Deposit & Copying of Dissertation Declaration

UNIVERSITY OF CAMBRIDGE

Board of Graduate Studies

Please note that you will also need to bind a copy of this Declaration into your final, hardbound copy of thesis - this has to be the very first page of the hardbound thesis.

1	Surname (Family Name)	Forenames(s)	Title
	NATRAJAN	MUKTHA	

2	Title of Dissertation as approved by the Degree Committee
	RETINOID X RECEPTOR ACTIVATION REVERSES AGE-RELATED DEFICIENCIES IN MYELIN DEBRIS PHAGOCYTOSIS AND CNS REMYELINATION

In accordance with the University Regulations in *Statutes and Ordinances* for the PhD, MSc and MLitt Degrees, I agree to deposit one print copy of my dissertation entitled above and one print copy of the summary with the Secretary of the Board of Graduate Studies who shall deposit the dissertation and summary in the University Library under the following terms and conditions:

1. Dissertation Author Declaration

I am the author of this dissertation and hereby give the University the right to make my dissertation available in print form as described in 2. below.

My dissertation is my original work and a product of my own research endeavours and includes nothing which is the outcome of work done in collaboration with others except as declared in the Preface and specified in the text. I hereby assert my moral right to be identified as the author of the dissertation.

The deposit and dissemination of my dissertation by the University does not constitute a breach of any other agreement, publishing or otherwise, including any confidentiality or publication restriction provisions in sponsorship or collaboration agreements governing my research or work at the University or elsewhere.

2. Access to Dissertation

I understand that one print copy of my dissertation will be deposited in the University Library for archival and preservation purposes, and that, unless upon my application restricted access to my dissertation for a specified period of time has been granted by the Board of Graduate Studies prior to this deposit, the dissertation will be made available by the University Library for consultation by readers in accordance with University Library Regulations and copies of my dissertation may be provided to readers in accordance with applicable legislation.

3	Signature	Date
	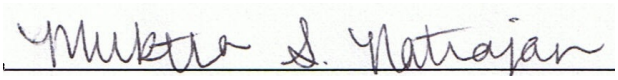	26/06/2015

Corresponding Regulation

Before being admitted to a degree, a student shall deposit with the Secretary of the Board one copy of his or her hard-bound dissertation and one copy of the summary (bearing student's name and thesis title), both the dissertation and the summary in a form approved by the Board. The Secretary shall deposit the copy of the dissertation together with the copy of the summary in the University Library where, subject to restricted access to the dissertation for a specified period of time having been granted by the Board of Graduate Studies, they shall be made available for consultation by readers in accordance with University Library Regulations and copies of the dissertation provided to readers in accordance with applicable legislation.

Retinoid X Receptor activation reverses age-related deficiencies in myelin debris phagocytosis and CNS remyelination

Muktha Sundar Natrajan

Newnham College, Cambridge
National Institutes of Health, USA

This dissertation is submitted for the degree of Doctor of Philosophy

April 2015

Preface

This dissertation is the result of my own work unless otherwise stated in the materials and methods section. None of this work has been submitted for any other qualification at any other University and does not extend the 60000 word limit established by the Department.

Muktha Sundar Natrajan

April 2015

Acknowledgements

Somehow, I have made it to the end of this PhD. I cannot account everything that has brought me to this point, but I certainly know who made it possible. To everyone in this list and to many others, you have given me the happiest and most transformative years of my life; I don't think it's possible to really thank you for such personal growth, but I would like to try.

First and foremost, I must thank my magnificent co-mentors, Robin and Bibi. Robin provided me with a fantastic beginning to my research. From chasing me down after work with his brilliant ideas to encouraging boldness in scientific thought, his passion for remyelination and his truly incredible ability to make complex ideas make sense to anyone still astounds me. I hope to take away at least a small portion of that brilliance and continue to learn from it for many years to come. I owe Bibi so much for a perfect introduction to clinical research. She has an incredible ability to understand all parts of biology, to take data and explain how so many complex pieces of science can work together. Her intelligence, sincerity, and unwavering ethics have inspired me to strive for excellence in research and mentorship.

To lab members from both sides of the Atlantic, thank you for your never-ending patience, knowledge, and kindness. I will start with my first teacher in Robin's lab, Alerie. She is the RXR queen and spent so much of her time teaching me techniques but also shared with me her wonderful friendship, compassion, and generosity. I must thank Abbe for spending many hours of her life helping me with surgeries, handling mice and dealing with the trials of animal work. I had not laughed so much or felt so connected at work before we met; truly an inspiration in every way!

To the wonderful post-docs and research scientists in Robin's lab, I could not have found such exceptional and talented people anywhere else. Chao, Dan, Peter, Pancho, Jeff, Mike, Daniel, and Ilias, thank you for all the tools I needed to believe I could finish the PhD. A special thanks to Chao and Daniel for their expertise in EM, to Jeff for his brilliance in nuclear receptor biology, and Peter and Ilias for their unparalleled humour and drive. And to our colleagues in Cambridge, specifically Lee Hopkins and Clare Bryant for the introduction to techniques in immunology, Jing-Wei Zhao for his knowledge on macrophages, Eimear Linehan for her microglia work, Vanessa Nunez and Mercedes Ricote for mouse breeding, and all the Innes Building staff for taking care of my animals.

To my partners in crime in the PhD office in Cambridge, Ginez, Sylvia, Sergey, Sonia, Bowei, Josephine, Laura, Caroline, and Katrin, thank you for always providing me with hearty laughs, exciting stories, and insightful comments. Sylvia and Ginez, you both are incredible sources of joy in my life, and I miss my smiling neighbours every day! And to everyone else I met in Cambridge, thank you for making it such a magical place. My Gates family, Olympia, Noham, Andrea, and Jorge, thank you for the adventures in Cambridge and beyond. I feel I could share anything with all of you, but mostly thanks for your commiseration in the PhD and for opening your homes when I travelled between the NIH and Cambridge.

To my wonderful NIH lab, thank you for accepting me halfway through this work. To Mika, Peter, Elena, Yen, Azita, and Simone, you took this little neophyte to many of the techniques and theories in immunology, and you never stopped teaching me. I certainly made mistakes, but you were all patient and kind throughout. I will miss

all of our delicious breakfasts and parties! To the post-baccs, Danish, Drew, Justin, and Paige -- thank you for making so many days in the lab fun. I have never had so many debates and exciting lunch discussions before.

And a big thanks to all members of the NIH community. It is a wonderful place to work, thanks to the amazing facilities and all of the people who make them function. Specifically, thanks to Kory and Tianxia for their incredible statistics and bioinformatics expertise and to Abdel and Weiwei for all the assistance with microarrays. And thanks to the NDU Clinical team and NIH blood bank, without whom I would not have had access to any of the patient samples that were so valuable to this work, specifically Jen and Tom who were always willing to take my orders and follow up on my research.

To my incredible cohort in the NIH-OxCam program – thank you for fully understanding how amazing and exciting this type of PhD experience can be. Thank you for the food, fun, and travels. Especially to Kristy, Adam, Coralie, Mike, and Caz, thank you for being sources of laughter and excitement whenever I came home.

I would also like to give a special thanks to those who got me started in science while at UGA. Steve Stice, Pam Kleiber, Frank West, and Jenny Mumaw, your support and drive always pushed me forward with no expectation of return. I still hope I can give more back to you some day!

I would like to thank my extended family, without whom I never would have gained the confidence and humility to pursue this type of degree. To my immediate family, thank you to my parents, who have never wavered in their support for anything I have aimed for. Dad, I have been so lucky to have such a hardworking, caring, and talented father. Amma, I hope to be at least half as patient, funny, loving, and inspiring to my children. Nithya, I will never meet anyone who cares so much and puts in such effort for those around her. And Mohan, despite all of our jokes, thank you for always understanding me.

Dave, you are my rock! Thank you for reading through this thesis so many times (along with every presentation, application, etc that I've ever done). Your insight and curiosity continue to impress me, and this PhD would not have been possible without your encouragement.

I am also appreciative of all the generous funding I have received. Thank you to the Gates Foundation and NIH-Oxford Cambridge Scholars Program for providing me with an amazing scholarship community. Thank you to the EG Fearnside Fund and Newnham College for the wonderful conference opportunities I've been able to partake in. Thank you to all those in the Brain Repair Centre, Vet School, and NINDS for the opportunity to study at the University of Cambridge and NIH. It has been an immense privilege to be able to complete this PhD with so much support.

Finally, thank you to all who make the effort to read this. I am very grateful for your time and insight into this incredible journey!

Summary

Muktha Sundar Natrajan

Retinoid X Receptor activation reverses age-related deficiencies in myelin debris phagocytosis and CNS remyelination

Remyelination is a regenerative process that occurs through the formation of myelin sheaths by oligodendrocytes, which are recruited as oligodendrocyte progenitor cells (OPCs) after demyelination in diseases such as Multiple Sclerosis (MS). A key environmental factor regulating OPC differentiation is the fate of myelin debris generated during demyelination. Myelin debris contains inhibitors of OPC differentiation and thus its clearance by phagocytic macrophages is an important component of creating a lesion environment conducive to remyelination. The efficiency of debris clearance declines with age, contributing to the age-associated decline in remyelination. Therefore, understanding the mechanisms of the age-related decline in myelin debris phagocytosis is important for devising means to therapeutically reverse the decline in remyelination. The aim of this study was to determine the functional/molecular differences between young and old phagocytes involved in myelin debris clearance, thereby identifying therapeutically modifiable pathways associated with efficient myelin debris phagocytosis.

In this study, we show that expression of genes involved in the retinoid X receptor (RXR) and peroxisome proliferator-activated receptor (PPAR) pathways are decreased with ageing in both myelin-phagocytosing human monocytes and mouse macrophages. Disruption of RXR and PPAR using synthetic antagonists in young macrophages mimics ageing by reducing myelin debris uptake. Macrophage-specific RXRα knockout mice revealed that loss of RXR function in young mice caused delayed myelin debris uptake and slowed remyelination. Alternatively, receptor agonists partially restored myelin debris phagocytosis in aged macrophages. The FDA-approved agonists bexarotene and pioglitazone, when used in concentrations achievable in human subjects, caused a reversion of the gene expression profiles in MS patient monocytes to a more youthful profile and enhanced myelin debris phagocytosis by patient cells. Activation of these pathways also enhances immunoregulatory markers on monocytes from MS patients, further suggesting the regeneration-promoting capacity of activating these pathways in phagocytes. These results reveal the RXR/PPAR pathway as a positive regulator of myelin debris clearance and a key player in the age-related decline in remyelination that may be targeted by available or newly-developed therapeutics.

Abbreviations

9CRA: 9-*cis* retinoic acid
AF: Alexa flour
AF-1: Activation function 1
ANOVA: Analysis of Variance
APC: Antigen presenting cell
ARG-1: Arginase-1
BBB: Blood brain barrier
BCA: Bicincotinic acid
BD: Becton Dickson
BDNF: Brain derived neurotrophic factor
BEX: Bexarotene
BMM: Bone marrow monocyte-derived macrophage
BSA: Bovine serum albumin
C-: Complement component -
CC1: Adenomatous polyposis coli
CCR-: Chemokine receptor -
CD-: Cluster of differentiation
CDNA: Complement deoxyribonucleic acid
CNPase: 2′,3’-cyclicnucleotide 3' phosphodiesterase
CNS: Central nervous system
CR-: Complement receptor -
CRE: Causes recombination protein
CRMPI: Complete RPMI Media for BMMs
CSF: Cerebrospinal fluid
CSPG: Chrondroitin sulfate proteoglycan
CV: Coefficient of variation
CXCL-: Chemokine ligand -
CXCR-: Chemokine receptor -
DBD: DNA binding domain
DIO: $DiOC_{18}(3)$
DMEM: Dulbecco’s modified eagle medium
DMSO: Dimethyl sulfoxide
DPL: Days post lesion
EAE: Experimental autoimmune encephalomyelitis
ECL: Electrochemiluminescence
EBNA-1: EBV-encoded nuclear antigen-1
EBV: Epstein Barr virus
EDN1: Endothelin-1
EDTA: Ethylenediaminetetraacetic acid
EM: Electron microscopy
ET-2: Endothelin-2
FACS: Fluorescence activated cell sorting
FBS: Foetal bovine serum
FDA: Food and drug administration
FITC: Fluorescein
GALC: Glactosylceramidase
GFP: Green fluorescent protein
GM-CSF: Granulocyte macrophage colony stimulating factor

H: Hours
HAT: Histone acetyl transferase
HDAC: Histone deacetylase
HV: Healthy volunteer
IBA-1: Ionized calcium-binding adapter molecule 1
ID2/4: Inhibitor of DNA binding
IFNγ: Interferon γ
IGF-1: Insulin-like growth factor 1
IL-: Interleukin -
INOS: Inducible nitric oxide synthase
IPA: Ingenuity pathway analysis
JC: John Cunningham
KO: Knockout
L929:Murine aneuploid fibrosarcoma (fibroblast) cell line
LBD: Ligand binding domain
LIF: Leukaemia inhibitory factor
LPS: Lipopolysaccharide
LXR: Liver X receptor
LYSM: Lysosyzme M
M1: Pro-inflammatory macrophage
M2: Anti-inflammatory macrophage
MAC-2: Galectin3
MAG: Myelin associated glycoprotein
MARCKS: Myristoylated alanine-rich C-kinase substrate
MBP: Myelin basic protein
MCP-1: Monocyte chemoattractant protein
M-CSF: Macrophage colony stimulating factor
MCT1: Monocarboxylate transporter 1
MFI: Mean fluorescence intensity
MHC: Major histocompatibility complex
MIN: Minutes
MO: Months old
MOG: Myelin oligodendrocyte glycoprotein
MOM: Mouse on mouse reagent
MOPS: 3-(N-morpholino)propansulfonic acid
MS: Multiple Sclerosis
NFAT5: Nuclear factor of activated T cells
NMDA: *N-methyl-D-aspartate*
NO: Nitric oxide
NR: Nuclear receptor
NS: Not significant
OL: Oligodendrocyte
OPC: Oligodendrocyte progenitor cell
ORO: Oil red O
PBS: Phosphate buffered saline
PBST: Phosphate buffered saline 0.1% tween 20
PDGFR: Platelet-derived growth factor receptor
PFA: Paraformaldehyde
PHODO: pH-sensitive Molecular Probes
PI3K: Phosphatidylinositol-3-kinase
PIO: Pioglitazone

PKC: Protein kinase C
PLP: Proteolipid protein
PML: Progressive multifocal leukoencephalopathy
PMN: Motoneuron domain
PPAR: Peroxisome proliferator activated receptor
PPMS: Primary progressive MS
PRMS: Progressive relapsing MS
P/S: Penicillin/Streptomycin
PSA-NCAM: Polysialylated-neural cell adhesion molecule
PTGES: Prostaglandin E synthase
QPCR: Quantitative polymerase chain reaction
RAR: Retinoic acid receptor
ROCKII: Rho-associated, coiled-coil containing protein kinase 2
ROS: Reactive oxygen species
RRMS: Relapsing remitting MS
RT: Room temperature
RXR: Retinoid X receptor
SCD14: Soluble CD14
SCD163: Soluble CD163
SDS: Sodium dodecyl sulfate
SEMA3A: Semaphorin 3A
SHH: Sonic hedgehog
SPMS: Secondary progressive MS
T007: N-(4′-aminopyridyl)-2-chloro-5-nitrobenzamide
TBS: Tris buffered saline
TCF4: Transcription factor 4
TGF-β: Transforming growth factor β
TLR: Toll-like receptor
TNF: Tumour necrosis factor
TR: Thyroid hormone receptor
TREM2: triggering receptor expressed on myeloid cells
VDR: Vitamin D receptor
VEGF: Vascular endothelial growth factor
WNT: Wingless-int
WT: Wildtype

Table of Contents

Chapter 1. Introduction & Literature Review

Retinoid X Receptor activation reverses age-related deficiencies in myelin debris phagocytosis and CNS remyelination

Introduction

The central nervous system (CNS) has long been considered an immune-privileged organ due to the presence of the blood brain barrier (BBB) made up of the meninges (pia, arachnoid, and dura) and tight junctions formed by endothelial cells. The BBB provides protection to the complex network of cells in the CNS, including neurons, astrocytes, oligodendrocytes, and microglia. Immune cells may enter the CNS to perform immune surveillance alongside microglia and astrocytes in the healthy brain, but in the absence of injury or disease, these activated cells tend to undergo apoptosis or exit the CNS (Bauer et al., 1998). In demyelinating diseases such as Multiple Sclerosis (MS), immune cells are recruited to the CNS and are involved in both the pathogenesis of disease and in the resolution of demyelinating events (Lassmann et al., 2012; Naegele and Martin, 2014).

This thesis focuses on the role of infiltrating monocytes and macrophages in the process of remyelination, the major regenerative process that occurs after demyelination. Our understanding of the beneficial role of innate immune cells in remyelination still remains incomplete, and discovering the most effective ways to harness these cells can lead to targeted therapies to promote regeneration. This introduction will provide a brief overview of the processes of demyelination and remyelination in the context of MS and the potential role of the innate immune response in overcoming barriers that prevent remyelination in the ageing population.

1.1 Myelin

Myelin is formed by oligodendrocytes (OLs) in the CNS to ensheath axons. OLs are the glial cell responsible for myelination, and by extending their plasma membranes, they are able to efficiently wrap axons in multiple myelin layers (Fig. 1.1). In addition to myelination, OLs interact with surrounding cells in the CNS and are able to communicate with axons, astrocytes, and endothelial cells. To communicate with axons, they form channel-like tubes from their nucleus to the axon (Paz Soldan and Pirko, 2012). OLs have also been shown to express receptors for neurotransmitters, such as NMDA receptors for glutamate (Karadottir et al., 2005), which play a role in transferring exosomes from the OL to the axon (Fruhbeis et al., 2013). They are connected to astrocytes via gap junctions, which are composed of two hemichannels (each of six connexin membrane proteins) to allow diffusion of

ions between OLs and astrocytes (Orthmann-Murphy et al., 2009). In addition, OLs form a complex interaction with endothelial cells at the blood brain barrier through the shuttling of glucose. Glucose is transferred to OLs and astrocytes via monocarboxylate transporter 1 (MCT1) and broken down into lactate molecules, which provide energy to myelin and axons (Lee et al., 2012). OLs have a high energy demand and use lactate and other sources of energy to expand their surface area by over 6,500-fold and can myelinate up to 60 axonal segments at a time (de Monasterio-Schrader et al., 2012; Freeman and Rowitch, 2013).

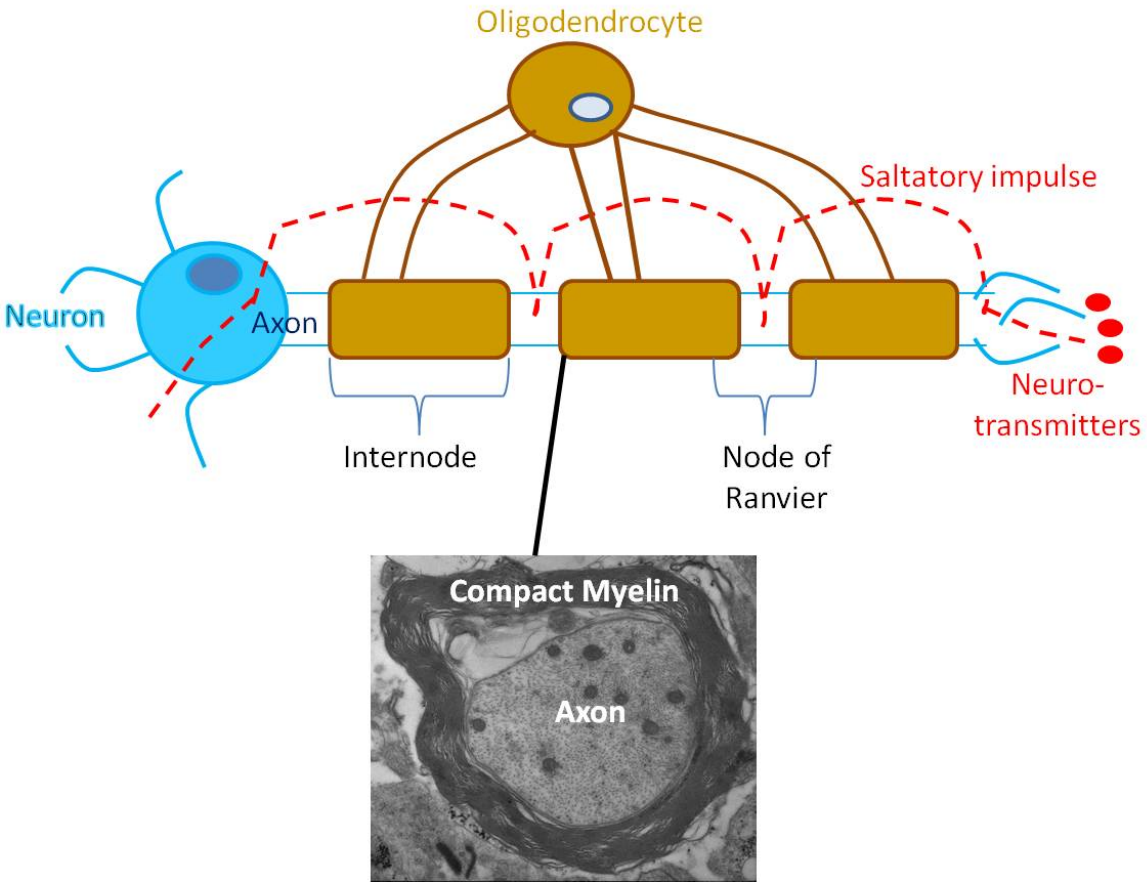

Figure 1.1: Myelin allows rapid saltatory conduction. Oligodendrocytes extend their plasma membranes to create multiple myelin sheaths around each axon. Myelinated portions of axon are known as the “internode” while unmyelinated portions are the “Nodes of Ranvier”. Myelination provides support and insulation to promote rapid firing of action potentials and electronic propagation down myelin segments (red dashed line), resulting in efficient neurotransmitter release. Electron micrographs of the spinal cord show the compact myelin sheath formed around the axon.

The uniquely polarised myelin membrane is primarily composed of lipids, which make up approximately 70% of its dry weight, in order to increase the speed of impulses up to one hundred-fold. The main lipids in myelin are cholesterol, phospholipids, and galactosylceramide (Edgar et al., 2009; Morell and Ousley, 1994; Norton and Poduslo, 1973). The remaining protein portion of myelin interacts with this high lipid content to create a properly folded, compact myelin sheath around segments of each axon (Baron and Hoekstra, 2010; Simons et al., 2012). The areas wrapped by myelin, known as the internode due to their placement between unmyelinated axon segments (Nodes of Ranvier), allow for rapid saltatory conduction of action potentials down the axon (Fig. 1.1). Myelin provides insulation to axons in an electrically charged environment by reducing capacitance and increasing membrane resistance, resulting in efficient neurotransmitter release at the end of axons (Aggarwal et al., 2011; Keirstead and Blakemore, 1999; Paz Soldan and Pirko, 2012).

In addition to allowing rapid saltatory conduction, the second major function of myelin is to preserve the long-term integrity of the axon (Griffiths et al., 1998). Myelin has evolved in high level nervous systems, allowing for better axonal support, higher muscle function, and more complex behaviour (Harris and Attwell, 2012; Nave, 2010). The myelin sheath especially protects the axon in diseased environments by providing trophic support to axons (via MCT1) and expressing neurotrophic factors such as brain derived neurotrophic factor (BDNF) and insulin-like growth factor (IGF-1). Unmyelinated axons contain more mitochondria than myelinated axons, suggesting that the axon must provide more of its own energy to maintain function in the absence of OLs (Smith et al., 2013). In addition, mice engaged in long term learning exercises preferentially generate myelin in adulthood, suggesting white matter changes in the brain (through an increase in OL production) occur during the learning process (McKenzie et al., 2014). This collection of evidence suggests that OLs are key to axonal survival by providing nutrients and a proper framework to support axonal health.

1.2 Oligodendrocyte Progenitor Cells

OLs in the adult CNS can be replenished by a population of adult stem cells known as oligodendrocyte progenitor cells (OPCs). These cells have the capacity to differentiate and generate myelin throughout adulthood (Young et al., 2013), explaining why myelination can continue late into life (Fields, 2008). OPCs are abundant in the adult CNS, making up 5-8% of total glial cells and are dispersed in both the white and gray matter (Dawson et al., 2003; Levine et al., 2001; Pringle et al., 1992). The majority of OPCs are derived from developmental OPCs, which originate from neural progenitor cells in the motoneuron domain (pMN) of the ventricular zone during development. Sonic hedgehog (SHH) signalling is released during nervous system development and transcribes Olig2, which initiates differentiation of neural progenitor cells to motor neurons and OPCs (Briscoe et al., 2000; Zhou and Anderson, 2002). OPCs are able to extend and retract processes as they migrate throughout the CNS during development and in adulthood, resulting in consistent spacing of OPCs in the parenchyma (Kirby et al., 2006). As they migrate, OPCs proliferate until they reach their final destination and exit the cell cycle (Wegner, 2008). OPCs are also able to regulate angiogenesis through their interactions with endothelial cells (Yuen et al., 2014), differentiate into astrocytes, Schwann cells, and neurons (Rivers et al., 2008; Tatsumi et al., 2008; Zawadzka et al., 2010), and in the majority of cases, differentiate to oligodendrocytes (Richardson et al., 2011).

Several markers of OPCs have been established to identify these cells in various stages of development (Fig 1.2). OPCs begin as neural progenitor cells in the pMN and express Polysialylated-neural cell adhesion molecule (PSA-NCAM), Nestin, and Vimentin during this time. As these progenitors grow, they start to express platelet-derived growth factor α (PDFRα) and mature into OPCs, which express NG2, Nestin, and A2B5. As they further differentiate into pre-oligodendrocytes, they also begin to express O4. Once they become pre-myelinating oligodendrocytes, they express GalC (a prominent myelin lipid), adenomatus polyposis coli (APC, also known as CC1), and 2’,3’-cyclic nucleotide 3’ phosphodiesterase (CNPase). Finally, mature myelinating oligodendrocytes express multiple myelin proteins, especially myelin basic protein (MBP), proteoplipid protein

(PLP), myelin oligodendrocyte glycoprotein (MOG), and myelin-associated glycoprotein (MAG) (Schumacher et al., 2012).

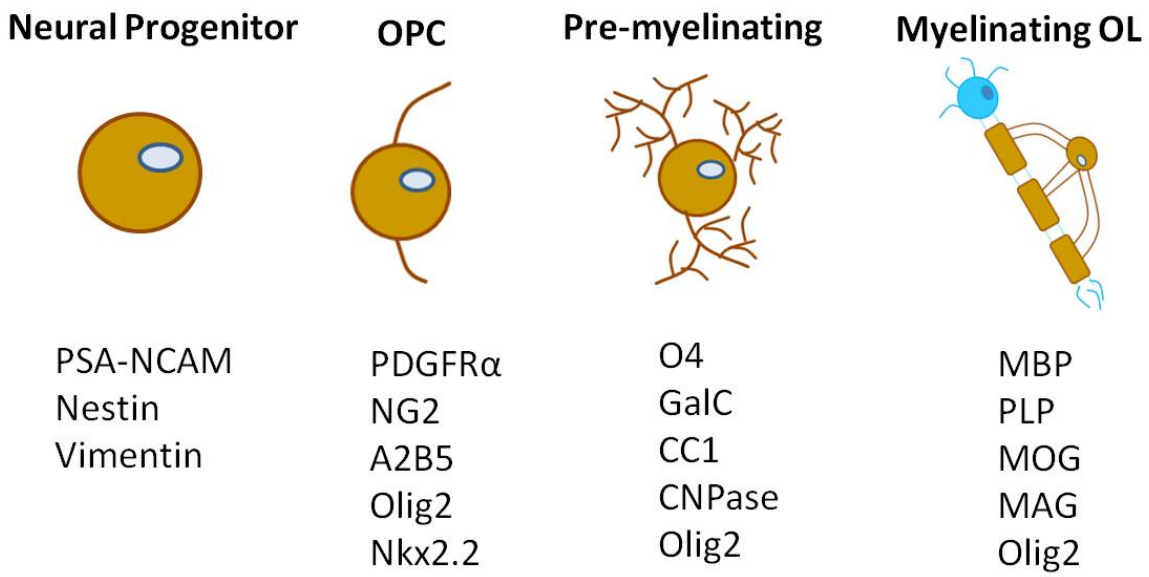

Figure 1.2: OPC differentiation markers. Specific markers in oligodendrocyte (OL) differentiation allow distinction of development along the OL lineage. OPCs begin as Neural Progenitors expressing PSA-NCAM, Nestin, and Vimentin. Once they become bipolar OPCs, they upregulate NG2, A2B5, and PDFRα. They then become pre-myelinating OLs and begin to branch out further and express OL-specific markers. Finally, they differentiate to myelinating OLs and ensheath axons while expressing myelin-specific proteins, such as MBP, PLP, MOG, and MAG.

To regulate differentiation, OPCs intrinsically control expression of several of these transcription factors to maintain a quiescent state. The repression model of myelination suggests that OPC differentiation is inhibited by continuous expression of transcription factors that inhibit myelin gene expression and mediate extrinsic signals. These factors include inhibitor of DNA binding-2 and 4 (ID2, ID4) and transcription factor 4 (Tcf4), which inhibit Olig2 expression (Kondo and Raff, 2000; Wegner, 2008). In addition, Wnt signalling stabilises Tcf4 transcription and disrupts OPC maturation by activating the Axin complex and releasing β-catenin (Fancy et al., 2009). To allow for differentiation, the surrounding environment of OPCs must promote downregulation of inhibitory transcription factors which allows for

transcription of myelinating OL genes. The promotion of OPC proliferation and differentiation is key to promoting myelin regeneration (remyelination) after a myelin destructive pathology (demyelination).

1.3 Demyelination & Remyelination

In normal adult white matter, an OL myelinates axons by extending cytoskeletal processes to form myelin around several axons (Asou et al., 1994; Matthews and Duncan, 1971). In diseases such as Multiple Sclerosis, demyelination occurs and these OLs and their processes are degraded, but remyelination and functional recovery can take place when OPCs are recruited and differentiated in distinct stages (Franklin and Ffrench-Constant, 2008; Murtie et al., 2005; Woodruff et al., 2004). In the recruitment stage, OPCs migrate to the demyelinated area of the axon. Then, they respond to both extrinsic and intrinsic factors to differentiate into oligodendrocytes and remyelinate axons (Fig 1.3) (Fancy et al., 2009; van Wijngaarden and Franklin, 2013).

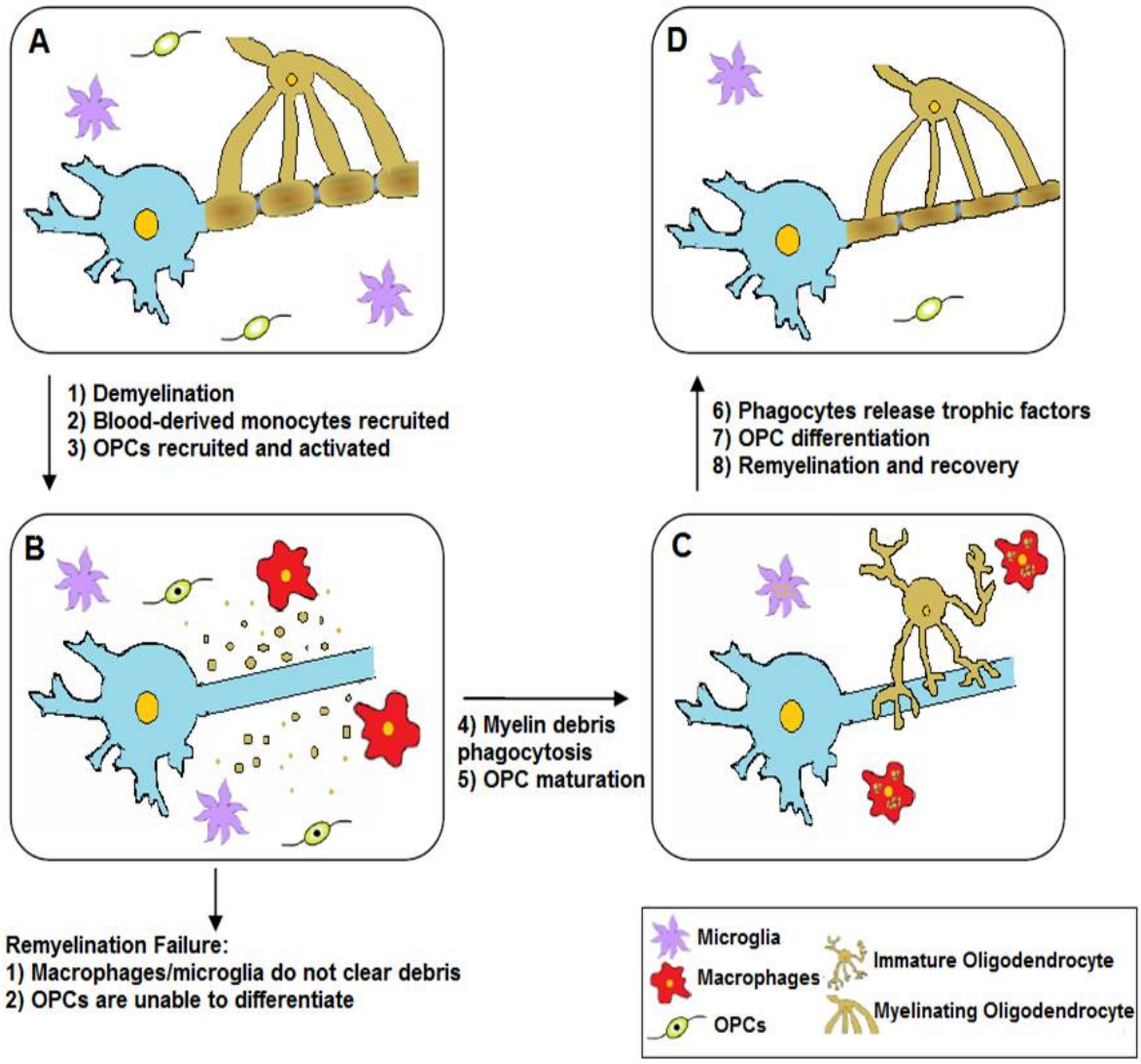

Figure 1.3: Macrophage and microglia involvement in the stages of demyelination to remyelination. A) Myelinating oligodendrocytes, microglia, astrocytes and OPCs populate healthy CNS white matter. B) After demyelination, myelin debris is formed around denuded axons and blood-derived monocytes are recruited to the lesion site. OPCs are recruited and activated as well in response to demyelination. However, if macrophages are not properly recruited and activated, myelin debris is not cleared and OPCs are unable to differentiate causing remyelination to fail. C) Myelin debris is phagocytosed by macrophages and microglia, clearing the way for OPC differentiation. Phagocytes also release various cytokines and growth factors that promote differentiation and remyelination of the CNS. D) After proper removal of myelin debris and activation of differentiation cues in OPCs, macrophages and microglia largely exit the lesion area and return to a resting state. Mature oligodendrocytes effectively remyelinate the exposed axons with a thinner myelin sheath and proper conductance is restored.

The loss of myelin from a healthy axon is known as demyelination and is a feature of several neurological conditions (Franklin and Ffrench-Constant, 2008; Franklin and Gallo, 2014). Due to demyelination, conduction of action potentials can be slowed and lack of trophic support from the OL leads to compromised axonal integrity and eventually, axonal degradation (Irvine and Blakemore, 2008; Nave, 2010; Smith and McLeod, 1979). When demyelination accumulates in the CNS, there is an associated decline in neurological function seen in many neurological disorders, including neuromyelitis optica, Transverse myelitis, Acute disseminated encephalomyelitis, Adult-onset leukodystrophies, and the most prevalent, Multiple sclerosis.

Remyelination and functional recovery can take place following demyelination. Remyelination is an endogenous process where OPCs are recruited to a site of injury and differentiate into myelinating OLs; it is vital for restoring function and preventing long-term neurodegeneration (Irvine and Blakemore, 2008; Kornek et al., 2000). Through the generation of new OLs, contact can be re-established between a myelinating OL and the demyelinated axon, resulting in concentric wrapping and compaction of a new myelin sheath. This sheath is thinner and shorter than before demyelination, but studies do not suggest any reduced function in a remyelinated sheath (Franklin and Ffrench-Constant, 2008). In order to distinguish remyelination, this thinner sheath is easily recognizable through the measurement of the “g-ratio.” The g-ratio is used to determine the relationship between axon diameter and myelin sheath thickness by calculating the circumference of the axon divided by the circumference of the myelin sheath. The remyelinated sheath (higher than normal g ratio) is able to provide effective trophic support and restore proper conductance across the axon (Franklin, 2002; Irvine and Blakemore, 2008; Kornek et al., 2000).

1.4 Multiple Sclerosis

Multiple Sclerosis (MS) is the most common inflammatory demyelinating disease of the CNS, affecting more than 2 million people worldwide (Compston and Coles, 2008; McFarland and Martin, 2007). MS is a complex disease with diverse symptoms and levels of progression, making it difficult to effectively treat. The demographics of MS patients have been extensively studied. Although the cause of

the disease remains uncertain, several factors have been associated with higher risks of MS. The average age of onset is 30 years old and ranges from 15-50 years in a predominantly female population (2-3:1, female:male ratio in relapsing-remitting disease) (Compston and Coles, 2008; Duquette et al., 1987). MS is more prevalent in Europe, North America, Australia, and New Zealand (Koch-Henriksen and Sorensen, 2010) and is associated with low vitamin D levels and cigarette smoking (Ascherio et al., 2014; Handel et al., 2010; Mikaeloff et al., 2007).

Several triggers of MS have been discussed; although no one cause has yet been confirmed, it is likely that the disease results from a combination of these factors (Fig 1.4). Genetic causes of MS have been extensively studied and have revealed a modest role of genetic effects. Approximately 20-25% of monozygotic twins both develop MS, in comparison to 2-5% of dizygotic twins and in the general population (Compston and Coles, 2008; Ebers et al., 1986), suggesting an increased susceptibility due to genetic traits. A more recent, large-scale study by the International MS Genetics Consortium identified genes within the major histocompatibility complex (MHC) and other immune-related genes as overrepresented in the MS population (International Multiple Sclerosis Genetics et al., 2011). In addition, there are >110 susceptibility loci reported in published literature, with the majority of these common allelic variants in non-coding regions with studies suggesting that these variants are specifically enriched for sequences involved in regulation of immune-related genes (International Multiple Sclerosis Genetics et al., 2013). These causes relate to the primary theory of MS as an autoimmune disease mediated by dysregulation of myelin-specific T-lymphocytes (Martin et al., 1992; McFarland and Martin, 2007). In this theory, autoreactive T cells invade the brain and elicit a local immune response resulting in demyelination; many studies report higher numbers or higher reactivity of myelin-specific T cells in MS (Martin and McFarland, 1995; Steinman, 2001; Wuest et al., 2014).

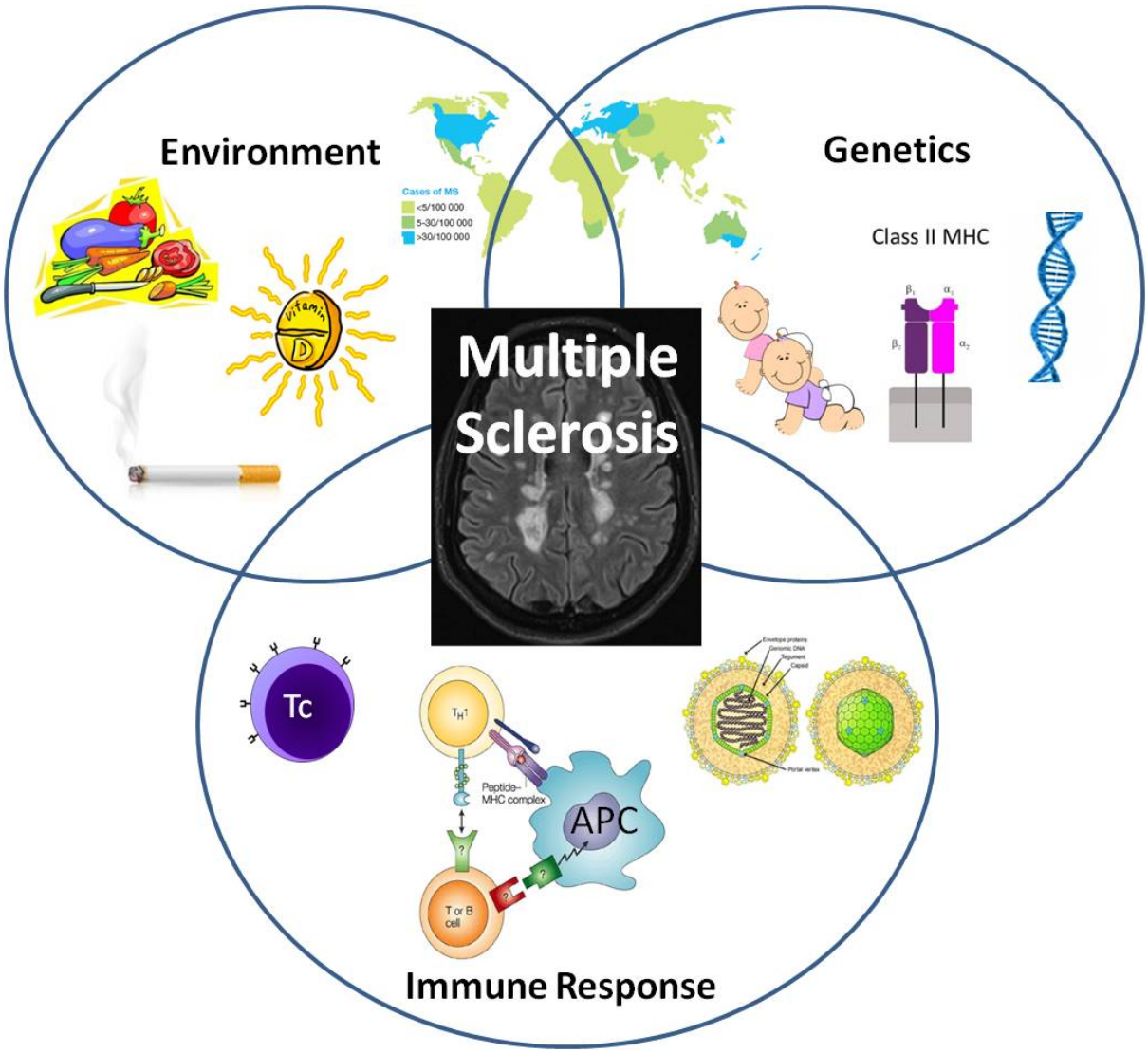

Figure 1.4: Multiple sclerosis (MS) is caused by an overlap of environmental, genetic, and immune factors. MS is a complex inflammatory neurodegenerative disease and is likely triggered by a combination of factors. Environmental factors such as low vitamin D exposure, cigarette smoking, diet, and distance from the equator have all been correlated to the disease. In addition, twins are more likely to develop MS, and large genetic studies have shown that several immune-related genes are more common among MS patients compared to the general population. These genes likely lend to the inflammatory reaction responsible for initial demyelination in the disease course.

Another theory is that MS is caused by primary OL apoptosis resulting in an inflammatory response. Due to evidence of demyelination before inflammation (Barnett and Prineas, 2004; Henderson et al., 2009), induction of OL apoptosis may be the primary cause of demyelination in some cases (Caprariello et al., 2012). However, genetic studies have clearly demonstrated that genetic predisposition to MS involves genes in immune regulation, and immunomodulatory therapies provide strong support for immune-mediated pathophysiology. Due to its likely immune-mediated nature, the disease is also related to viral infections that prime immune cells to target OLs. The most commonly associated virus with MS is the Epstein Barr Virus (EBV) (Serafini et al., 2013; Tzartos et al., 2012), which displays significantly elevated levels of viral copies in MS patients compared to the general population and is present in 99.5% of MS cases, making it a likely necessary component of MS (Pakpoor and Ramagopalan, 2013). Studies have shown that EBV-encoded nuclear antigen-1 (EBNA1)-specific T cells accumulate in MS cases and allow cross-recognition of autoantigens (Lunemann et al., 2006). EBV is a γ-herpesvirus and acts by infecting and expanding B cells. The latent EBV infection remains within B cells and is present in ~90% of the adult population (Pender and Burrows, 2014), so alone it is not sufficient to identify MS as it is common in the overall population. These studies together with genetic and epidemiological evidence suggest that MS is an immune-mediated disease, but the triggers of this immune response and which antigens specifically are targeted in MS remains unknown.

A definitive cause remains elusive, and the symptoms of MS also vary greatly among patients and disease course. In general, patients suffer from sensory and motor symptoms during an MS attack. These include visual loss, gait disturbance, balance problems, vertigo, bladder problems, fatigue, and tremors (Compston and Coles, 2008). Symptoms develop from demyelinated lesions at specific sites within the CNS, in both the gray and white matter (Geurts and Barkhof, 2008), and an MS diagnosis requires demonstration of these lesions and their dissemination in time as well as exclusion of alternative diseases that cause CNS lesions separated in space and time (Polman et al., 2011). This demyelination often leads to degradation of axons (Evangelou et al., 2001). In addition, inflammation is readily apparent in MS lesions, including activated macrophages with ingested myelin, perivascular T-cell infiltrates, and a few B-cells (Lassmann, 2007; Lassmann, 2011). This inflammation

can result from and/or cause disruption of the blood brain barrier (BBB), which is recognised by enhanced accumulation of gadolinium in active MS lesions (Kirk et al., 2003). The disease course of MS is unpredictable, but can generally be defined in four main groups.

Relapsing-remitting MS (RRMS) is the most common form of the disease and is characterised by short timeframes of disability followed by recovery periods with no decline. Most cases (~85%) are first diagnosed as RRMS, and patients generally do not experience any symptoms between their attacks (Bethoux et al., 2001). This is partially due to the efficiency of remyelination in these patients. At early stages of RRMS, areas of acute demyelination undergo robust regeneration due to a conducive environment for remyelination. On patient pathology, this remyelination is visualised by “shadow plaques,” areas with thinner myelin sheaths and higher than normal g ratios (Bramow et al., 2010; Lassmann, 2007; Patrikios et al., 2006). In 50-65% of RRMS cases, the disease begins to progress between relapses and remyelination begins to decline; this type of MS is called secondary progressive MS (SPMS). In SPMS, patients accumulate disabilities over time, usually over the course of decades. There does not appear to be increased mortality in these patients but rather an increase in disability burden with no remission (Weinshenker et al., 1989).

One less common forms of MS involves progression of disability from the onset of disease. A further 10% of patients are diagnosed directly with primary progressive MS (PPMS), where there are no periods of relapse or remission from disease onset and disabilities worsen with little recovery. PPMS patient MRIs tend to show a lower T2 and T1 focal lesion load compared to SPMS patients and also have a higher number of diffuse abnormalities in both the brain and spinal cord (Ingle et al., 2002; Lublin et al., 2014; van Walderveen et al., 1998). Also, PPMS tends to show abnormalities in the spinal cord rather than the brain (as in RRMS and SPMS) (Nijeholt et al., 1998). However, the course of the disease can be indistinguishable from SPMS and is based purely on clinical diagnosis.

Several therapeutic agents are currently used to treat MS and especially assist in relapse reductions and reduce formation of new lesions. The most common and longest used treatments are Interferon β-1a/b. They have been shown to reduce frequency of relapses but have several side effects (Walther and Hohlfeld, 1999).

The strongest second-line treatment is Natalizumab, a selective monoclonal antibody against α4 integrin receptor on leukocytes, preventing their entry into the CNS (Yednock et al., 1992). However, natalizumab can reactivate John Cunningham (JC) polyomavirus and cause progressive multifocal leukoencephalopathy (PML) (Brew et al., 2010; Clifford et al., 2010). Fingolimod, a new oral drug, modifies the sphingosine-1-phosphate receptor on lymphocytes to prevent them from leaving the lymph nodes and crossing the BBB (Mandala et al., 2002). Glatiramer acetate, made up of a subset of amino acids in MBP, is used to prevent relapses by limiting T cells attacking myelin (Comi et al., 2001). Alemtuzumab, a recently FDA-approved treatment for RRMS, is a monoclonal antibody against CD52 on mature lymphocytes, causing depletion of lymphocytes and reduction of relapses compared to interferon β (Cohen et al., 2012; Coles et al., 2012). The currently prescribed agents for MS are highlighted in Table 1.1.

These agents do not successfully promote structural recovery and remyelination and have limited efficacy when applied in late stages of MS. All the current treatments have limited effects on damage resulting in accumulated disability and progression of disease. There is still a great amount of research to be done on treatments that provide strategies to overcome demyelination and axonal degeneration in MS, and in order to fully research the spectrum of treatments, ideal models of the disease must be utilised.

Drug	Trade names	Target	Administration	Side effects
Interferon β-1a/b	Avonex, Rebif, Cinnovex, Extavia, Betaferon	Reduces MHC II expression, Th1, and Th17 production	Subcutaneous, 1-3 /week	Skin site reactions, flu-like symptoms, thyroid dysfunction, liver abnormalities
Natalizumab	Tysabri	Monoclonal antibody against α4 integrin receptor on leukocytes	Intravenous, 1/month	Headache, joint pain, skin site reactions, infections, PML
Glatiramer acetate	Copaxone	T cells recognise this subset of amino acids from MBP	Subcutaneous, 1-3 /week	Skin site reactions, nausea, joint pain, headaches
Fingolimod	Gilenya	Retains lymphocytes within lymph nodes	Oral, 1/day	Back pain, cough, diarrhoea, headache
Teriflunomide	Aubagio	Blocks enzyme dihydoorotate dehydrogenase and T cell proliferation	Oral, 1/day	Diarrhoea, nausea, tingling in skin, hair loss
Alemtuzumab	Lemtrada	Monoclonal antibody against CD52 on mature lymphocytes	Intravenous, 1x3-5 day cycle/year	Fever, chills, dizziness, muscle stiffness, increased risk of other autoimmune diseases
Dimethyl fumarate	Tecfidera	Activates nuclear factor-like 2 (Nrf2), Nicotinic receptor agonist	Oral, 2/day	Redness, itching, stomach pain, diarrhoea, nausea, vomiting, PML

Table 1.1. Drugs available for MS treatment. This table lists several drugs currently approved for reducing relapses in MS patients with varying adverse effects and administration routes/frequency. Adapted from (Tullman, 2013)

1.4.3 Animal Models of MS

As the aetiology of MS is incredibly complex, achieving representative *in vivo* models of the disease remains difficult. One of the oldest and most well-characterised models is experimental autoimmune encephalomyelitis (EAE). In this model, clinical symptoms can be induced by several myelin epitopes as well as some non-myelin antigens, and myelin-reactive T-cells induce demyelinating lesions resembling those seen in MS. EAE is characterised by infiltration of blood-derived immune cells to the CNS and complex demyelination/remyelination process resulting in relapsing disability and clinical symptoms in mice (Gold et al., 2000). When studying questions of the adaptive immune response in MS, this model is ideal. It maintains a complex immune response that may mirror the components of autoimmune CNS disease. However, when studying remyelination of the CNS and progressive stages of MS, where several immunomodulatory therapies have shown little efficacy (Miller and Leary, 2007), the EAE model is not ideal.

Remyelination biology is more easily manipulated in toxin models of demyelination, where demyelination can be induced and subsequent remyelination efficiency can be studied using markers for stages of oligodendrocyte (OL) differentiation (Fig .1.2). Oral cuprizone, a copper chelator causing dysfunction in mitochondrial complex IV, results in selective OL toxicity throughout the corpus callosum and hippocampus. This model is used for studies of response of resident CNS inflammatory cells, such as microglia and astrocytes, because little infiltration of recruited monocytes occurs (Krauthausen et al., 2014; McMahon et al., 2002). However, in studies of the infiltrating innate immune response to demyelination and remyelination biology, lysolecithin and ethidium bromide-induced demyelination cause prompt demyelination followed by distinct stages of remyelination. These models allow for isolated demyelination in the CNS and can identify important cellular mechanisms that change during manipulation of this system. In addition, in young healthy mice, a consistent timeframe of OL differentiation can be followed. After initial infiltration of innate immune cells, OPC migration and proliferation mainly occurs from 4-7 days post lesion (dpl). OPC maturation and differentiation begins around 10dpl and continues to increase around 14-15dpl. Then, remyelination mainly occurs until around 21dpl, when most of the lesion is remyelinated. By 28dpl,

remyelination is fully complete in this model (Blakemore and Franklin, 2008; Hinks and Franklin, 1999).

Remyelination therapies are necessary to improve disability outcomes; therefore, accurate modelling of this process and therapeutic targets that remove barriers to OPC differentiation must be created to allow this process to occur. Currently, several barriers have been identified that delay remyelination, and removing these barriers is an ideal way to promote OPC differentiation.

1.5 Ageing and Myelin Debris inhibit remyelination

In MS lesions, OPCs fail to remyelinate due to defective recruitment of OPCs and impaired OPC differentiation. In some MS patients, antibodies to NG2 cause OPC depletion, leading to chronic lesions due to defective recruitment (Mason et al., 2004; Niehaus et al., 2000). However, the major delay in remyelination failure results from reduced OPC differentiation (Franklin, 2002; Franklin and Ffrench-Constant, 2008; Kuhlmann et al., 2008). Many studies have suggested several factors that are involved in reduced OPC differentiation, from intrinsic factors in OPCs to extrinsic factors in the demyelinated lesion (Fig 1.5). Within OPCs, some pathways have been identified that prevent maturation. Activation of the Wnt signalling pathway inhibits developmental myelination and remyelination (Fancy et al., 2009). In addition, shuttling of the transcription factor Olig1 to the nucleus of OPCs is imperative for effective differentiation (Arnett et al., 2004).

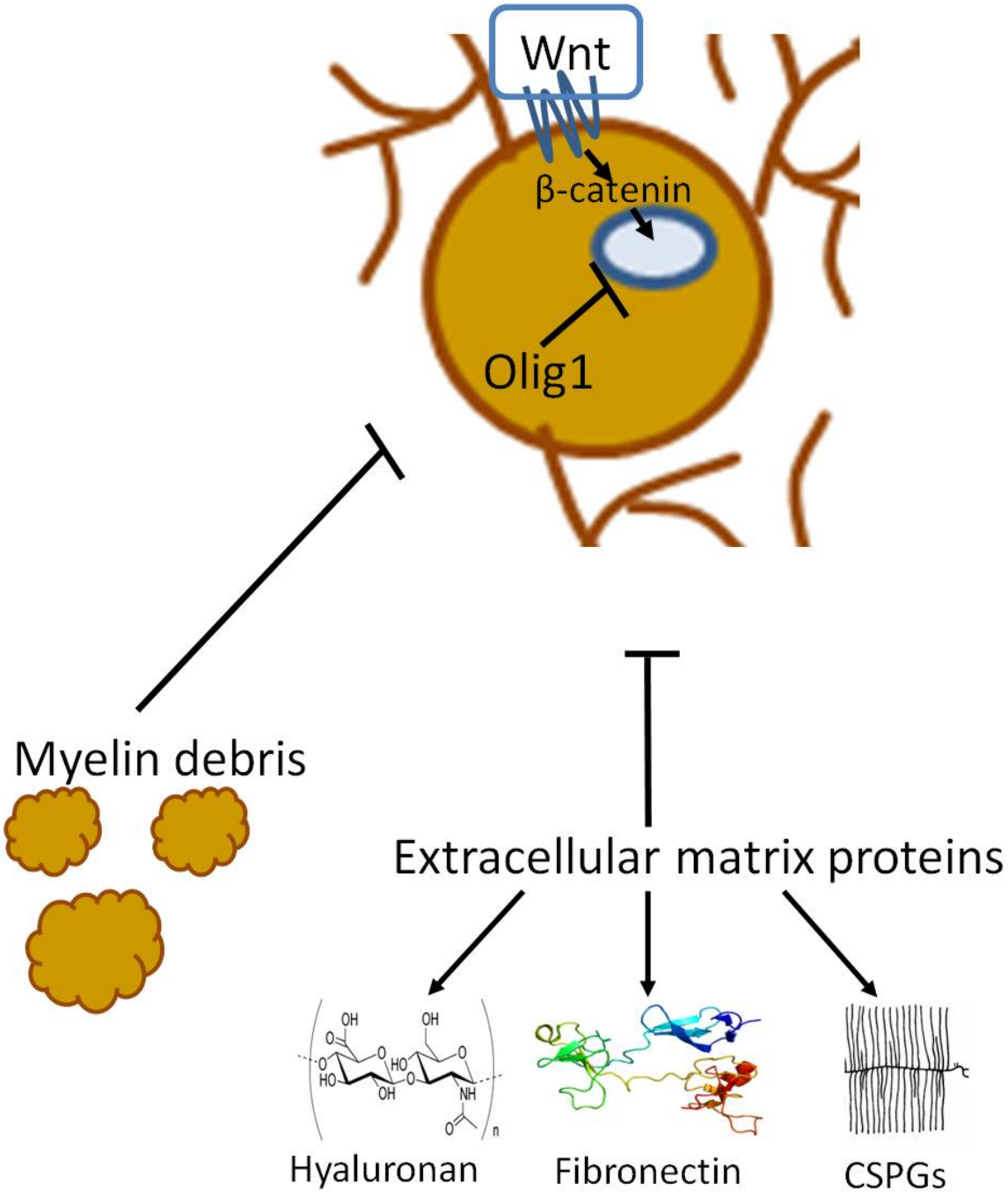

Figure 1.5: Intrinsic and extrinsic factors prevent OPC differentiation. Several factors have been identified that prevent OPC maturation to myelinating oligodendrocytes. Intrinsic factors include Wnt activation of the β-catenin and Tcf4 pathway and prevention of shuttling of Olig1 to the nucleus of the OPC. In addition, several environmental factors have also been identified that directly inhibit OPC differentiation. Accumulation of myelin debris and extracellular matrix proteins, such as hyaluronan, fibronectin, and chondroitin sulfate proteoglycans (CSPGs), also inhibit remyelination.

1.5.2 Ageing

As with many other cellular processes, a major inhibitor of remyelination is ageing. There is an obvious age-dependent pattern of reduced remyelination in animal models (Franklin and Kotter, 2008). The aged rodent CNS has an abundance of OPCs (Rivers et al., 2008; Sim et al., 2002), which are efficient at repopulating various regions of the CNS in the face of recurrent demyelination (Penderis et al., 2003). Remyelination is regulated by age-dependent epigenetic control in OPCs. Downregulation of HDACs in aged OPCs results in reduced differentiation and reduced remyelination in ageing animals (Shen et al., 2008). The protein klotho, which declines with age in the CNS, enhances OPC differentiation via activation of the Akt pathway in cuprizone-induced demyelination (Chen et al., 2013). Aged OPCs are also less responsive after toxin-induced demyelination, showing reduced expression of late myelin markers such as MBP (Sim et al., 2000). As animals grew older, they experienced a decline in both recruitment and differentiation of OPCs
(Sim et al., 2002). Demyelinated lesions are fully remyelinated in young rats by one month post lesion, while aged rates do not fully remyelinate until two months post lesion (Shields et al., 1999). In animal models, remyelination is delayed and the rate of remyelination is compromised in the aged CNS, but it can still proceed to completion with time.

However, ageing has also proven to be a significant, persistent barrier to remyelination in progressive MS. In humans, both cognitive ability and white matter volume decline with age (Bartzokis et al., 2001; Bartzokis et al., 2010; Mabbott et al., 2006). During the clinical course of MS, ageing results in accumulated disabilities (Scalfari et al., 2011). Age is a greater determinant of disability milestones in MS than number/presence of preceding MS attacks (Confavreux and Vukusic, 2006), suggesting that age-associated defects in tissue repair, including remyelination, may be the driving force behind accumulation of progressive disability. Older patients tend to have more physical limitations than younger, irrespective of disease duration (DiLorenzo et al., 2004). As patients age, OPCs become less effective at remyelination and the number of shadow plaques is reduced (Suzuki et al., 1969). OPCs remain abundant in these lesions (Chang et al., 2002; Kuhlmann et al., 2008; Wolswijk, 1998), further suggesting impairment in differentiation and not recruitment. OPC differentiation is also largely inhibited by extrinsic factors.

1.5.3 Myelin debris

Many extrinsic factors can also inhibit OPC differentiation. Fibronectin was recently shown to aggregate in demyelinated lesions and impair remyelination in EAE mice (Stoffels et al., 2013). PSA-NCAM is produced by axons as a negative regulator of remyelination and was present in demyelinated MS lesions as compared to remyelinated shadow plaques (Charles et al., 2002). Hyaluronan, a glycosaminoglycan, accumulates in demyelinated MS lesions and mice with EAE, and OPC cultures do not mature in the presence of this protein (Back et al., 2005). Another glycosaminoglycan, chondroitin sulfate proteoglycan, also accumulates in MS lesions and prevents OPC differentiation *in vitro* and *in vivo* (Lau et al., 2012) (Fig. 1.5).

One major external barrier to remyelination is the presence of myelin debris. Primary demyelination produces large amounts of debris as myelin sheaths degrade (Franklin, 2002). Upon demyelination of the CNS, degenerating oligodendrocytes form debris around denuded axons. This debris can create a dense matrix that may present a physical barrier to the demyelinated axon. Previous studies have shown that myelin debris does not affect the number of OPCs recruited to the lesion site; however, differentiation of OPCs into myelinating oligodendrocytes is impaired by the extracellular accumulation of debris (Franklin and Kotter, 2008; Kuhlmann et al., 2008). Cultured OPCs plated onto CNS myelin substrates and myelin protein extracts *in vitro* were unable to effectively differentiate (Baer et al., 2009; Robinson and Miller, 1999). Increased intracellular calcium in the OPC in response to myelin also leads to decreased process motility and collapse of the oligodendrocyte structural formation on contact with myelin (Moorman and Hume, 1994). Observations in animal models of focal demyelination reveal an association between myelin debris removal and effective OPC differentiation and rapid remyelination (Fancy et al., 2010). Injection of excess myelin debris into demyelinated lesion sites further confirmed impairment of rapid CNS remyelination by degenerated myelin (Kotter et al., 2006).

Myelin debris is a major cause of impaired OPC maturation through the expression and release of molecules that inhibit differentiation (Fig. 1.6). This impairment is mainly due to interactions between the protein extracts from myelin

and OPCs, not the lipids or salts present in the debris (Syed et al., 2008). More than 100 proteins were identified in these myelin extracts, including MAG, MBP, PLP, and MOG; however, the current datasets only reveal a list of potential candidates that cause the inhibitory effects of myelin debris (Baer et al., 2009). Although the specific inhibitory proteins have not yet been identified, differentiation pathways that the debris targets and soluble factors released by debris have been studied. One of the proteins released by degraded myelin is Semaphorin3A (Sema3A), a molecular guidance cue. Semaphorins play a role in diverting OPC processes through negative guidance cues, and Sema3A is specifically upregulated in active demyelinating lesions of MS patients. Sema3A also prevents OPC differentiation *in vitro* in OPC cultures and *in vivo* in animal models of demyelination. Artificially increasing Sema3A in demyelinated lesions leads to more demyelination and further induces failure of remyelination (Syed et al., 2011). Several signalling processes activated by myelin debris proteins also result in a similar failure of remyelination. Protein kinase C (PKC) signalling is involved in translocation of myristoylated alanine-rich C-kinase substrate (MARCKS) from the OPC membrane to the cytosol, which is known to regulate differentiation. In differentiating OPCs, MARCKS is present in the cell membrane, and in OPC inhibition, it is localised to the cytosol (Baron et al., 1999). Myelin protein extracts activate PKC signalling, thereby promoting MARCKS translocation to the cytosol and impairing OPC differentiation.

Fyn-1 is an Src family tyrosine kinase, and activation of this molecule is one of the earliest events triggered in OPC differentiation. This receptor regulates process extension of OPCs to form myelin sheaths, and myelin debris inhibits phosphorylation and activation of this kinase. Impairment of Fyn-1 allows for activation of RhoA, an important negative regulator of oligodendrocyte differentiation. RhoA activates Rho-associated, coiled-coil containing protein kinase 2 (ROCKII) which leads to actin depolymerization and prevents OPC process extensions from expanding and forming new myelin sheaths (Baer et al., 2009). Effective removal of myelin debris to prevent activation of PKC, Sema3A, and RhoA/ROCKII signalling will improve OPC differentiation and enhance effective remyelination.

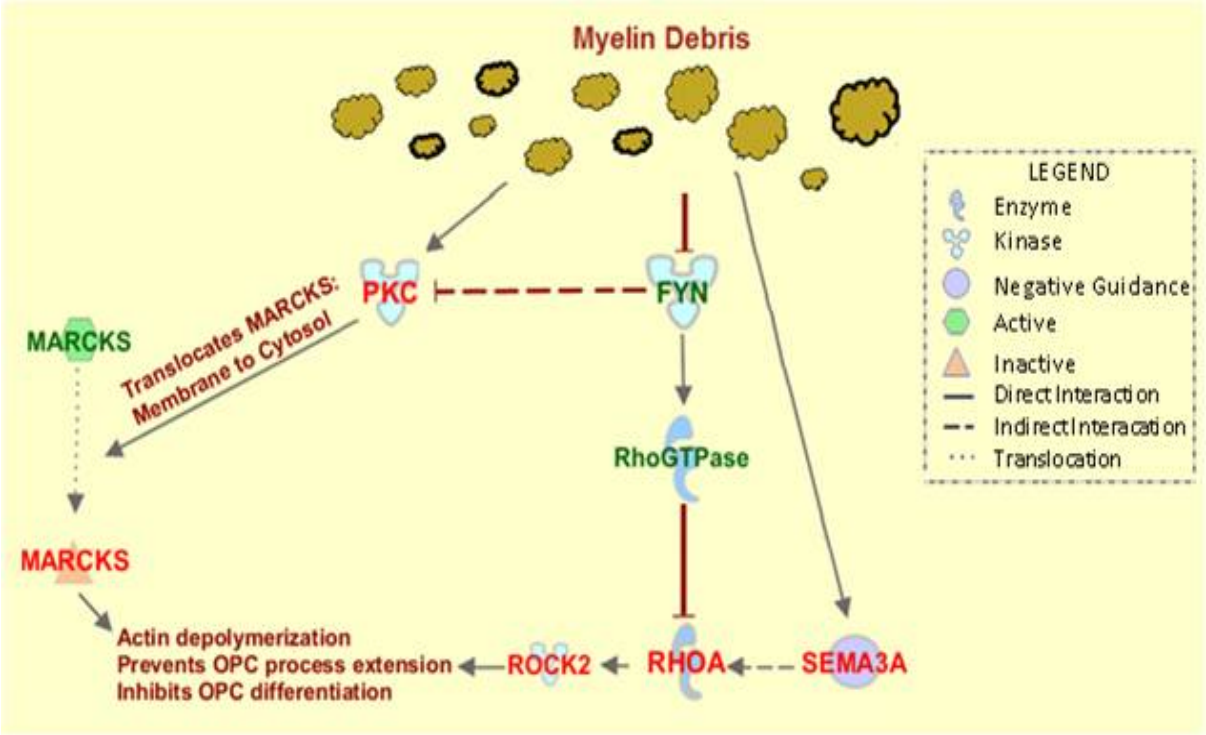

Figure 1.6: Myelin debris prevents OPC differentiation via Sema3A, RhoA, and PKC pathways. The inhibitory effects of degraded myelin on remyelination regulate several pathways in OPCs. Fyn-1 is a positive regulator of OPC differentiation and prevents RhoA phosphorylation by activating Rho-GTPases (O'Meara et al., 2011). When Fyn-1 is dysregulated in the presence of myelin debris, RhoA-GTP activates ROCK2, resulting in actin depolymerization and inhibited remyelination. PKC is also activated when Fyn-1 is dysregulated, and it prevents OPC differentiation by translocating the MARCKS protein from the plasma membrane, where it is active during OPC differentiation, to the cytosol, where it is inactive during OPC quiescence. PKC has also been shown to play a role in RhoA activation. Finally, the negative guidance cue Sema3A has been shown to impair OPC differentiation and remyelination, possibly through activating the RhoA pathway. Myelin debris activates and releases these negative regulators of OPC differentiation to prevent remyelination. *Green text = Activates OPC differentiation. Red text = Inhibits OPC differentiation.*

1.6 Beneficial Role of Monocyte-derived Macrophages and Microglia in Remyelination

The healthy brain is largely depleted of adaptive immune cells, with T-cells predominating in the CSF. However, cells with innate immune functions are present in the CNS at all times, primarily astrocytes and microglia, but also a minority of

monocytes are settled in the meninges and perivascular spaces of parenchyma capillaries and arteries (Ransohoff and Engelhardt, 2012). As the brain is relatively immune-privileged, antigen presenting cells (APCs) have limited capacity to present antigens (Ransohoff and Cardona, 2010). However, adaptive immune cells can enter the CNS by trafficking across the BBB to the CNS allowing for some activation of innate immune cells in both the healthy brain and when the BBB has been compromised due to disease or injury (Ransohoff and Engelhardt, 2012).

Macrophages and microglia have many roles as APCs of the CNS, including monitoring the tissue environment for pathogens, maintaining homeostasis, and phagocytosing dead cells (Diemel et al., 1998; Giulian et al., 1989; Rawji and Yong, 2013). Although macrophages and microglia are both myeloid cells, they are derived from different origins and maintain unique markers within the CNS. Microglia are derived from the yolk sac during early development and reside in the CNS through adulthood, whereas blood-derived monocytes are differentiated from bone marrow cells and are usually recruited to the CNS in response to an insult (Ginhoux et al., 2010; Neumann et al., 2009; Ousman and Kubes, 2012).

1.6.1 Microglia

Microglia are the resident macrophages of the CNS and constitute approximately 15% of CNS cells (Lawson et al., 1992). They mediate innate immune responses in this system and originate during early development. These cells express many toll-like receptors to recognise pathogens and protect the brain and spinal cord (van Noort and Bsibsi, 2009). Microglia can display other innate immunity via these receptors; they also help maintain homeostasis independent of this immune activity. In contrast to blood-derived macrophages, microglia express low levels of CD45 and do not express the C-C chemokine receptor 2 (CCR2), which is targeted in monocyte recruitment. Also, circulating monocytes are short-lived, while microglia can self-renew and are long-lived (Perry et al., 2010). Due to this, they are extremely malleable cells and can rapidly change their function and phenotype.

Based on their environment, microglia can display different morphologies and functions. In their resting state of the healthy CNS, microglia display a ramified morphology, with small soma and fine cellular processes (Streit et al., 1988; Vinet et al., 2012). These microglia elongate and retract their processes to monitor their

surrounding environment (Nimmerjahn et al., 2005). They have also been known to promote the survival and maturation of developing OPCs (Nicholas et al., 2001). They contribute to myelin turnover through macropinocytosis of exosomes from OLs (Fitzner et al., 2011). Due to infection, trauma, disease, etc., a profound change occurs in microglial phenotype. During this activation, microglia become less complex than the ramified state and take on a more amoeboid phenotype. They are able to become more active and move to lesion sites in this activated state (Haynes et al., 2006; Stence et al., 2001). They may proliferate in response to the diseased state as well. They can also phagocytose tissue debris, damaged cells, and pathogens in their activated state as well as upregulate TLRs, MCHII, and CD68 (Beyer et al., 2000; Kettenmann et al., 2011; Olson and Miller, 2004).

Although neuroinflammation has traditionally been considered a pathogenic driver of MS (Lassmann, 2007; Nataf, 2009), it has more recently been associated with myelination and remyelination as well (Foote and Blakemore, 2005; Setzu et al., 2006). Using a cuprizone model, one study was able to distinguish the effects of microglia and monocytes in remyelination. They found that activation of microglia supported remyelination through the activation of MHCII with effective phagocytosis of myelin debris (Olah et al., 2012). A more recent study of microglia in the EAE model also suggested microglia are more involved with debris clearance early in the demyelination process and express several receptors associated with MS tissue sections, including CCR7 and CD40 (Yamasaki et al., 2014). Through the use of CX3CR1 labelling to identify microglia, the authors were also able to show that microglia act earlier in debris clearance. However, at later stages of EAE progression, during remyelination, both cell types are indistinguishable and both act in myelin debris phagocytosis and neuroinflammation.

1.6.2 Monocyte-derived macrophages and remyelination

Although microglia and monocyte-derived macrophages are difficult to distinguish once they are activated, studies have suggested that monocyte-derived cells play the pivotal role in myelin debris clearance and CNS remyelination (Kotter et al., 2005; Ruckh et al., 2012), but both cell types are able to phagocytose debris (Neumann et al., 2009; Olah et al., 2012; Yamasaki et al., 2014). Monocytes and macrophages can enhance remyelination through the release of protective cytokines

and growth factors in response to demyelination. Macrophages have been shown to release growth factors that specifically promote OPC differentiation thereby stimulating recovery (Table 1.2). In a study looking for growth factors upregulated during remyelination, insulin-like growth factor 1 (IGF-1) and transforming growth factor β (TGFβ) were both released by myelin-phagocytosing macrophages and had been shown to enhance OPC differentiation in culture. The release of IGF-1 by M2 microglia *in vitro* exerts beneficial effects on neural progenitor cells and encourages oligodendrogenesis (Butovsky et al., 2006). Both growth factors become more abundant after monocyte-derived macrophage infiltration rather than astrocyte or microglia activation, indicating that they are primarily produced by blood-derived phagocytes. IGF-1 and TGFβ exhibit increased expression in a similar temporal pattern as new myelin sheaths are formed, so they seem to share a similar function in OPC maturation (Hinks and Franklin, 1999). These growth factors also show lowered peak expression in aged animals and are associated with delayed remyelination, indicating their expression is importation for effective recovery (Hinks and Franklin, 2000).

Leukemia inhibitory factor (LIF) is released by macrophages as a member of the interleukin (IL)-6 family and is known to be a neuropoietic cytokine that encourages OPC differentiation both *in vitro* and *in vivo* (Deverman and Patterson, 2012). When LIF binds to receptor complexes on macrophages, it activates phosphatidylinositol-3-kinase (PI3K) pathways known to activate myelin debris phagocytosis and has been shown to stimulate phagocytosis in models of demyelination and remyelination. Release of LIF inhibits production of reactive oxygen species (ROS) and stimulates proliferation and differentiation of OPCs through the activation of the gp130 receptor (Hendriks et al., 2008). Another secretory peptide released by macrophages is endothelin 2 (ET-2). ET-2 is a cytokine and growth factor that regulates chemotaxis and activation of macrophages and affects their inflammatory capacity. In cerebellar slice cultures, ET-2 was released by macrophages in demyelinated environments and promoted remyelination. The receptor for ET-2, endothelin receptor B, responds to this release and is expressed on oligodendrocytes during remyelination. Blocking ET-2 activity by using an antagonist for this receptor inhibited OPC maturation, indicating that ET-2 release is necessary for efficient remyelination (Yuen et al., 2013). The cysteine protease inhibitor cystatin F is activated during acute demyelination and stays active

in remyelinating areas. Cystatin F is expressed by macrophages and microglia, and myelin debris phagocytosis induces its release. This induction is specific to the phagocytosis of myelin debris and results in the overexpression of cystatin F specifically in remyelinating areas, indicating that its expression in phagocytes may play a unique role in OPC differentiation (Ma et al., 2011).

In addition to growth factors and cytokines, macrophages can also regulate other molecules that encourage OPC differentiation. Iron is required for the proliferation and maturation of cells due to its role in DNA synthesis and oxidative metabolism. Regulation of iron content is also specifically involved in oligodendrogenesis and is necessary for OPC differentiation and remyelination (Schulz et al., 2012). Ferritin, an effective iron storage component, is present in activated macrophages and allows them to colocalise with areas of cell genesis in a dose-dependent manner. Ferritin can sequester thousands or iron atoms and functions to oxidise the more toxic Fe^{2+} to the less reactive Fe^{3+}. Since iron is a pro-oxidant and oxidation causes cell cycle arrest, the release of iron from macrophages can help enhance OPC differentiation. M2 myelin-phagocytosing macrophages release iron after myelin debris phagocytosis and are the main source of iron for OPCs. Excess ferritin can also negatively regulate OPC differentiation, but when iron is released by macrophages at the appropriate timepoint after demyelination, it improves OPC maturation and helps replace lost oligodendrocytes (Mehta et al., 2013; Schonberg et al., 2012). By enhancing OPC differentiation, all of these trophic factors can encourage recovery in demyelinating disorders and confirm the beneficial effects of macrophages in remyelination.

Released factor	Mechanisms causing OPC differentiation	Reference
IGF-1 (Insulin-like Growth Factor 1)	Binds IGF1R to enhance both 2'-3' cyclic nucleotide 3'-phosphohydrolase (CNP) and myelin basic protein (MBP) expression	(Mozell and McMorris, 1991)
TGFβ (Transforming GF β)	Downregulates PDGF and FGF, both of which promote OPC proliferation and precursor cell state, thereby promoting maturation	(McKinnon et al., 1993a; McKinnon et al., 1993b)
LIF (Leukaemia inhibitory factor)	Limits ROS production; Activates gp130 on OPCs	(Hendriks et al., 2008)
ET-2 (Endothelin 2)	Activates Endothelin Receptor A & B on OPCs, which mediate ERK and CREB phosphorylation and transcription of mature oligodendrocyte genes	(Gadea et al., 2009; Yuen et al., 2013)
Iron/Ferritin	Acts in oxidative metabolism to cause cell cycle arrest in OPCs and promote maturation	(Todorich et al., 2008)

Table 1.2: Factors released by myelin-phagocytosing macrophages and microglia that promote OPC differentiation and remyelination. Both growth factors and other trophic molecules promote remyelination by activating receptors and downstream pathways involved in OPC differentiation. Several studies have shown that monocytes and macrophages are primary sources of these molecules.

1.7 Ageing reduces phagocytosis of myelin debris

CNS remyelination occurs more rapidly in young animals partly due to extrinsic factors such as the macrophage response, so it is important to consider the effects of age on these cells (Hinks and Franklin, 2000; Sim et al., 2002). Ageing has a profound impact on the immune system, and several studies have shown significant changes in the gene expression profiles of innate immune cells as they age (Lloberas and Celada, 2002; Stout and Suttles, 2005). Recruited monocytes and macrophages display impaired phagocytic function in respiratory disorders, and wound-healing macrophages show a considerable reduction in phagocytosis of cell

debris in response to age. The tissue remodelling and repair function of macrophages declines through decreased release of growth factors and impaired cytoskeletal rearrangement in these models (Ashcroft et al., 1997; Mancuso et al., 2001; Swift et al., 2001). Human monocytes are also altered with age, and these age-related changes include impaired phagocytosis, shortened telomeres, and weakened anti-inflammatory functions (Hearps et al., 2012). Similar to other systems, the macrophage response to demyelination declines with age (Hinks and Franklin, 2000). Lesions in old animals contain more myelin debris, while lesions in young animals contain less debris and more remyelinated axons (Ruckh et al., 2012; Shields et al., 1999). There is a delay in both the recruitment and proliferation of monocyte-derived macrophages in aged animals; there was also an increase in expression of various pro-inflammatory cytokines, including tumour necrosis factor (TNF) α, IL1β, IL6, IL12, and IL23. These pro-inflammatory macrophages contribute to the decline in remyelination of aged animals (Shields et al., 1999; Zhao et al., 2006).

Monocytes and blood-derived macrophages appear to be the key regulators in the age-related decline in remyelination. By connecting the circulatory systems of young and aged animals, a model called heterochronic parabiosis, aged mice were exposed to the systemic milieu of young mice. Young mice were GFP+, so Ruckh, et al. were able to distinguish the young cells recruited to the demyelinated lesions in the aged partner. These cells proved to be blood-derived monocytes; impairing recruitment of young monocytes to demyelinated lesions prevented effective remyelination. Conversely, recruitment of young monocytes improved remyelination in this model. In addition, there was significantly more myelin debris in the lesions of old animals compared to that of young animals, indicating the efficiency of myelin debris clearance is impaired with age. However, when myelin debris clearance in old mice is accelerated with monocytes from young mice, there is a significant decrease in fractionated myelin and a considerable increase in remyelination (Ruckh et al., 2012). This study proved that in CNS biology, signals from the systemic environment, such as those from young macrophages, are able to override age-related deficits in myelin debris phagocytosis and CNS remyelination (Fig 1.7).

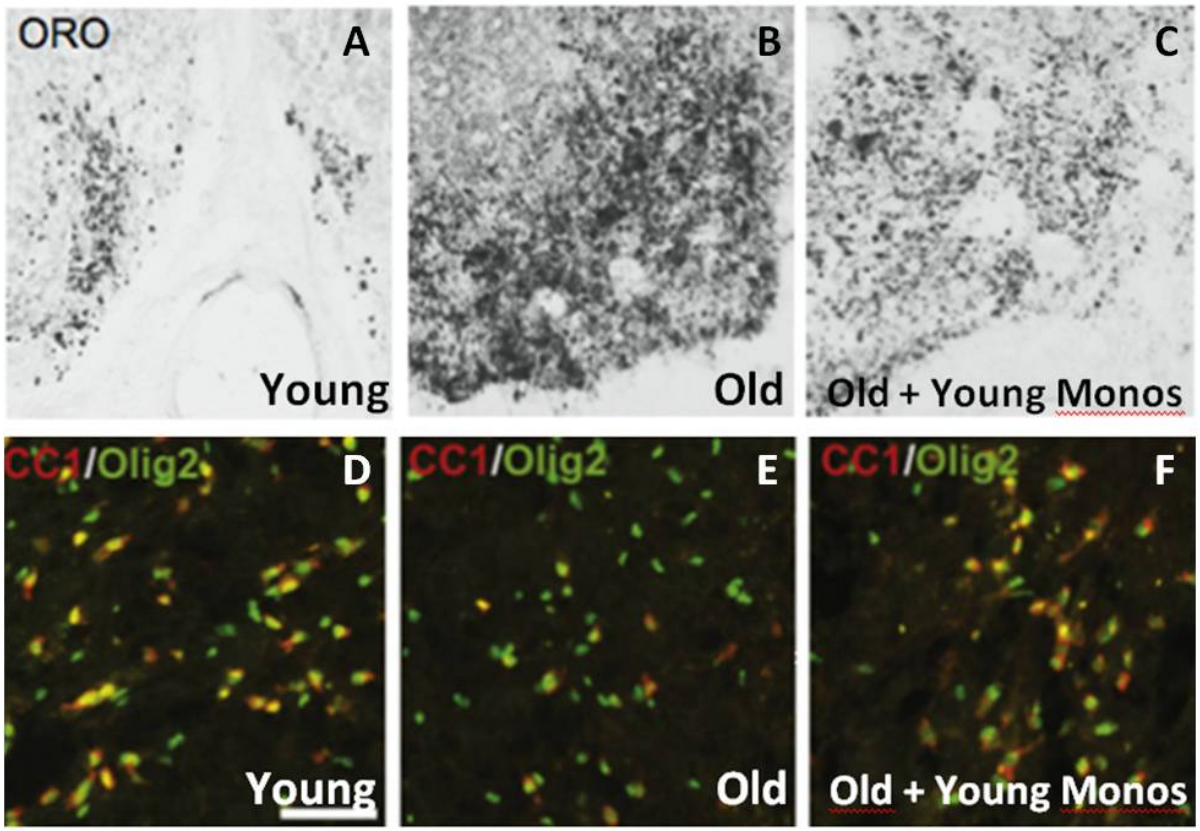

Figure 1.7: Efficient myelin debris clearance and the recruitment of young monocytes restore remyelination in aged animals. Aged mice experience impaired remyelination and reduced myelin debris phagocytosis compared to their young counterparts. One of the key differences between young and old demyelinated lesions is the efficiency of circulating monocytes to promote remyelination in young animals. A-C) Oil red O staining in lysolecithin-induced focal demyelination reveals myelin debris in the lesion. There is significantly less inhibitory myelin debris in the lesions of young animals (A) and old animals exposed to young monocytes (C) as compared to old animals (B). D-F) CC1, a mature oligodendrocyte marker, and Olig2, a pan-OPC and oligodendrocyte marker, were used to measure efficient differentiation of OPCs. Young animals (D) and old animals exposed to a young systemic milieu (F) expressed significantly more CC1+/Olig2+ mature oligodendrocytes as compared to old animals (E) (Ruckh et al., 2012).

1.7.2 Macrophage Receptors involved in Myelin Debris Clearance

Macrophages act as efficient phagocytes in response to demyelination by removing excess myelin debris. Other cell types, such as astrocytes and Schwann cells, may also be involved in debris clearance, but the major actors in the CNS are macrophages. Phagocytically active macrophages containing myelin degradation

products are present in both animal models of demyelination and in actively demyelinating MS lesions (Shi et al., 2011; Vogel et al., 2013). When macrophages are artificially depleted before inducing demyelination, a greater number of axons remain demyelinated and remyelination is impaired (Kotter et al., 2001). Persistent myelin debris after spinal cord injury is correlated with a decrease in infiltrating monocytes (Imai et al., 2008). Release of chemotactic factors, such as monocyte chemoattractant protein-1 (MCP-1) and gelsolin, is also impaired in the presence of degenerated myelin. Gelsolin is necessary for macrophage motility and actin polymerization, so it has a role in phagocytosis after monocyte recruitment. Gelsolin knockouts experience both impaired recruitment of monocytes and delayed remyelination of the peripheral nervous system due to a decreased macrophage response (Goncalves et al., 2010). Myelin debris phagocytosis by myeloid cells is a vital component of remyelination; therefore, macrophages provide an essential role in enhancing OPC differentiation and recovery.

The mechanisms of myelin phagocytosis are dependent upon expression of multiple receptors and soluble compounds in macrophages, most importantly complement receptor 3 (CR3), Galectin3 (MAC-2), C1q, nuclear receptors, and triggering receptor expressed on myeloid cells (TREM2) (Fig. 1.8). The presence of complement component 3 (C3) on degenerating myelin encourages phagocytosis via CR3 (Carroll, 2009). CR3 is expressed by myelin-phagocytosing, monocyte-derived macrophages and microglia in EAE models. As an integrin composed of two transmembrane subunits, CD11b and CD18, CR3 mediates many cell functions including adhesion, motility, and phagocytosis. After binding to ligands from myelin debris such as C3, CR3 transmits signals across the cell membrane to engage filamentous actin, resulting in actin rearrangement and phagocytic activity (Reichert et al., 2001). Expression of this receptor has proven to be essential in myelin debris removal via PI3K-dependent phagocytosis (Lutz and Correll, 2003). PI3K is also controlled by the MAC-2 pathway. Galectins are a family of β-galactosidases binding lectins, with MAC-2 perpetually expressed in macrophages and microglia that phagocytose myelin. When conditioned media from MAC-2 expressing microglia is added to OPC cultures, it promotes oligodendrocyte differentiation in culture (Pasquini et al., 2011). MAC-2 regulates scavenger receptor II and Fcγ receptors, which are both involved in myelin phagocytosis, and stabilises Ras GTPases, which phosphorylate PI3K. When PI3K pathways are enhanced, actin polymerization and

myelin debris phagocytosis are also enhanced (Rotshenker et al., 2008). Another component of the complement system, C1q, is importantly linked to phagocytosis mechanisms and is upregulated after myelin phagocytosis. Macrophages release C1q and then bind and opsonise apoptotic cells to signal phagocytosis (Bogie et al., 2012; Nauta et al., 2003).

Modulating expression of TREM2 also enhances myelin debris clearance. TREM2 is a receptor belonging to the Ig superfamily and serves to induce cytoskeletal reorganization, augment phagocytosis, and reduce TNF-α and nitric oxide synthase production in monocytes, macrophages, and microglia. Blocking TREM2 results in exacerbation of demyelination in EAE mice by removing the protective functions of macrophages, such as the control of local inflammation and clearance of debris (Piccio et al., 2007). Enhancing TREM2 function in EAE limits tissue destruction and allows macrophages to maintain CNS homeostasis after demyelination. These TREM2 enhanced macrophages also maintain an anti-inflammatory cytokine profile, further proving their regulatory and regenerative capacity (Neumann et al., 2009; Takahashi et al., 2007). These receptors and proteins specifically expressed in myeloid-derived cells respond to myelin debris signals and show the particular role of macrophages and microglia in the phagocytosis of degraded myelin.

Macrophages also upregulate many members of the nuclear receptor subfamily in response to phagocytosis. Liver X receptors (LXRs), peroxisome-proliferator activated receptors (PPARs), and retinoid X receptors (RXRs) are members of the nuclear receptor family. LXRs are activated by oxysterols and lipoproteins such as those in myelin fragments, and their downstream genes have been linked to immunoregulatory functions in monocytes and macrophages. PPARs have been shown to ameliorate symptoms in mouse models of MS, and they also regulate anti-inflammatory gene function in macrophages. RXRs form a heterodimer with both of these receptors to enhance their functions. Upregulated gene expression of these receptors is seen in myelin-phagocytosing macrophages, resulting in suppressed inflammation and activated lipid metabolism (Bogie et al., 2013; Bogie et al., 2012).

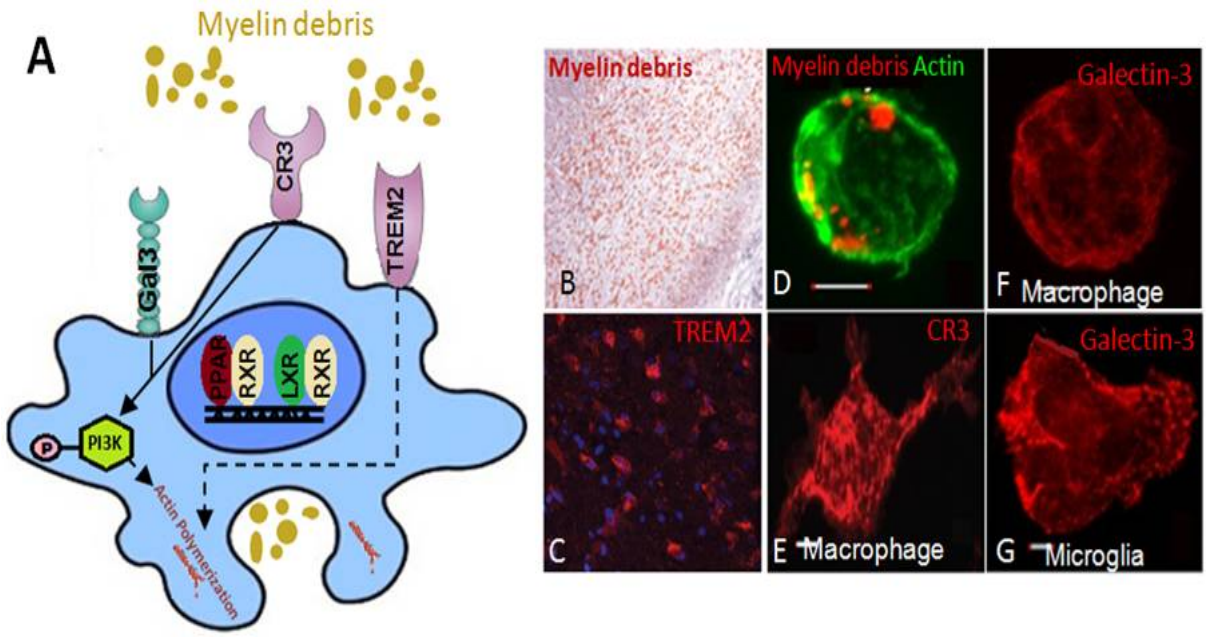

Figure 1.8: Macrophages express unique receptors and compounds that promote myelin debris phagocytosis. Monocytes, macrophages, and microglia are primarily responsible for the removal of inhibitory myelin debris to enhance remyelination. Through signals such as MCP-1 and Gelsolin, these myeloid-derived cells are recruited to the CNS and express membrane receptors, nuclear receptors, and complement components to enhance phagocytosis mechanisms. A) Activation of CR3 and MAC-2 leads to PI3K phosphorylation and phagocytosis. LXR, PPAR, and RXR are activated by lipid-derived ligands and act as transcription factors to enhance phagocytosis and immunoregulation. TREM2 pathways activate cytoskeletal rearrangement and response to apoptotic cells which results in effective myelin debris clearance. B) Oil Red O stained myelin debris in a demyelinated lesion; C) TREM2 staining of region (B) showing phagocytic TREM2+ macrophages; D) Actin rearrangement during myelin debris phagocytosis by macrophages; E) CR3 activation in (D); F) Galectin-3 activation in (D); G) Galectin-3 activation in myelin-phagocytosing microglia (Adapted from: (Gitik et al., 2011; Hadas et al., 2010; Piccio et al., 2007))

1.7.3 Macrophage polarization

The phagocytosis of cellular debris is considered to be mainly an anti-inflammatory process. Two extreme types of macrophages, known as M1 and M2, have been identified and are classified into distinct categories based on their inflammatory properties such as induction factors, cytokine production, and phagocytosis type. However, macrophages show phenotypic plasticity and may fall

anywhere along this continuum. Cells are also not committed to the M1 and M2 phenotype terminally; rather, these are transient differentiation states in macrophages (Laskin, 2009; Olah et al., 2012). The presence of these two extreme categories has not been shown to be easily distinguished in humans and is likely an *in vitro* paradigm. Specific pathologies may be more associated with one extreme or the other depending on stage of disease and timecourse, but mixed populations of macrophages with different phenotypes often coexist in these states. In addition, among the M1/M2 states, several subcategories exist along the spectrum, resulting in a complex mix of macrophage subtypes and functions (Chinetti-Gbaguidi et al., 2015; Sica and Mantovani, 2012). Nonetheless, this categorization is useful in identifying targets in macrophages that may affect diseased states as it allows for identification of specific stimuli, signalling pathways, and transcription factors within these cells.

The hallmarks of the two major polarization states are discussed here (Fig 1.10). M1 macrophages are classically activated macrophages that express pro-inflammatory cytokines and cell markers while M2 macrophages are alternatively activated macrophages that express anti-inflammatory and immunomodulatory markers. M1 polarization is induced by interferon-γ (IFNγ) and TNFα from Th1 cells and lipopolysaccharide (LPS) released by bacteria. Activation by these three molecules results in a high production of pro-inflammatory mediators and destruction of micro-organisms and tumour cells. M1 macrophages express CD80 and CD86 co-stimulatory molecules as well as chemokine receptor 7 (CCR7), resulting in efficient antigen presentation. They also release TNFα, nitric oxide (NO), IL6, and IL1β in response to stimulation. When macrophages produce NO, they create cytotoxic ROSs and also stimulate the secretion of IL-12, another pro-inflammatory cytokine. These cytokines increase antigen-presenting activity and may assist in perpetuating the autoimmune response (Mikita et al., 2011; Shechter and Schwartz, 2013; Vereyken et al., 2011).

The switch from M1 to M2 macrophages occurs between the OPC recruitment and differentiation stage in the lysolecithin model of remyelination and is central to recovery after demyelination (Miron et al., 2013). M2 macrophages are induced by IL-4, IL-10, IL-13, and lipid mediators from Th2 type inflammation, which are inhibitors of the Th1 response. Their primary functions are scavenging cellular debris and apoptotic cells, remodelling tissues, and expressing anti-inflammatory molecules

(Vereyken et al., 2011). In remyelination, myelin-containing foamy macrophages are characterised as M2 macrophages conferring immunoregulatory functions. These foam cells in MS lesions express anti-inflammatory molecules and lack pro-inflammatory cytokines (Boven et al., 2006). Various surface markers such as CD209 (on microglia), CD23, CD163, CD206, and mannose receptors indicate M2 macrophages, which are known to be better at phagocytosing opsonised particles. They also produce growth factors that assist in tissue remodelling and repair (Laskin, 2009).

M2 cytokines are known to reduce inflammation and have higher angiogenic potential. They express high levels of arginase-1 (Arg-1), an enzyme that competes with inducible nitric oxide synthase (iNOS). iNOS converts L-arginine to NO and exacerbates inflammation, while Arg-1 consumes L-arginine by converting it to ornithine and urea, both noninflammatory molecules. Higher levels of Arg-1 in M2 macrophages are associated with phagocytosis of myelin debris in EAE and contribute to modulating neuroinflammation. The increase in iNOS levels at early and peak stages of the disease is followed by a decrease during recovery and high arginase-1 levels, suggesting that M2 macrophages are important for improvement (Ahn et al., 2012; Durafourt et al., 2012). Arg-1 positive macrophages also express the M2 cytokine activin A, which is a member of the TGFβ family known to be a neuroprotective cytokine expressed in the CNS. Addition of activin A to microglia cultures also reduced NO production and downregulated IL-6 and IL-18, showing its anti-inflammatory characteristics (Sugama et al., 2007; Wilms et al., 2010). Blocking activin A expression inhibits OPC differentiation *in vitro* and is associated with inhibited remyelination *in vivo*, while adding M2-conditioned media containing activin A enhanced OPC differentiation by binding to ACvr2, the activin receptor on OPCs (Miron et al., 2013).

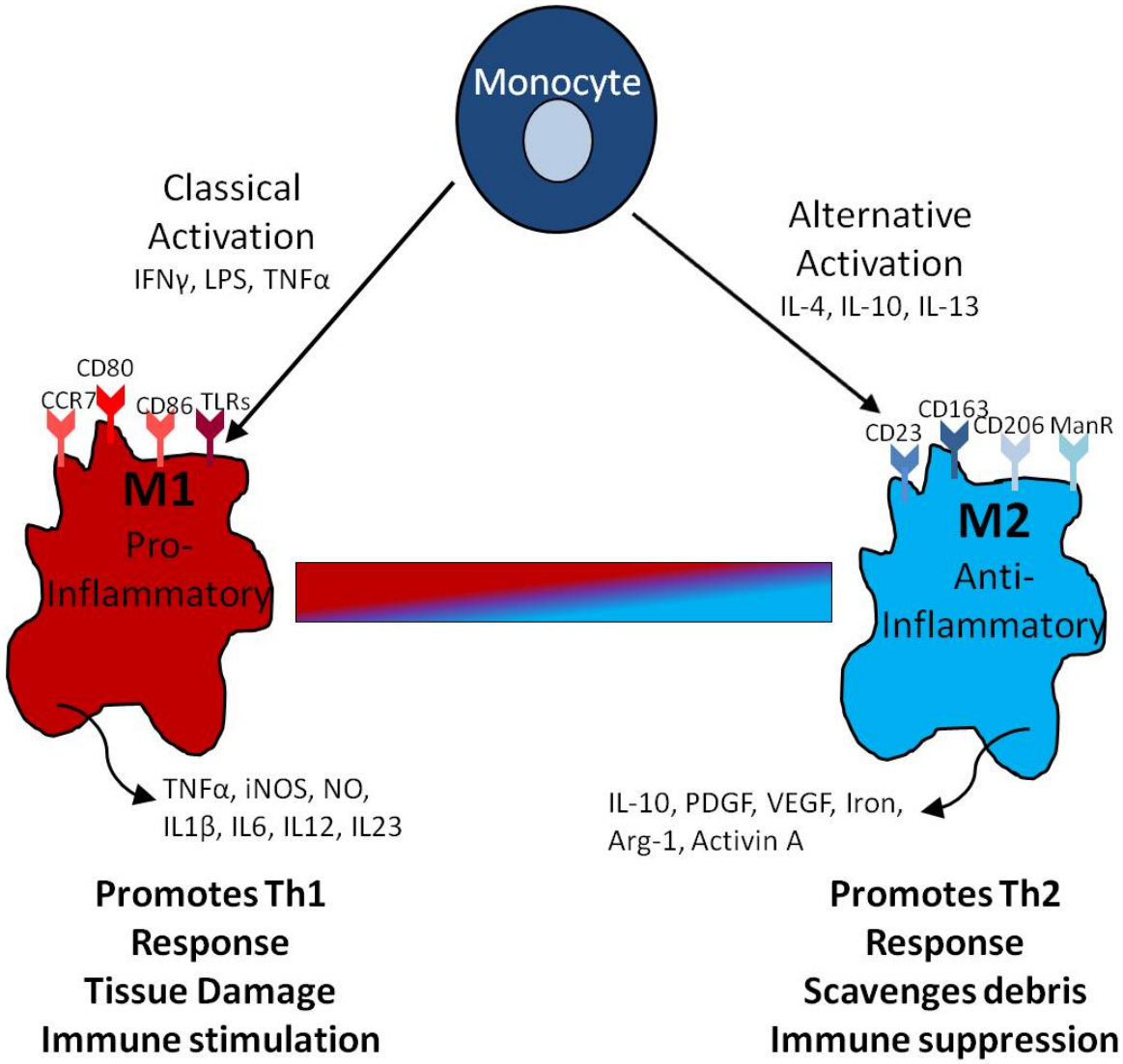

Figure 1.10: Expression profiles of M1 and M2 macrophages. CNS monocytes and microglia can change their expression profiles based on activation cues present in the local environment. The two major subsets are M1 (pro-inflammatory) or M2 (anti-inflammatory) macrophages. M1 macrophages express CD80, CD86, CCR7, and TLRs and release TNFα, iNOS, NO, IL1β, IL6, IL12, and IL23. M2 macrophages maintain an immunoregulatory profile in response to IL4 stimulation, and they express CD23, CD163, CD206, and mannose receptors and release IL10, PDGF, VEGF, iron, Arg-1, and activin A. In response to myelin debris phagocytosis, macrophages have a more M2-like phenotype and can help support tissue repair, suppress the detrimental immune response, and promote CNS remyelination (Adapted from (Laskin, 2009)).

Since the balance of regulating inflammation is pivotal for efficient remyelination (Miron et al., 2013; Vogel et al., 2013; Zhao et al., 2006), the modulation of two monocyte-specific soluble and surface markers, CD14 and CD163, can be used to identify M1 and M2 type monocytes. CD14 is an LPS binding protein and is associated with activating inflammation. It is a co-receptor for LPS along with toll-like receptor 4 (TLR4), and it is expressed on the surface of monocytes with no intracellular domains due to being anchored to the surface of cells by glycosylphophatidylinositol-anchored protein. When LPS binds to the CD14-TLR4 complex, it induces inflammatory pathways and the release of several inflammatory cytokines, including IL-6, CXCL8, and TNFα. Dysregulating CD14 in monocyte cultures results in suppression of IL-10, TNFα, and CXCL8 release (Levy et al., 2009). In addition, CD14 has an important role in LPS-mediated injury (Triantafilou and Triantafilou, 2002).

CD163 has been identified as a primarily immunoregulatory marker. As a member of the class B scavenger receptor cysteine-rich superfamily, it is responsible for endocytosing haemoglobin complexes. CD163 acts as an anti-inflammatory scavenger receptor recognizing free haemoglobin-associated damage and results in secretion of anti-inflammatory cytokines such as IL-10. In addition, CD163 surface expression is increased in response to M2 activation by IL-10 and M-CSF. CD163 is shed from monocytes after proteolytic cleavage due to stimulation by pro-inflammatory LPS or TLR activation. Soluble CD163 (sCD163) is thought to be involved in inflammation resolution as shedding of CD163 occurs in response to inflammatory activation by LPS and results in the release of TNFα (Møller, 2011; Tippett et al., 2011). In MS, proteolytic shedding of CD163 in the plasma of patients results in increased sCD163 levels due to increased matrix metalloproteinase activity in plasma (Davis and Zarev, 2005; Fabriek et al., 2007).

1.8 Summary

OPCs respond to both intrinsic and extrinsic factors to differentiate into oligodendrocytes and remyelinate axons (Franklin and Ffrench-Constant, 2008; Groves et al., 1993). When remyelination fails in clinical disorders, OPC recruitment is often not greatly affected; it is generally due to a failure in the maturation and differentiation of OPCs (Dyall et al., 2010; Fancy et al., 2010; Kuhlmann et al., 2008). There are multiple extrinsic factors involved in the failure of OPC differentiation, including the accumulation of inhibitory myelin debris, age-related decline, and the lack of growth factor signalling in the demyelinated area (Hinks and Franklin, 2000; Kotter et al., 2006; Robinson and Miller, 1999). Myelin debris clearance and growth factor signalling can be the result of an innate immune response performed by monocyte-derived macrophages and resident microglia. Innate immune cells, such as macrophages, play a prominent role in the remyelination process, and discovering a rapid remyelination course is imperative to preventing axonal loss, protecting vulnerable axons, and organizing the neural environment for optimal signal conduction (Franklin and Ffrench-Constant, 2008). The function of innate immune cells in neuroimmunological disorders is currently a complex topic, and determining the best method to harness the beneficial role of phagocytes in remyelination is an important step in identifying the therapeutic capability of these cells.

1.9 Scope of this thesis

Due to the axon-protective properties of myelin, promoting remyelination is a therapeutic goal in demyelinating diseases, specifically for MS, the most prominent demyelinating disorder. The beneficial effects of monocytes and monocyte-derived macrophages in myelin debris clearance and CNS remyelination can be beneficial in remyelination therapies for MS through the peripheral blood system. Ageing has also proven to be a significant barrier in macrophage activity and impairs remyelination.

The overall aim of this project was to address the impact of ageing on myelin debris clearance and CNS remyelination. Using both human and murine model systems, this project allowed for modulation of receptor activation and expression in the genetically controlled mouse system and sought to translate these results to the more heterogeneous human population. Using these tools, four key questions were investigated:

1. What are the intrinsic differences between young and old macrophages that allow young macrophages to clear myelin debris more efficiently?
2. Is myelin debris phagocytosis deficient in ageing human monocytes and those from MS patients?
3. Can aged macrophages be made to behave like young macrophages?
4. What are the therapeutically-modifiable targets in monocytes and macrophages that can create a more youthful state and enhance myelin debris clearance?

Chapter 2. Methods

Materials and Methods:

Animal and Human Models

2. Materials and Methods

Animal Models

2.1 Animals

Female C57Bl/6 mice from Charles River Laboratories were used for *in vitro* cell isolations. All mice used for *in vitro* studies were euthanised by the United Kingdom Home Office Schedule 1 methods using a CO_2 chamber. All experiments were performed under the UK Home Office project licenses issued under the Animals (Scientific Procedures) Act.

2.2 Mouse Bone Marrow Monocyte-Derived Macrophage Cultures (BMMs)

Bone marrow cells were collected from the tibiae and femurs of C57Bl/6 mice by scraping and flushing with a 23-25g needle and 5 ml syringe and using complete RPMI (cRPMI) medium consisting of RPMI 1640 (Invitrogen) supplemented with 15% heat-inactivated foetal bovine serum (FBS, Biosera), 20% L929 fibroblast-conditioned media (to provide macrophage colony stimulating factor, M-CSF), 100 u/ml penicillin, 100 µg/ml streptomycin, 2 mM L-glutamine, 0.05 mM β-mercaptoethanol, and 0.1 mg/ml Na-pyruvate.

For collection of L929 conditioned media, approximately 200,000 L929 fibroblast cells were seeded in 75 cm^2 flasks in 20 ml of: RPMI 1640 supplemented with 10% heat-inactivated FBS. Cells were incubated at 37 °C in a humidified 5% CO_2 atmosphere incubator (used for all further studies) and grown to confluency. Media were discarded, and cells were scraped into 5 ml of pre-warmed media per T-75 flask. Cells from 3 flasks were pooled in a 15 ml conical tube and centrifuged at 250 *g* for 5min. Supernatants were aspirated and cells were resuspended in 20 ml pre-warmed media. The cell suspension was equally distributed to 10 T-175 flasks containing 100 ml L929 media. After ~1 week, the conditioned media of the confluent fibroblasts were harvested and filtered using a 1000 ml, 0.22µm pore Millipore Stericup Filter and aliquoted at 25 ml in 50 ml conical tubes and stored at -20 °C for up to 1 year.

Cell numbers from the bone marrow cells were counted using a haemocytometer, and the cells were seeded in tissue culture plates in fresh cRPMI at $1x10^7$ cells per 100 mm tissue-culture treated dishes (Corning) in 10 ml cRPMI. Cells were incubated at 37 °C in a humidified 5% CO_2 chamber for 3 days, and the non-adherent population was aspirated on Day 3. Media was replaced with 10 ml fresh cRPMI. On Day 7, numerous adherent cells were evident and remaining non-adherent cells were aspirated and removed. BMMs were gently washed with 5 ml warm phosphate buffered saline (PBS) 1X (per dish), and then scraped and collected in 3 ml cRPMI. Each 100 mm dish yielded approximately $7\text{-}10x10^6$ macrophages. Macrophages were pooled into a 15 ml conical tube (BD), and cells were centrifuged for 10min at 200 *g*. Supernatant was aspirated, and cells were resuspended in 3-5 ml cRPMI to count macrophages on the haemocytometer. Cells were plated in cRPMI at a density of $1x10^5$ cells/well in a 24-well plate (for immunocytochemistry analysis) or $7\text{-}10x10^6$ cells/dish in a new 100 mm dish (for Western blots and flow cytometry). After plating overnight, media were changed to Macrophage Serum-free Media 1X (Gibco 12065-074) with 1 ml/well in a 24-well plate and 10 ml/dish in 100 mm dishes. Macrophage isolation procedure is highlighted in Figure 2.1. All agonist, antagonist, and myelin treatments below were performed in serum-free media. The adherent cells were identified with a macrophage surface antigen, CD11b or Iba1 (Primary antibodies in Table 2.1), to confirm that they were bone marrow monocyte-derived macrophages (BMMs).

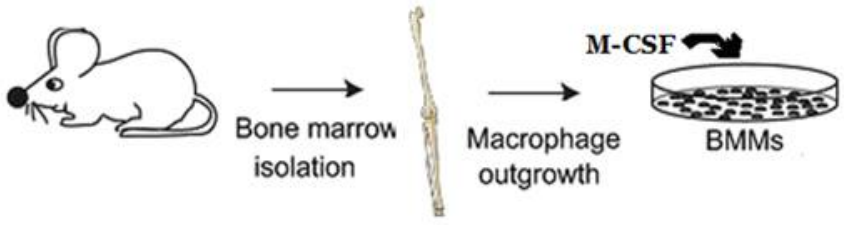

Figure 2.1 Collection of bone marrow from hind limbs. Bone marrow was isolated from femurs and tibiae of C57Bl/6 mice and cultured in media conditioned with M-CSF from L929 media to promote macrophage growth and differentiation from pre-monocytic cells. Cells can then be used to study macrophage activity, including phagocytosis, nuclear receptor expression and modulation, and ageing.

2.3 Myelin Isolation

Whole brains were collected post-mortem from C57Bl/6 mice from age 1-32 mo. Myelin was isolated using a discontinuous sucrose gradient (Norton and Poduslo, 1973) as shown in Figure 2.2. Sucrose was dissolved in sterile-filtered 2.5 mM Tris/HCl, pH 7.0, to form 0.32 M and 0.85 M solutions. The brains were homogenised in ice-cold 0.32 M sucrose (10 ml/brain) using a 40-ml Dounce homogeniser. The homogenate was layered over 10 ml 0.85 M sucrose in 37.5 ml thick-walled Beckman ultracentrifuge tubes and ultracentrifuged at 75,000 *g* for 30 min (Beckman-Coulter). The interface was collected and pelleted in 0.32 M sucrose (75,000 *g*, 30 min). The pellet was resuspended in 40 ml distilled H_2O and washed (75,000 *g*, 20 min) and then osmotically shocked with 40 ml ice-cold distilled H_2O (40,000 *g*, 20 min). After centrifugation, the pellet was washed once more in 40 ml ice-cold H_2O (40,000 *g*, 15 min), and the weight of purified myelin was determined. The protein concentration was determined using a bicinchoninic acid (BCA) Assay Kit (Thermoscientific). BCA works by colourimetric detection of the cuprous cation (Cu^{+1}) chelating with two molecules of BCA, producing a purple-coloured reaction product with absorbance at 562nm. This absorbance is linear with protein concentration from 20-2000 µg/ml. BCA assay revealed that age did not affect protein content in myelin fragments (Fig 2.3). Myelin fractions were resuspended in PBS 1X at 20 mg/ml and stored in 500 µl aliquots at -70 °C. For all experiments, myelin was added to BMMs at 50 µg/ml. For phagocytosis assays, 50 µg/ml fractionated myelin was added to 24-well plates or 100 mm dishes for 8h after agonist/antagonist treatment and before collection.

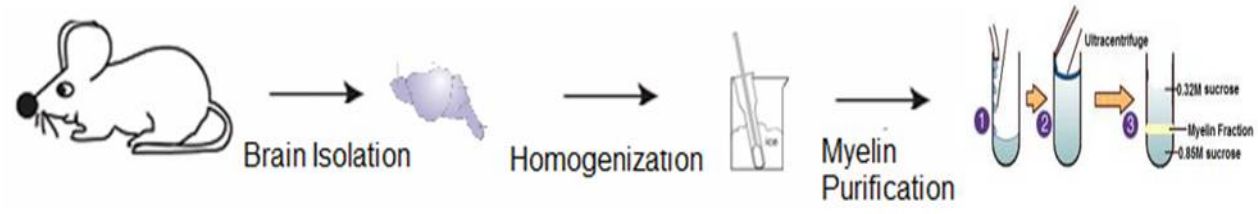

Figure 2.2 Purified myelin fractions. Overview of myelin isolation from whole brain tissue.

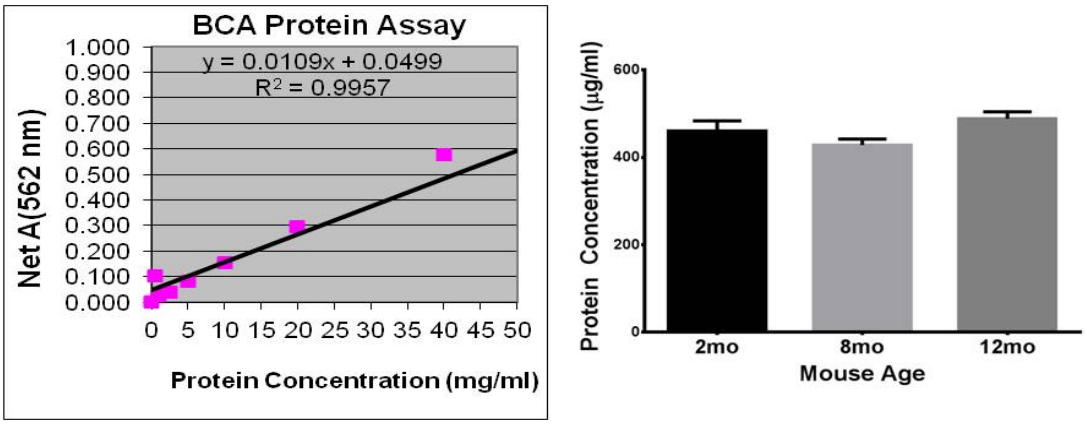

Figure 2.3 Age does not have an effect on protein concentration in isolated myelin. The BCA assay was used to measure protein concentration in myelin fragments. Myelin fragments from the brains of mice aged 2mo, 8mo, and 12mo were compared. One-way ANOVA, post-hoc t-test, n=3/age group.

2.4 Peritoneal Macrophages and Microglia Cultures

Experiments performed by Eimear Linehan at the University of Belfast.

Peritoneal macrophages were harvested by peritoneal lavage with 10ml of cold PBS 1X. Peritoneal macrophages were plated in Dulbecco's Modified Eagle Medium (DMEM, Invitrogen) supplemented with FBS (10%), l-glutamine (2mM) and penicillin/ streptomycin (100U/ml). For Microglia, a cell suspension from CNS tissue of C57Bl/6 mice was prepared using a Neural Tissue Dissociation Kit (Miltenyi). Myelin debris was removed using Myelin Removal Beads II (Miltenyi). Microglia were then isolated using anti-CD11b MicroBeads (Miltenyi). Peritoneal macrophages and microglia were seeded on chamber slides ($7x10^4$/well) for immunocytochemistry or in 96-well plates for flow cytometry. Fluorescently-labelled myelin debris (10 µg/ml protein) was added for 2h. Cells for flow cytometry were incubated with anti-CD16 and anti-CD32 to block Fc receptors, stained with anti-CD11b and anti-CD45 (eBioscience) and fixed with Medium A (Invitrogen) prior to acquisition on BDFACSCantoII. Chamber slides were fixed with 4% paraformaldehyde (PFA) then washed and blocked with 10% normal goat serum (NGS, Sigma). Cells were stained with CD11b-APC (eBioscience), washed and stained with DAPI. Finally, slides were washed, mounted and visualised with a Leica DM5500 microscope using a Leica DFC340 FX camera. Objectives: 40X HCX PL APO 0.85 Corr, 100X HCX PL 1.40-0.7 Oil and quantified using ImageJ software.

2.5 Immunocytochemistry of BMMs

BMMs were fixed in 4% PFA for 10 min and washed twice with PBS 1X. Before staining, the coverslips were blocked in 5% NGS with 0.1% Triton-X-100 (Sigma) for 1h at room temperature (RT). Then the coverslips were incubated with primary antibodies (Table 2.1) diluted in blocking solution for 1h at RT. After washing 3x10min with PBS 1X, secondary antibodies diluted in blocking solution were applied for 1h RT (Table 2.2). After the incubation, coverslips were washed 3x10min and cell nuclei were stained 5min RT with Hoechst (Sigma), 10mg/ml diluted 1:5000 in PBS 1X. Coverslips were washed 2x10min with PBS and mounted with Fluoromount G (Southern Biotech) onto polysine slides and dried overnight. Quantification was performed by obtaining pictures of five randomly chosen areas of the 13mm coverslip with a 20X objective using Zeiss Axiovision Observer A1 fluorescence microscope. Using ImageJ software and the cell counter plug-in, the number of cells positive for Iba1 (macrophage marker), Retinoid X Receptor (RXR) α, RXRγ and/or MBP (myelin basic protein) (Table 2.1) were determined and used to visualise intracellular, phagocytosed myelin.

2.6 Western Blots

BMMs treated and not treated with myelin from ages 1-24mo were lysed with 10% sucrose with Halt protease and phosphatase inhibitor cocktail 1:100 (ThermoScientific) and homogenised by pipetting. The protein concentration was determined using a BCA Assay Kit (ThermoScientific). Samples were incubated with BCA reagents for 30 min at 37 °C and protein concentration measured using a nanodrop spectrometer.

The lysate was mixed with NuPAGE sample LDS loading buffer with 1X NuPAGE Reducing Agent (10X). The samples were boiled at 95 °C for 10min. 5-15µg of sample in a volume of 40µl was loaded in NuPAGE Novex 4-12% Bis-Tris gels. Gels were run at 100V for 2h 30min in MOPS SDS running buffer 1X. In the inner chamber, 250µL of NuPage antioxidant (Invitrogen) was added per 100 mL of MOPS SDS running buffer 1X. Precision Plus standard protein ladder (Bio-Rad) was used to determine protein molecular weight. Once the proteins were properly separated, gels were transferred onto nitrocellulose membrane (GE Healthcare Amersham

Hybond ECL membrane). Transfer was run in a Bio-Rad tank for 100min at 90V at 4°C on ice using Tris/Glycine/SDS transfer buffer 1X (Bio-Rad).

Nitrocellulose membranes were blocked with 5% milk in PBS 0.1% Tween-20 (Sigma) for 1h at RT. Primary antibodies diluted in 5% milk in PBS-T were used to detect RXRα, RXRβ, RXRγ, and Peroxisome Proliferator Activated Receptor γ (PPARγ) (Table 2.1) in an overnight incubation at 4°C. Three 10min washes with PBS-T removed excess primary antibody. HRP-conjugated goat anti-mouse and rabbit secondary antibodies in 5% milk in PBST were added for 2h at RT to detect the primary antibodies (Table 2.2). Three 10min washes with PBS-T removed excess secondary antibody. Proteins were detected with the highly sensitive enhanced chemiluminescent reagent (ECL, Amersham) peroxidase substrate, and the horse radish peroxidase (HRP) reaction was detected using exposure films (ThermoScientific) which were exposed for 2min, 5min, 15min, or 30min. The film was developed by immersion in Kodak GBX developer for 1min and fixing the film in Kodak GBX fixer for autoradiography for 1min (Sigma). Developed films were quantified using ImageJ software. The films were scanned as an 8bit image and each band was surrounded and selected and its integrated density measured. Each of the bands was normalised using the correspondent β-actin band measured in the same way.

2.7 Treatment with agonists and antagonists

RXR and its binding partner PPARγ agonists and antagonists were used to modulate these pathways in BMM cultures. The agonists and antagonists were added for 24h before beginning the myelin phagocytosis assay for a further 8h. The following concentrations of agonists and antagonists were used: RXR agonist 9 *cis* Retinoic Acid (9cRA) at 1μM, RXR antagonist HX531 at 10 μM, and PPARγ antagonist N-(4′-aminopyridyl)-2-chloro-5-nitrobenzamide (T007) at 10 μM (Yamauchi et al., 2001).

2.8 Fluorescence Activated Cell Sorting (FACS) for BMMs

BMMs were replated to 100 mm dishes (Corning) and allowed to adhere overnight. Media was changed and 10 μM of the antagonists HX531, T007, or DMSO controls were added for 24h to 2mo young controls. Subsequently, DiO-labelled myelin (50

µg/ml) was added to phagocytosing groups for 8h. Cells were then washed, detached, and centrifuged at 300 *g* for 5 min. Pellets were resuspended in FACS buffer (PBS 1X, 1% FBS) and CD11b-APC (eBioscience, 1:300) was added for 30min at 4ºC. Cells were then washed and resuspended in FACS buffer prior to acquisition on a BD FACSCalibur. Phagocytosis index was determined by the percentage of macrophages CD11b-APC+/DiO Myelin-FITC+ using SigmaPlot software.

Myelin was labelled with the lipophilic dye $DiOC_{18}(3)$ (DiO, Sigma) by taking 0.0020 g DiO and resuspending in 1ml DMSO. 375 µl of DiO/DMSO solution was added to 10 ml PBS 1X. Then, 40 mg of isolated myelin was added to DiO-PBS solution. Myelin was incubated in diluted DiO solution for 30 min at 37°C. Then, the solution was centrifuged at 300 *g* for 10 min in a 15 ml conical tube. Labelled myelin was resuspended in 2 ml PBS 1X and stored at –80°C.

2.9 Co-Immunoprecipitation

BMMs were replated and kept in serum-free media for 24h in 100 mm dishes and then phagocytosing groups were treated with myelin for 8h. Cells were washed with PBS 1X and then lysed with 50 µL IP lysis/wash buffer from the kit (0.025M Tris, 0.15M NaCl, 0.001M EDTA, 1% NP40, 5% glycerol) together with Halt protease and phosphatase inhibitor cocktail 1:100 (ThermoScientific). Protein amount was measured with BCA protein assay (ThermoScientific). Immunoprecipitation was performed following the protocol of Pierce crosslink immunoprecipitation kit (ThermoScientific). 10µg of the antibody against PPARγ (Table 2.1) were bound to the Protein A/G agarose beads at RT on rotation for 1h. Then antibodies were crosslinked to the agarose beads with 2.5mM DSS crosslinker for 1h to avoid the elution of antibodies with the proteins. After crosslinking, between 200 and 600µg of the cell lysates were added and incubated at 4°C overnight. Antigen elution was performed in 30µL elution buffer and the samples were prepared for SDS-page gels and used for western blot (explained above). In order to analyse the binding of RXRα to the same pulled down protein, western blot membranes were stripped with stripping buffer (50mM Tris-HCL pH 6.8, 2% SDS, 50mM DTT or 100mM β-mercaptoethanol diluted in water) for 30 min at 75°C. Then the membranes were washed 2x10min with double distilled water and another 3x with PBST. Membranes

were blocked for 1h at RT with 5% milk in PBST and incubation with PPARγ was repeated. After western blots, each band was selected and integrated density was measured in ImageJ. Each band was normalised by dividing their integrated density by the integrated density of the co-immunoprecipitation protein, PPARγ.

2.10 Knockout Mice

Knockout mice bred and genotyped by Vanessa Nunez at the CNIC Madrid. Mice with floxed RXRα alleles were crossed with lysozyme-M (LysM) Cre recombinase transgene (Cre) mice to generate offspring with macrophage-specific loss of RXRα (Núñez et al., 2010). Mice were bred on a mixed C57Bl/6 and 129/Sv background. The offspring containing the lox-P-targeted RXRα gene and the Cre transgene (LysM-Cre+/ RXRα$^{fl/+}$) were then crossed with RXRα$^{fl/fl}$ mice to generate mice with an active Cre transgene and the RXRα floxed allele (LysM-Cre+/RXRα$^{fl/fl}$). LysM-Cre-negative RXRα floxed mice were considered wildtype (WT) and RXRα floxed-LysMCre+ mice were considered knockout (KO) animals. Mice aged 4mo were used for experiments. Mice were bred and genotyped at the CNIC, Madrid, Spain. Mice were genotyped by PCR using the primers P1, P2, and P3 as described (Ricote et al., 2006). KO and WT distinction is visualised in Fig. 2.4.

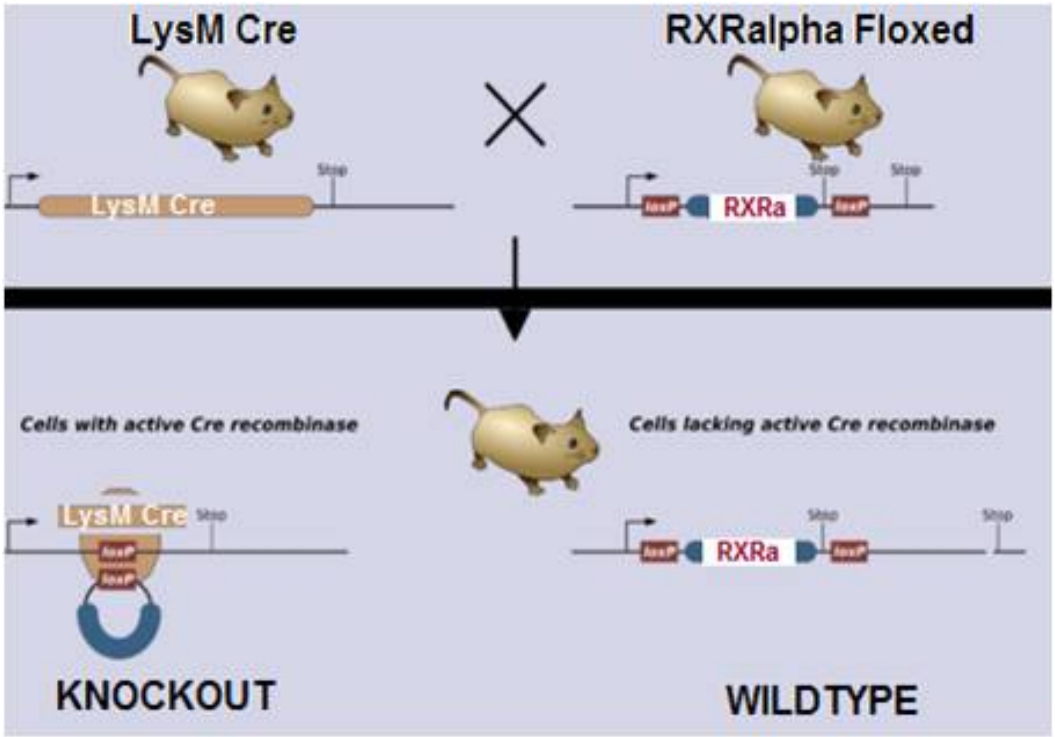

Figure 2.4 Generation of Lysozyme-M Cre-RXRα floxed WT and KO mice.

2.11 Lysolecithin-induced Demyelination

Demyelinating lesions were induced in the ventral funiculus of the thoracic spinal cord with 1 µl 1% lysolecithin (lysophosphatidylcholine, vol/vol). Lysolecithin was prepared by dissolving powder (Sigma) in sterile PBS 1X and storing it at -20°C. Solution was defrosted and sonicated for 15min and vortexed to eliminate any micelles or particles. Mice were induced under general anaesthesia with 2.75% isofluorane (Abbott) in oxygen. Buprenorphine (Vetergesic, Alstoe) was administered subcutaneously at 0.02 mg/kg and used for preoperative analgesia. Hair was clipped from the dorsal cervical and thoracic regions and skin was prepared with diluted chlorhexidine (Hibiscrub). A skin incision (5 mm) was made over the caudal thoracic vertebrae. The subcutaneous fascia and paravertebral muscle were dissected between the T12 and T13 vertebrae. The dorsal spinal cord was visualised, and the dura was pierced. Using a 10 µl Hamilton syringe with a pulled glass microelectrode pipette, lysolecithin was injected in the ventral funiculus for 2min for solution to disperse. Muscle and skin were closed using nylon stitches (Ethilon). Mice were placed in a warm incubator for recovery.

Mice were intracardially perfused with 4% glutaraldehyde (for electron microscopy) or 4% PFA at 5 days post lesion (dpl), 14dpl, and 21dpl. These timepoints represent significant events in the demyelination/remyelination process: 5dpl = OPC recruitment and proliferation, 14dpl = OPC differentiation, 21dpl = complete remyelination. Before perfusion, mice were heavily anesthetised with 3% isofluorane in oxygen and sacrificed with intraperitoneal injection of pentobarbitone (Pentoject). Once fully anesthetised, the thoracic cavity was opened and left ventricle was pierced with a 23g butterfly catheter hooked to a pre-filled pump. The left atrium was pierced and perfusion was continued for 3 min. Spinal cords were dissected from the vertebral canal and transferred to 20% sucrose (Fischer). PFA-fixed spinal cords were post-fixed overnight and cryoprotected in sucrose before optimal cutting temperature (OCT) embedding (Tissue-Tech) and storage at −80 °C. OCT-embedded tissue was cut in 12µm segments using a Leica Cryostat Microtome, collected on poly-l-lysine coated glass slides, and stored at −80 °C prior to staining.

2.12 Oil Red O Staining (ORO)

Tissue sections were dried in 100% propylene glycol (Sigma) for 1min then stained at 60°C in 0.5% Oil Red O solution (ORO, Sigma) dissolved in propylene glycol for 6min. Then, slides were switched to 85% propylene glycol for 2min followed by rinsing with distilled water for 1min in coplin jars. Nuclei were stained with haematoxylin (Sigma) for 1min and washed with tap water. Slides were mounted with jelly mounting media and visualised in brightfield at Nikon Eclipse E600 microscope and DS-Vi1 camera using 20X (Plan Fluor 20X / NA 0.3) and 40X (Plan Fluor 40X / NA 0.75) objectives. Area of ORO and Haematoxylin staining were quantified using ImageJ Software, with lesion area denoted by haematoxylin+ staining and ORO staining quantified by ORO+ area/total lesion area.

2.13 Immunohistochemistry

Cryostat cut sections were dried for 1h at RT and washed with PBS 2x10min. Slides were blocked in 7% NGS (Sigma) with 0.1% Triton in PBS for 1h at RT. Primary antibodies diluted in blocking solution were applied for 12h at 4°C (Table 2.1). Slides were washed 3x10min with PBS 1X and secondary antibodies in blocking solution were applied (Table 2.2) for 2h at RT. Slides were washed again and stained with Hoechst nuclear stain (1:5000). Slides were washed 2x10min PBS1X and mounted with coverslips using Fluoromount G. For nuclear antigens (Olig2), tissue sections were incubated for 10min at 75 °C with pre-boiled 1X citrate buffer pH 6 antigen retrieval solution (Dako) diluted in double distilled water and continued as above. For mouse antibodies (CC1), slides were washed in tris-buffered saline (TBS, Fischer) with 0.05% tween-20 (TBST) after initial blocking. Before adding primary antibodies, slides were incubated with mouse on mouse (MOM, VectorLabs) for 1h at RT. Slides were further washed in TBS-T for the remaining protocol as above. Slides were mounted and visualised with 40X objective (EC PLAN 40X / 0.50 Ph1 numerical aperture) using a Zeiss Axiovision Observer A1 AX10 fluorescence microscope with AxioCam HRC HAL100 camera. Cells were counted using ImageJ software.

2.14 *In Situ* Hybridisation

Proteolipid protein (PLP) probe was prepared and diluted in hybridisation buffer and denatured for 10min at 75°C then 150 µL of the probe was added to spinal cord sections. Slides were coverslipped and incubated in a chamber with 50% formamide and SSC in diethylpyrocarbonate-treated dH_2O and hybridised overnight at 65°C. Slides were then incubated in wash buffer (1X SSC, 50% formamide, 0.1% Tween-20) at 65°C for 15min. Slides were washed in wash buffer at 65°C and washed twice for 10min in MABT (100mM maleic acid, 150mM NaCl, 0.1%Tween-20, pH 7.5) at RT. Slides were then incubated in blocking solution (2% blocking reagent and 10% heat-inactivated sheep serum in MABT) for 1h at RT. Anti-digoxygenin-alkaline phosphatase fragments (Roche Molecular Biochemicals) were diluted to 1:1500 in blocking solution and added to slides, and slides were incubated overnight at 4°C. Slides were then washed 3x10min in MABT and twice in staining buffer (100mM Tris-HCl, 100mM NaCl, 5mM $MgCl_2$, pH 9) followed by incubation in 5-bromo-4-chloro-3-indolyl-phosphate/nitro blue tetrazolium (BCIP/NBT) stock solution (Roche) at 37°C for 1-2h. Slides were rinsed in double distilled water containing Hoechst followed by 2x1min soaks in 100% ethanol and 2x1min soaks in xylene. Slides were coverslipped with Aquamount and visualised in brightfield with a Nikon Eclipse E600 microscope and DS-Vi1 camera using 20X (Plan Fluor 20X / NA 0.3) and 40X (Plan Fluor 40X / NA 0.75) objectives. PLP^+ cells and $Hoechst^+$ area were quantified using ImageJ Software.

2.15 Electron Microscopy

Glutaraldehyde-perfused spinal cords were post-fixed in 2% osmium tetroxide (Oxkem Ltd) in phosphate buffer at 4°C overnight followed by dehydration in 70% ethanol for 15min, 95% for 15min, and 100% for 3x10min. Tissue was then put in propylene oxide twice for 15min and left in 50% propylene oxide, 50% resin mix (TAAB embedding resin mix) for 3h and transferred to 100% resin mix overnight. Embedding capsules were incubated at 60 °C for 12-24h until resin was solid. Embedded samples were cut in 90 nm sections on an ultramicrotome (Reichert Ultracut E) with a diamond knife (Diatome) and visualised using a Transmission Electron Microscope (Hitachi H600). Electron microscope films (Kodak) were developed and scanned at high resolution and analysed with ImageJ software. The

g-ratio was used to determine extent of remyelination on all axons. G-ratio = (axon diameter) / (diameter of the axon including outer myelin).

2.16 Statistics for Animal Studies

Data are presented by mean ± S.E.M in all graphs. All the statistical analysis was done using Excel 2010 and Graphpad Prism 6. When comparing more than two groups with only one independent variable, one-way ANOVA was used followed by Tukey's multiple comparisons test as a post-hoc test, as in the cases of comparing protein expression by western blot. In this case, the single explanatory variable (age) had multiple levels (from 2mo-24mo). When two or more variables were involved, a two-way ANOVA was used to check interaction amongst the variables and if interaction was positive, further analysis was done by Sidak's multiple comparisons test considering these variables separately, as in comparing agonist treatment and protein expression by immunohistochemistry. Two-tailed unpaired Student t-tests were used to compare antagonist treatment. Results were considered significant if $p<0.05$. Technical replicates were performed at least two or more times for each experiment, with $n\geq4$ biological replicates (animals) per experiment. Specific *n* numbers and significance values are indicated in the results section.

Human Models

2.17 Subjects

Studies were performed according to US National Institutes of Health guidelines and all subjects signed informed consent. Study subjects were healthy volunteers in 2 age groups, Young donors (≤35 years old) and Old donors (≥55 years old) or multiple sclerosis (MS) patients in the same age groups. MS patients were previously diagnosed as relapsing remitting (RRMS), secondary progressive (SPMS), or primary progressive (PPMS) patients based on the 2010 revisions of the McDonald diagnostic criteria.

2.18 Human Monocyte Isolation

Peripheral blood mononuclear cells (PBMCs) were isolated from whole blood using lymphocyte separation medium (LSM, Lonza). Whole blood (30 ml) and 10ml PBS1X were mixed and layered over 10 ml LSM in a 50 ml conical tube (BD). Tubes were spun at 1200 rpm for 30min at RT. Diluted serum was aspirated, and the remaining PBMC layer (above LSM and red blood cells) was carefully removed with a 1 ml pipette. Collected cells were washed with 30ml cold PBS 1X and centrifuged at 300 *g* for 10 min at 4°C. Cells were resuspended in 10ml cold MACS buffer (2 mM EDTA, 0.5% Bovine Serum Albumin, BSA in PBS 1X) and spun again. Buffer was aspirated, and the cell pellet was lightly dislodged. Cells were resuspended in 200 µl MACS buffer and 50 µL CD14+ magnetic microbeads (Miltenyi) and incubated at 4°C for 15min. Cells were washed with 10 ml MACS buffer and centrifuged at 300 *g* for 10min. Supernatant was aspirated and cells were resuspended in 500 µl MACS buffer. CD14+ monocytes were isolated by positive selection by running magnetically-labelled cells through an LS column attached to MACS magnetic separator (Miltenyi). Columns were washed 3x3 ml with MACS buffer. Columns were removed from the magnet and 5ml MACS buffer was loaded into each column. Columns were then immediately plunged so positively selected cells could be collected. Cells were counted by a Neubauer haemocytometer (Hausser Scientific). Monocytes were plated in 6-well plates at $1x10^6$/well (for RNA/supernatants) or in suspension in 96-well plates at $1x10^5$/well (for flow cytometry) in X-vivo without phenol red (Lonza). Monocyte isolation is highlighted in Fig. 2.4.

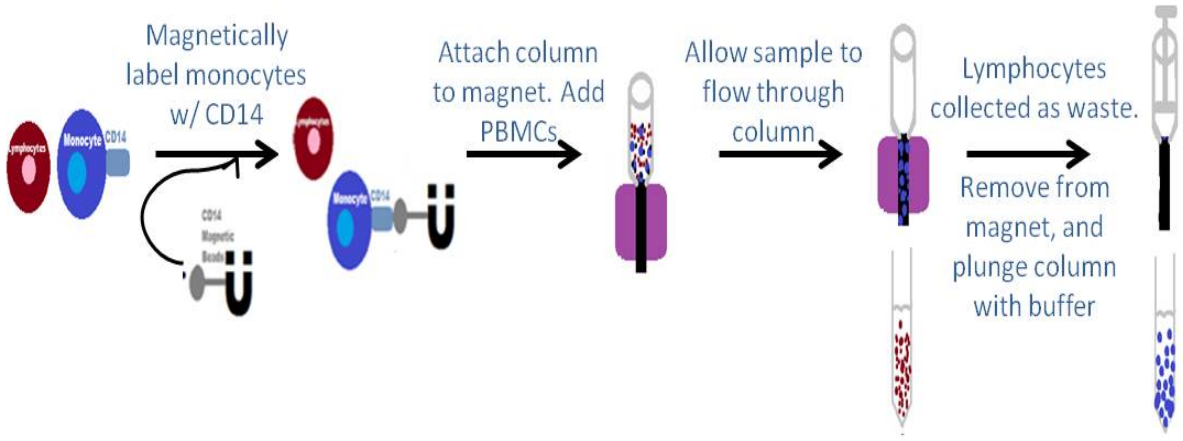

Figure 2.5 Monocyte isolation from PBMCs. Monocytes were isolated from PBMCs by CD14+ selection using CD14 magnetic microbeads (Miltenyi).

2.19 Human Myelin Isolation and Labelling

Brain tissue was obtained post-mortem from a PPMS patient. The same protocol used for myelin isolation in mice was followed to isolate human myelin (Section 2.3). Myelin was stored in 100 µl aliquots at -80 °C. For FACS, myelin was labelled with pHrodo green STP ester (Life Technologies). pHrodo dyes are pH-sensitive, suitable for studying low pH environments of the phagosome. The dye increases fluorescein+ (FITC+) fluorescence upon engulfment by monocytes and macrophages. pHrodo dye was reconstituted to 1 mg/ml in DMSO, and 1µL of dye was added to 100 µl of myelin. Myelin was protected from light and incubated at RT on a shaker for 30 min. Myelin suspension was then washed with 1 ml PBS1X and spun at 250 *g* at 4°C for 10min in a microcentrifuge. PBS was aspirated, and pHrodo-labelled myelin was resuspended in 100 µl PBS1X and stored at -20 °C for further experiments.

2.20 Fluorescence Activated Cell Sorting (FACS) of Human Monocytes

Monocytes in 96-well plates were incubated with 1 µM Bexarotene or Pioglitazone (treated groups, Sigma) or the equivalent DMSO (controls) in 100 µl/well of X-vivo without phenol red for 30min at 37 °C. Cells were then stained with CD14-APC (eBioscience) and CD163-PE (R&D Systems) for 10min at 37 °C. Cells were washed

in cold FACS buffer (1 g/L Sodium Azide, 1% FBS, 1X PBS) by adding an equal volume of FACS buffer (100 µl/well) and centrifuging at 250 *g,* 5min, 4 °C. Cells were then resuspended in 100 µl warm X-vivo. 10 µg/ml pHrodo-labelled myelin was added to phagocytosing groups for 20min at 37 °C. An equal volume of cold FACS buffer was then added, and cells were immediately acquired on a BD LSR II and analysed with BD FACSDiva 6.1 software. Gating was based on non-phagocytosing controls, and myelin-phagocytosing FITC+ cells were normalised to controls. Amount of myelin phagocytosis in each treated group was calculated by by the phagocytosis index = (Myelin+ fluorescence in treated groups) / (Myelin+ fluorescence in non-phagocytosing controls)

2.21 Microarrays

Monocytes were separated in 6-well plates at $1x10^6$/well. There were 4 donor groups: Young HVs (≤35 years old), Old HVs (≥55 years old), Young MS Patients, and Old MS Patients. There were 6 wells per donor (1 well/treatment): Control cells (no treatment), Phagocytosing cells (treated with myelin (10µg/ml)), Bexarotene-treated cells (Sigma, 1µM), Bexarotene-treated Phagocytosing cells, Pioglitazone-treated cells, Pioglitazone-treated phagocytosing cells. All treatments were 2h. Supernatants were incubated for 24h, collected, centrifuged at 250 *g* at 4°C for 10min in a microcentrifuge, and stored at −80 °C (for cytokine detection, see Section 2.25). Cells were then collected in Trizol (Invitrogen) and stored at −80 °C until RNA isolations. RNA was isolated using the miRNeasy kit (Qiagen) according to manufacturer's instructions with n=4 per treatment/group. RNA concentration was measured using a Nanodrop ND-2000, and RNA integrity was assessed using Bioanalyzer 2100 (Agilent). RNA was sent to the NIH Microarray Core Facility, and microarrays were performed on GeneChip Human Gene 1.0 ST Arrays (Affymetrix). Ingenuity Pathway Analysis software was used to create diagrams for comparing biological pathways. Microarray experiments performed by core facilities are below.

2.21.1 Sample Preparation for Microarray Hybridisation

Performed by Abdel Elkahloun at NIH Microarray Core Facility.
RNA quality control, quantitation, cRNA (complementary RNA) synthesis and labelling were performed on a sample-by-sample basis according to manufacturer's guidelines for use

with the Affymetrix Human 1.0 ST GeneChip (Affymetrix). DNase treatment was included as part of isolation to remove possible contaminating DNA. Bioanalyzer nanochip (Agilent) and NanoDrop were used to validate and quantitate the RNA prior to cRNA synthesis and labelling. For cRNA synthesis and labelling, 5 µg of total RNA was used per sample in conjunction with the Affymetrix 3' one-cycle Target labelling Kit (Affymetrix).

2.21.2 Microarray Hybridisation

Labelled cRNA were hybridised to Affymetrix Human 1.0 ST GeneChips (Affymetrix) in a blinded, interleaved fashion. The Affymetrix scanner 3000 was used in conjunction with Affymetrix GeneChip Operation Software to generate more than 750,000 oligonucleotide probe measurements for each hybridised cRNA.

2.21.3 Microarray Data Analysis

Performed by Kory Johnson as the NIH Bioinformatician. Probe measurement summarisation and normalisation was accomplished using the Affymetrix Expression Console with the "RMA Sketch" option selected (Affymetrix). Subsequent analysis of the data generated by the Console was done in "R". Data quality was first inspected and assured via sample-level Tukey box plot, covariance-based PCA scatter plot, and correlation-based Heat Map using the "box.plot()", "princomp()", "cor()", and "image()" functions respectively. After, gene fragments not having at least one expression value greater than system noise were deemed "noise-biased" and discarded. System noise was defined as the expression value across experiment groups at which the observed C.V. (Coefficient of Variation) grossly deviates from linearity. For gene fragments not discarded, expression values were floored to equal system noise if less than system noise then subject to the one-factor ANOVA test under BH (Benjamini and Hochberg) FDR (False Discovery Rate) MCC (Multiple Comparison Correction) condition using Experiment Group as the factor. For gene fragments having a corrected p-value < 0.05 only, the Tukey HSD (Honestly Significant Difference) test was applied and the fold-

change between all possible group means calculated. Gene fragments having both a Tukey HSD p-value < 0.05 and a fold-change ≥ 1.5 for a pair-wise group comparison were flagged as having expression significantly different for that comparison. Subsequent annotation for each gene fragment flagged and corresponding enriched pathways and functions was obtained using IPA (http://www.ingenuity.com).

2.22 PCR Arrays and Semi-quantitative Real-Time PCR

Isolated RNA was converted to cDNA using the QuantiTect Reverse Transcription Kit (Qiagen) according to the manufacturer's instructions. cDNA was stored at −20°C prior to experiments. cDNA was pooled from 4 samples in each group and added to SYBR Green qPCR SuperMix (Bio-Rad). Each sample was aliquoted on the Human Retinoic Acid Signalling PCR Array (SABiosciences), with primer pairs for 84 genes in the RXR signalling pathway. Plates were run on a CFX96 Touch Real-Time PCR Detection System (Bio-Rad) for 10min at 95 °C, then 40 cycles of 15s 95°C, 60s 60°C. Data normalisation was performed using Excel 2010 to correct Ct values to average Ct values for several constantly expressed housekeeping genes on the array. To analyse PCR-data, relative quantification was used to compare samples to untreated, Young (≤35 years old) controls, resulting in ΔCt values used to calculate relative fold changes. The effect of bexarotene treatment ($|FC| > 1.5$) was plotted.

2.23 Electrochemiluminescence (ECL)

Electrochemiluminescent assays were developed and optimised to quantify the concentrations of selected biomarkers in cell culture supernatants using the Meso Scale Discovery (MSD) detection system. The MSD detection system provides a combination of high sensitivity with low background and a 5-log-order of magnitude dynamic range. The concentrations of soluble CD14 (sCD14) and sCD163 were developed in the NDU laboratory. All samples were run in duplicate. Each assay contained additional reference samples (minimum of 2) on each plate to check the intra- and inter- assay reliability.

The standard protocol for the developed assays was as follows; standard binding plates (MSD) were coated with 30 µl of working solution of capture antibody and stored at 4 °C overnight. The next morning, the coating solution was aspirated, and plates were blocked with 150 µl of 1% BSA in PBS 1X for 2h at RT on a shaker at 200 rpm. After washing plates 3 times with PBS-T, 25 µl of each supernatant sample was added to each well, and the plates were incubated for 2h at RT on a shaker at 200 rpm. Plates were washed again 3x with PBS-T. 25 µl of working solution of detection antibody was added to each well, and the plates were incubated as above. The plates were then washed and incubated 1h with 25 µl of 0.25 µg/ml Sulfo-tag labelled Streptavidin solution (MSD). Finally, plates were washed 3 times with PBS-T and 150 µl of 2 fold-concentrated Read Buffer was added for the SI2400 image analyser (MSD). The standard curve was generated from a serial dilution of standard proteins in 1% BSA in PBS. The details are depicted in Table 2.3.

2.24 Human M1/M2 Macrophage Cultures

Monocytes were isolated as in Section 2.8 and plated at $1x10^6$/well in 12-well plates (Corning). Two groups were studied: Young HVs (≤35 years old) and Old MS patients (≥55 years old, progressive). For each donor group, 8 treatment groups were studied:

1) M1-polarised Cells
2) M1-polarised myelin-phagocytosing cells
3) M1-polarised Pioglitazone-treated cells
4) M1-polarised Pio-treated phagocytosing cells
5) M2-polarised Cells
6) M2-polarised myelin-phagocytosing cells
7) M2-polarised Pioglitazone-treated cells
8) M2-polarised Pio-treated phagocytosing cells

All cells were plated in 1 ml media/well. Media and protocol were adapted from (Mia et al., 2014). Basic media was composed of RPMI 1640, 10% FBS, 100 u/ml Pen/Strep, and 20 µM β-mercaptoethanol. For M1-polarised cells, 50 ng/ml granulocyte macrophage colony stimulating factor (GM-CSF) was added to media. For M2-polarised cells, 50 ng/ml M-CSF was added to media. On Day 3, media was

changed on both M1 and M2 cells, and 1 μM pioglitazone was added to the treatment groups. On Day 6, cells were further polarised to M1 and M2 phenotypes. M1 cells were plated in basic media plus: 20 ng/ml IFNγ, 20 ng/ml TNFα, and 50 ng/ml LPS (Peprotech). M2 cells were plated in basic media plus: 20 ng/ml IL-4 and 20 ng/ml IL-10 (Peprotech).

After 24 hours of polarisation, cells were collected and analysed by FACS. Using a cell lifter, cells were gently scraped and centrifuged in a microcentrifuge at 2000 rpm for 10 min in 2 ml tubes. Cells were resuspended in X-vivo without phenol red and $1x10^5$ cells/treatment group were stained with M1 and M2 markers (highlighted in Table 2.1) for 15 min at 37°C in a 96-well plate. For M1 markers, CD80 and CCR7 were used. For M2 markers, CD206 and CD163 were used. For all macrophages, CD11b was used. After staining, 10 μg/ml pHrodo labelled myelin was added to phagocytosing groups for 20 min at 37°C. Cells were washed with FACS buffer and fixed using BD FACS Cytofix buffer (100 μl/well) for 20 min at 4°C. Plates were centrifuged at 250 *g* at 4°C for 5min. Then, cells were resuspended in FACS 1X Perm/Wash Buffer (BD) and centrifuged as before. Cells were finally resuspended in 150 μl FACS buffer/well and run on a BD LSR II flow cytometer using BD FACSDiva 6.1 Software. Mean fluorescence intensity for all markers was determined by dividing the MFI of each treated group to the MFI of the control, resting macrophages.

2.25 Statistics for Human Studies

SAS and power analysis performed by Tianxia Wu, NIH statistician. Data are presented by mean ± S.E.M in all graphs. All the statistical analysis was done using SAS 9.2 and Graphpad Prism software. Initial power analysis was performed on a small cohort of young HVs, old HVs, young MS patients, and old MS patients. Power analysis was conducted using an internal pilot study including 18 young HVs and 17 old HVs with outcome measures from pre-treatment, and 48 MS patients with outcome from both pre- and post-treatment. Based on a significance level of 0.05, a sample size of 18 subjects was required to have 80% power for detecting the difference between pre and post-treatment using a paired t-test; a sample size of 34 subjects per group was required to have 80% power for detecting the difference between the young HV and old HV group using a two-sample t-test. nQuery program was used for the power analysis. Two-way repeated measures ANOVA was performed to evaluate the effect of group (between-subject factor, MS,

young-HV, old-HV) and treatment (within-subject factor, pre- and post- treatments), and the interaction between group and treatment. When the interaction was significant, pairwise comparisons among the combinations (group x treatment) were conducted with Tukey's correction procedure. Natural-logarithm was applied to the outcome, Myelin debris phagocytosis, since the distribution had a long right tail. SAS 9.2 and Graphpad Prism software were used for the statistical analysis and $p<0.05$ was used as the significance level. In the case of measuring ECL cytokines and surface markers, if interaction was positive, further analysis was done using Sidak's multiple comparisons test. Results were considered significant if $p<0.05$. Each biological replicate also represented a technical replicate as patients/donors were collected at independent times.

2.26 Antibodies

Antigen	Species	Manufacturer	Cat. No.	Dilution
RXRγ	Rabbit	Abcam	Ab15518	1:100
RXRβ	Rabbit	Santa Cruz	SC-774	1:100
PPARγ	Rabbit	Santa Cruz	SC-1008	1:100
PPARγ	Mouse	Santa Cruz	SC-271392	1:100
RXRα	Rabbit	Santa Cruz	SC-553	1:100
β-actin	Mouse	Sigma	A5441	1:5000
MBP	Rat	Serotec	MAC409S	1:500
Olig2	Rabbit	Millipore	AB9610	1:1000
CC1	Mouse	Calbiochem	OP80	1:200
Iba1	Rabbit	Wako	019-19741	1:500
CD11b	Rat	Serotec	MCA711	1:250
CD11b-APC	Mouse	eBioscience	9017-0118	1:300
CD45-PE	Rat	eBioscience	12-0451	1:500
Hoechst	N/A	Biotium	40043	1:5000
CD14-APC	Mouse	eBioscience	17-0149	1:500
CD163-PE	Mouse	R&D Systems	FAB1607P	1:250
CD206-APC	Mouse	R&D Systems	FAB25342A	1:250
CD80-PerCP	Mouse	eBioscience	46-0809-41	1:500
CCR7-PeCy7	Rat	eBioscience	25-1979-41	1:500
CD11b-AF450	Mouse	R&D Systems	FAB16991V	1:250

Table 2.1 Primary Antibodies.

Species	Manufacturer	Cat. No.	Dilution
HRP Goat anti-mouse	Dako	P0447	1:1000
HRP Goat anti-rabbit	Dako	P0448	1:1000
Goat 488 anti-rabbit	Invitrogen	A11034	1:1000
Goat 488 anti-mouse	Invitrogen	A11029	1:1000
Goat 568 anti-rabbit	Invitrogen	A11036	1:1000
Goat 568 anti-mouse	Invitrogen	A11031	1:1000
Goat 568 anti-rat	Invitrogen	A11077	1:1000

Table 2.2 Secondary Antibodies.

Molecule	Manufacturer (Antibodies)	Dilution factor	Detection limit	CV
sCD14	R&D systems (MAB3833, BAF383)	10	4 ng/mL	≤20%
sCD163	R&D systems (MAB16071, BAM16072)	10	2 ng/mL	≤20%

Table 2.3 ECL reagents and detection limits for sCD14 and sCD163.

Chapter 3. Results

Age-related changes in monocytes and macrophages reduce myelin debris phagocytosis *in vitro*

3. Results

Age-related changes in monocytes and macrophages reduce myelin debris phagocytosis in vitro

The aim of the present study was to elucidate the causes of impaired myelin debris clearance previously seen in ageing rodent models of remyelination (Ruckh et al., 2012; Shields et al., 1999). These studies prompted us to use *in vitro* macrophage cultures to study myelin debris phagocytosis in aged macrophage subtypes. Determining the effects of age on phagocytes *in vitro* would then allow us to further study the mechanisms of the age-related decline in myelin debris clearance in cultures.

3.1 Bone marrow monocyte-derived macrophages phagocytose myelin debris

Bone marrow monocytes were isolated from the tibia and femurs of female C57Bl/6 mice and differentiated to bone marrow monocyte-derived macrophage (BMM) cultures. These cultures were then exposed to myelin debris, isolated from the brains of C57Bl/6 mice, for 8 hours. Light micrographs of BMMs reveal bipolar, amoeboid, and branched morphologies among activated BMMs at 20X (Fig 3.1A) and 40X (Fig 3.1B) magnification. This phenotypic heterogeneity is represented in previous studies of these cultures as well (Trouplin et al., 2013; Wang et al., 2013; Wang and Harris, 2011). Electron microscopy of myelin-phagocytosing BMMs shows a myelin-laden BMM (Fig 3.1C-D). The multilamellar myelin fragments are located throughout the intracellular compartment of the BMM after 8h of incubation, confirming ingestion of myelin particles.

Immunocytochemistry was used to label BMMs and myelin debris to confirm myelin debris phagocytosis *in vitro* (Fig 3.1E-H). The activated macrophage marker, Iba1 (Fig 3.1G), was used to label myelin-phagocytosing macrophages, and myelin basic protein (MBP) was used to label myelin debris (Fig 3.1H). Degraded myelin was determined by punctate debris staining, and MBP+ debris within Iba-1+ macrophages was deemed intracellular, phagocytosed myelin debris.

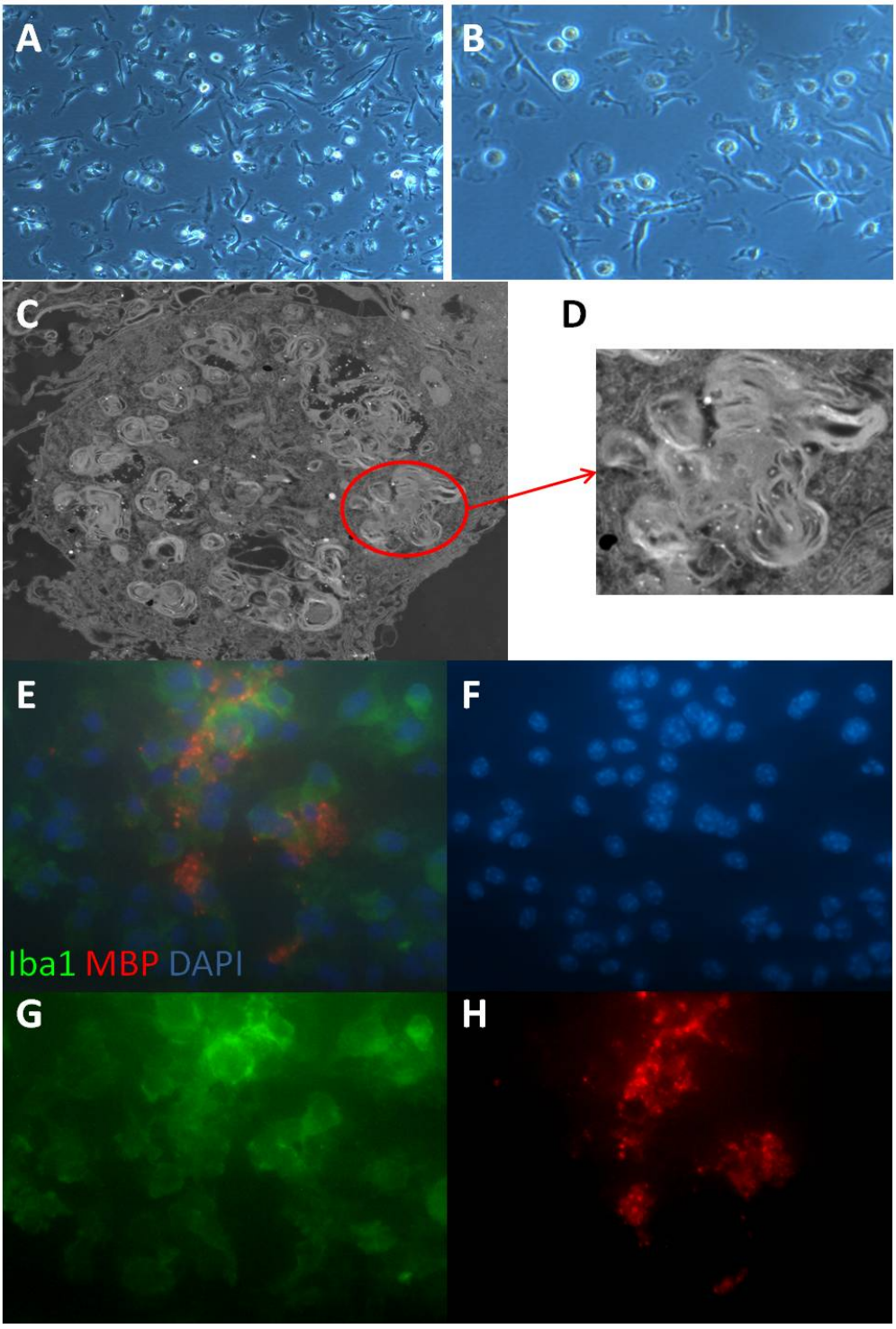

Figure 3.1 Bone marrow monocyte-derived macrophages (BMMs) consume myelin debris *in vitro*. A-B) Light micrographs of BMMs *in vitro* at 20X (A) and 40X (B). BMMs were incubated with myelin isolated from the brains of 2mo mice and phagocytosis was analysed. C-D) Electron microscopy was used to show a micrograph of a heavily laden, myelin-phagocytosing macrophage and allows visualisation of intracellular myelin debris (D). E-H) An overlay showing myelin debris (red=Myelin Basic Protein, MBP) contained inside BMMs (green=Iba1). DAPI (F), Iba1 (G), and MBP (H) labelling of myelin-phagocytosing BMMs.

3.2 Ageing impairs myelin debris phagocytosis in tissue-derived macrophages

Previous studies have revealed an age-associated decline in myelin debris clearance following experimental induction of primary demyelination (Ruckh et al., 2012; Shields et al., 1999; Sim et al., 2002). In addition, research also indicates a decrease in phagocytosis by various types of macrophages with age (Aprahamian et al., 2008; Hearps et al., 2012; Plowden et al., 2004). Both CNS-resident microglia and infiltrating macrophages are present in MS lesions and both are involved in myelin debris clearance (Franklin and Ffrench-Constant, 2008).

To test whether a change in myelin debris phagocytosis occurs because of an age-associated decline in the intrinsic function of phagocytic cells, the effects of ageing on myelin debris phagocytosis using peritoneal macrophages, CNS-derived microglia, and BMMs from mice were determined. These subtypes produced a comparison of the phagocytic ability of macrophages derived from different tissues. The phagoctostosis index (a % of myelin-phagocytosing cells) was calculated either by counting the number of macrophages containing myelin and dividing by the total number of macrophages (immunocytochemistry) or by the cells staining positive for both macrophage and myelin fluorescence markers (flow cytometry).

After incubating cells with myelin fragments, immunostaining suggested that peritoneal macrophages from young mice (2 months old, 2mo = young) (Fig 3.2A) were more efficient at engulfing myelin debris compared to their aged (15-20mo = old) counterparts (Fig 3.2B). Flow cytometry analysis confirmed this impairment in phagocytosis by aged peritoneal macrophages (Fig. 3.2C, H). BMMs also showed an age-dependent decrease in myelin phagocytosis by immunocytochemistry (Fig 3.2D-E), with more than 50% of young cells phagocytosing myelin while less than 25% of aged BMMs (24mo) cleared debris (Fig 3.2H).

Since microglia-derived macrophages are also likely to be involved in myelin debris clearance (Yamasaki et al., 2014), adult microglia cultures were used and showed a similar affect of ageing in mice (Fig 3.2F-G). Adult microglia isolated from the brains of young and aged (2mo and 15-20mo) mice also experienced a significant decrease in myelin debris phagocytosis with age (Fig 3.2G-H). In general, the number of phagocytosing microglia was significantly less than other macrophage types, with only 19% of young microglial cells phagocytosing myelin debris

compared to 50-70% phagocytosis in other young tissue-derived macrophages (Fig 3.2H). This result may further indicate that monocyte-derived macrophages are more important in phagocytosing myelin debris than resident microglial cells in response to myelin debris accumulation in the CNS. These *in vitro* data indicate that ageing impairs myelin debris phagocytosis in tissue macrophages and that these cells can be used to study the effects of ageing on myelin debris phagocytosis.

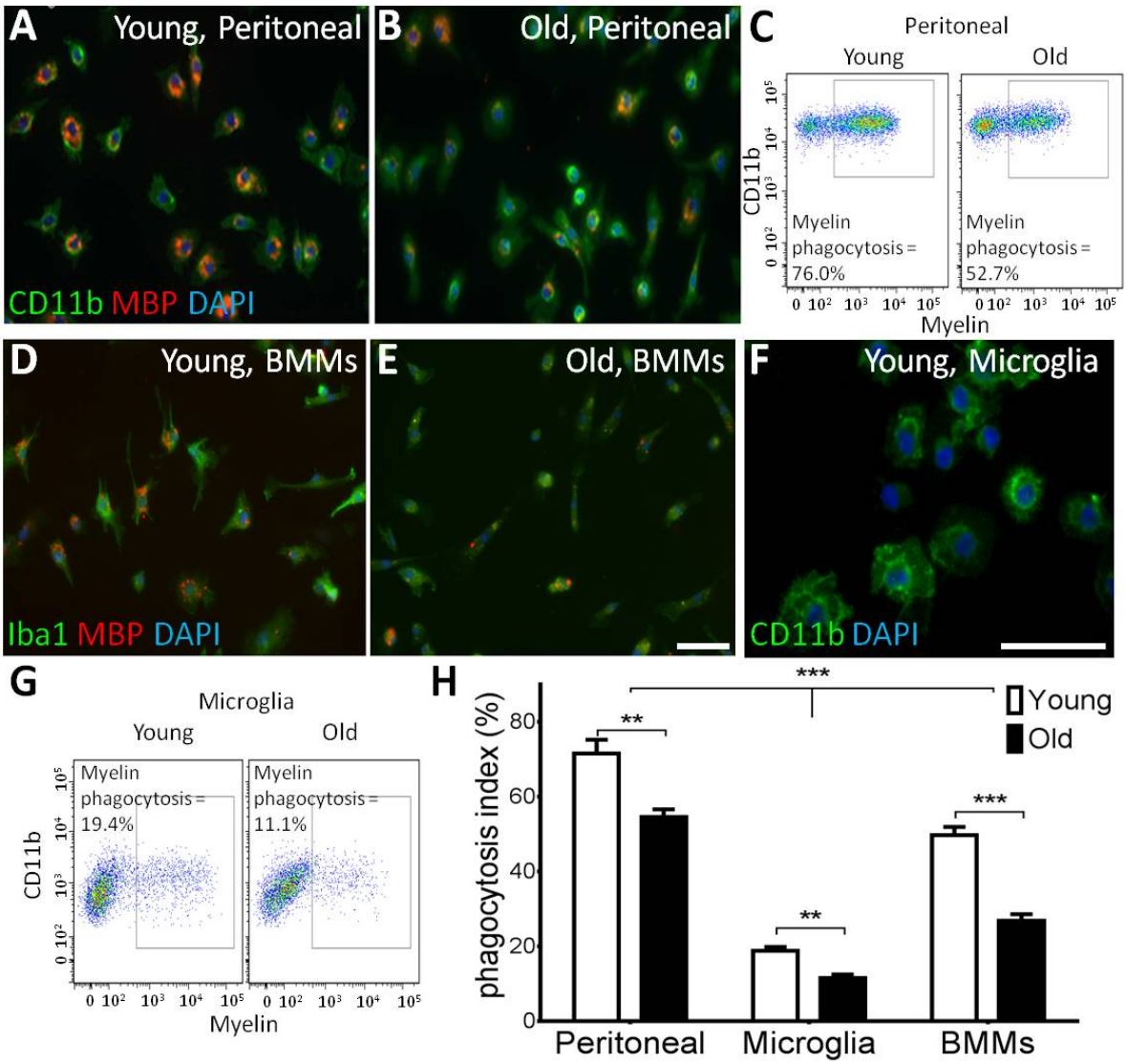

Figure 3.2 Ageing impairs myelin debris phagocytosis. Macrophage cultures were incubated with fluorescent myelin and phagocytosis was analysed. A-C) Aged peritoneal macrophages showed impairment in myelin phagocytosis by both immunocytochemistry (CD11b-green; Myelin-red, A-B) and flow cytometry (C). D-E) Bone marrow monocyte-derived macrophages (BMMs) showed a decrease in myelin debris phagocytosis with age. F-G) Myelin debris uptake is reduced in microglia cultures from aged mice compared to young (G). H) All 3 macrophage subtypes showed significantly reduced myelin debris phagocytosis with age. There were significantly fewer myelin-phagocytosing microglia compared to peritoneal or BMMs regardless of age. Young=2mo mice, Old=15-24mo mice. Scale bars = 50µm. Two-way ANOVA, posthoc Sidak's multiple comparisons test *=p<0.05, **=p<0.01, ***p<0.001, n=4/age group. *Microglia experiments performed by Eimear Linehan

3.3 Ageing does not affect BMMs grown in serum-containing media

Although ageing reduced myelin debris phagocytosis in these macrophage cultures, the phagocytic ability of BMMs was not significantly affected when phagocytosis assays were performed in media containing serum (Fig 3.3A-D). Immunocytochemistry (Fig 3.3A-B) of young and old BMMs did not show a difference in the percentage of MBP+ myelin-phagocytosing macrophages. In addition, flow cytometry confirmed that there was no difference in myelin phagocytosis with age (Fig 3.3C-D). Aged BMMs had enhanced myelin phagocytosis when grown in serum-containing compared to serum-free media. Factors in the fetal bovine serum (FBS) enhanced phagocytosis in our aged BMM cultures, suggesting environmental factors in the media improved phagocytosis in aged BMMs. Therefore, all further experiments were conducted using serum-free, well-defined media, as suggested by previous studies (Eske et al., 2009; Flesch et al., 1986). In all other experiements using BMMs, cells were placed in serum-free conditions 24 hours before incubation with fragmented myelin debris, resulting in a signifcant decrease in phagocytosis in aged BMMs (Fig 3.2H).

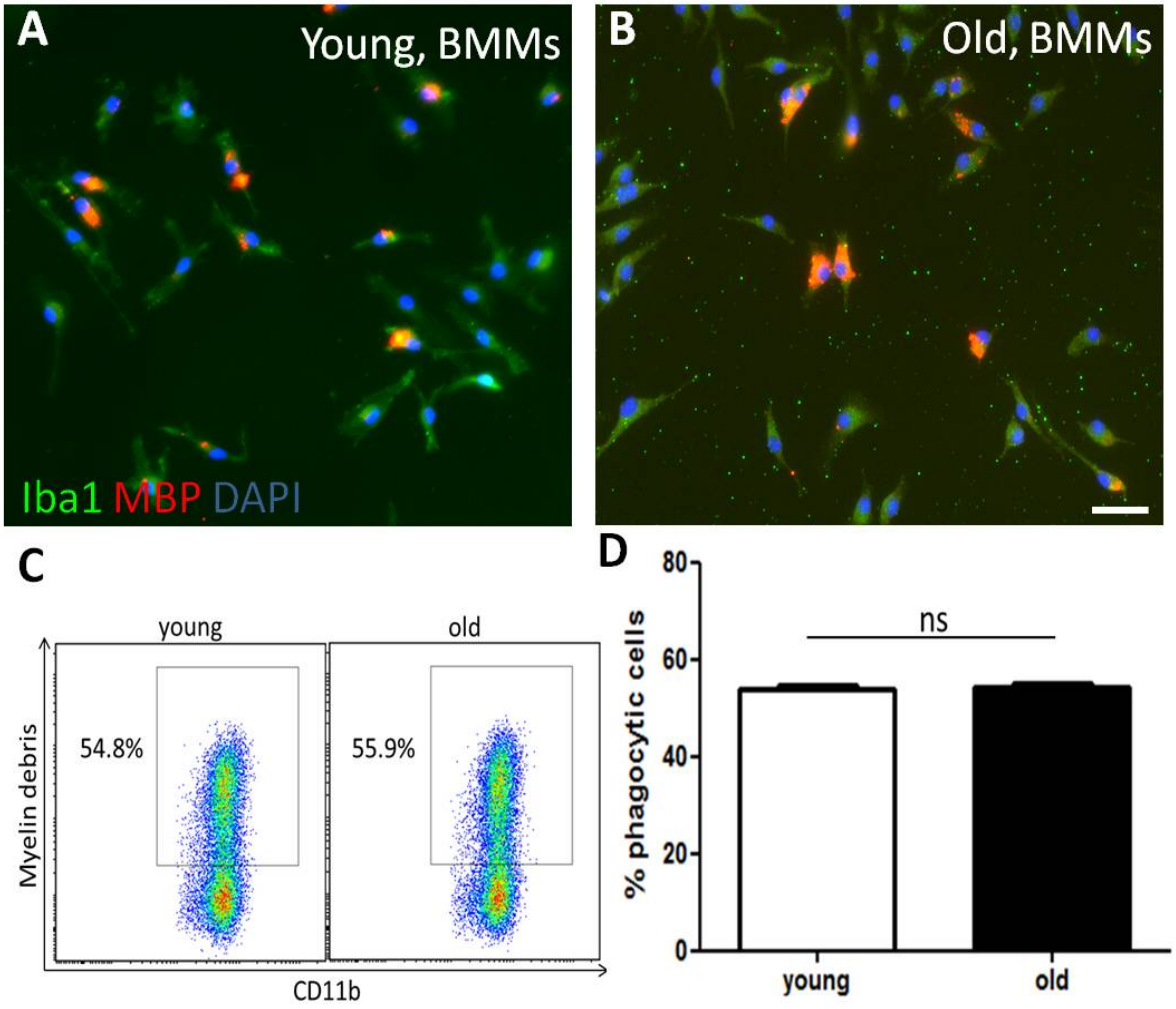

Figure 3.3 Ageing does not affect phagocytosis by BMMs in serum-containing media. BMMs cultured in serum-containing media were incubated with fluorescent myelin and phagocytosis was analysed. A-D) Aged BMMs showed no impairment in myelin phagocytosis by both immunocytochemistry (A-B) and flow cytometry (C). D) There was no significant difference when comparing myelin phagocytosis by young and old BMMs in serum-containing media. Young=2mo mice, Old=15-24mo mice. Scale bar = 25μm. Mann-Whitney test, n=4/age group.

3.4 Myelin debris phagocytosis and RXR pathways are downregulated in aged myelin-phagocytosing monocytes

As impaired myelin debris uptake was seen in animal models of phagocytosis (Fig. 3.2), this study sought to determine whether analogous defects in myelin phagocytosis observed in ageing animals are also present in ageing humans. Using blood-derived monocytes isolated from healthy volunteers (HVs), large numbers of

cells were obtained for both transcriptional and functional studies. Myelin phagocytosis index was calculated as follows for FACS experiments with human monocytes: (Myelin+ fluorescence in phagocytosing treated groups) / (Myelin+ fluorescence in non-phagocytosing controls). Pilot myelin-phagocytosis data was provided to the biostatistician for calculating sample size for functional comparison of monocytes derived from young (≤35 years old) and old (≥55 years old) HVs. Myelin debris phagocytosis was determined by comparing FITC+ fluorescence in phagocytosing cells to control cells. Myelin debris was labelled with pHrodo-green dye (Invitrogen), which activates FITC+ fluorescence in the low pH environment of the phagosome. Upon acquiring pre-determined sample sizes (n=34 for each group), there was a modest, but highly significant decrease observed in the efficiency of myelin phagocytosis in monocytes derived from old HVs (Fig. 3.4A-D). Monocytes from young HVs were highly effective at phagocytosing myelin debris in culture (Fig. 3.4A, 2.44±0.06), while cells from old HVs were not (Fig. 3.4B, 205 ±0.04). The change in myelin debris phagocytosis was also highly correlated with age (Fig. 3.4D, R^2=0.31).

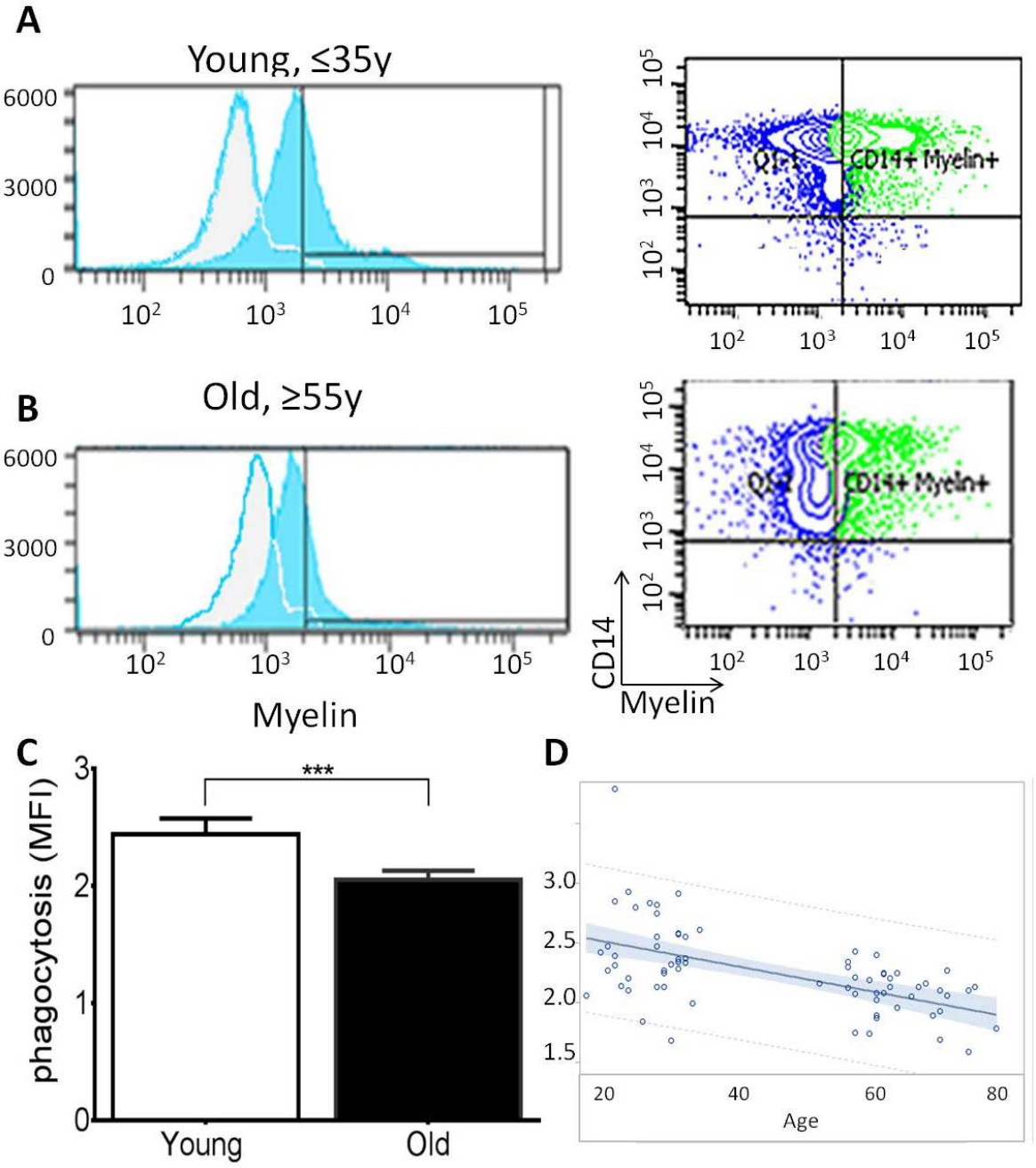

Figure 3.4 Myelin debris phagocytosis is reduced in aged myelin-phagocytosing human monocytes. A) CD14+ monocytes from HVs (≤35 years old) effectively phagocytose myelin debris (Phagocytosis index = 2.44±0.06). $FITC^+$ gate was determined by non-phagocytosing control cells (gray background plots). B-C) Monocytes from aged volunteers (≥55 years old) show significantly impaired myelin debris uptake (2.05±0.04). D) Age is significantly negatively correlated to myelin debris phagocytosis (slope=0.011, R-square=0.31). Adjusted p-values for pairwise comparisons in a Two-way repeated measures ANOVA with Tukey's procedure based on log-transformed outcomes, p=0.0014, n=36/group.

To identify possible mechanisms involved in the age-associated changes in phagocytic cells responsible for myelin debris clearance, we undertook gene expression profiling. We argued that human experiments might provide more general data, due to broad genetic heterogeneity among human subjects. This would also provide data that could be of direct relevance to patients and whose mechanisms could be explored subsequently using laboratory animal models. Microarrays were performed on myelin-phagocytosing monocytes from young and old HVs (Fig. 3.5). To define the mechanistic pathways enriched in monocytes upon phagocytosis, Ingenuity Pathway Analysis (IPA) found that the RXR pathway was differentially regulated upon myelin phagocytosis in young compared to old monocytes. RXRs are nuclear receptors that act both homodimerically and heterodimerically as ligand-activated transcription factors. In young cells, RXR heterodimer pathways were largely upregulated, with 19 positive regulators upregulated and 7 downregulated, while these pathways were largely downregulated in old cells. As RXR has several binding partners, activation and inhibition of several pathways were shown to be affected. Multiple RXR binding partners and downstream target genes were plotted with IPA, and the genes identified in the microarray of young cells showed mostly upregulation of positive regulators of RXR (Fig. 3.6A), while the profile of old cells showed mostly downregulation of genes in this pathway (Fig. 3.6B). Genes in green are upregulated upon phagocytosis in monocytes, and those in red are downregulated upon phagocytosis.

To confirm the results from the microarray in an independent cohort, quantitative real-time PCR was performed with a Retinoic Acid Signalling PCR Array (SABiosciences). This array measures 84 genes in the RXR pathway, providing insight into RXR regulation. After monocytes were exposed to myelin debris, cells were collected and relative gene expression was determined from isolated cDNA. Groups of pooled young or old myelin-phagocytosing cells were compared to young controls. The PCR arrays confirmed the results seen in the microarray, with RXR genes more highly upregulated upon myelin phagocytosis in young monocytes (Fig. 3.6C). This array also confirmed the changes seen in RXR protein expression in myelin-phagocytosing mouse macrophages, with an increase in RXRα and β expression in young monocytes and a decrease in aged cells. In addition the RXR binding partners RAR and PPAR are both similarly upregulated in young cells compared to old. These results further suggest a decrease in RXR in ageing cells.

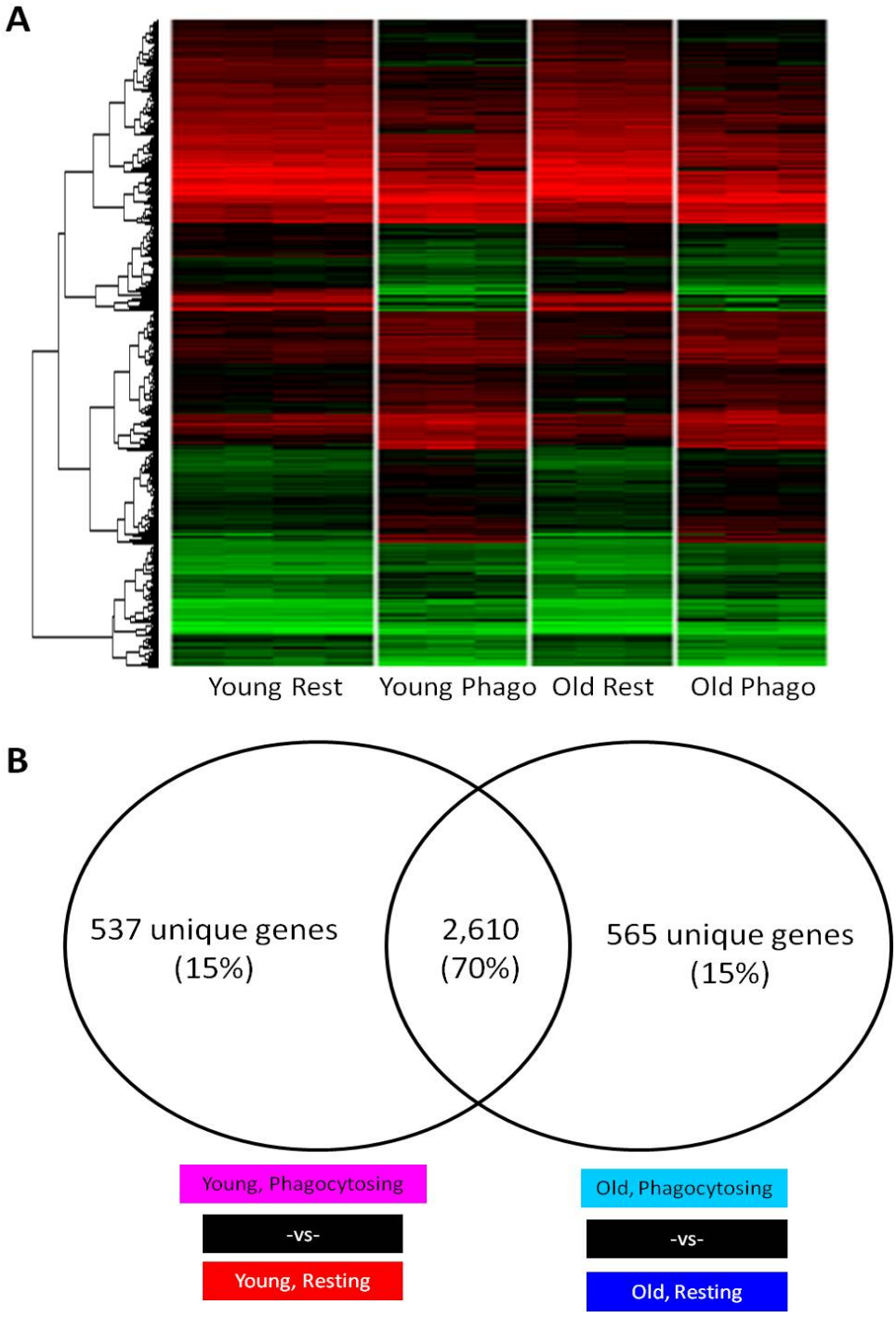

Figure 3.5 Myelin phagocytosis causes upregulation of a unique set of genes in young monocytes compared to old. Myelin was added to young (≤35 years old) and old (≥55 years old) human monocytes, and myelin-phagocytosing groups were compared to resting cells A) Heat maps of resting controls compared to phagocytosing cells show differential gene expression upon phagocytosis in young and old monocytes. B) Venn diagram of microarray data with significantly different gene sets upon phagocytosis in young and old groups, with 537 genes of interest in young and 565 in old.

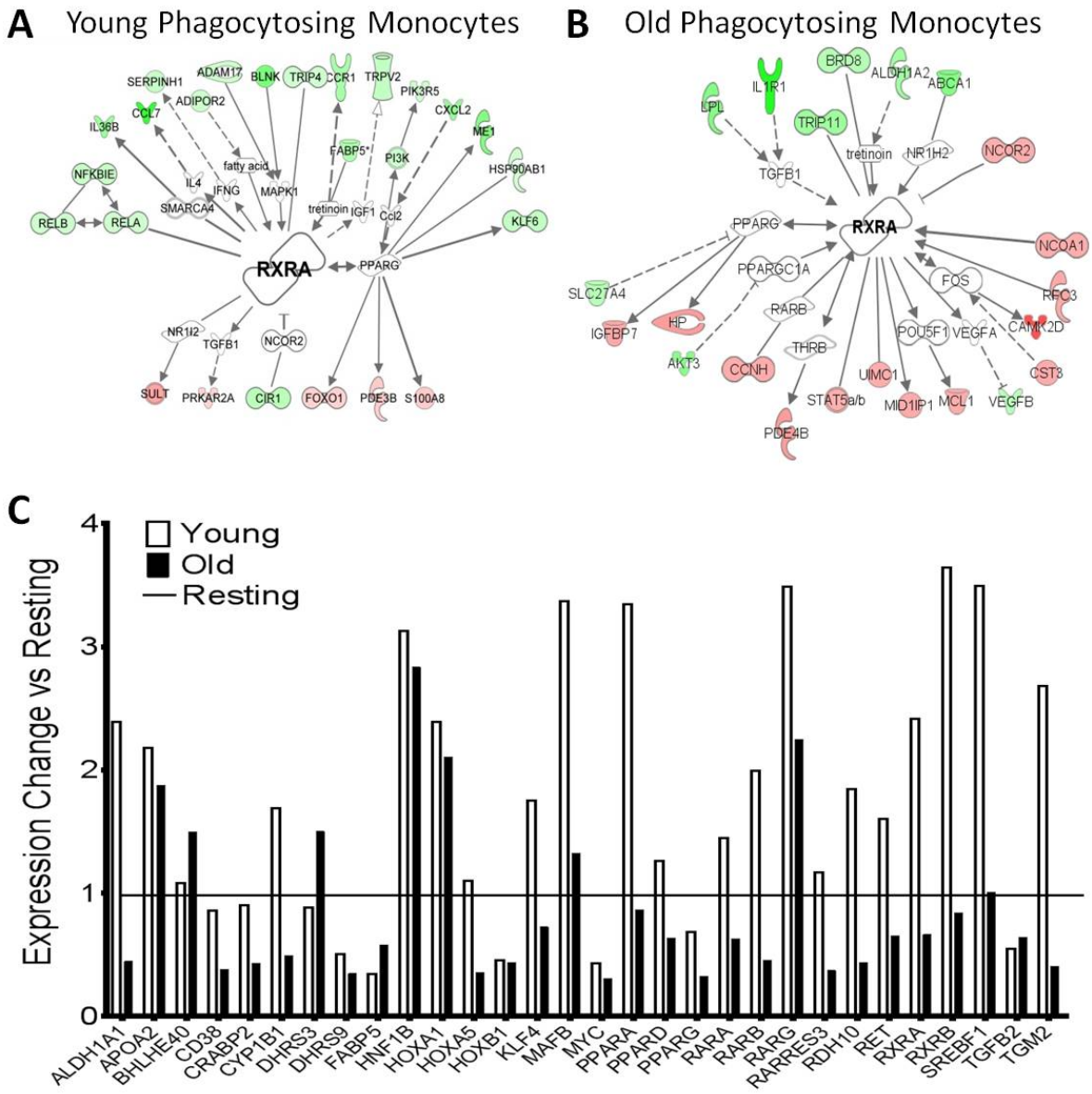

Figure 3.6 RXR pathways are downregulated in aged myelin-phagocytosing monocytes. A-B) Ingenuity Pathway Analysis (IPA) of microarray results showed that RXR-related genes with significant fold changes ($p<0.05$, $|FC| > 1.5$) were more highly upregulated in young-phagocytosing (A) compared to old-phagocytosing (B) groups (Green=upregulated, Red=downregulated). n=3/group. C) qPCR was performed using a Retinoic Acid Signalling RT2 Profiler PCR Array (SABiosciences). Expression changes were calculated by comparing young or old phagocytosing cells to resting controls. Genes in the RXR pathway with $|FC| > 1.5$ are shown here (White bars=Young cells vs Resting, Black bars=Old cells vs Resting). n=6/group.

3.5 Conclusions

In a heterochronic parabiosis model of remyelination, the circulatory systems of young and aged animals were connected, and the major young cell population recruited to the old animal's lesion site was identified as blood-derived monocytes, resulting in improved remyelination in aged animals (Ruckh et al., 2012). However, the underlying mechanisms of the age-related decline in myelin debris phagocytosis have not been fully elucidated. The *in vitro* data in this chapter indicate that ageing impairs myelin debris phagocytosis in blood-derived macrophages and microglia and this age-related decline may be related to a reduction in RXR pathways. The findings shown here indicate that the age-related decline in remyelination efficiency could be in part due to a deficiency in RXR activity in aged monocytes and macrophages, resulting in reduced phagocytosis by monocyte-derived macrophages. This pathway was further studied in subsequent chapters to determine if the defects in RXR signalling may be utilised to reverse this age-associated decline.

These data also confirm that there is a defect in the phagocytic ability of myelin debris phagocytosing macrophages with age, suggesting that increased myelin debris load in aged subjects is not only due to a decreased number of recruited phagocytes or an increase in the amount of myelin debris in aged animals. Microglia are also impaired *in vitro*, but monocyte-derived macrophages appear to phagocytose more myelin debris in both young and aged groups. Previous studies have indicated that microglia play a pivotal role in myelin debris phagocytosis; however, these studies used models where infiltrating monocytes did not play a role (Olah et al., 2012) or were only measured during the early stages of demyelination (Yamasaki et al., 2014), also suggesting that later stages of remyelination may be modulated by a blood-derived monocyte response.

This finding suggests that factors affecting macrophage plasticity in the ageing environment *in vivo* affect phagocytic ability. Since these cells have a great deal of heterogeneity and can adapt to different biological cues, modulating their environment and expression profiles can help recover age-related deficits, making them an ideal target for endogenous repair.

Chapter 4. Results

Retinoid X Receptor activation reverses the age-related deficiency in myelin debris phagocytosis and enhances remyelination

4. Results

Retinoid X Receptor activation reverses the age-related deficiency in myelin debris phagocytosis and enhances remyelination

We next asked whether the age-associated defects in RXR pathways in myelin-phagocytosing cells have *in vivo* consequences for remyelination by testing the hypothesis that RXR signalling is involved in the delayed myelin clearance that limits efficient remyelination with ageing. To do this, we reverted to animal models where this hypothesis could be tested experimentally.

RXRs belong to a family of receptors known as nuclear receptors (NRs). NRs contain both a DNA-binding domain and a ligand-binding domain, allowing them to act as transcription factors to directly activate gene expression by binding to low-affinity ligands (Nagy and Schwabe, 2004). These hormone receptors have a wide-reaching capacity as they are expressed in several cell types and regulate a complex array of genes. NRs are classified into six different families depending on their evolutionary divergence. Many of the receptors in Class III-VI are defined as “orphan receptors,” meaning they currently have no known ligands. The Class I receptors, the most well characterised, and their currently defined natural ligands are described in Table 4.1. The Class II receptors include RXR, chicken ovalbumin upstream promoter transcription factor (COUP-TF), hepatocyte nuclear factor 4 (HNF-4), Tailles-related receptor (TLX), Photoreceptor specific nuclear receptor (PNR) and testis receptor (TR). Of these, RXR binds to several Class I receptors and regulates genes expression of their downstream targets. Class III receptors are steroid receptors and include glucocorticoid receptor (GR), androgen receptor (AR), progesterone receptor (PR), oestrogen receptor (ER), and oestrogen related receptor (ERR). Class IV includes NGF induced clone B (NGFI-B), Nurr1, and Nor1; Class V is steroidogenic factor 1 (SF-1); and Class VI is germ cell nuclear factor (GCNF) (Aranda and Pascual, 2001).

Due to their complex function, these receptors have several components that allow for gene transcription and receptor function. They consist of six domains: an amino terminal region (consisting of two domains), DNA-binding domain (DBD), hinge region, ligand binding domain (LBD), and the C-terminal domain (Fig 4.1). The amino terminal region generally contains an autonomous transcriptional activation

function (AF-1) to activate the receptor in the absence of ligands. The DBD consists of two helix-forming Zn^{2+} fingers containing four cysteines, zinc ions, and carboxy terminal extension all acting together to recognise DNA-response elements. The hinge region acts to rotate the DBD. The most significant region for receptor activation is the LBD. This domain allows for ligand binding, homo/hetrodimerisation of NRs, and activation of downstream transcription. The LBD varies greatly in size between NRs, depending on the size of ligands and their receptor affinity (Aranda and Pascual, 2001).

Nuclear Receptor	**Isoforms**	**Ligands Identified**	**FDA-Approved Drugs**	**Binding to RXR**
Retinoic Acid Receptor (RAR)	α,β,γ	All-trans Retinoic Acid	T-retinoin	Nonpermissive Heterodimer
Vitamin D Receptor (VDR)	N/A	Vitamin D3	Cholecalciferol	Nonpermissive Heterodimer
Thyroid Hormone Receptor (TR)	α,β	Thyroid hormone	Levothyroxine	Nonpermissive Heterodimer
Pregnane X Receptor (PXR)	N/A	Pregnolone, Glucocorticoid	N/A	Nonpermissive Heterodimer
Constitutive androstane receptor (CAR)	α,β	Androstenol	N/A	Nonpermissive Heterodimer
Peroxisome proliferator-activated receptor (PPAR)	α,γ,δ	Unsaturated fatty acids, Eicosanoids	Pioglitazone, Rosiglitazone, Finofibrate	Permissive Heterodimer
Liver X Receptor (LXR)	α,β	Oxysterol	N/A	Permissive Heterodimer
Farnesoid X Receptor (FXR)	N/A	Chenodeoxycholic acid, Fexaramine	N/A	Permissive Heterodimer
Retinoic acid orphan receptor (ROR)	α,β,γ	Unknown	N/A	Unknown
Retinoid X Receptor (RXR) – Class II	α,β,γ	9-*cis* Retinoic Acid, Docosahexanoic acid	Bexarotene	Homodimer, Homotetramer

Table 4.1: Class I Nuclear Receptors and their association with Retinoid X Receptors. Class I NRs bind to RXR to form permissive and nonpermissive heterodimers. This table highlights the currently classified Class I NRs along with their known ligands, approved drugs, isotypes, and binding to RXR. Adapted from (Aranda and Pascual, 2001).

Once the LBD is activated, the DBD binds to hormone response elements for each NR (Szanto et al., 2004; Zilliacus et al., 1994). In general, RXR heterodimers consist of the RXR element upstream and the binding partner downstream (Kurokawa et al., 1993). When the LBD is activated, many NRs perform auto-regulatory functions by synthesising or degrading their own ligands (Baker, 2011; Dave, 2012; Evans and Mangelsdorf, 2014; Sarang et al., 2014). In the absence of a ligand, NRs repress activation of downstream genes by binding to the hormone response elements and co-repressors. Several co-repressors have been identified, including silencing mediator for retinoic and thyroid hormone receptors (SMRT), nuclear co-repressor (NCoR) or small ubiquitous nuclear co-repressor (SUNCoR) and histone deacetylases (HDACs) (Chen and Privalsky, 1995; Chen and Evans, 1995; Horlein et al., 1995). These co-repressors prevent transcription of downstream genes and allow NRs to perform transcriptional repression of their target sequences (Chen and Evans, 1995; Moras and Gronemeyer, 1998; You et al., 2013). When a ligand binds to the LBD, co-activators are recruited to this site and co-repressors are released. These co-activators include steroid receptor coactivator 1 (SRC-1), nuclear coactivator 2 (NCoA2), steroid receptor coactivator 2 (SRC-2), p300, and cyclic adenosine monophosphate-response element binding protein (CBP). Through histone acetyl transferase (HAT), HDAC co-repression is released and acetylation leads to an activated state (Lonard and O'Malley, 2012). These mechanisms are highlighted in Fig 4.1.

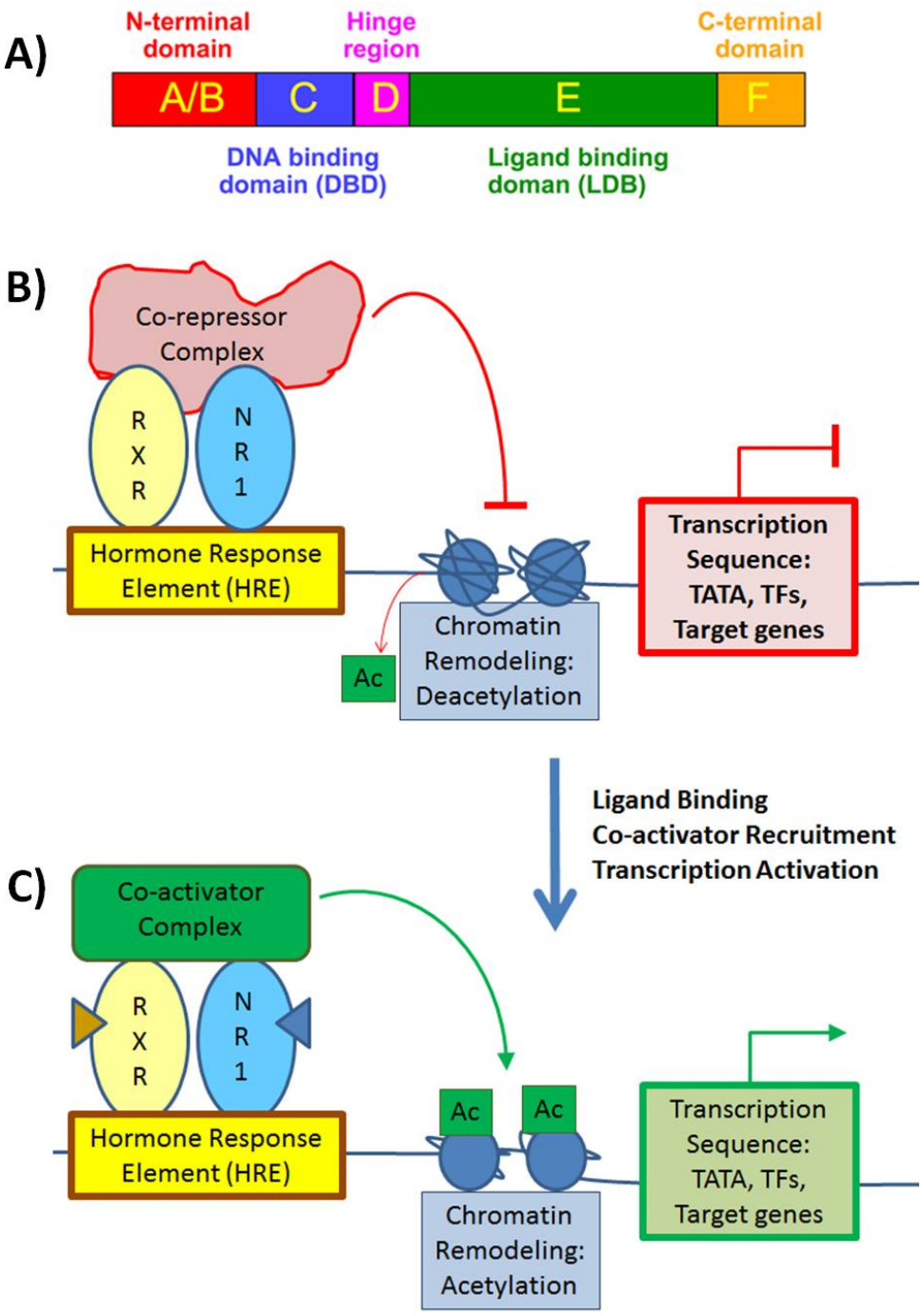

Figure 4.1: Nuclear receptors act as ligand-binding transcription factors. A) NRs are composed of both a DNA-binding (DBD) and a Ligand-binding domains (LBD). Once the NRs dimerise through the LBD dimerisation motif, they use the DBD to bind to their respective hormone response elements (HREs). B) Co-repressors, such as NCoR, SUNCoR, and SMRT, bind to RXR and its NR binding partners to prevent activation of the HRE by deacetylating histones and stopping transcription. C) Once ligands for RXR and its NR binding partner activate their respective receptors, co-activator complexes consisting of SRC1-3, NCoA2, CBP, and p300 are recruited and allow for histone acetylation and transcription of downstream target genes. (Adapted from Aranda and Pascual, 2001).

Retinoid X Receptors

Retinoid X receptors (RXRs) act as a binding partner for several Class I NRs, resulting in the expression of a large variety of genes. Due to extensive heterodimerisation, RXR pathways have a far-reaching effect in different cell types. They are known to be activated by endogenous ligands (Table 4.1) and can function as permissive and non-permissive heterodimers with other NRs. Permissive heterodimers allow for activation of the target sequence by ligands for either RXR or one of its NR binding partners. Permissive binding parts include, PPAR, LXR, and FXR. Ligands for both receptors may also act together synergistically to increase downstream expression (Chawla et al., 2001; Ogawa et al., 2005; Roszer et al., 2013). Non-permissive heterodimers form when the RXR ligand is not sufficient to activate the complex, and the binding partner's ligand must be present for transcription of downstream genes. In these cases, RXR activation is inhibited even in the presence of its ligand. Examples of non-permissive binding partners are VDR, RAR, and TR (Shulman et al., 2004). RXR can also form homodimers with other RXRs. These homodimers are activated by RXR ligands and result in RXR-specific gene transcription (Yasmin et al., 2010; Yasmin et al., 2004).

Three main isoforms of RXR exist throughout the body. They regulate many processes from cellular proliferation to lipid metabolism. Each isoform has expression in various regions. RXRα is most commonly expressed in the liver, kidney, spleen, and epidermis. It also has the highest expression in monocytes and monocyte-derived macrophages (Roszer et al., 2013). RXRβ is largely expressed in the CNS as well as throughout the body. RXRγ shows the highest expression in the muscle and CNS (Brown et al., 2000; Kastner et al., 1996; Krezel et al., 1996). All three isoforms of RXR can provide compensatory functions for each other when the others are downregulated. They can be expressed in both the cytoplasm and nucleus of cells. Upon activation of NRs, RXRs are shuttled and localise to the nucleus. Through this nuclear localisation, RXRs are able to homo- and heterodimerise to activate downstream genes (Baumann et al., 2001; Katagiri et al., 2000; Prufer et al., 2000).

In this chapter, the role of RXRs in ageing myelin-phagocytosing macrophages was studied to determine if this extensive pathway plays an age-related role in myelin debris phagocytosis and can be targeted to reverse the age-related decline in myelin debris clearance and CNS remyelination.

4.1 RXRα expression declines with age in myelin-phagocytosing BMMs

As many genes in the RXR pathway were downregulated with age (Fig. 3.5), we first assessed the levels of protein expression of this receptor family in monocyte-derived macrophages, since they appear to play a key role in myelin debris phagocytosis (Kotter et al., 2001; Kotter et al., 2005; Ruckh et al., 2012). BMMs were used to study expression and modulation of nuclear receptor pathways during myelin debris phagocytosis. RXRα expression in myelin-phagocytosing macrophages was confirmed using immunocytochemical staining of Iba1+ BMMs (Fig. 4.2A) with RXRα found to be localised to the nucleus (Fig. 4.2B). BMMs from ageing mice (from 2mo to 24mo) were incubated with myelin debris, and phagocytosing cells were lysed and collected for protein analysis. Using western blots, the protein expression of RXRα in myelin-phagocytosing BMMs was determined and compared to β-actin controls at 2mo, 8mo, 12mo, 16mo, and 24mo (Fig. 4.2A-C). The RXRα band has a weight of 55kd with another non-specific band indicated on the gel (Fig. 4.2C); this distribution of bands has also been seen in previous studies (Kuhla et al., 2011; Menéndez-Gutiérrez et al., 2015). By isolating BMMs from mice of different ages, the change in RXRα expression was correlated with ageing. In young, 2mo macrophages, RXRα expression was highest. BMMs isolated from adult mice had a slow decline in RXRα protein expression, which reached statistical significance ($*p<0.05$) when comparing RXRα expression in the youngest (2mo) to the oldest age group (24mo) (Fig. 3.4D), indicating that this receptor is significantly affected by ageing in myelin-phagocytosing macrophages.

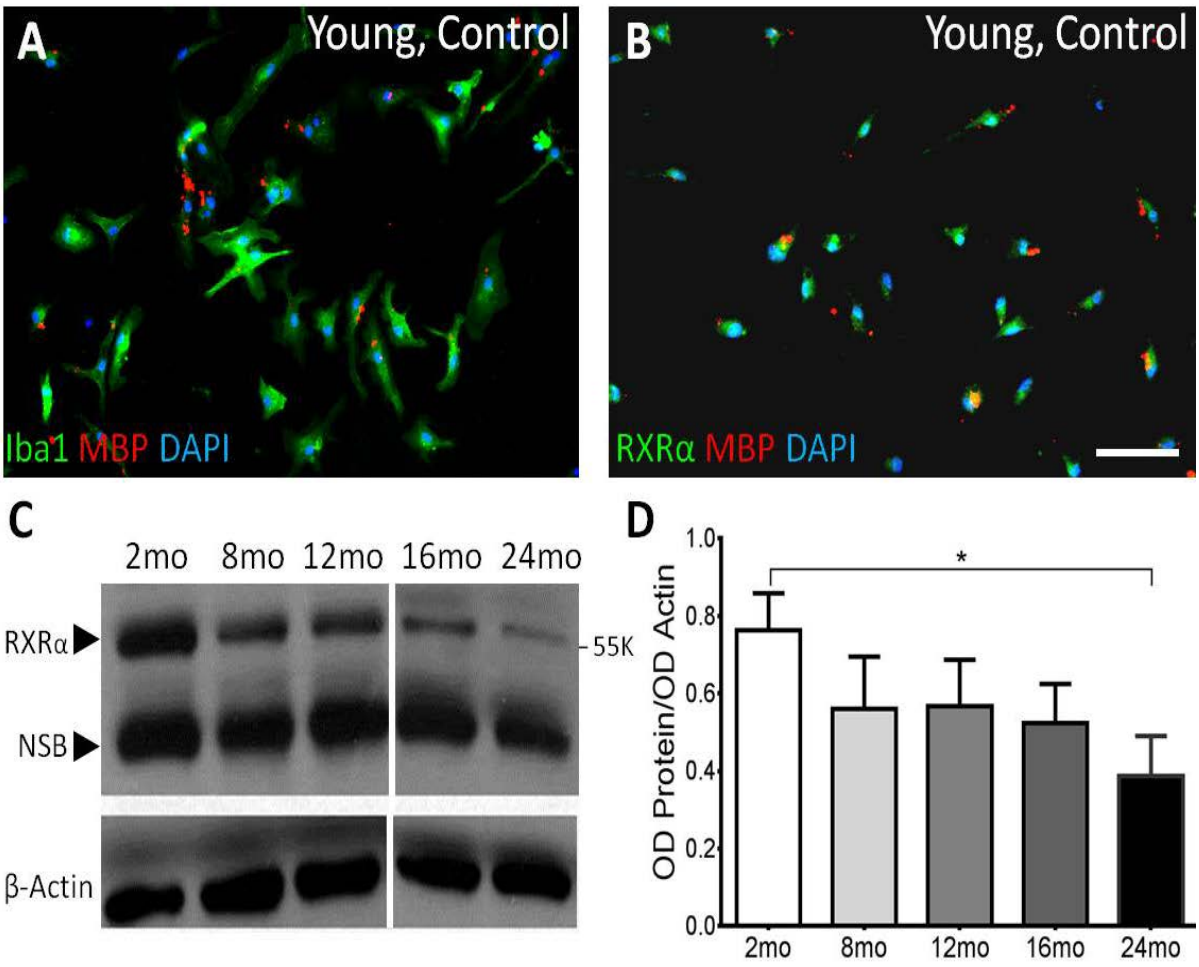

Figure 4.2 Myelin-phagocytosing BMMs undergo an age-related decline in RXRα expression. A-B) Immunocytochemistry of Iba1+ cells revealed (B) nuclear localisation of active RXRα in myelin-phagocytosing macrophages. Scale bar = 50μm. C) Levels of RXRα expression in macrophages derived from 2-24mo mice were determined by western blot and analysed by ImageJ. Dividing line indicates different gels. RXRα band is indicated at 55K, with nonspecific bands (NSB) at lower values indicated on the gel. D) There was a significant reduction in RXRα expression in macrophages between 2mo and 24mo mice, measured by optical density (OD) of RXRα relative to actin controls. One-way ANOVA and post-hoc Tukey's multiple comparisons test, *p<0.05, n=3/age group.

Although the other two isoforms of RXR show little expression in macrophages (Roszer et al., 2013), expression levels of both RXRβ and RXRγ were examined in BMM cultures as all three isoforms of RXR are expressed in the CNS (Dyall et al., 2010) and can show compensatory functions due to the loss of one isoform (Li et al., 2000). Immunocytochemistry staining of RXRβ did not have any reactivity in culture, while RXRγ cultures did show some nuclear localisation (Fig 4.3A). However, this result was not reproducible, suggesting nonspecific binding of this antibody *in vitro*. Western blots against both isoforms analysed with ImageJ also revealed inconsistent band expression, with only an n=2 in each age group (Fig 4.3B-C). These bands were only visible after 30min of incubation time with the Supersignal detection reagent, used for proteins with low immunoreactivity. These results further suggest that the main isoform expressed in myelin-phagocytosing BMMs is RXRα.

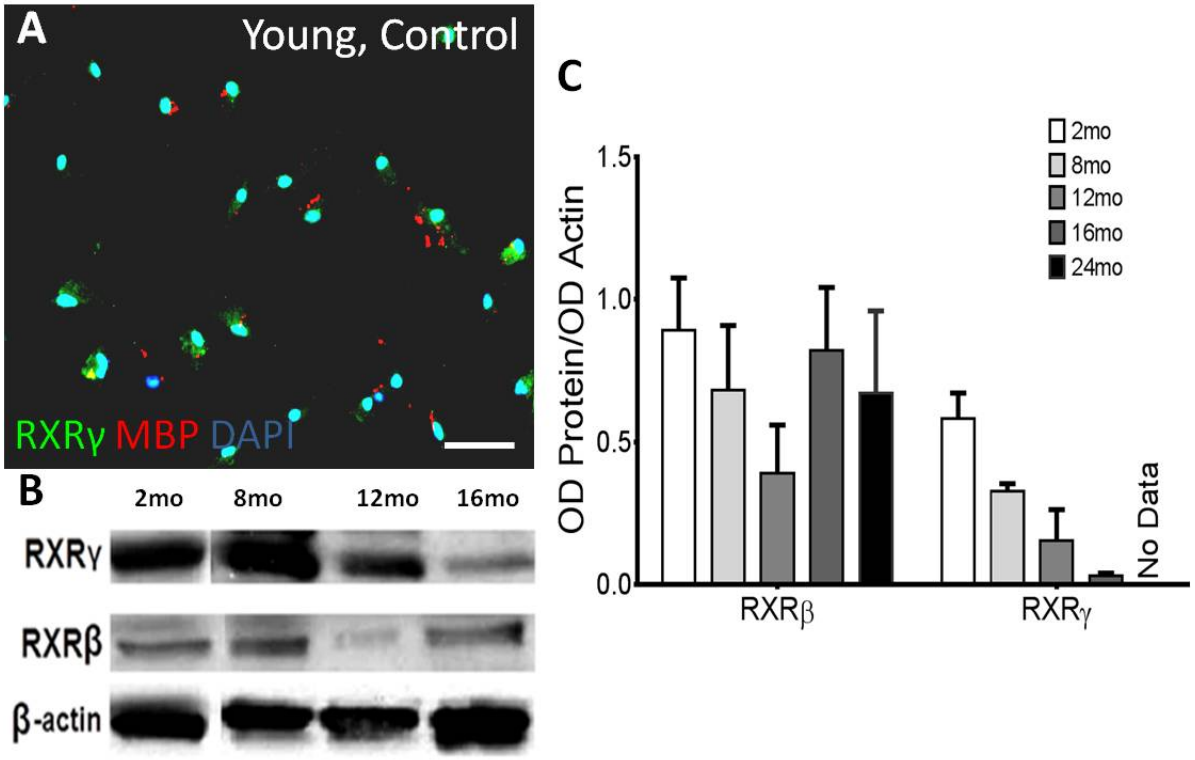

Figure 4.3 RXRβ and RXRγ expression are not consistent in ageing BMMs. A) Immunocytochemistry showed nuclear localisation of RXRγ in myelin-phagocytosing macrophages, but expression was not highly reproducible (n=2). Scale bar = 50μm. B-C) Levels of RXRβ and RXRγ expression in macrophages derived from 2-24mo mice were determined by western blot and analysed by ImageJ. n=2/age group. Blots were not reproducible

4.2 The RXR agonist 9-*cis* retinoic acid enhances myelin phagocytosis in aged macrophages

There are several synthetic ligands for RXR, and one of the most common is the 9-*cis* form of retinoic acid (9cRA). 9cRA is known to be a high affinity ligand for RXR and may be produced endogenously during retinoid metabolism (Heyman et al., 1992). Here, 1μM 9cRA was added to myelin-phagocytosing BMMs for 24h to activate RXR *in vitro* before adding myelin debris to macrophage cultures. Macrophages were labelled with the myeloid marker Iba1 and ingested myelin was labelled with MBP. Young (2mo) controls were able to effectively clear myelin, and the addition of 9cRA did not augment phagocytosis (Fig 4.4A-B). However, old (32mo) macrophages showed significantly reduced myelin debris clearance (Fig. 4.4C, 10%±SEM) compared to young. When RXR was activated by 9cRA, significantly more old BMMs were able to phagocytose debris (Fig. 4.4D-E, 34%±SEM). Myelin debris phagocytosed per macrophage was also calculated by determining the area of MBP+ staining per BMM. There was also a decrease in the amount of myelin debris phagocytosed per aged macrophage (Fig 4.4F). There was still a significant difference in myelin debris phagocytosis between 2mo and 32mo+9cRA treated cells, indicating that RXR activation cannot restore phagocytic ability completely, but the addition of 9cRA has the potential to enhance debris clearance in aged animals.

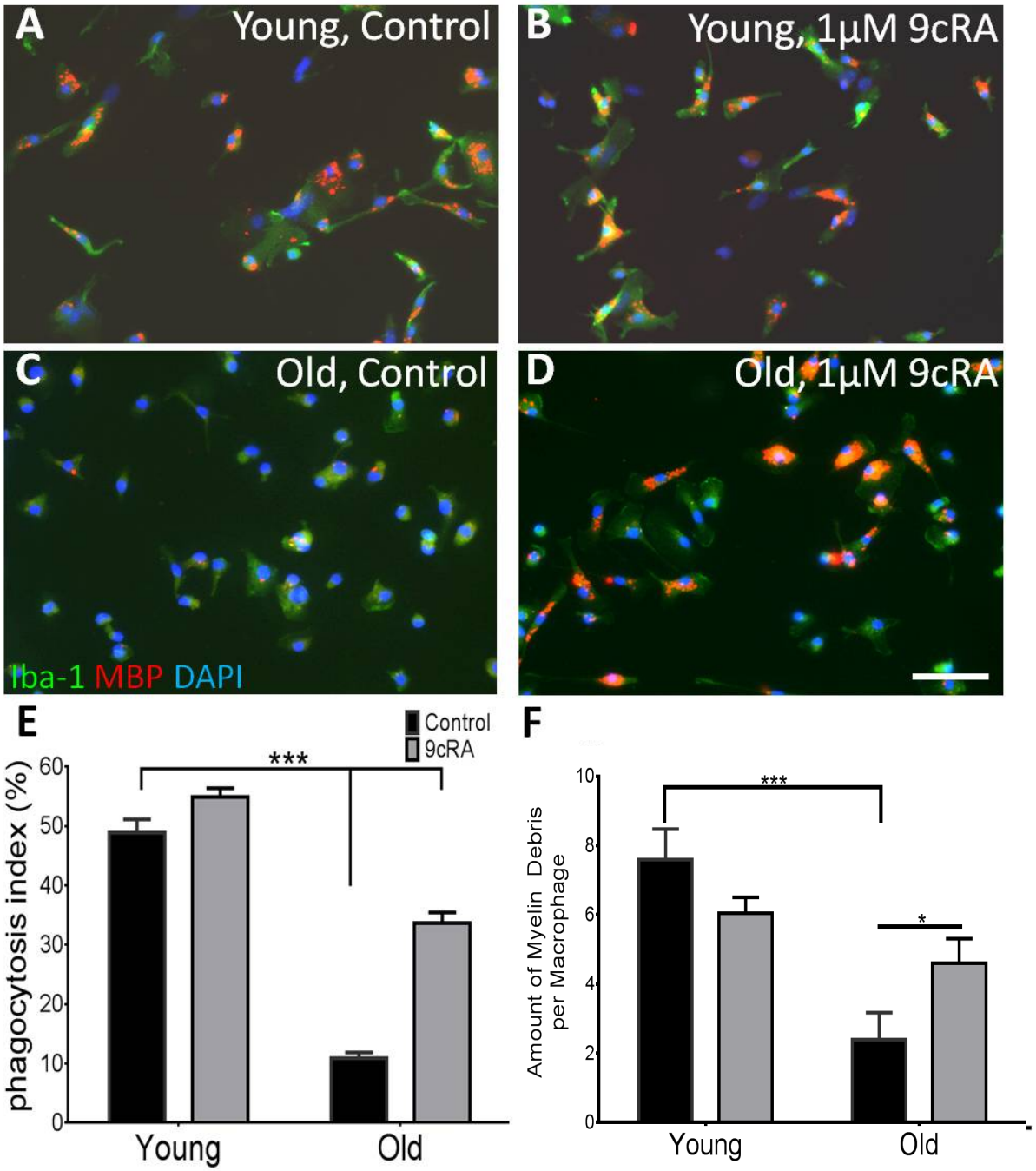

Figure 4.4 RXR agonist 9cRA stimulates myelin debris phagocytosis in aged macrophages. A-B) Macrophages from 2mo mice are able to effectively consume myelin debris, both before (A, 48.9%±2.6%) and after treatment with 9cRA (B, 54.9%±1.5%). C) However, 32mo senescent macrophages were not able to efficiently phagocytose debris. D-E) Adding 1µM 9cRA significantly increased myelin debris consumption in aged macrophages. >50% of young macrophages were able to effectively clear myelin, while only 10.9% (±1%) of old macrophages were able to; however, 9cRA significantly increased myelin clearance to 33.6% (±1.7%) in aged cells. F) The amount of myelin debris phagocytosed per macrophage was also measured, showing a similar effect as (E). Scale bar = 50µm. Two-way ANOVA and posthoc Sidak's multiple comparisons test, ***$p<0.001$, *$p<0.05$ n=6/age group.

4.3 Loss of RXR function in young macrophages impairs myelin debris clearance

Since there was no significant difference when 9cRA was added to 2mo BMMs, we hypothesised that ligand-independent, constitutive RXR activation (Laursen et al., 2012; Nagpal et al., 1993) may be one of the key differences between young and old cells. The synthetic antagonist for RXR, HX531, was used to block RXR and determine if RXR activation was necessary for efficient myelin debris phagocytosis in young BMMs. After antagonist treatment and incubation with myelin debris, cells were stained with CD11b. Myelin+/CD11b+ cells were quantified by immunocytochemistry and flow cytometry. Young cells efficiently phagocytosed the DiO-labelled myelin (Fig. 4.5A-B, 36.6-42%), while macrophages treated with 10μM HX531 showed reduced myelin debris uptake and significantly fewer double positive cells (Fig. 4.5C-E, 19.8-23.8%). When RXR activation is inhibited by HX531, myelin debris phagocytosis is significantly impaired in young BMMs, suggesting that RXR is necessary for efficient myelin debris phagocytosis in young macrophages.

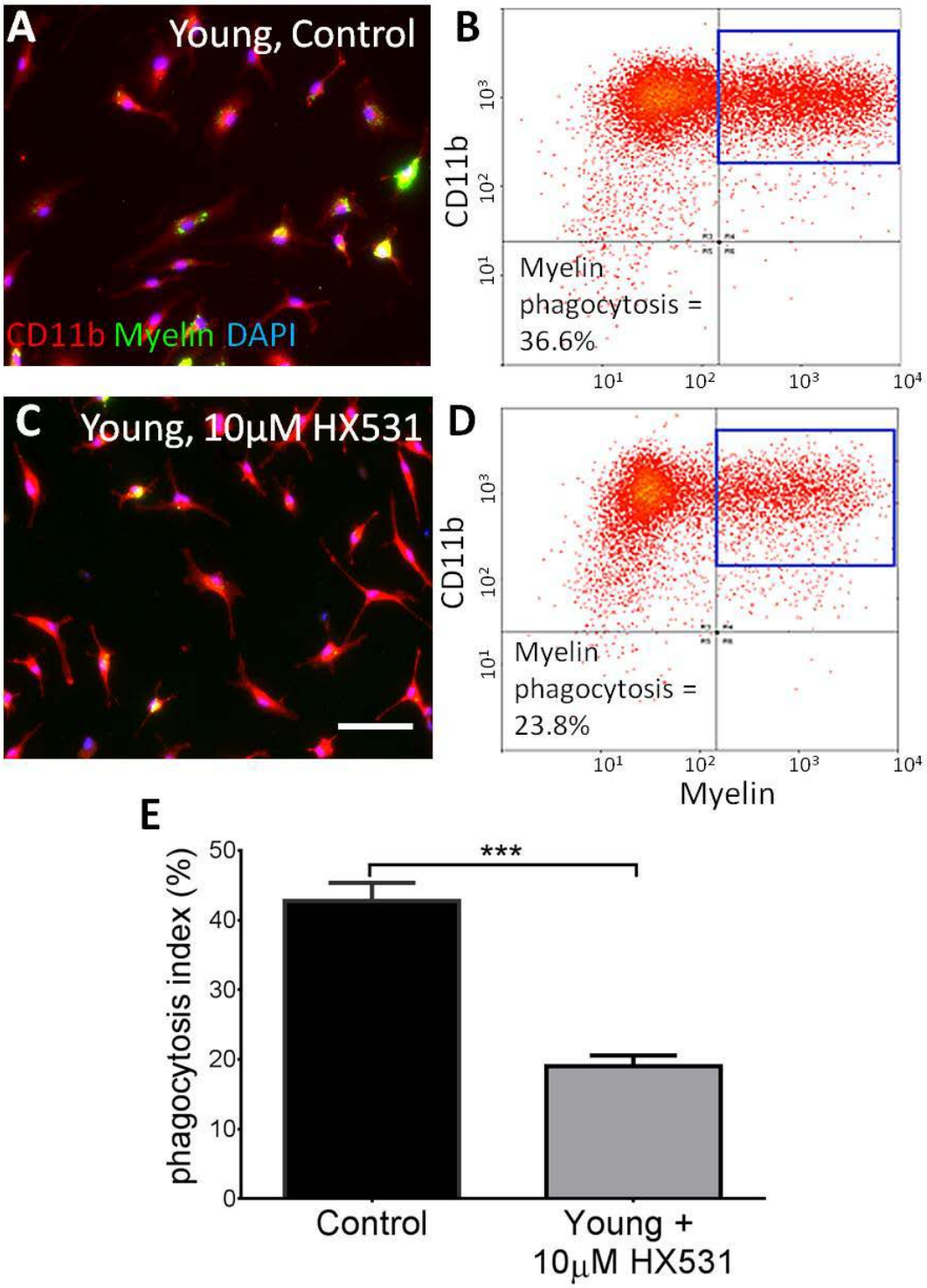

Figure 4.5 RXR antagonist slows myelin debris uptake in young macrophages. A-D) DiO-labelled myelin was used to measure myelin debris clearance by immunocytochemistry and flow cytometry in young macrophages (A,B) and young macrophages treated with a synthetic RXR antagonist, HX531 (C,D). E) Blocking RXR with 10μM HX531 reduced myelin debris uptake in young BMMs from 42.8% (±2.5%) in young controls to 19.06% (±1.5%). Scale bar = 50μm. Student's t-test, ***p<0.001, n=4/treatment.

4.4 Loss of RXR function slows myelin debris uptake *in vivo*

This study utilised lysolecithin-induced demyelination due to its focal capacity, synchronous timeframe, mainly OL loss and OL remyelination, and infiltration of innate immune cells (highlighted in section 1.4.3). A Cre-lox model system was used to specifically target genes in myeloid-derived cells during toxin-induced demyelination. The Lysozyme M (LysM) Cre driver is expressed in all myeloid lineage cells. However, since microglia are derived from the yolk sac during early development, the LysM Cre has shown little recombination in these cells (Goldmann et al., 2013). Therefore, the major targets in LysM Cre recombination are the monocyte-derived cells. RXRα floxed mice were crossed with LysM Cre mice to produce both LysM-RXRα knockouts, mice with active Cre recombinase and the efficient deletion of RXRα from myeloid-derived cells, and LysM-RXRα wildtype mice, mice lacking active Cre recombinase with active expression of RXRα in myeloid-derived cells. The RXRα isoform was specifically chosen due to its high expression in macrophage cell types (Fig. 4.2-4.3, (Roszer et al., 2013)); it was expected to have the greatest effect. The following experiments tested the efficiency of remyelination with the absence of RXR in myeloid-derived cells.

Lysolecithin-induced focal demyelination was performed on 4mo WT ($LysMCre^{-}$ $RXR\alpha^{fl/fl}$) and KO ($LysMCre^{+}$ $RXR\alpha^{fl/fl}$) mice, and demyelinated lesions were stained with oil red O (ORO) to quantify myelin debris accumulation. ORO labels neutral lipids and effectively measures myelin debris in the demyelinated lesion. There was little ORO staining at 5dpl in the WT at early stages of demyelination, while there was significantly more diffuse ORO staining in the KO at this timepoint when OPC recruitment into the lesion is maximal (Arnett et al., 2004) (Fig 4.6A-B, G), indicating reduced myelin debris clearance in the KO at 5dpl. Myelin debris clearance was more advanced at 14dpl (Fig 4.6C-D) and 21dpl (Fig 4.6E-F) in both WT and KO, the staining being more punctate and consistent with intracellular staining of phagocytosed myelin (Kotter et al., 2005). The greater level of myelin debris accumulation at early timepoints in the RXRα KO (Fig 4.6G) suggests impaired myelin debris phagocytosis at early stages of OPC differentiation in these mice.

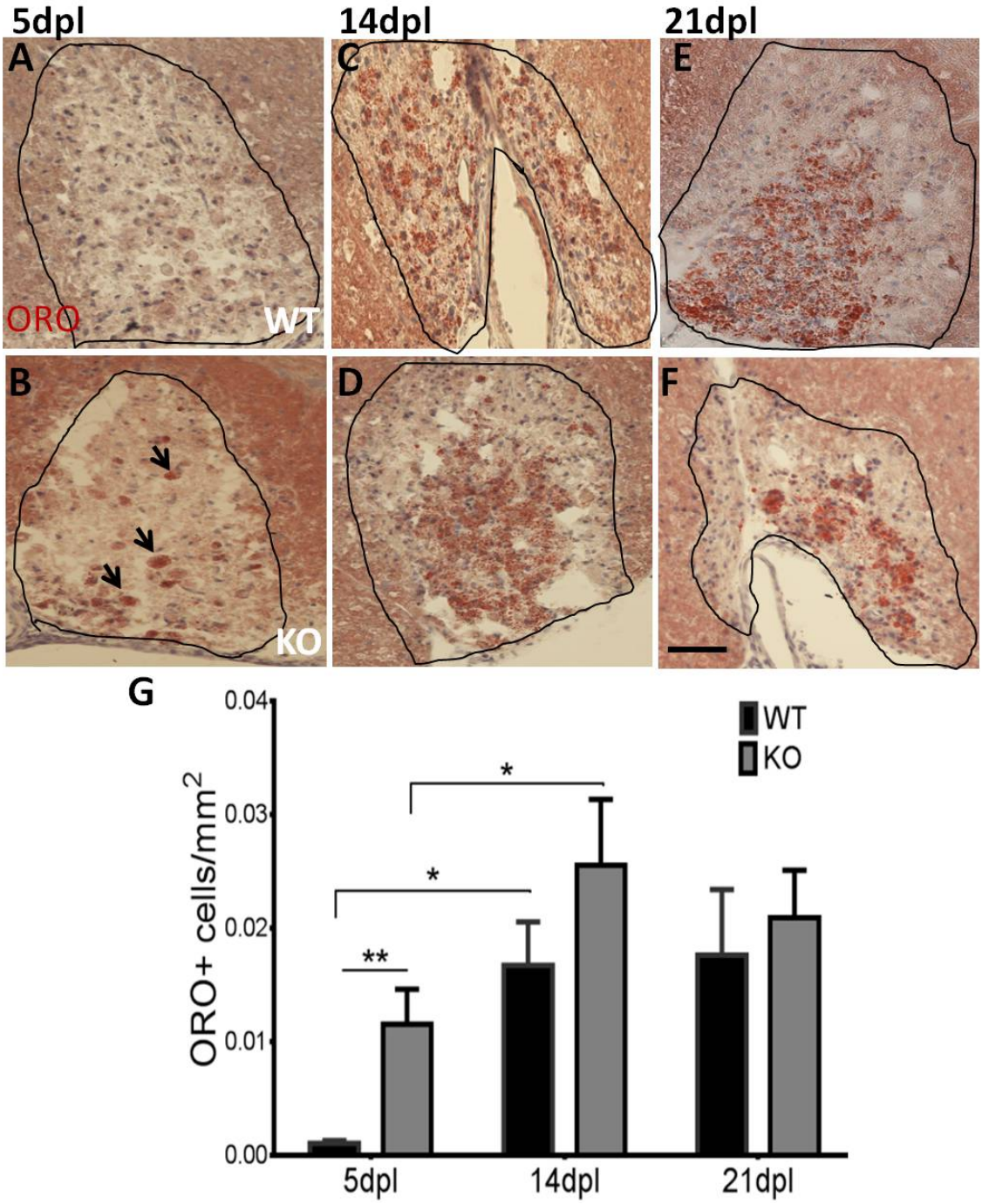

Figure 4.6 Loss of RXRα function in young macrophages slows myelin debris uptake *in vivo*. Lysolecithin-induced focal demyelination is denoted by black outlines. A-G) Oil red O was used to label neutral lipids in demyelinated lesions of RXRα myeloid-specific knockouts at 5dpl (A-B), 14dpl (C-D), and 21dpl (E-F). G) Myelin debris uptake was significantly slowed in KOs at 5dpl, with extracellular myelin debris indicated by black arrows in (B). At 14dpl and 21dpl, there is an increase in intracellular lipids, consistent with previous studies (Kotter, Zhao et al. 2005). Staining is more punctate and less diffuse at these timepoints. Scale bar = 100µm. Two-way ANOVA and post-hoc Sidak's multiple comparisons test, *p<0.05, **p<0.01, n=4/timepoint

Iba1, a marker of activated macrophages and microglia, was used to label phagocytosing cells (Fig 4.7A-B). Iba1 was visualised with diffuse staining throughout the lesion, providing effective demarcation of the lesion but was difficult to quantify as almost all DAPI-labelled cells appeared Iba1+. The staining provided evidence of macrophage activation throughout the lesion. The effects of this early accumulation of myelin debris were next studied with markers of OPC differentiation.

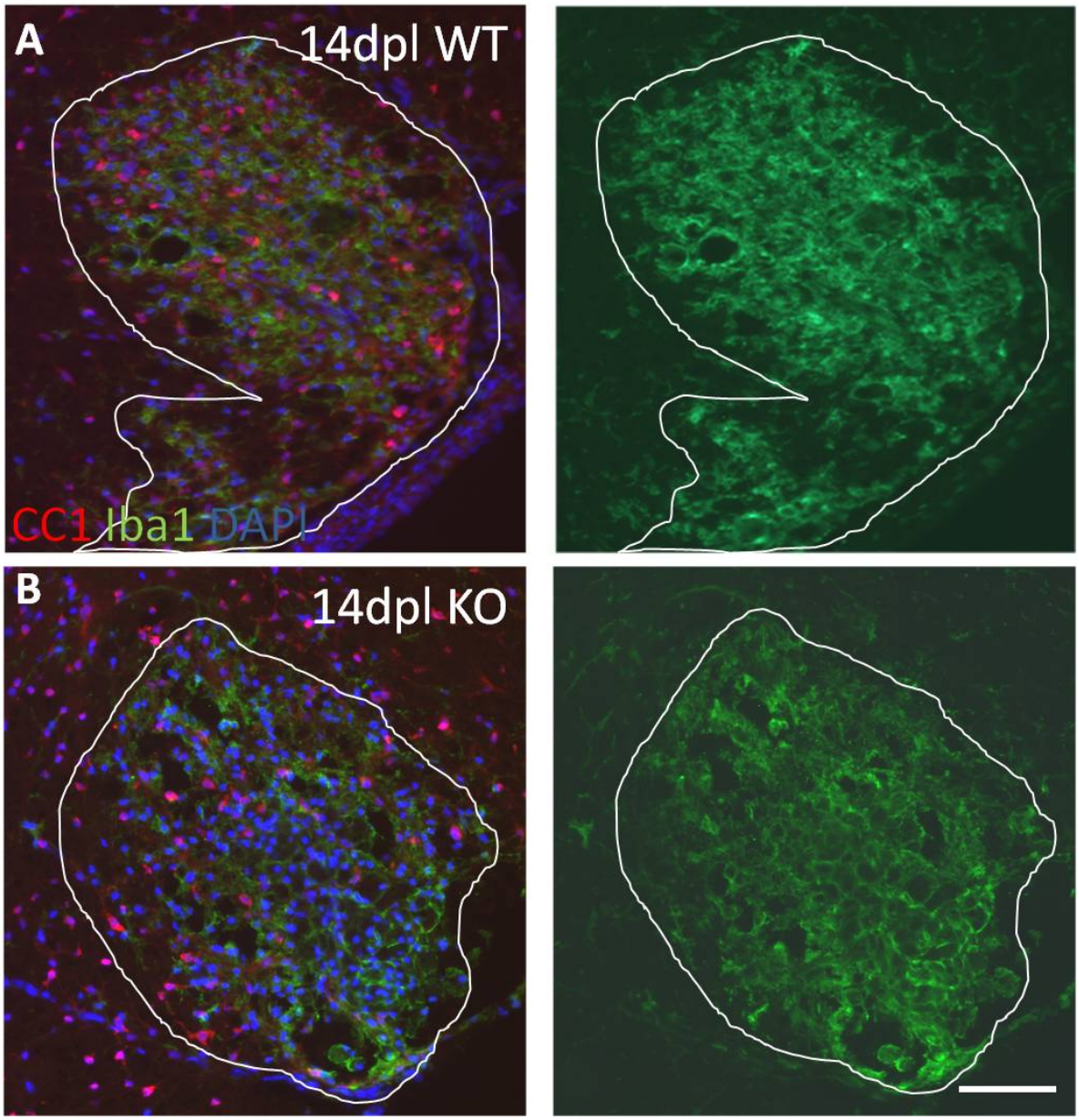

Figure 4.7 Macrophages invade the demyelinated lesion. Lysolecithin-induced demyelinated lesion is denoted by DAPI-labelling, and Iba1 was used to label blood-derived macrophages and microglia. A-B) In both WT and KO lesions, a prominent macrophage response is evident. Scale bar = 100µm.

4.5 Macrophage-specific RXR knockouts experience slowed OPC maturation

Since myelin debris contains inhibitors of OPC differentiation (Baer et al., 2009; Kotter et al., 2006; Syed et al., 2011), a delay in myelin debris clearance can impact OPC differentiation. To assess remyelination in the absence of myeloid-specific RXRα, several oligodendrocyte lineage and myelination markers were used: Olig2 is a marker for all stages of the OL lineage, from OPC to mature OL; CC1 is a marker for mature OLs and labels the cell body; and proteolipid protein (PLP) is a marker of myelinating OLs (Emery, 2010; Lu et al., 2002). The density of CC1+ and Olig2+ cells was determined using immunohistochemistry. Antibodies against CC1 stained mature OLs at 14dpl (Fig 4.8A-B) and 21dpl (Fig 4.8C-D). At 5dpl, few CC1+ cells were present in the demyelinated lesion. By 14dpl, these CC1+ cells were more prevalent in both WT and KO lesions. However, there were significantly fewer CC1+ OLs in KO lesions at this timepoint. By 21dpl, there was no difference between CC1+ cells in the WT and KO lesions (Fig 4.8E). To confirm that this difference was not due to impaired recruitment of OPCs to the lesion, the total number of OL lineage cells was accounted for by dividing by the number of Olig2+ cells in each lesion. There were still significantly fewer CC1+/Olig2+ cells (Fig 4.8F) in the KO at 14dpl, suggesting delayed OPC differentiation in the myeloid-specific KO. In addition, Olig2+ cells in the same lesions (Fig 4.9A-D) showed a higher population of CC1-/Olig2+ cells (OPCs and early OLs) in the KO lesions at 14dpl, further suggesting that there are a greater number of OPCs present in the KO that have not differentiated. The OPC numbers were reduced and comparable to WT by 21dpl (Fig 4.9E), suggesting effective differentiation of OPCs by 21dpl in the KOs.

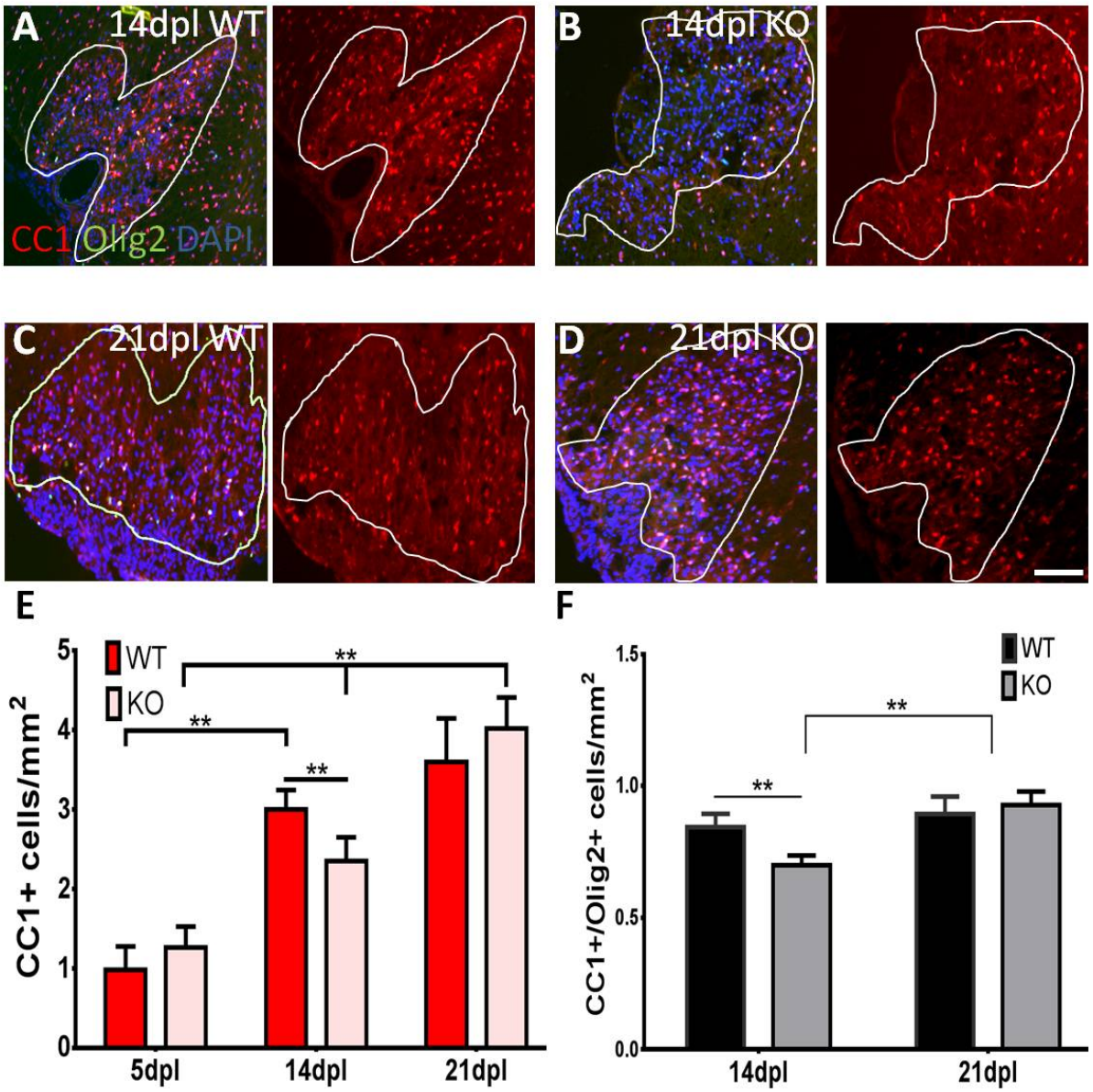

Figure 4.8 OPC maturation is impeded in RXR KOs. Lysolecithin-induced demyelinated lesion is denoted by DAPI-labelling. A-B) CC1 staining for mature OLs in the LysM-RXRα WT (A) and KO (B) mice. C-D) By 21dpl, CC1 marks many mature OLs in both the WT (C) and KO (D) lesions. E) At 14dpl, there are significantly more CC1+ cells in the lesions of WT mice compared to KOs. From 5dpl to 14dpl, there is a dramatic increase in CC1+ cells in both groups. From 14dpl to 21dpl, there is a significant increase in CC1+ cells in the KO. F) Olig2 is a pan-OL marker, so CC1+/Olig2+ cells indicate accurately marked mature OLs. At 14dpl, there is a significant difference in CC1+/Olig2+ cells between WT and KO. There is also an increase in CC1+ cells from14dpl to 21dpl in the KO, indicating slowed differentiation. Scale bars = 100µm. Two-way ANOVA and post-hoc Sidak's multiple comparisons test, **p<0.01.

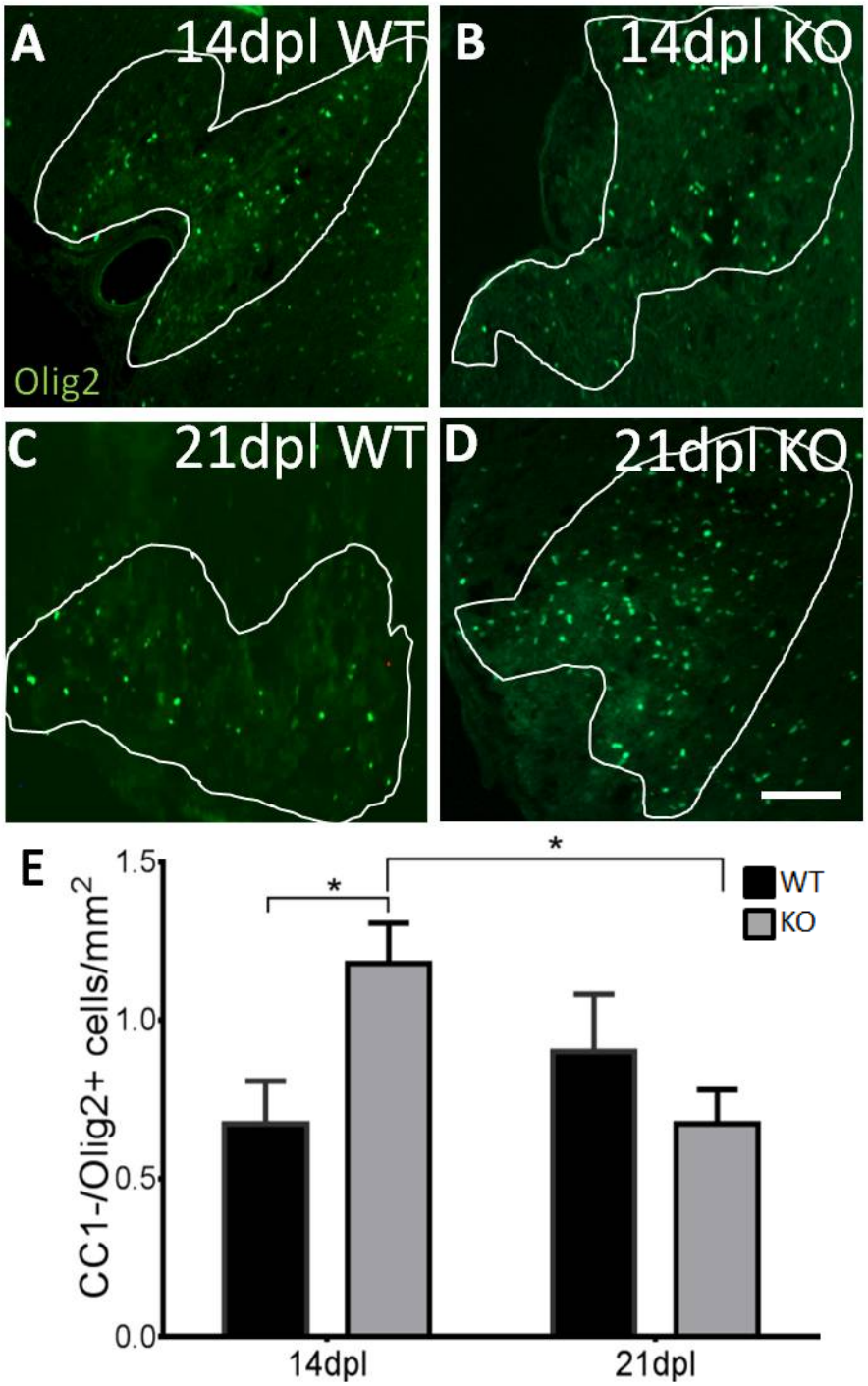

Figure 4.9 OPCs are more prevalent in LysM-RXRα KO lesions at 14dpl. Lysolecithin-induced demyelinated lesion is denoted by DAPI-labelling in previous figure (shown here in white lines). A-B) At 14dpl, there is a significant difference in CC1-/Olig2+ (OPCs) between WT and KO. C-E) There is also a decrease in CC1-/Olig2+ cells from 14dpl to 21dpl in the KO, indicating fewer undifferentiated OPCs by 21dpl. Scale bar = 100µm. Two-way ANOVA and post-hoc Sidak's multiple comparisons test; *p<0.05.

4.6 Delayed remyelination occurs in LysM-RXRα knockouts

In situ hybridisation of the myelinating marker PLP was performed at 14 and 21dpl. Unlike immunohistochemistry, ISH can be used to measure cell numbers of later myelinating markers such as PLP since this technique visualises mRNA expression localised to the nucleus (Fig 4.10A-D). The delay in OPC differentiation was confirmed in this experiment with less PLP+ myelinating OLs in the KO at 14dpl, indicating reduced differentiation. This impairment was again recovered by 21dpl, when there was no significant difference in PLP+ cells (Fig 4.10E).

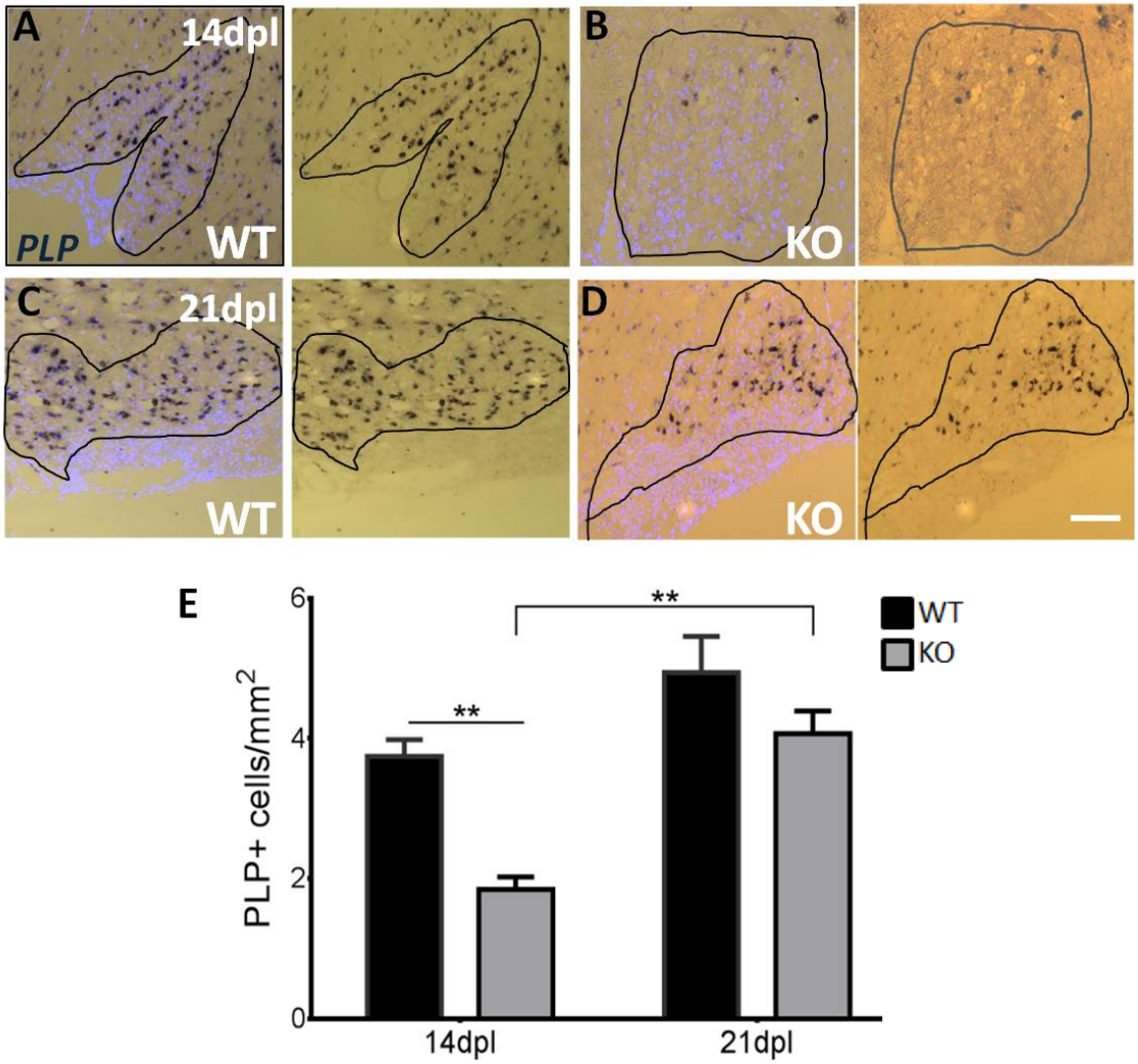

Figure 4.10 Macrophage-specific RXRα knockouts display delayed remyelination markers. A-E) *In situ* hybridisation of the myelinating marker proteolipid protein (PLP) in WT and KO lesions at 14dpl (A-B) and 21dpl (C-D). F) PLP+ myelinating OLs were decreased in KOs at 14dpl but not at 21dpl, suggesting a delay in PLP expression. Scale bar = 100µm. Two-way ANOVA and post-hoc Sidak's multiple comparisons test; n=4/group, **p<0.01.

Resin-embedded spinal cord tissues were stained and processed for electron microscopy (EM) analysis. EM was used to quantify the thickness of myelin sheaths within the demyelinated lesions (Fig 4.11A-B). EM images allowed visualisation of axonal cross-sections and myelin sheaths along with active mitochondria within axons. The relative amount of remyelination was measured using the g-ratio by comparing the thickness of the unmyelinated axon to the myelinated axon. The diameter of each axon was measured and divided by the total diameter including its myelin sheath. A higher g-ratio indicates a thinner myelin sheath (Fig 4.11C). A normally myelinated axon has a g-ratio of approximately 0.6-0.7, while a remyelinated axon has a g-ratio of >0.8 due to its thinner myelin sheath (Aharonowiz et al., 2008; Guy et al., 1989). Fully demyelinated axons with almost no myelin sheath have a g-ratio closer to 1. The delay in OL differentiation in KOs was associated with significantly thinner myelin sheaths (a larger g ratio) compared to WT at 14dpl, during the remyelination process (Fig 4.11D). WT mice at 14dpl had a mean g-ratio of 0.875, suggesting more remyelinated axons than KOs, with an average of 0.901. These findings indicate that RXRα plays an essential role in macrophage function during myelin debris clearance and CNS remyelination.

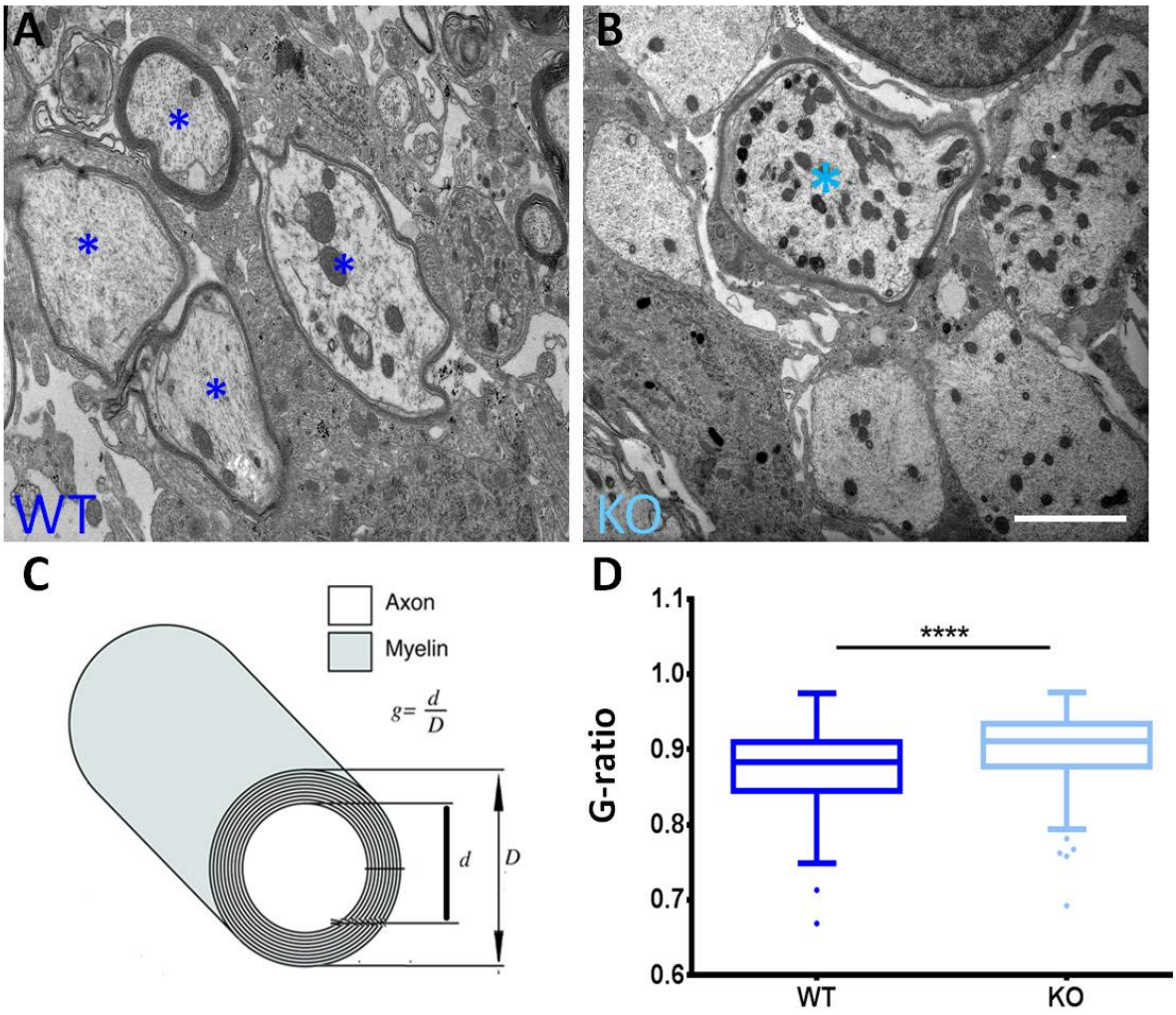

Figure 4.11 Macrophage-specific RXRα knockouts have decreased remyelination. A-B) Electron micrographs of demyelinated lesion tissue from both (A) WT and (B) KO mice at 14dpl. C) The g-ratio, used as a measure of myelin thickness and remyelination, was calculated by dividing diameter of each axon by the total diameter of the myelinated axon in representative lesions. D) Micrographs confirmed that KOs have a higher g-ratio (Mean=0.901, S.E.M =0.024) than WT (Mean=0.875, S.E.M.=0.026) and less remyelination at 14dpl. *Remyelinated axons. Scale bar = 2µm. Student's t-test; ****p<0.0001, n=4/group

4.7 Conclusions

In this chapter, the role of RXR in remyelination and macrophage function was studied using *in vitro* BMM cultures and a targeted knockout of RXR. RXR activation enhanced myelin debris clearance in aged macrophages and impairing RXR function *in vitro* reduced phagocytosis in young macrophages. To determine if RXR is a necessary component of efficient myelin debris clearance in young animals, RXR was knocked out specifically in myeloid-derived cells and resulted in significantly reduced OPC differentiation in knockout lesions, indicating that RXR has an important role in macrophage biology during remyelination. In the KOs, myelin debris clearance was reduced at 5dpl, in the early stages after demyelination and during OPC recruitment. By 14dpl and 21dpl, there was no difference in the myelin debris load between WT and KO mice. In addition, ORO staining at these timepoints was punctate and localised to cells within the lesion, likely macrophages and microglia. The accumulation of myelin debris at the early timepoint led to a delay in the OPC differentiation process.

Loss of RXR in young macrophages further resulted in slowed remyelination in lysolecithin-induced focal demyelination, indicating that this receptor is necessary for efficient remyelination. Although mice do fully recover in this model and it is difficult to see persistent demyelination, this model can be used to determine changes in OPC differentiation and identify potential barriers to remyelination. In this case, the KO showed decreased OPC differentiation and remyelination at 14dpl, while these processes occurred efficiently in the WT. By 21dpl, there was no difference between KO and WT mice, and remyelination completed successfully. This recovery in delayed remyelination may be due to the KO of only the most significant form of RXR in monocytes, RXRα. The other isoforms, β and γ, may help compensate for the loss of RXRα by 21dpl. These observations indicate that RXRα is necessary for active myeloid cell activity in the demyelinated lesion, and without this receptor, young mice experience delayed recovery after demyelination. This study identified RXR in myeloid-derived cells as a target for enhancing myelin debris clearance and promoting endogenous remyelination in the murine system, which led to the question of how activation of this receptor may affect myelin debris clearance in the human population.

Chapter 5. Results

Bexarotene reverses the decline of RXR pathways and myelin debris phagocytosis in MS patient monocytes

5. Results

Bexarotene reverses the decline of RXR pathways and myelin debris phagocytosis in MS patient monocytes

RXR activity was shown to be necessary in both *in vitro* and *in vivo* models of myelin debris phagocytosis and remyelination in chapters 3-4. Murine models provide a genetically-controlled, easily manipulated system to study this class of receptors. Due to the homogeneity between animal subjects, a smaller *n* number and fewer studies are required to test the function and expression of RXR in this system. As such, the studies shown here allowed for manipulation of RXR activity through ligand-modulated activation/inhibition and a knockout system of remyelination. It was possible to see the effects of targeting RXR in this controlled system due to the ease of experimental manipulation in models of demyelination/remyelination. However, the absolute predictive value of animal models in treatment strategies for disease remains difficult (van der Worp et al., 2010).

Although animal models provide an incredibly powerful predictive tool to study potential drug targets in human disease, confirmation of these targets should be performed in human studies as well. The heterogeneity and complex environment of human systems provides a barrier to well-controlled studies, but a large *n* number and effective control of certain variables in subjects (such as disease status, age, sex, race, etc.) can effectively overcome this barrier. This then allows for use of the human system to elucidate the efficacy of targets identified in animal models. Both healthy subjects and subjects with a disease of interest, in this case MS, can be manipulated in human models and studied. The last two results chapters in this thesis utilised samples from human MS patients and healthy volunteers (HVs) to study the role of RXR and its binding partner, PPARγ, in myelin debris clearance.

Monocytes were isolated from the PBMCs of HVs and MS patients from two age groups. Subjects were considered “young” if they were ≤35 years old and “old” if they were ≥55 years old. This distinction was made due to the chronic and progressive nature of MS as well as the impairment of many biological processes

with age. The average age for MS diagnosis is 30 years old, so ≤35 years old constituted the young group of patients and HVs (Kremenchutzky et al., 2006). In addition, to provide a significant age difference and a greater likelihood to discover changes between age groups, an age difference of ≥20 years was chosen. Human *in vitro* models provide a more genetically diverse system compared to mice, so testing therapeutics and determining their effects on monocytes from humans allows for a more direct comparison of the effects of patient status and ageing in the human system.

There is currently only one FDA-approved drug that directly targets RXR: Bexarotene. Bexarotene (brand-labelled Targretin) is currently used as an antineoplastic agent to treat cutaneous T cell lymphoma. As a vitamin A derivative and retinoid, this drug has been shown to control cellular differentiation and proliferation *in vitro* and inhibits growth of tumour cell lines from haematopoietic and squamous cells. It is currently prescribed in an oral dose of 300 mg/m^2/day and has a terminal half-life of about seven hours. The prescribed dosage results in a maximum plasma concentration of 911 µg/L. The molecular weight of bexarotene is 348.48 g/mol, so the concentration of the drug achieved in the serum of patients and the *in vivo* achievable maximum concentration is approximately 2.55 µM. In the following studies, a conservative concentration of 1 µM bexarotene was used on monocytes. Due to the complex nature of RXR interactions, bexarotene does have several associated side effects. Common adverse effects include increased triglycerides and cholesterol in the blood, sensitivity to sunlight, and underactive thyroid resulting in weight gain and low energy (Henney, 2000; Lowe and Plosker, 2000; Richardson et al., 2007).

Bexarotene was used to study the transcriptional and functional effects of modulating RXR in human monocytes with Affymetrix microarrays, confirmatory qPCR, fluorescence activated cell sorting (FACS), and electrochemiluminescence assays (ECL). Microarrays allow the determination of gene expression and comparative analysis between groups of a large set of commonly expressed human genes. This platform makes it possible to determine the specific genetic changes resulting from MS diseases status, myelin debris phagocytosis, and bexarotene treatments in *in vitro* monocytes. Arrays can compare the roles of known genes in various states of cell conditioning. In addition, several tools for analysing large

microarray datasets allow identification of functional analysis of genetic changes captured by this system. Ingenuity Pathway Analysis (IPA) contains a large database of frequently updated scientific findings that identify pathways, functions, and interactions of genes discovered by each array. These pathways include those involved in disease processes, basic biological processes of cells, and signalling pathways modulating cellular function.

Using FACS and ECL, myelin debris uptake and receptor modulation in large cohorts of samples can be tested. Since the balance of regulating inflammation is pivotal for efficient remyelination (Miron et al., 2013; Vogel et al., 2013; Zhao et al., 2006), the modulation of two monocyte-specific soluble and surface markers, CD14 and CD163, was studied in this system. The dual functions of these two monocyte-specific receptors in M1/M2 polarisation (see section 1.7.3) as well as their ability to be released in soluble forms made them ideal targets to study the inflammatory effects of modulating myelin debris phagocytosis with bexarotene in MS patients and HVs.

5.1 Monocytes from MS patients show altered gene expression which is modulated by bexarotene treatment

Microarrays were again used to determine if monocytes from MS patients could be distinguished from monocytes from healthy controls. Although there was a great deal of homogeneity among monocytes from both groups, monocytes from MS patients were still clearly distinguishable from those from HVs. RNA was isolated from MS patient monocytes and HVs (n=4/group) both before and after myelin debris phagocytosis. Disease status was a greater determinant of genetic make-up than myelin debris phagocytosis, with phagocytosing groups more similar to their resting controls within each group. The heat map comparing gene expression (green=higher value, red=lower value) showed clustering of MS patients and HV monocytes separately (Fig. 5.1A). This heat map also shows that many genes are commonly regulated amongst all monocytes, regardless of phagocytosis or disease state. However, significant differences can be seen between MS patients and HVs. This difference was confirmed in a principal component analysis of the microarray

data (Fig. 5.1B), showing clear clustering of MS monocytes separately from HV monocytes. In addition, monocytes from each subject were more likely to cluster with the myelin-phagocytosing monocytes from that subject than with other phagocytosing monocytes. IPA was used to determine which canonical pathways were differentially regulated in MS monocytes compared to HVs. The analysis showed that the most highly expressed pathways were involved in inflammatory functions of monocytes, including IL-17 signalling, which has previously been largely associated with MS (Matusevicius et al., 1999; McFarland and Martin, 2007), expression of pattern recognition receptors, and IL-8 signalling (Fig. 5.1C). The specific genes involved in each of these pathways that are differentially regulated in myelin-phagocytosing MS patient monocytes compared to HVs are shown in Table 5.1. Several of these genes are involved in lipid metabolism and are downstream of the RXR pathway. In addition, genes involved in promoting/inhibiting actin rearrangement in phagocytosis are shown as well as genes associated with IL-17 signalling and immunological diseases.

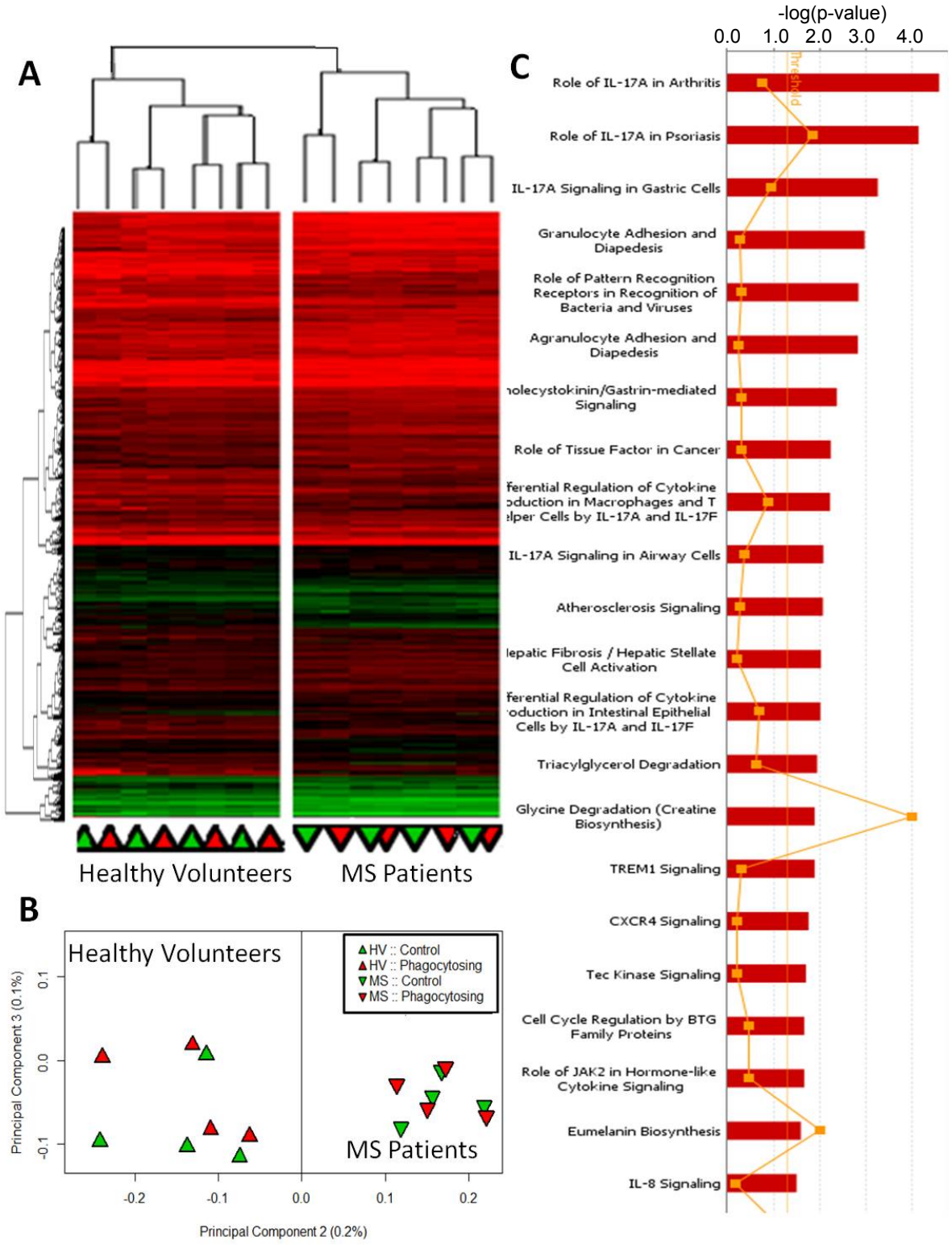

Figure 5.1 Monocytes from MS patients cluster independently of monocytes from HVs and show enhanced inflammatory pathways. Microarrays were used to compare MS patient monocytes to monocytes from HVs. A-B) Heat maps (A) and principal component analysis (B) of microarray data clearly distinguish clustering of MS patient monocytes and HVs. C) IPA identified highly expressed canonical pathways upregulated in MS patient monocytes. Several of the top pathways are important in pro-inflammatory functions of monocytes (IL-17 signalling, bacteria recognition, IL-8 signalling). n=4/group.

	Fold Δ in MS Patients vs HVs		Fold Δ in MS Patients vs HVs
IL-17 Signalling in Immune Cells			
CCL20	3.37	CXCL3	2.39
CXCL1	2.23	CCL5	2.00
Pattern Recognition & IGF-1 Signalling			
NLRP3	2.27	SOCS3	2.55
RIPK2	1.63	SRF	1.63
TRAF1	1.88		
Immunological Diseases			
TGFBR1	-1.51	GBP1	2.28
STAT4	3.09	TNFSF15	2.44
CXCR4	-2.95	GFTP1	-1.75
ARL5B	1.53	MS4A4A	1.79
CCRN4L	2.17	TBC1D2	-1.83
CLEC4E	1.60		
Lipid Metabolism			
ACAT2	1.72	LIPA	-1.53
BTG2	1.54	LPL	1.97
EDN1	2.23	NR4A1	2.12
GBP2	2.15	PRLR	-1.83
Actin Rearrangement			
CD180	-3.81	GFPT1	-1.75
DUSP16	1.67	NFKBIZ	1.63
E2F7	3.85	NLRP3	2.27
GBP3	2.99	ZC3H12A	1.87

Table 5.1 Genes important in monocyte function and phagocytosis are dysregulated in MS patient monocytes. IPA revealed genes in several key monocyte and macrophage functions significantly changed by MS disease status.

As monocytes from MS patients were clustered independently from HVs, we next aimed to determine if these transcriptional effects led to functional differences in myelin debris phagocytosis. Monocytes were isolated from young and old HVs and both young (≤35 years old) and old (≥55 years old) MS patients exposed to FITC+ pHrodo-labelled myelin. As in the initial experiment, the statistician first performed a sample size estimate on pilot data. After obtaining the pre-determined

n=18 volunteers per age group, we observed that monocytes from MS patients displayed significantly impaired myelin debris phagocytosis (Fig. 5.2A-B). However, there was no significant difference in myelin phagocytosis between young (RRMS) patients and old (progressive MS) patients (Fig. 5.2C). Due to this functional similarity, further studies analysed MS patients in one group, regardless of age.

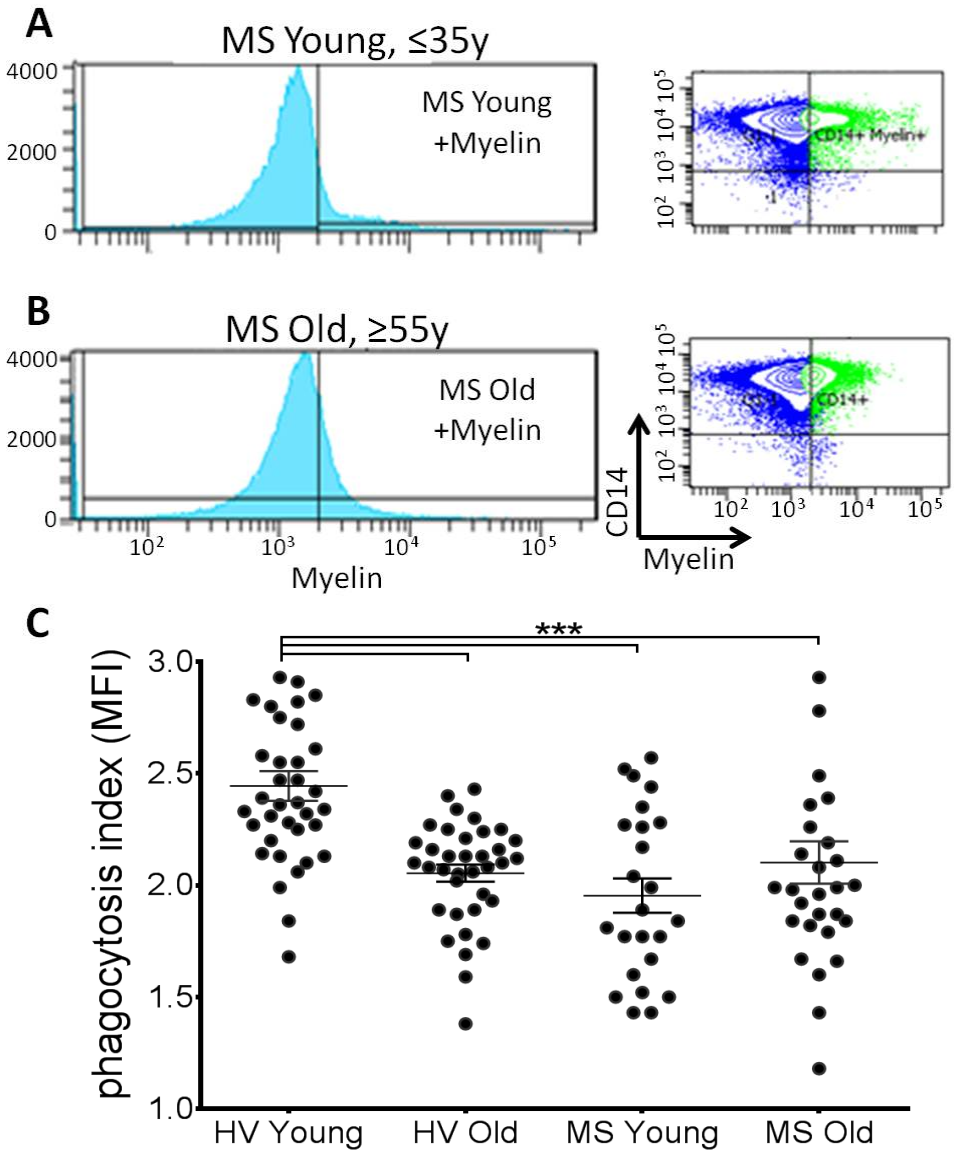

Figure 5.2 Myelin debris phagocytosis is reduced in MS patient monocytes regardless of age. A-B) Monocytes from young (A, ≤35 years old) and aged (B, ≥55 years old) MS patients were treated with myelin debris, and phagocytosis was compared to HVs. C) Monocytes from MS patients show significantly impaired myelin debris uptake, in both young (Phagocytosis = 1.95±0.12) and aged (2.10±0.09) MS groups compared to young HVs (2.44±0.06). One-way ANOVA and post-hoc Tukey's multiple comparisons test, **p<0.01, n≥24/group.

5.2 Bexarotene enhances RXR expression and myelin debris phagocytosis in MS patient monocytes

Based on the significant effects of modulating this pathway in the murine system, we next aimed to determine the effects of this potent RXR agonist on myelin-phagocytosing human monocytes to elucidate its efficacy in human subjects. Since monocytes were significantly altered by MS disease status, both functionally and transcriptionally, the potential effects of bexarotene on myelin-phagocytosing monocytes were determined using microarrays. This study would ascertain the effects of bexarotene on MS patient monocytes. Bexarotene treatment significantly increased the expression of several genes in the RXR pathway (shown in green) and significantly decreased expression of negative regulators of RXR (shown in red) in monocytes from MS patients. The treatment significantly affected 4 groups of RXR-related genes.

RXR activators, highlighted by the green box, were primarily upregulated upon bexarotene treatment compared to untreated MS monocytes (Fig. 5.3A). Nuclear receptor binding partners of RXR and the genes they regulate are in the purple box, including receptors in the RAR and PPAR families, and were primarily upregulated as well. In addition, genes inhibited by PPAR-RXR signalling were largely downregulated, including the inflammatory cytokines CXCL1 and CXCL3 as well as the negative regulator of remyelination, endothelin-1 (EDN1) (Hammond et al., 2014). Inhibitors of RXR in the red box are mainly downregulated upon bexarotene treatment. In addition, a select few other binding partners of RXR (blue box), were differentially upregulated upon treatment. Of the many genes upregulated upon bexarotene treatment, 10 statistically significant genes made patient monocytes behave more like young, healthy controls (Fig. 5.3B). For example, genes such as EDN1 and CXCL3 are more highly expressed in MS patient monocytes compared to young HVs. However, when MS patient monocytes were treated with bexarotene, the expression of these genes decreased to levels similar to those seen in HVs. Thus, the gene profiles of patient monocytes became more similar to the profiles of healthy controls. This result further suggests that bexarotene treatment is able to create a healthier, more youthful state in human myelin-phagocytosing monocytes via activation of the RXR pathway.

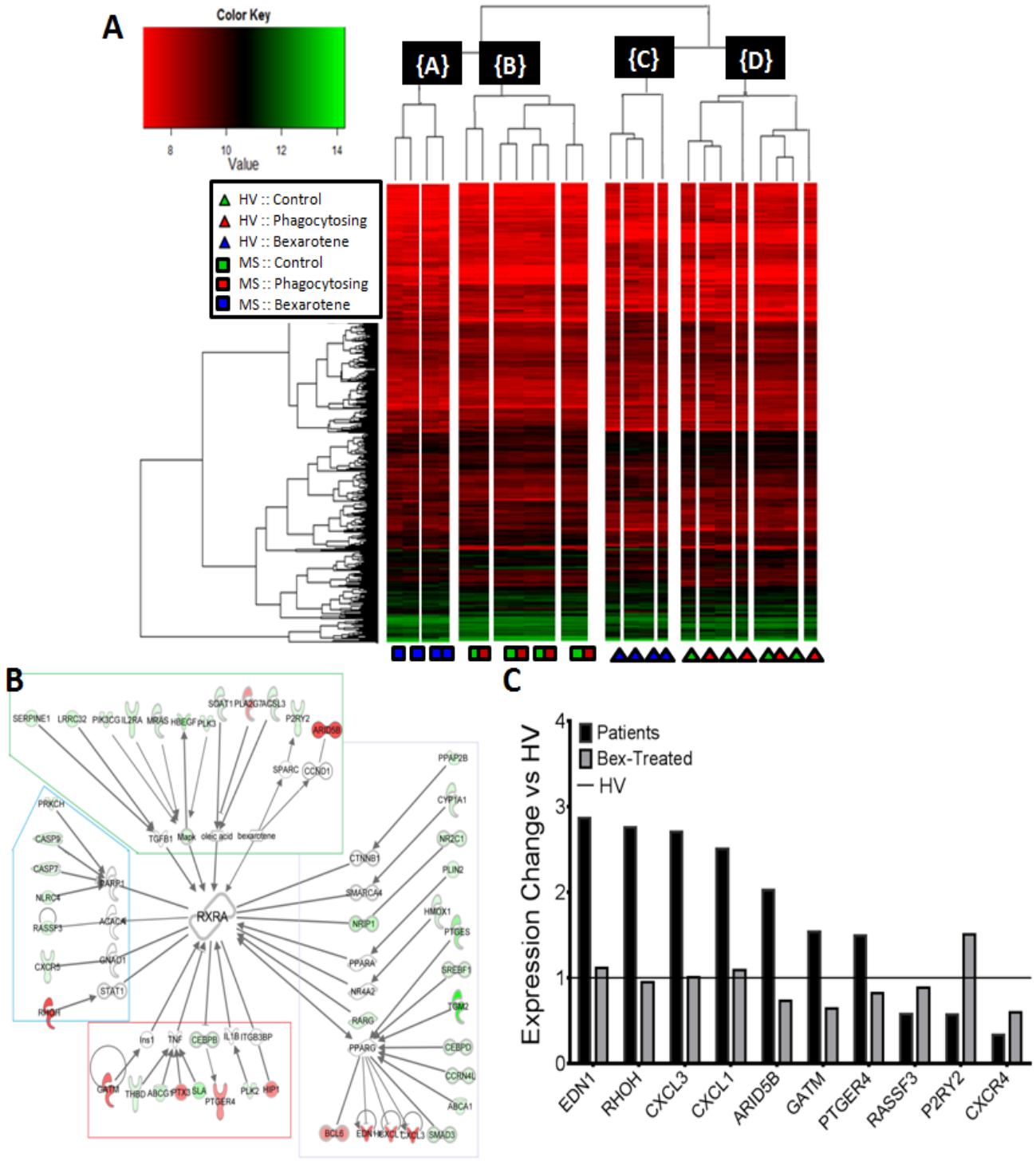

Figure 5.3 Bexarotene activates the RXR pathway in MS patient monocytes. A) Heat map showing independent clustering of bexarotene-treated samples in HVs and MS patients. B) IPA was used to analyse microarrays comparing MS patient monocytes to treated MS monocytes. Several RXR-related genes are upregulated with bexarotene treatment, shown here. Green box=RXR Activators, Purple box=Nuclear Receptor Binding partners, Red box=RXR inhibitors, Blue box=Other binding partners. B) Upon bexarotene treatment, 10 genes had significant fold changes ($p<0.05$) and expression profiles more like HVs (HV=1) compared to patient monocytes. n=4/group. MS patients ages (years old): 32, 38, 60, 69

Due to the significant upregulation of RXR pathways upon bexarotene treatment and significant difference between MS and HV monocytes, functional studies of myelin debris phagocytosis assessed the effects of bexarotene treatment on monocytes. Monocytes from young HVs were not significantly affected by bexarotene treatment (Fig. 5.4A, 2.39±0.07), while monocytes from MS patients showed significantly improved myelin debris phagocytosis compared to untreated cells (Fig. 5.4B-C, 2.20±0.06), further suggesting that altering this pathway in patients will enhance myelin debris phagocytosis.

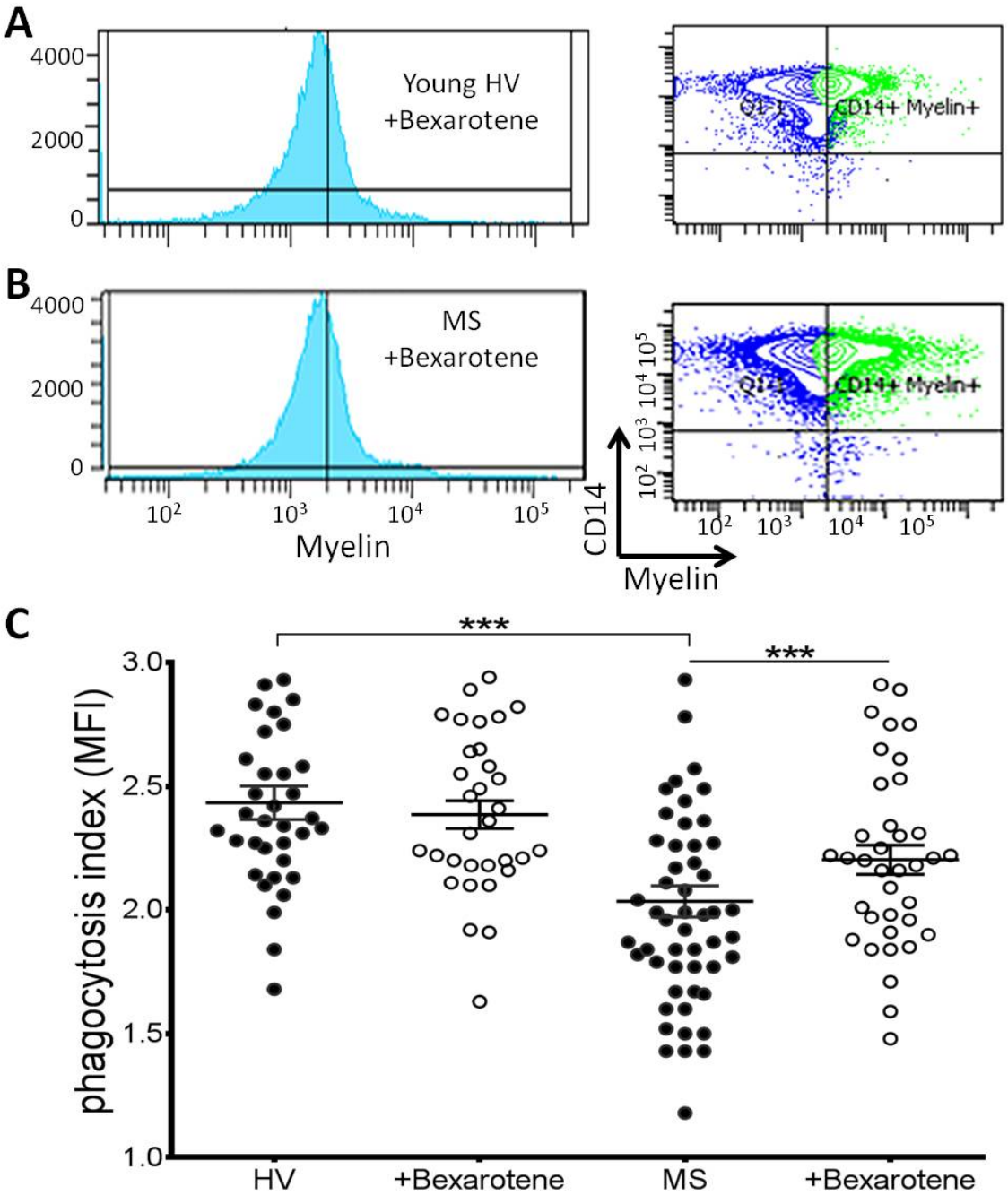

Figure 5.4 Bexarotene increases myelin debris phagocytosis by MS patient monocytes. A-B) Monocytes from young HVs (A, ≤35 years old) and all MS patients (B) were treated with myelin debris and bexarotene, and phagocytosis was compared to untreated, young HVs. C) The impairment in myelin debris phagocytosis was significantly improved by adding 1 μM Bexarotene in MS patient monocytes (2.20±0.06), while it had no significant effect on young HVs (2.39±0.07). However, there was still a significant difference between treated MS monocytes and young HVs. Two-way repeated measures ANOVA and post-hoc Tukey-Kramer adjustment for multiple comparisons, ***$p<0.001$, n≥36/group.

5.3 CD14 and CD163, monocyte markers of inflammatory activity, show small changes due to age, disease status, and activation

Due to their proven roles in affecting inflammatory pathways in monocytes, CD14 and CD163 were studied in myelin-phagocytosing monocytes. In addition, the role of bexarotene in modulating these two receptors and soluble molecules was determined in activated, myelin-phagocytosing cells. In order to establish the optimum incubation time to measure CD163 and CD14 in the supernatants of monocytes, cells were plated for 1-24 hours and supernatants were collected at pre-selected time intervals. Using an ECL assay, the release of both sCD14 and sCD163 was determined over the time course (Fig. 5.5A-D). sCD14 reached a peak at 24 hours in all three groups tested (control resting cells, myelin-phagocytosing cells, and phagocytosing bexarotene-treated cells) (Fig. 5.5A). The standard curve developed for sCD14 followed a precise curve, with a coefficient of variation (CV) ≤15.5% (Fig. 5.5B). sCD163 also reached a peak at 24 hours, but showed less accumulation in supernatants compared to sCD14 (Fig. 5.5C). For further experiments, supernatants were collected after 24 hours to measure sCD14 and sCD163.

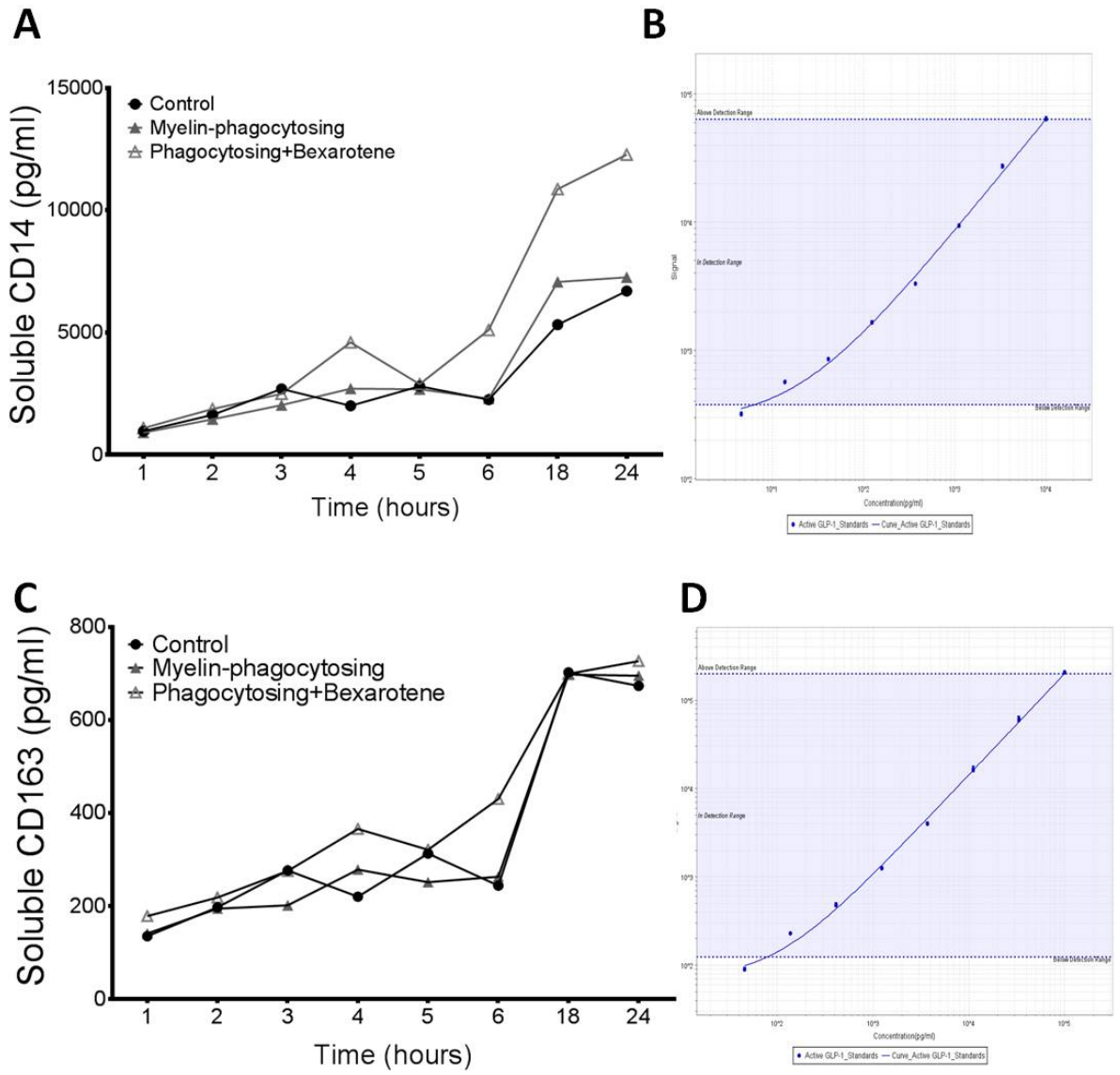

Figure 5.5 Optimisation of soluble CD14 and CD163 time course. MesoScale Discovery ECL Assays were used to detect soluble CD14 (sCD14) and soluble CD163 (sCD163) levels in monocyte supernatants. Levels (pg/ml) were calculated in supernatants from monocytes plated for 1-24 hours with myelin and bexarotene treatments. A) sCD14 increased over time, and peaked at 24 hours incubation (6701-12,276 pg/ml). B) The standard curve for sCD14, with low CVs (≤15.5%), is shown here. C-D) sCD163 also peaked at 24 hours incubation (673-726 pg/ml) and had an accurate standard curve.

Both sCD163 (measured by ECL) and surface CD163 expression (measured by FACS) were determined in 2 different groups with 3 separate treatments. The effects of MS disease status, phagocytosis, and bexarotene treatment were determined for each group. For sCD163, MS disease status resulted in significantly higher sCD163 shedding compared to HVs in all 3 groups (resting controls, phagocytosing monocytes, and bexarotene-treated phagocytosing cells) (Fig. 5.6). These results suggest an increase in pro-inflammatory regulation of CD163 via shedding of this receptor in monocytes from MS patients. In addition, surface CD163 expression was determined across all groups. Upon phagocytosis, both monocytes from MS patients and HVs display a significant increase in surface CD163 expression, confirming an increase in the immunoregulatory phenotype upon phagocytosis. However, bexarotene treatment had no additional effect on surface CD163 expression in either group. Conversely, HV monocytes have significantly less surface CD163 expression overall, suggesting a less immunoregulatory phenotype in HVs perhaps due to less activation of this receptor. Since CD163 was affected by MS patient status, the effects of treatment and disease status on CD14 expression were determined in those cells. Compared to young HVs, bexarotene increased shedding of sCD14 in MS patient monocytes (Fig. 5.7A), suggesting activation of a more anti-inflammatory, M2 cell type upon treatment with bexarotene and myelin debris. Although this increase was seen in sCD14, there was no significant difference in CD14 surface expression among monocytes (Fig. 5.7B). These results suggest that there is a mechanism for balancing sCD14 and surface CD14 expression in monocytes, with bexarotene tending to increase shedding of CD14.

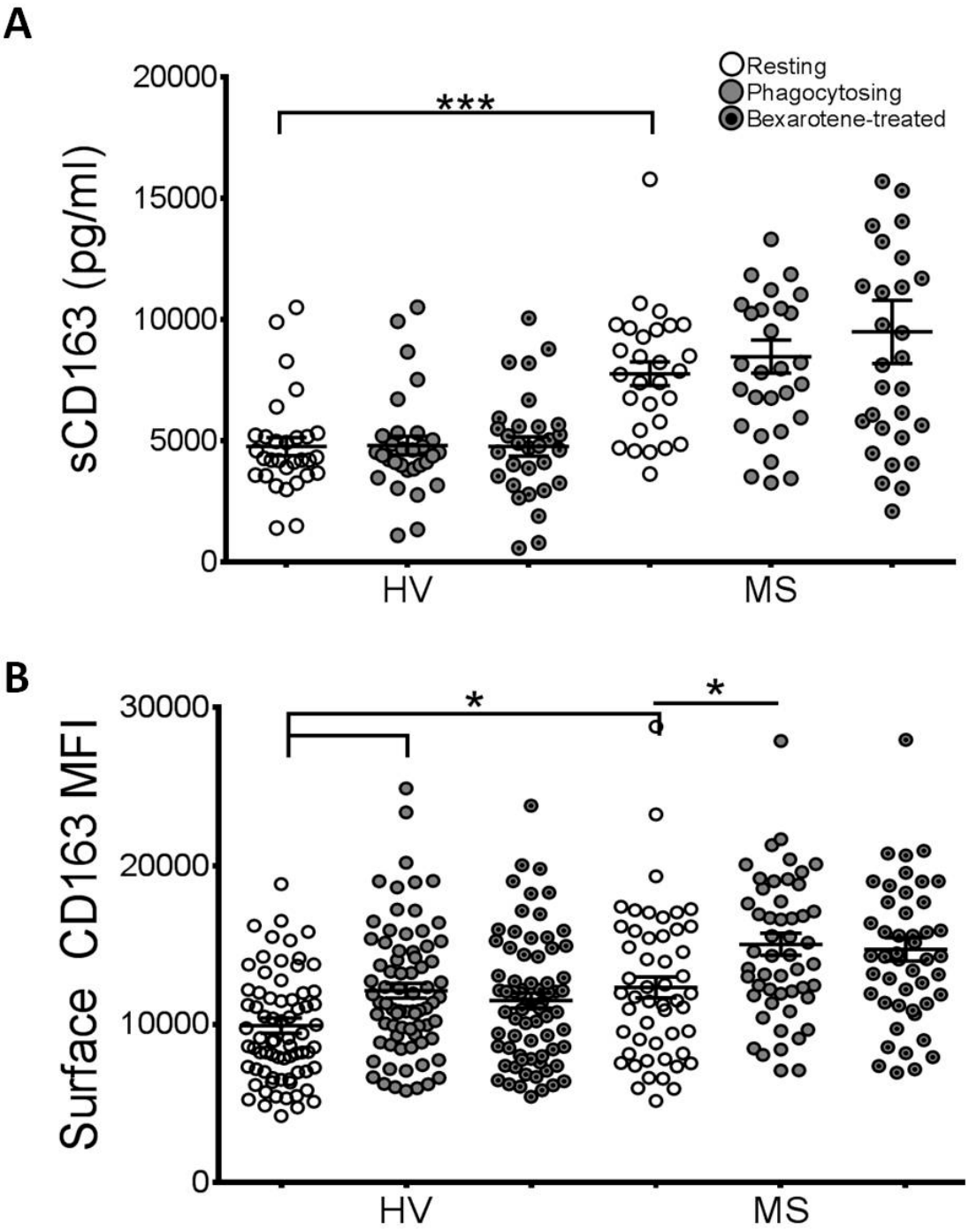

Figure 5.6 sCD163 and surface CD163 are increased in monocytes from MS patients. Soluble CD163 (sCD163) in supernatants and Surface CD163 expression on monocytes (MFI) were calculated for monocytes from HVs and MS patients. A) sCD163 was compared in HVs and MS patients. Phagocytosis and bexarotene treatment had no significant effect on sCD163 expression. sCD163 was increased in supernatants from MS patients (7.8±0.5 ng/ml) compared to HVs (4.8±0.4 ng/ml). This increase was significant across all 3 treatment groups. B) Surface CD163 expression in monocytes was increased due to myelin phagocytosis in both HVs and MS patients. MS monocytes displayed increased surface CD163 expression across all 3 groups. Two-way ANOVA and post-hoc Sidak's multiple comparisons test. ***p<0.001, p<-0.05. A) n=30/group; C-D) n≥50/group.

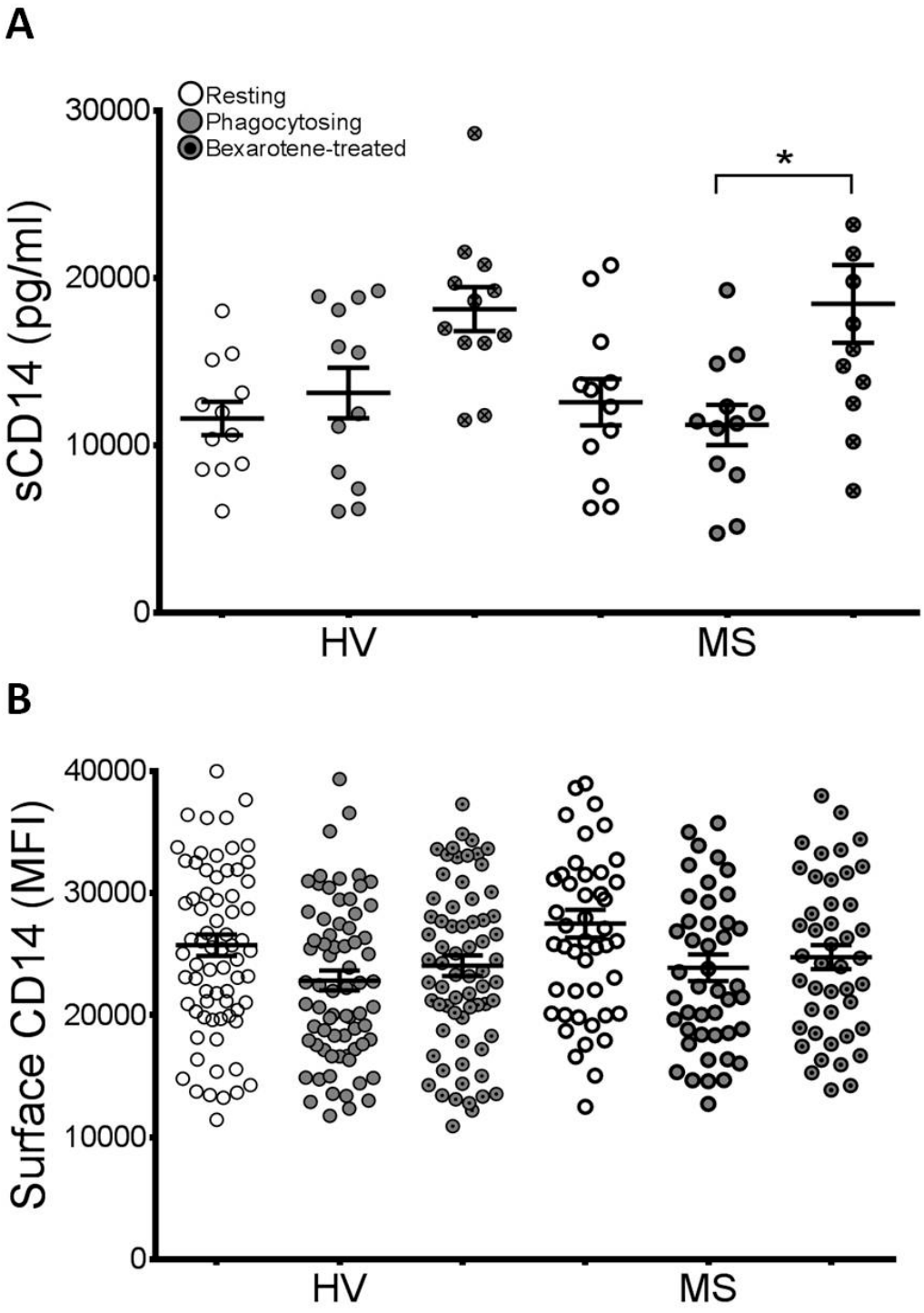

Figure 5.7 Bexarotene enhances sCD14 release in monocytes from MS patients. sCD14 in supernatants (pg/ml) and Surface CD14 expression on monocytes (MFI) were calculated for monocytes from HVs and MS patients. A) MS patient status had no significant effect on sCD14 expression in monocyte supernatants; however, bexarotene treatment did significantly increase sCD14 (18.5±2.3 ng/ml) compared to untreated cells from MS patients (11.2±1.2 ng/ml). B) Surface CD14 expression was not changed due to disease status, phagocytosis, or treatment. Two-way ANOVA and post-hoc Sidak's multiple comparisons test. *$p<0.05$. A) n=12/group; B) n≥50/group.

5.4 Conclusions

The goal of this study was to examine functional and molecular differences between young and MS patient myelin-phagocytosing monocytes, in order to identify therapeutically-modifiable pathway(s) that may enhance defective myelin debris clearance and therefore potentially also enhance remyelination in aged subjects with demyelinating disorders such as MS. By using multiple complementary assays, systemic differences in the RXR pathway were discovered between efficiently-phagocytosing young and poorly-phagocytosing MS monocytes from humans.

Similar to the results seen in mice, treatment with bexarotene enhanced activation of the RXR pathway as well as enhanced impaired myelin debris phagocytosis seen in MS patients, suggesting that activating this pathway has functional significance in human monocytes. The specific genes upregulated in response to bexarotene and RXR activation in young cells are related to several monocyte functions. Determining how to harness the specific activation of positive regulators of phagocytosis due to RXR activation will further provide evidence of the beneficial role of RXR in myelin debris phagocytosis.

The balance of pro- and anti-inflammatory effects of m o nocytes are key to harnessing the beneficial role of these cells in remyelination. In this chapter, two important surface and soluble markers of inflammatory capacity in monocytes are highlighted. CD14 and CD163 both have complex roles in monocyte regulation, and the results shown here indicate that both receptors have an important role in modulating myelin phagocytosis in disease. Increased shedding of sCD163 in MS patient monocytes suggests that these cells tend toward a more pro-inflammatory state. The increase in surface CD163 upon phagocytosis further suggests that myelin debris phagocytosis induced a more immunoregulatory phenotype in human monocytes, skewing them towards M2, wound-healing macrophages. In addition, increased shedding of CD14 upon bexarotene treatment implicates a role for RXR activation in reducing pro-inflammatory surface markers.

Since the genetic regulation of the RXR pathway is an incredibly complex and ongoing topic, highlighting the role of RXR binding partners in further affecting myelin debris phagocytosis may provide a more complex but more effective therapy in progressive MS. Several downstream genes have been discovered and are

highlighted here, but much work remains to determine other genes that are pivotally regulated by this pathway. Specifically, elucidating the role of nuclear receptors in anti-inflammatory pathways may enhance further knowledge on the effects of activating RXR in monocytes and will be highlighted in the next results chapter.

Chapter 6. Results

PPARγ activation enhances immunomodulation and myelin debris phagocytosis in MS patient monocytes

6. Results

PPARγ activation enhances immunomodulation and myelin debris phagocytosis in MS patient monocytes

RXR activity was shown to be important in myelin debris clearance and CNS remyelination in both murine models and human monocytes. However, RXR activation did not fully recover myelin debris phagocytosis in aged BMMs or MS patient monocytes nor did RXR inhibition completely impair phagocytosis or remyelination in young subjects. In addition, there was a trend towards a more immunomodulatory phenotype in macrophages upon bexarotene treatment, but RXR activation could not largely enhance anti-inflammatory functions in myelin-phagocytosing monocytes that have previously been shown to be important in the beneficial role of monocytes and macrophages in promoting remyelination (Miron et al., 2013; Takahashi et al., 2007; Zhao et al., 2006). These results suggest that other binding partners of RXR may also be playing a pivotal role in myelin debris clearance and beneficial macrophage functions. One of RXR's permissive binding partners, PPARγ, has been shown to enhance M2 activation in macrophages and may also play a role in improving remyelination or treating MS. In addition, activating both RXR and its permissive binding partners has been shown to have a synergistic effect in downstream gene transcription (Chawla et al., 2001; Ogawa et al., 2005; Roszer et al., 2013); therefore, the additional role of modulating RXR's binding partner, PPARγ, was further studied here.

As a permissive binding partner of RXR, PPARγ, has also been shown to play an important role in remyelination biology and macrophage function (Bernardo et al., 2009; De Nuccio et al., 2011; Lloberas and Celada, 2002; Ricote et al., 1999). PPARs have large ligand binding sites that are only partially filled by ligands, so multiple fatty acids can activate these receptors, and this activation has been shown to regulate gene expression in macrophages (Nagy and Schwabe, 2004). Unsaturated fatty acids largely activate PPARγ (Committee, 1999), and as myelin debris is composed of lipids, mainly galactocerebrosides with an unsaturated fatty acid tail (Hu et al., 2004), phagocytosis of myelin debris may assist in NR activation.

Due to its immunoregulatory capacity, PPARγ has been considered a therapeutic target in MS (Drew et al., 2008). An MS mouse model revealed that the addition of PPAR and RXR agonists activated transcriptional pathways that resulted

in anti-inflammatory effects on macrophages, ultimately resulting in greater recovery of treated animals (Diab et al., 2004; Feinstein et al., 2002). In addition, treatment with pioglitazone in a small set of RRMS patients resulted in a reduction in gray matter atrophy and a reduced number of lesions (Shukla et al., 2010); however, there was no significant decrease in disability in these patients (Kaiser et al., 2009). Elevated levels of soluble PPARγ have been detected in the CSF of MS patients (Szalardy et al., 2013), and PPARγ agonists have also been shown to enhance OL maturation and differentiation (Bernardo et al., 2009; De Nuccio et al., 2011).

PPARγ also plays a significant role in macrophage function. RXR and PPARγ heterodimerise during hematopoietic stem cell differentiation and are associated with their development into monocytes and myeloid cells (Safi et al., 2009; Schneider et al., 2014; Tabe et al., 2012). PPARγ activation affects lipid accumulation in macrophages and proper lipid metabolism (Chawla et al., 2001; Chinetti et al., 2001; Moore et al., 2001). Several studies suggest that PPARγ activates an anti-inflammatory phenotype in macrophages (Huang et al., 1999; Odegaard et al., 2007; Ricote et al., 1998).

Pioglitazone was used as the primary activator of PPARγ in the following studies. Pioglitazone is a thiazolidinedione, a class of drug also known as glitazones and currently used in the treatment of type 2 diabetes. Thiazolidinediones are oral drugs known to decrease triglycerides, increase cholesterol, and block pro-inflammatory genes. Other thiazolidinediones have also been prescribed for type 2 diabetes but have been associated with severe toxicities and removed from the market, including rosiglitazone (increased cardiovascular risks) and troglitazone (increased hepatitis). Even pioglitazone, brand labelled as Actos, has been associated with bladder cancer (Lewis et al., 2014), but this has not been confirmed and the drug is still FDA-approved. Common side effects include sore throat, muscle pain, eye problems (such as blurred vision), and weight gain (DeFronzo et al., 2011). Pioglitazone is currently prescribed at a dose of 30 mg/day and achieves a maximum plasma concentration of 800 ng/ml, which is approximately 2 μM in the serum (Eckland and Danhof, 2000). Therefore, the *in vivo* achievable dose used in the following *in vitro* studies was 1 μM.

Due to slight immunomodulatory effects of bexarotene treatment and pan-RXR activation, this study further aimed to determine the effects of the RXR binding

partner PPARγ by studying the expression levels of this receptor in ageing and the effects of modulating this receptor in myelin debris phagocytosis.

6.1 RXRα and PPARγ bind in BMMs, and PPARγ plays a role in efficient myelin debris phagocytosis

As ageing played a significant role in RXR expression (Chapters 3-4) and as previous studies have indicated a role for ageing in PPARγ expression (Dyall et al., 2010; Sung et al., 2006), the role for ageing on expression of PPARγ heterodimers in myelin-phagocytosing BMMs was studied here. In order to confirm PPARγ-RXRα interaction in BMM cultures, protein was lysed from control and myelin-phagocytosing BMMs, and co-immunoprecipitation was performed by eluting PPARγ-expressing isolates. After collecting specific PPARγ expressing proteins, western blots were performed on the elutes with antibodies against RXRα to determine the amount of PPARγ-RXRα co-expression. Nitrocellulose blots were stripped overnight and re-incubated with PPARγ antibodies to determine consistency of PPARγ expression across samples (used as a control). RXRα-PPARγ heterodimers experienced interaction in both control and myelin-phagocytosing BMMs (Fig. 6.1A-B).

Once it was determined that these receptors do bind in BMMs, the effects of age on PPARγ expression were determined by western blots. Protein was lysed from myelin-phagocytosing, ageing BMMs (2mo, 8mo, 12mo, 16mo, 24mo). Resulting bands reached significantly decreased expression when comparing 2mo and 8mo BMMs to 24mo BMMs (normalised to β-actin and 2mo controls) (Fig. 6.1C-D). There was a trend towards decreased PPARγ expression with age, suggesting that this receptor has a similar expression pattern as RXRα and may also play a role in decreased myelin debris phagocytosis with age.

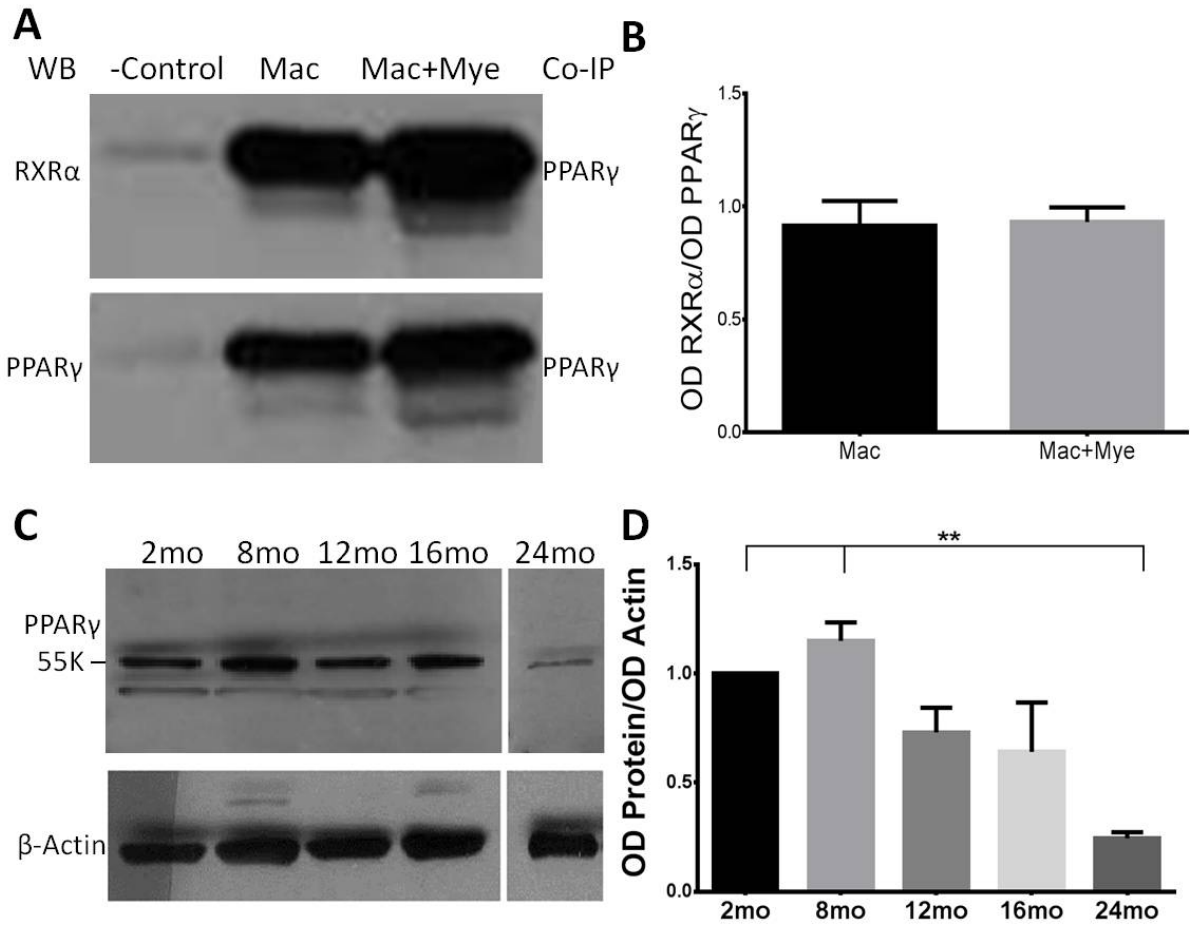

Figure 6.1 PPARγ binds to RXRα and declines with age in BMMs. A) Co-immunoprecipitation followed by Western Blot was used to determine PPARγ and RXRα association in young BMMs. These receptors bind in BMMs, and B) myelin phagocytosis (mac+mye) does not significantly affect PPARγ-RXRα binding compared to resting controls (mac). C) Levels of PPARγ expression in macrophages derived from 2-24mo mice were determined by western blot and normalised to 2mo by ImageJ (C). Dividing line indicates different gels. D) There was a significant reduction in PPARγ expression in macrophages between 2mo and 24mo mice as well as 8mo and 24mo. One-way ANOVA and posthoc Tukey's multiple comparisons test, **p<0.01, n=3/age group.

Since there was a significant decline in PPARγ expression with age, loss of PPARγ activity in young BMMs and its effects on myelin debris phagocytosis were studied. The synthetic antagonist for PPARγ, N-(4′-aminopyridyl)-2-chloro-5-nitrobenzamide (T007), was used to determine if PPARγ activation was necessary in young BMMs for efficient myelin debris phagocytosis. After antagonist treatment for 24h and incubation with myelin debris, cells were stained with CD11b to identify BMMs. Myelin+CD11b+ cells were counted by immunocytochemistry and flow cytometry. Young cells were able to efficiently phagocytose DiO-labelled myelin (Fig 6.2A-B, 36.6-42%), while macrophages treated with 10μM T007 showed reduced myelin debris uptake and significantly fewer double positive cells (Fig 6.2C-E, 22.3-26.3%). These results suggested that PPARγ activity may also be important in efficient myelin debris phagocytosis. These studies led to the question of how activating PPARγ would affect transcriptional profiling and function in ageing and patient myelin-phagocytosing human cells.

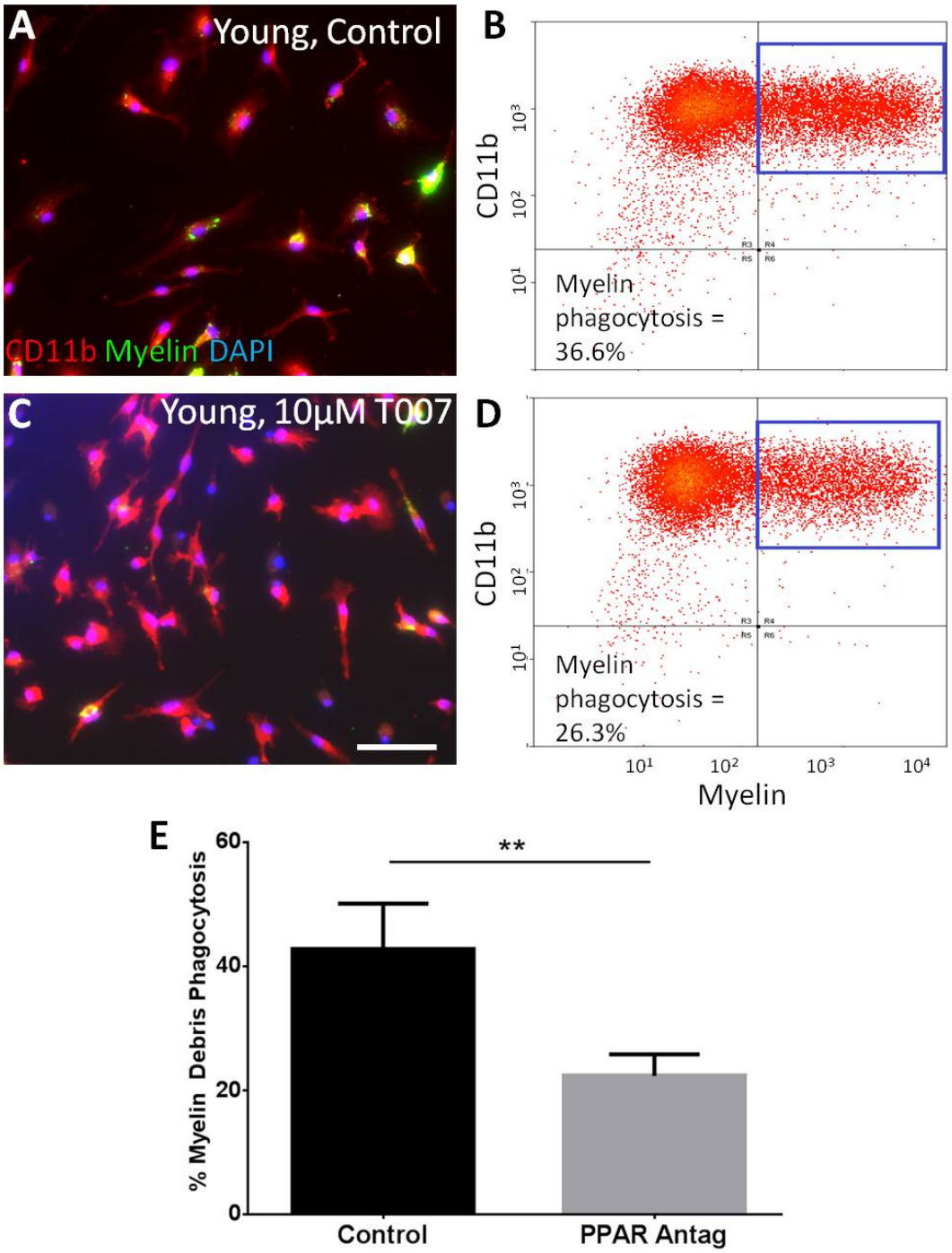

Figure 6.2 PPARγ antagonist slows myelin debris uptake in young BMMs. A-D) DiO-labelled myelin was used to measure myelin debris clearance by immunocytochemistry and flow cytometry in young macrophages (A-B) and young macrophages treated with a synthetic PPARγ antagonist, T007 (C,D). E) Blocking PPARγ with10µM T007 reduced myelin debris uptake in young BMMs from 42.8% (±2.5%) in young controls to 22.3% (±3.5%). Scale bar = 50µm. Student's t-test, **p<0.01, n=4/treatment.

6.2 Pioglitazone treatment enhances immunoregulatory pathways and reduces inflammatory CD14 expression

Pioglitazone and bexarotene-treated monocytes were compared to controls from both MS patients and HVs. Microarrays were again used to study gene expression in these groups, and IPA was performed to determine the pathways affected. A principal component analysis was performed on monocyte groups to compare clustering of gene expression between 8 groups: HV Controls, HV Phagocytosing, HV Bexarotene-treated, HV Pioglitazone-treated, MS Controls, MS Phagocytosing, MS Bexarotene-treated, and MS Pioglitazone-treated. As previously shown (Fig. 5.3), bexarotene significantly affected myelin-phagocytosing monocytes and, in a select few genes, made MS patients monocytes more like HVs. However, bexarotene treatment caused significantly different clustering of monocytes from both treated MS patients and treated HVs compared to controls (Fig. 6.3A), suggesting a significant difference from normal HV monocytes. Alternatively, pioglitazone treatment only significantly affected gene expression of 8 specific genes in myelin-phagocytosing monocytes from MS patients. The expression of all of these genes was made more similar to expression in HVs compared to untreated MS monocytes. The relation of these eight genes to the PPARγ pathway are mapped here (Fig. 6.3B). The functions of these genes in macrophages are also shown in Fig. 6.3C. Several of these genes have been shown to be involved in immunoregulatory, M2 differentiation, such as the cytokine IL-19, which is a member of the anti-inflammatory IL-10 family (Richards et al., 2015). In addition, LRG1 has been shown to enhance the release of the growth factor TGF-β in macrophages, increasing their role in regeneration (Song and Wang, 2015). In addition, NFAT5 regulated the expression of VEGF (Wiig et al., 2013), another important growth factor. Finally, PTGES promotes production of prostaglandin and encourages M2 differentiation (Sica and Mantovani, 2012; Sica et al., 2006).

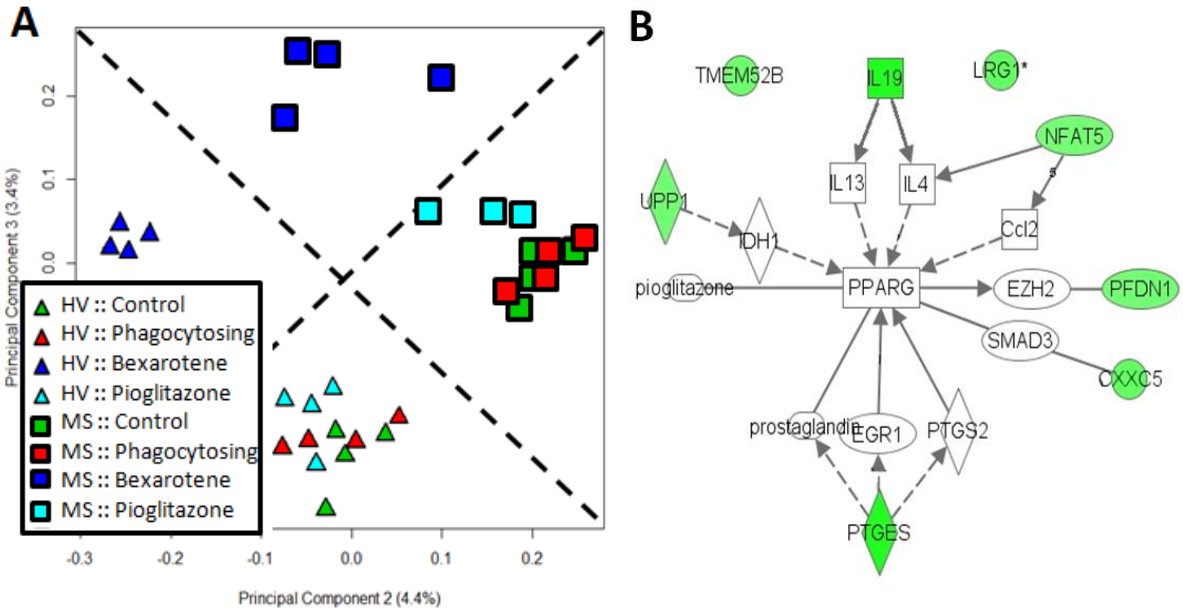

C

Gene	Fold Δ with Pio	Function in Macrophages
CXXC5	1.72	--
Interleukin-19 (IL19)	2.44	Part of IL-10 subfamily. Can lead to activation of M2 phenotype in macrophages **(Richards et al. 2015)**
Leucine-rich alpha-2-glycoprotein (LRG1)	1.83	Involved in enhancing TGF-β signaling **(Song 2015)**
Nuclear factor of activated T cells (NFAT5)	1.50	Regulates expression of VEGF-C in macrophages **(Wiig 2013)**
Prefoldin subunit 1 (PFDN1)	1.53	Stabilizes newly synthesized polypeptides
Prostaglandin E Synthase (PTGES)	2.43	Promote production of prostaglandin, which encourages M2 differentiation **(Sica 2006)**
Transmembrane protein 52B (TMEM52B)	1.59	--
Uridine phosphorylase 1 (UPP1)	1.55	Catalyzes phosphorylsis of uridine

Figure 6.3 MS patient monocytes treated with pioglitazone experience a significant change in select genes related to immunoregulation. Microarrays were used to compare MS patient monocytes and HV monocytes to those treated with either pioglitazone or bexarotene. A) Principal component analysis of microarray data (performed by Dr. Kory Johnson) clearly distinguished clustering of MS patient monocytes treated with pioglitazone or bexarotene compared to HVs. Bexarotene treatment significantly altered both normal, HV monocytes and MS patient monocytes, while pioglitazone treatment did not cluster away from HVs. However, pioglitazone does have a small effect on MS monocytes. B) IPA mapped eight genes that were significantly upregulated in pioglitazone-treated MS monocytes and had expression levels more similar to HVs. Most genes have also been shown to be regulated by PPARγ activity. C) Gene function related to immunoregulatory macrophages. $p<0.05$, n=4/group.

Due to the increased expression of immunoregulatory genes upon pioglitazone treatment, the effects of pioglitazone on CD163 and CD14 expression were expected to be more pronounced than in monocytes treated with bexarotene. This study determined the balance of these M1/M2 markers on the surface and in the supernatants of myelin-phagocytosing monocytes. As previously shown (Fig. 5.6-5.7), phagocytosis and patient status affect sCD163 and surface CD163 expression compared to resting controls. Treatment with pioglitazone had no significant effect on either sCD163 or surface CD163 expression in monocytes (Fig. 6.4A-B). Although there was no change in CD163 expression, the more inflammatory monocyte marker CD14 was affected by pioglitazone treatment. More sCD14 was found in the supernatants of myelin-phagocytosing monocytes from MS patients treated with pioglitazone compared to untreated controls (Fig. 6.5A), suggesting increased shedding of this inflammatory surface marker upon treatment. Surface CD14 trended towards reduced expression upon pioglitazone treatment in HVs and MS patients (Fig. 6.7B). With the reduction in inflammatory CD14 surface expression and increased sCD14 upon pioglitazone treatment, these results further suggest a trend towards a less inflammatory, more immunoregulatory phenotype upon treatment with pioglitazone.

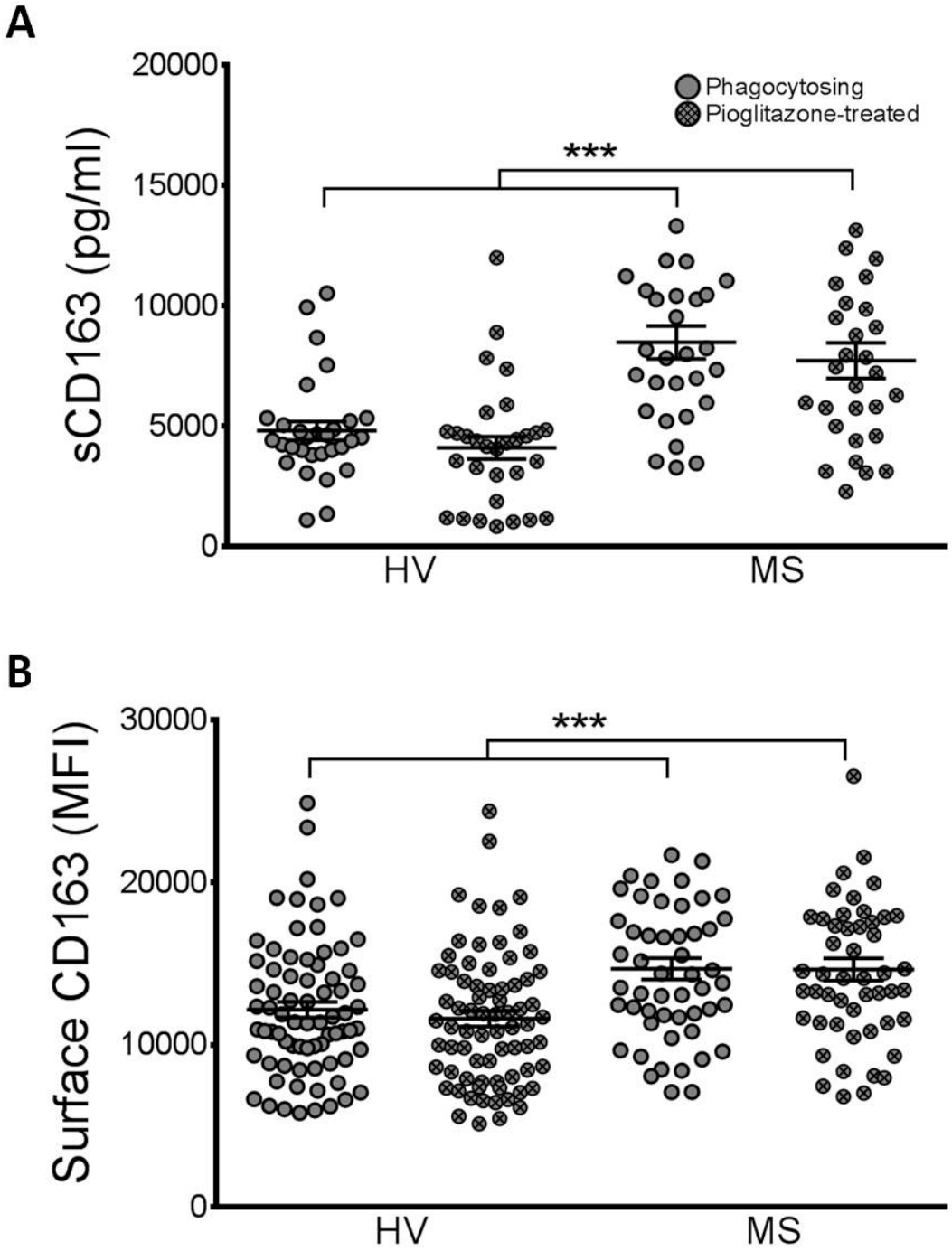

Figure 6.4 sCD163 and surface CD163 in monocytes are not significantly affected by pioglitazone treatment. Soluble CD163 in supernatants and Surface CD163 expression on myelin-phagocytosing monocytes (MFI) were calculated before and after pioglitazone treatment. A) Pioglitazone treatment had no significant effect on sCD163 expression in either HVs or MS patients. B) Surface CD163 expression in monocytes was also not affected by pioglitazone. As before, both surface and sCD163 were significantly higher in MS patients compared to HVs. Two-way ANOVA and post-hoc Sidak's multiple comparisons test. ***p<0.001, A) n=30/group; B) n≥50/group.

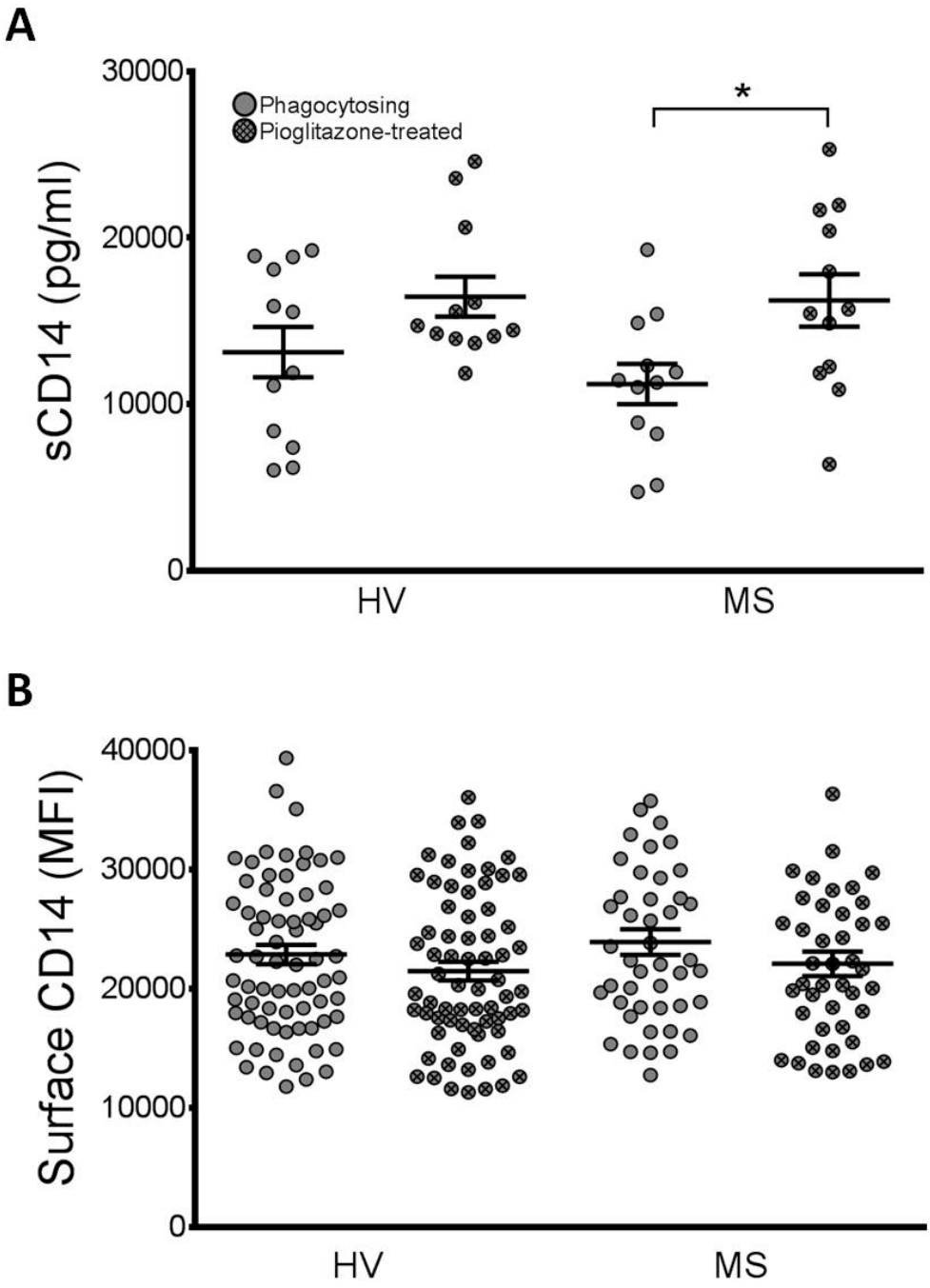

Figure 6.5 Pioglitazone enhances sCD14 release and reduces surface CD14 expression in MS patient monocytes. Soluble CD14 in supernatants and Surface CD14 expression on myelin-phagocytosing monocytes (MFI) were calculated before and after pioglitazone treatment. A) Pioglitazone treatment significantly increased sCD14 in MS patients (16.2±1.6 ng/ml) compared to myelin-phagocytosing controls (11.2±1.2 ng/ml). B) Surface CD14 expression in monocytes was not significantly affected due to pioglitazone treatment; however, both HVs and MS patients showed a trend (ns) towards decreased surface CD14 upon pioglitazone treatment. Two-way ANOVA and post-hoc Sidak's multiple comparisons test. *$p<0.05$, A) n=12/group; B) n≥50/group.

6.3 M1/M2 polarised cells show increased CD163 expression upon pioglitazone treatment in MS patient macrophages

Since PPARγ activation tended to cause a less inflammatory phenotype in myelin-phagocytosing monocytes, the direct effects of pioglitazone treatment on M1 and M2 polarisation were studied by polarising monocytes towards an M1 or M2 macrophage phenotype. As previously described, these extreme states are largely an *in vitro* paradigm that can provide insights into the potential for modulating inflammatory capacity in macrophages. It was hypothesised that since PPARγ reduced CD14 expression and promoted immunoregulatory genes in non-polarised monocytes, activation by pioglitazone may also assist in converting M1, pro-inflammatory macrophages to a more M2-like, regenerative phenotype. Monocytes were cultured and differentiated with M1, pro-inflammatory cytokines (granulocyte macrophage-colony stimulating factor, IFNγ, LPS, TNFα) or M2, anti-inflammatory cytokines (macrophage colony-stimulating factor, IL-10, IL-4). After 7 days of differentiation, cells were deemed M1 or M2 type cells. M1 macrophages tended to have a more rounded appearance compared to more bipolar M2 macrophages in culture (Fig. 6.86-D), also previously seen in other studies characterising these cells (Edin et al., 2013). Pioglitazone treatment did not appear to have a large effect, but some M1 cells took on a more elongated phenotype upon treatment (Fig. 6.6B). This difference in phenotype led to further investigation of expression of M1 and M2 surface markers in these two macrophage cultures.

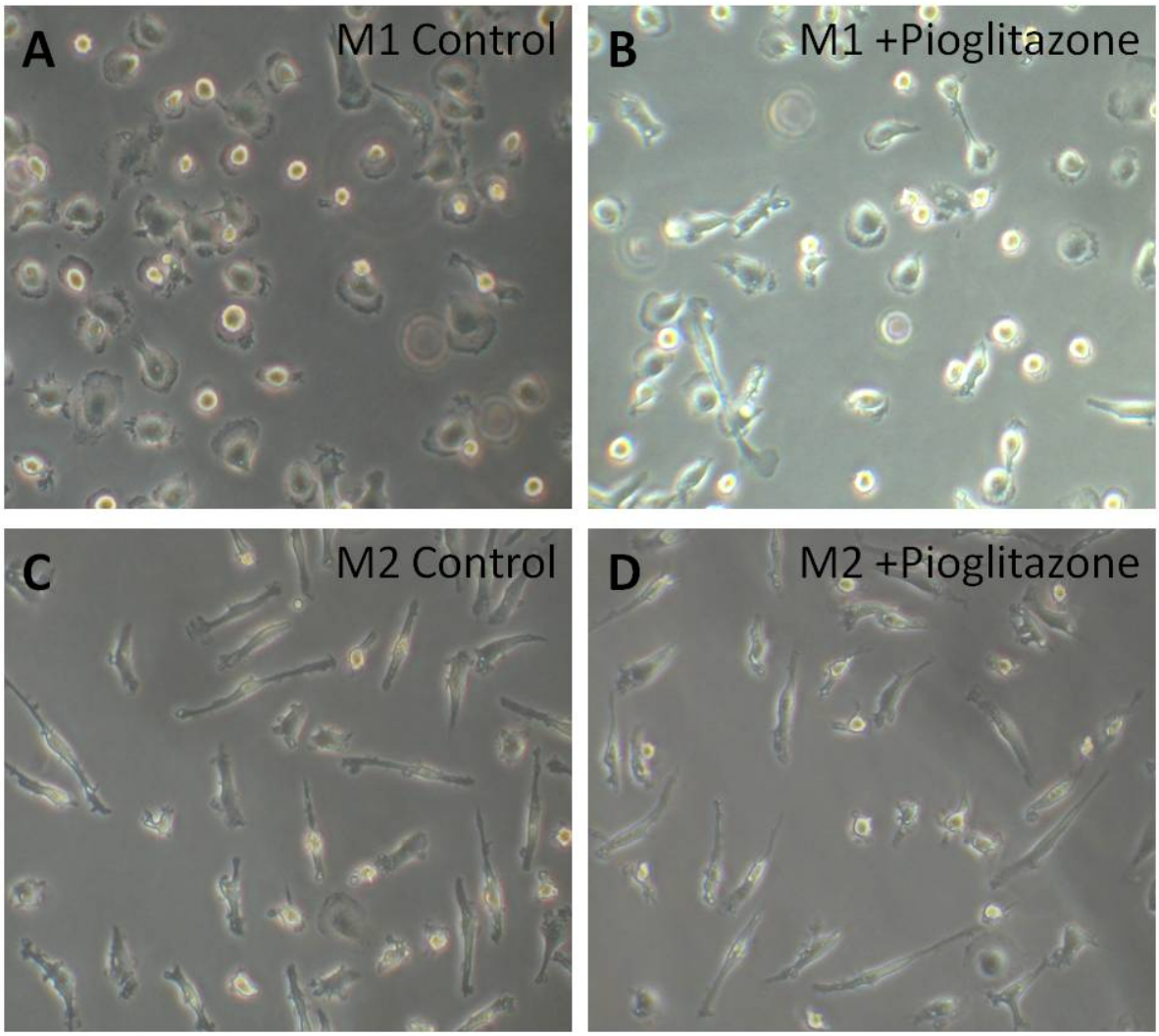

Figure 6.6 M1 human macrophages have an amoeboid phenotype, and M2 polarisation results in a bipolar structure. Light micrograph images of M1 and M2 human monocyte-derived macrophages. A-B) M1 polarised macrophages have a flattened, amoeboid appearance. When treated with 1 μM Pioglitazone, some cells show a more elongated phenotype. C-D) M2 polarised macrophages display a bipolar appearance and maintain that with pioglitazone treatment.

Myelin debris phagocytosis has previously been associated with a more M2-like phenotype (Boven et al., 2006). This study aimed to determine the effects of polarising macrophages from young HVs and old MS patients. CD80 and CCR7 (M1 markers) and CD163 and CD206 (M2 markers) expression was determined in different treatment conditions for both HV and MS macrophages. However, the only marker that showed any significant or appreciable differences between M1/M2 macrophages upon phagocytosis or pioglitazone treatment was CD163, with data

shown here. CD163 expression was determined by comparing 1) polarised cells treated with pioglitazone and/or myelin debris to 2) non-phagocytosing, untreated controls. In young HVs, there was no significant change in CD163 expression upon phagocytosis or pioglitazone treatment in M1-polarised macrophages (Fig. 6.7A-B). However, CD163 expression was significantly increased in pioglitazone-treated M1 macrophages from MS patients (Fig. 6.7C-E). These results suggest that pioglitazone treatment does enhance M2 marker expression in M1-polarised macrophages from MS patients, but it has no significant effect on those macrophages from HVs, consistent with the microarray results in myelin-phagocytosing monocytes.

The effect of pioglitazone on CD163 surface expression on M2-polarised macrophages was also determined. Again, pioglitazone and myelin debris phagocytosis did not significantly affect CD163 expression in HVs, although there was a trend towards increased expression in both cases (Fig. 6.8A-B). In M2 macrophages from MS patients, pioglitazone treatment significantly enhanced CD163 surface expression on myelin-phagocytosing macrophages compared to all other groups (Fig. 6.8C-E), indicating that pioglitazone treatment can enhance CD163 on M2-phagocytosing macrophages as well, further promoting the immunoregulatory state in these cells.

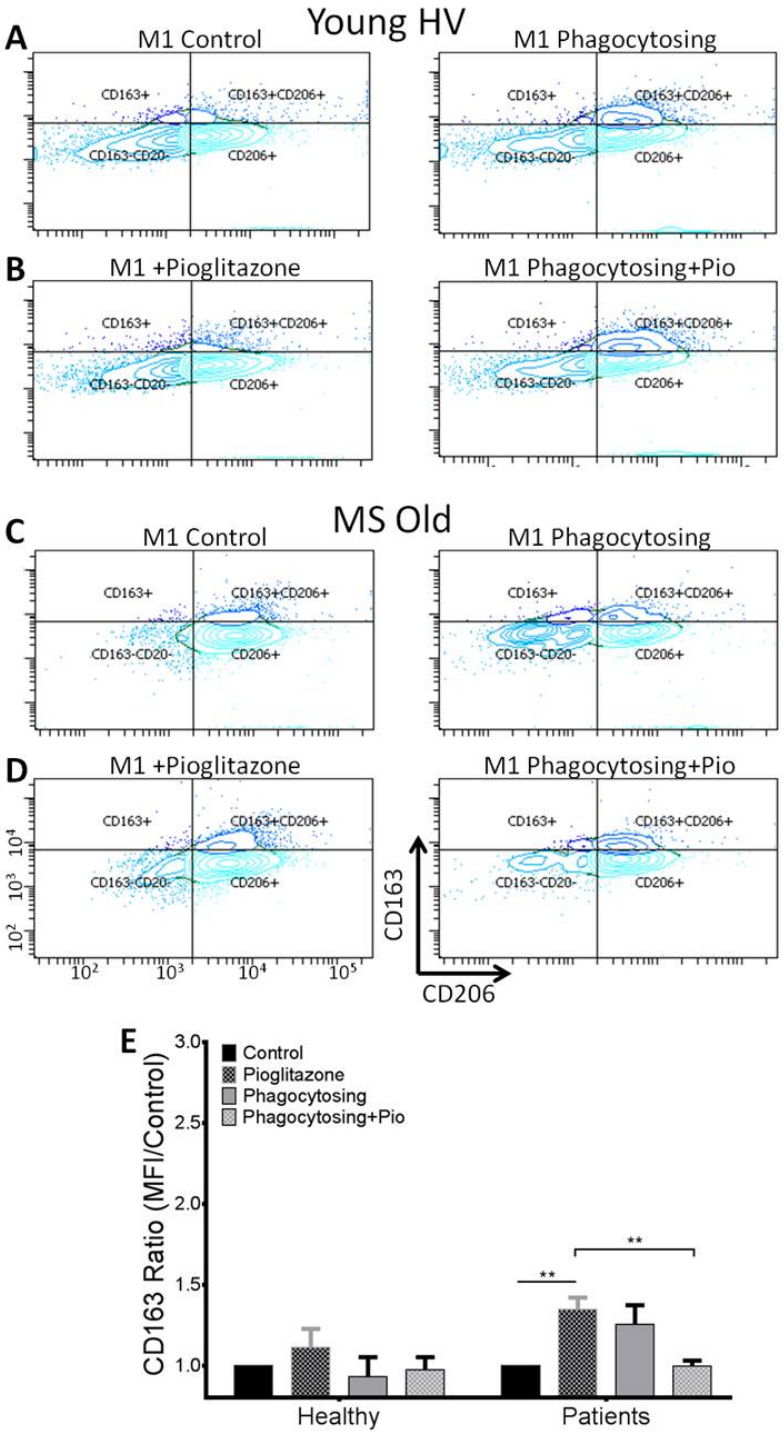

Figure 6.7 M1-polarised macrophages from old MS patients experience an increase in CD163 surface expression upon pioglitazone treatment. A-B) There is no change in CD163 expression in either resting or myelin-phagocytosing M1 polarised macrophages from young HVs, both before and after treatment with 1 μM pioglitazone. C) M1 polarised cells from MS patients do not experience a significant change in CD163 upon phagocytosis. D-E) However, CD163 expression is increased upon pioglitazone treatment compared to controls. This increase in expression is not maintained in myelin-phagocytosing M1 macrophages. Two-way ANOVA, post-hoc Sidak's multiple comparisons, **p<0.01. n=10/group.

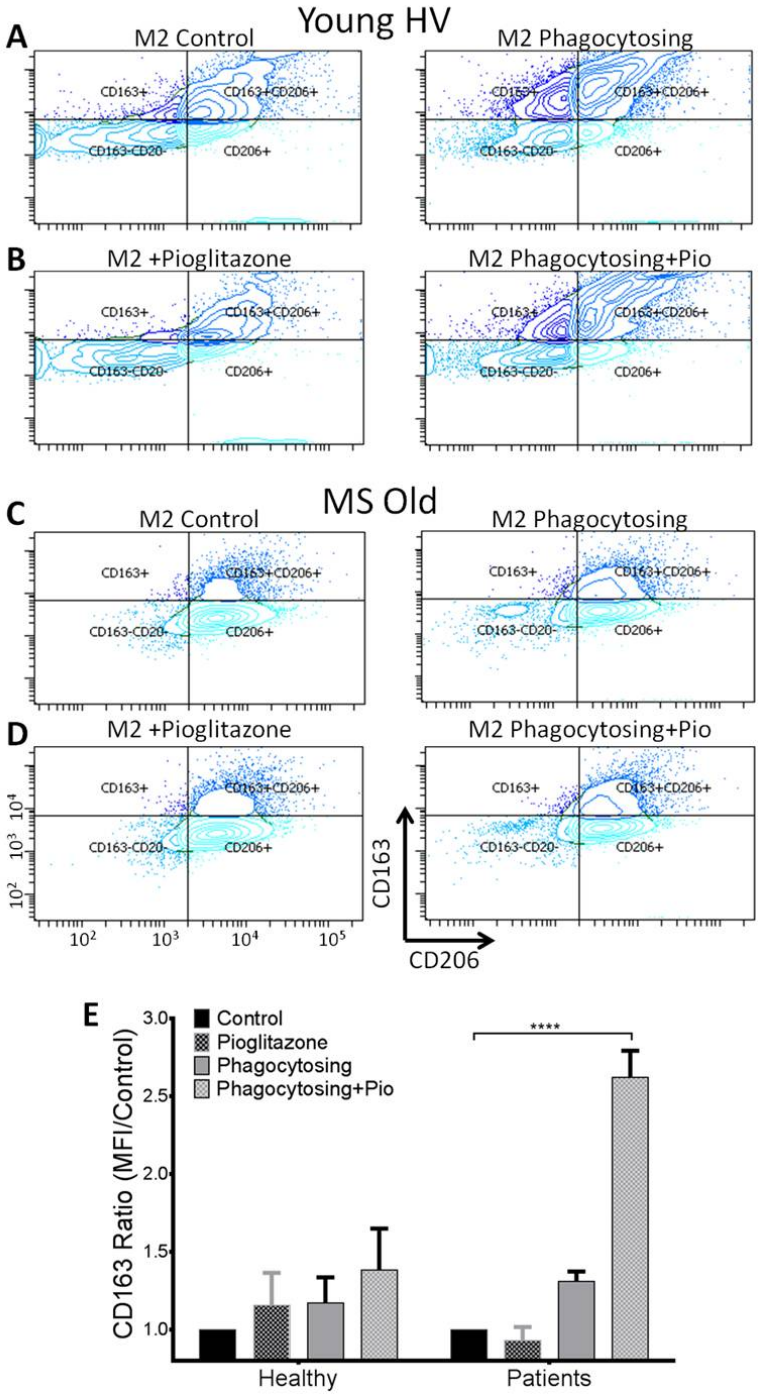

Figure 6.8 Myelin-phagocytosing M2 macrophages from MS patients experience an increase in CD163 surface expression upon pioglitazone treatment. A-B) There is no change in CD163 expression in either resting or myelin-phagocytosing M2 polarised macrophages from young HVs, both before and after treatment with 1 μM pioglitazone. C-E) M2, pioglitazone-treated macrophages show increased CD163 expression upon myelin debris phagocytosis compared to control and pioglitazone-treated resting cells. Two-way ANOVA, post-hoc Sidak's multiple comparisons, ****p<0.0001. n=10/group.

6.4 PPARγ activation promotes myelin-phagocytosis in monocytes from MS patients

As CD163 and M2-like phenotypes were promoted and CD14 and M1-lke phenotypes were downregulated by pioglitazone-treatment, the functional effects of pioglitazone on myelin debris phagocytosis were also determined. To determine if PPARγ activation can also enhance myelin debris phagocytosis and further study the role of PPARγ in MS patient monocytes, pioglitazone was added to myelin-phagocytosing human monocytes. After pioglitazone treatment, cells were exposed to myelin debris and phagocytosis was determined by FACS. Young monocytes were able to effectively phagocytose debris both before (2.44±0.07) and after (2.56±0.08) pioglitazone treatment (Fig. 6.9A-B). As previously seen, there was a significant decrease in myelin debris phagocytosis in MS patient monocytes (Fig. 6.9C, 2.01±0.06). When MS patient monocytes were treated with 1 μM pioglitazone, phagocytosis significantly increased to 2.33 (±0.06) (Fig. 6.9D). In addition, myelin debris phagocytosis by pioglitazone-treated MS monocytes was not significantly different from young HVs (Fig. 6.9E), suggesting that pioglitazone treatment is able to induce efficient phagocytosis by MS patient monocytes.

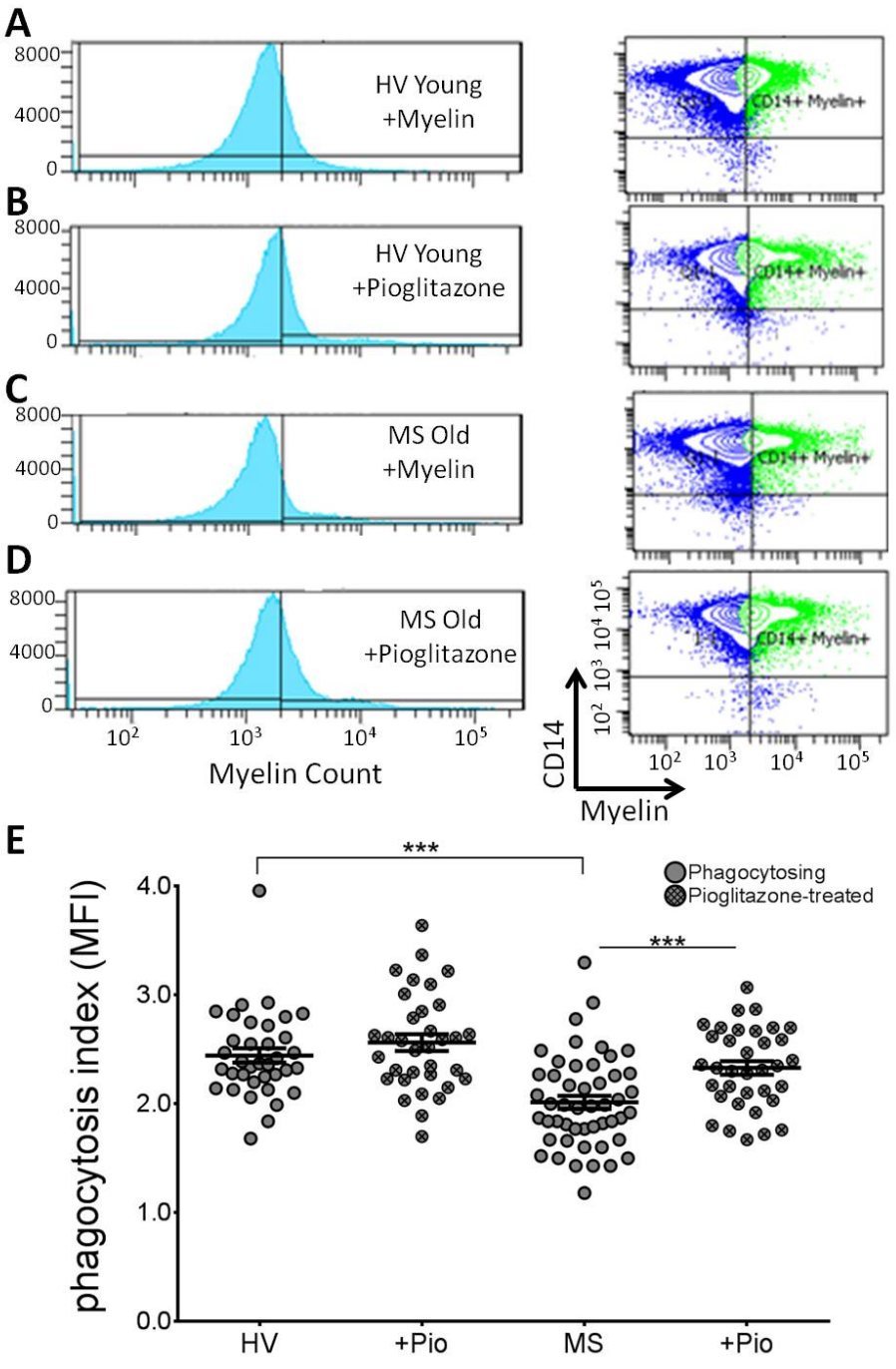

Figure 6.9 Pioglitazone significantly improves myelin debris phagocytosis in MS patient monocytes. A-D) Monocytes from young HVs (A-B, ≤35 years old) and MS patients (C-D) were treated with myelin debris (A, C) and pioglitazone (B, D). Histograms and FACS plots are shown. E) Monocytes from MS patients (2.01±0.06) show significantly impaired myelin debris uptake by flow cytometry compared to young HVs (2.44±0.06). This impairment was significantly improved in MS patients by adding 1 μM Pioglitazone (2.33±0.06) and was not significantly different from HVs after treatment. Two-way repeated measures ANOVA, ***p<0.001, *p<0.05, n≥35/group.

6.5 Conclusions

The results shown in this chapter provide further evidence that RXR activation and enhancement of RXR-related pathways, specifically through PPARγ activation, provide enhancement of myelin debris phagocytosis and control of immunoregulatory pathways in monocytes and macrophages. The confirmation of RXRα-PPARγ binding in myelin-phagocytosing macrophages and decrease in PPARγ expression with age highlighted the importance of this permissive heterodimer in ageing macrophage functions. In addition, loss of PPARγ in young BMMs impaired myelin debris phagocytosis in these cells. Activating PPARγ, via treatment with the FDA-approved drug pioglitazone, enhanced myelin debris phagocytosis and immunomodulatory pathways in aged monocytes and monocytes from MS patients. This enhancement is likely through downmodulation of M1, pro-inflammatory markers such as CD14. In addition, pioglitazone was able to increase the M2 marker CD163 on M1-polarised macrophages, further suggesting that this receptor may provide the capacity to enhance both myelin debris phagocytosis and immunoregulatory pathways in macrophages. These results further suggest that targeting RXR and PPARγ together may synergistically increase the beneficial functions enhanced by these receptors and allow them to act together to promote remyelination therapies in MS patients via myelin debris phagocytosis.

Chapter 7. Discussion

Discussion and Conclusions

7. Discussion and Conclusions

The aim of this study was to examine functional and molecular differences between young and old myelin-phagocytosing myeloid cells to identify therapeutically-modifiable pathway(s) that may enhance defective myelin debris clearance and therefore potentially enhance remyelination in aged subjects with demyelinating disorders. By using multiple complementary assays, we identified systemic differences in nuclear receptor pathways, specifically RXR and PPARγ, between efficiently-phagocytosing young and poorly-phagocytosing old cells from both animal and human models. We further demonstrated the link between measured efficiency of phagocytosis of myelin debris by cells of the myeloid lineage and the speed of remyelination in the experimental model of focal demyelination. The experimental focus of this study was to determine the role of RXRs and their binding partner PPARγ in myelin debris phagocytosis and ageing monocyte/ macrophage function with the objective of determining the role of these proteins and complexes in the clearance of myelin debris and efficient remyelination.

Although myelin debris clearance is mediated by an innate immune response performed by both monocyte-derived macrophages and microglia, we observed greater efficiency in myelin phagocytosis in BM-derived monocytes/macrophages in comparison to CNS-derived microglia. Macrophages and microglia are both myeloid cells with different origins and unique markers within the CNS. Microglia are derived from the yolk sac during early development and reside in the CNS through adulthood, whereas blood-derived monocytes are differentiated from bone marrow cells and are usually recruited to the CNS in response to an insult (Ginhoux et al., 2010; Neumann et al., 2009; Ousman and Kubes, 2012). These cells are difficult to distinguish once they are activated, but studies have suggested that monocyte-derived macrophages play a pivotal role in myelin debris clearance and CNS remyelination (Kotter et al., 2005; Ruckh et al., 2012), although both cell types can become phagocytic macrophages (Lampron et al., 2015; Neumann et al., 2009; Olah et al., 2012; Yamasaki et al., 2014).

In two of these previous studies suggesting a greater involvement of microglia in myelin debris clearance, the cuprizone model of demyelination was used

(Lampron et al., 2015; Olah et al., 2012). In this model, a copper chelator causing dysfunction in mitochondrial complex IV, results in selective oligodendrocyte toxicity in various CNS regions. This model is used for studies of resident CNS inflammatory cell response because little infiltration of recruited monocytes occurs (Krauthausen et al., 2014; McMahon et al., 2002). A recent study using fluorescently-labelled resident microglia and infiltrating monocytes determined that monocyte-derived cells are involved with myelin stripping from the axon and demyelination while microglia play a greater role in debris clearance in early stages of EAE (Yamasaki et al., 2014). However, this study failed to determine the roles of microglia and monocyte-derived macrophages during later stages of remyelination and only focused on initial demyelination. In this thesis, we found evidence that blood-derived macrophages play a larger role in myelin debris clearance and remyelination. This has previously been shown in other studies of remyelination as well (Kotter et al., 2005; Ruckh et al., 2012; Zhao et al., 2006). In addition to showing a significantly greater ability to phagocytose myelin debris *in vitro* (Fig. 3.2), changes affecting monocyte-derived macrophage function also impaired remyelination *in vivo* (Chap. 4), as the LysM-Cre shows little recombination in microglia (Goldmann et al., 2013), indicating the delayed myelin debris clearance seen in KOs is mainly due to RXR impairment in recruited myeloid cells.

As myelin debris phagocytosis was impaired in both ageing BMMs and human monocytes, further studies on pathways involved in remyelination were considered here. Microarrays of human monocytes suggested that RXR pathways are less activated upon myelin phagocytosis in aged monocytes compared to young (Fig. 3.5). Although human monocytes were grouped from a heterogeneous population, the effects of ageing on monocytes were clear. Variations in gene expression profiles between individuals reduce sensitivity in this model, but microarrays are still a valuable tool to study large-scale gene expression profiles. Due to the homogeneity among genes expressed by all monocytes, fold changes were relatively small among the two age groups. The low fold changes likely reflect the similarity among all monocytes, but nevertheless, these arrays identified multiple genes involved in RXR activity as primarily upregulated in young cells and downregulated in old monocytes. The fact that several genes in the same pathway show similar up/downregulation based on age group alone enhances the broader implication of these differences

regardless of the small fold changes of each individual gene. In addition, these genes were confirmed using qPCR and PCR arrays of RXR signalling in a larger group of subjects, suggesting that this result was not simply an artefact of large-scale gene expression comparisons. The implications of these genetic changes were further studied in functional characterisation of monocytes and macrophages in response to myelin debris and in a focal demyelination model. In ageing, RXR expression declines (shown here in Fig. 4.2, previously shown in (Dyall et al., 2010)), likely resulting in reduced transcription of downstream genes. By activating RXR in aged monocytes and macrophages, we showed that recovery of this diverse pathway can restore a youthful state.

In macrophage biology, RXRs have proven to be important. RXR expression is involved in macrophage differentiation from monocytes (Kazawa et al., 2009) as well as in the control of chemokine expression in macrophages (Nunez et al., 2010). RXR can form homodimers but also acts as a binding partner for several other nuclear hormone receptors. In resulting permissive heterodimers, such as PPAR and LXR, both RXR and its binding partner can bind their cognate ligands and cause ligand-dependent trans-activation. Moreover, each heterodimer has different DNA-binding specificity, resulting in the expression of genes downstream of both RXR and its permissive binding partner (Evans and Mangelsdorf, 2014). Due to this combinatorial heterodimerisation, RXR pathways have far-reaching effects in different cell types. For example, in a previous study, RXRγ was highly expressed during OPC differentiation. Treatment with an RXR ligand (9cRA) improved remyelination in aged rats in this study (Huang et al., 2011). Furthermore, macrophage-specific knockouts of RXRα in mice resulted in impaired clearance of apoptotic cells in a model of autoimmune kidney disease (Roszer et al., 2011), and a clinically approved RXR agonist increased clearance of amyloid deposits in an animal model of Alzheimer's disease (Cramer et al., 2012). Both of these studies support the conclusion derived from the current results in this thesis, that RXR plays a role in phagocytosis in general and in myelin-debris clearance in particular. The role of thyroid hormone in differentiation and the epidemiological link between Vitamin D deficiency and risk for development of MS (Ascherio et al., 2014) further strengthen our conclusions and suggest that modulating RXR pathways may influence the MS disease process.

In addition to this receptor having a positive role in remyelination and enhanced activity in young monocytes and macrophages, vitamin A (the precursor to the *in vivo* RXR ligand 9cRA) has also shown to be beneficial in patients with MS. Vitamin A is an essential, fat-soluble vitamin capable of crossing the BBB. Treatment with vitamin A activated anti-inflammatory functions in EAE and helped balance the pro-/anti-inflammatory response in mice, resulting in protection from reduced clinical scores in this model of MS. However, excess amounts of vitamin A have also proven to be harmful in MS, so an active balance in vitamin A concentration is imperative to harnessing its beneficial role (Massacesi et al., 1987; Salzer et al., 2013). Part of this beneficial activity may be through the conversion of vitamin A to 9cRA, which activates RXR pathways. Young BMMs were able to phagocytose myelin debris efficiently regardless of the presence of 9cRA. However, aged BMMs did not show impaired phagocytosis in the presence of serum (when more vitamin A was present), but they did show reduced myelin debris clearance in the absence of serum. This reduction was partially and significantly recovered when 9cRA was added to serum-free media (Fig. 4.4), suggesting that RXR activation is one of the key regulators of myelin debris clearance in BMMs.

Bexarotene also partially reverses the observed functional defect in myelin phagocytosis of MS monocytes, while changing their expression profile to a more “youthful” state, possibly through the autoregulatory activation of RXR. As RXR is downregulated with ageing, activating the receptor may not only enhance activation of RXR but also increase RXR expression in aged cells because RXR has previously been shown to act as a transcription factor for its own expression as well as for other nuclear receptors (Baker, 2011; Dave, 2012; Evans and Mangelsdorf, 2014). In young monocytes and macrophages, activation of RXR does not have a functional effect on myelin phagocytosis. We hypothesise that this is because young cells can optimally phagocytose myelin debris; therefore, further activating RXR does not affect function in these efficiently phagocytosing cells. In addition, RXR and its binding partners have previously been shown to display constitutive, ligand-independent activation (Laursen et al., 2012; Nagpal et al., 1993), which may be the case in young cells and not in old. The functional necessity of RXR in young macrophages was confirmed by inactivating the receptor with an RXR antagonist (Fig. 4.5), further proving that this receptor is necessary for efficient myelin debris

phagocytosis. By activating this receptor with 9cRA or bexarotene, it is possible that we increased expression of this receptor, thus enhancing its activity and creating a more youthful state in aged monocytes and macrophages. Activation of this pathway may have then resulted in enhanced myelin debris clearance in ageing cells. Together, these data suggest that RXR may be a key regulator of myelin debris phagocytosis in ageing monocytes and macrophages.

In order to determine the role of RXRs in myelin debris phagocytosis and remyelination, a LysM Cre-RXRα floxed knockout was created to remove RXRα function specifically in myeloid cells. Although the effect was not large, there was a time-dependent reduction in remyelination in the macrophage-specific RXR KOs. This recovery in delayed remyelination at later timepoints may be due to the KO of only the most significant form of RXR in monocytes, RXRα. We hypothesise that the other isoforms, β and γ, helped compensate for the loss of RXRα by 21dpl. In addition, nuclear receptor binding partners of RXR can still experience downstream transcription without RXR activation, so these other receptor pathways may also be playing a role in the recovery of remyelination at later timepoints. This finding suggests that RXRα is necessary for efficient myelin debris clearance at early stages of OPC differentiation and results in faster remyelination *in vivo,* and without this receptor, young mice experience delayed recovery after demyelination.

While these observations are highly encouraging, they nevertheless cannot assure that RXR activation will promote remyelination in ageing subjects with MS. The major drawback of all models of experimental demyelination is the fact that remyelination is generally complete even without therapeutic interventions. Consequently, all remyelination-promoting therapies identified thus far are only speeding up remyelination, rather than inducing it in a system where spontaneous remyelination failed. We predict that this slowed remyelination is relevant to human disease despite the lack of functional deficit. Although this is different from the situation in progressive MS, where OPCs are recruited to demyelinated lesions but fail to differentiate into myelinating OLs (Chang et al., 2002), we also see the presence of OPCs at 14dpl and no defect in recruitment at earlier timepoints, suggesting that the defect in differentiation is common across models. While the persistent or delayed presence of inhibitors in myelin debris may indeed be one of

the factors underlying observed remyelination failure in MS, this hypothesis requires experimental confirmation. Interventional clinical trials can provide definitive answers on whether therapeutic agents that promote OPC differentiation, either directly or indirectly, via enhanced clearance of myelin debris, will promote remyelination in humans. Availability of bexarotene and pioglitazone makes such a proof-of principle clinical trial in human subjects with MS feasible. Determining the therapeutic window available for treatments that promote remyelination can help us understand how to boost regeneration in progressive MS. In this study, we also were able to further study the effects of bexarotene and pioglitazone in samples from MS patients that assist in translation of these results by studying measurable CSF biomarkers (Komori et al., 2015) and functional effects.

As MS patients monocytes showed such a clear distinction in gene expression profiles compared to HVs (Fig. 5.1), we expected that this change in genetic make-up may also be reflected in functional activity, both in myelin debris phagocytosis and in the balance between pro/anti-inflammatory (M1/M2) markers and cytokines. Monocytes from MS patients displayed significantly reduced myelin phagocytosis compared to young HVs (Fig. 5.2). Interestingly, there was no significant difference in myelin debris phagocytosis between monocytes from RRMS patients and those from progressive MS patients, contrary to the expectation that young patients are likely able to clear myelin debris more efficiently than old patients. The similarity between RRMS and PPMS/SPMS patient monocyte phagocytosis has been suggested by previous studies as well (Brettschneider et al., 2002), where CD14-expressing cells (activated monocytes) were increased in both PPMS and RRMS. This similarity along with the similarity in phagocytosis among all MS monocytes further suggests that the MS disease state affects monocyte and macrophage function. However, since RRMS patients are likely able to overcome barriers to OPC differentiation, these findings may suggest that other factors in the *in vivo* situation for RRMS monocytes allows for remyelination in earlier stages that are prevented in later stages of progression. For instance, our study suggests that activation of the RXR pathway is an inhibitor of myelin debris phagocytosis, so activation of this pathway *in vivo* in RRMS patients compared to progressive MS patients may lead to more myelin debris phagocytosis in young MS patients compared to aged. Other effects *in vivo,* such as activation towards a more M2

phenotype *in vivo* in RRMS which allows for more phagocytosis by these monocytes in subjects may not be recapitulated in the *in vitro* situation. Additionally, disease duration and rate of newly developing lesions were not considered in this study, so the similarity in RRMS and progressive patients may also reflect the similarity of disease duration among patients in these groups. Overall, MS patient monocytes showed consistent differences in functional, genetic, and biomarker studies, highlighting that modulating monocyte function and myelin debris phagocytosis may be relevant to all stages of the MS disease course.

The functional changes in RXR-related pathways and expression of these genes were highly increased in response to bexarotene treatment. In addition, bexarotene treatment also changed the expression of 10 specific genes to be more similar to HVs (Fig. 5.3). This finding suggests that these specific proteins may be highly valuable downstream effectors in the RXR pathway. Determining the specific targets in the RXR pathway that create a “healthier” state in MS monocytes may be necessary to target this pathway more effectively because bexarotene also significantly altered gene expression in HVs (Fig. 6.3). Due to the role of RXR in several nuclear receptor pathways, activating this pathway may lead to unexpected off-target effects, and since it had a significant effect on healthy monocytes as well, a more targeted approach may be necessary.

Recently, a study of remyelination highlighted that M2 cell densities increased in the lesions of old mice that were exposed to a young environment (Miron et al., 2013). The findings from this study led us to not only determine the effect of MS disease status and bexarotene treatment on myelin debris phagocytosis in monocytes but also on M1 and M2 markers. Overall, bexarotene treatment did not have a large effect on the modulation of these representative surface markers and cytokines. MS patients released more sCD163, suggesting a reduction in M2 markers in MS patients, which has also been previously suggested (Fabriek et al., 2007; Stilund et al., 2014). Bexarotene increased sCD14 shedding, suggesting a more anti-inflammatory phenotype in these monocytes upon treatment; however, there was no effect on CD163 or M2-related genes in the microarray, leading us to study more anti-inflammatory effects of one of RXR’s permissive binding partners, PPARγ. Previous studies have shown a role for RXR and its nuclear receptor binding partner PPARγ in changes in macrophage gene expression and cytokine profiles

(Lloberas and Celada, 2002). The activation of the RXR/PPARγ pathway has previously been shown to lead to the transcription of molecules associated with anti-inflammatory pathways (Diab et al., 2004). These pathways have immunoregulatory functions, orchestrate encapsulation and containment of particles, and promote tissue repair (Boven et al., 2006; Vereyken et al., 2011).

In the present study, PPARγ showed similar functional characteristics to RXR, with decreased expression with age and modulation of myelin debris clearance upon activation/inhibition of this receptor. However, in comparison to bexarotene's effects, the PPARγ activator pioglitazone led to a larger and more significant increase in myelin debris phagocytosis in MS patients (Fig. 6.9), and reached an efficiency in myelin debris phagocytosis that was not significantly different from HV monocytes. In addition to this important functional effect, this FDA-approved drug also caused no difference in gene clustering in young HVs and a slight but significant difference in clustering of MS monocytes upon pioglitazone treatment. This result suggests that this drug may allow for a more targeted change in monocytes. In this case, the genes upregulated upon pioglitazone treatment were largely related to anti-inflammatory, M2 pathways. Pioglitazone treatment did not appear to affect CD163 in early monocyte phagocytosis; however, it did show a significant reduction in surface CD14 expression and increased sCD14 in MS patient monocytes (Fig. 6.5), suggesting a more M2-like phenotype upon pioglitazone treatment. Then, at later stages of monocyte differentiation and macrophage polarisation, in our M1/M2 culture conditions, pioglitazone did significantly increase surface CD163 expression in both M1 and M2 macrophages from MS patients. Again, this drug caused no significant difference in receptor expression in young HVs. This study using the functional results on myelin debris phagocytosis and the modulation of measurable CSF biomarkers (Komori et al., 2015) can be utilised to compare functional effects that can be observed with clinical tests in MS, and the effects of pioglitazone can also be correlated to the change in sCD14/sCD163 in the CSF of MS patients. This will allow us to determine whether these *in vitro* studies display similar pharmacodynamic effects that can be observed *in vivo* as the clinical tools to study these changes are readily available.

Further combined and targeted modulation of both the RXR and PPARγ pathway may lead to both a more controlled system (as seen with pioglitazone

treatment) and a larger activation of RXR/PPARγ pathways and enhanced myelin debris phagocytosis (as seen with animal models of RXR and bexarotene treatment). Currently, some modulators exist that function to activate both of these receptors, such as the synthetic agonist LG 100754 (Tocris). However, in order to effect enhanced synergistic activation of these receptors, both ligand binding domains must be activated and engaged. In the case of current modulators, they only function to enhance PPARγ binding to the ligand when RXR is present. Development of a drug that can activate both pathways and reduce the off-target effects of activating all forms of RXR may further enhance our understanding of these pathways and allow for a more targeted and more effective approach to enhancing myelin debris clearance and anti-inflammatory pathways to promote CNS remyelination. In addition to identifying a more applicable activator of this pathway, further correlation between the role of monocyte function and disease status in MS may lead to a greater understanding of how these cells directly affect disease status and disability. The current study is able to correlate activation of these pathways in *in vitro* monocyte cultures from MS patients and animal models of demyelination. However, further studies on the disability state of the MS patients that monocytes were isolated from may increase our understanding of how deficiencies in myelin debris phagocytosis and enhanced inflammatory markers may affect disability in these patients. Through studying MRI scans, biomarkers of MS, and clinical disability scales, we can further correlate the role of monocytes to remyelination in patients.

In CNS biology, signals from the systemic environment, such as those from young macrophages, can improve CNS recovery. When these cells are targeted in aged subjects, enhancing the RXR and PPARγ pathways results in efficient phagocytosis of myelin debris and may override age-related deficits in CNS remyelination. In the pathogenesis of progressive MS, OPC differentiation is inhibited and removing barriers to remyelination is critical to the therapeutic efficacy of future treatments. In addition, we know that factors affecting macrophage plasticity in the ageing environment affect phagocytic ability. Since these cells have a great deal of heterogeneity and can adapt to different biological cues, modulating their environment and expression profiles can help recover age-related deficits, making them an ideal target for endogenous repair. Through the activation of the RXR-PPARγ pathway in monocyte-derived macrophages, we have shown that it is

possible to reverse the age-related decline in nuclear receptor expression and enhance myelin debris phagocytosis, thus making this an intriguing therapeutic target for progressive stages of demyelinating diseases.

In conclusion, we identified activation of therapeutically-modifiable pathways during efficient clearance of myelin debris by phagocytes in humans and mice. We observed that efficiency of myelin phagocytosis declines in ageing and that this age-related defect can be partially reversed, in both animal and human systems, by activating nuclear receptor pathways. Efficient clearance of myelin debris enhances remyelination in experimental models, while ageing in humans is associated with defective/insufficient remyelination. These combined observations raise a possibility that pharmacological enhancement of myelin phagocytosis in humans through the RXR-PPARγ pathway may promote OPC differentiation and enhance remyelination in ageing patients with demyelinating diseases.

References

1. Aggarwal, S., L. Yurlova, and M. Simons. 2011. Central nervous system myelin: structure, synthesis and assembly. *Trends in cell biology* 21:585-593.
2. Aharonowiz, M., O. Einstein, N. Fainstein, H. Lassmann, B. Reubinoff, and T. Ben-Hur. 2008. Neuroprotective Effect of Transplanted Human Embryonic Stem Cell-Derived Neural Precursors in an Animal Model of Multiple Sclerosis. *PloS one* 3:e3145.
3. Ahn, M., W. Yang, H. Kim, J.K. Jin, C. Moon, and T. Shin. 2012. Immunohistochemical study of arginase-1 in the spinal cords of Lewis rats with experimental autoimmune encephalomyelitis. *Brain Res* 1453:77-86.
4. Aprahamian, T., Y. Takemura, D. Goukassian, and K. Walsh. 2008. Ageing is associated with diminished apoptotic cell clearance in vivo. *Clin Exp Immunol* 152:448-455.
5. Aranda, A., and A. Pascual. 2001. Nuclear hormone receptors and gene expression. *Physiol Rev* 81:1269-1304.
6. Arnett, H.A., S.P. Fancy, J.A. Alberta, C. Zhao, S.R. Plant, S. Kaing, C.S. Raine, D.H. Rowitch, R.J. Franklin, and C.D. Stiles. 2004. bHLH transcription factor Olig1 is required to repair demyelinated lesions in the CNS. *Science* 306:2111-2115.
7. Ascherio, A., K.L. Munger, R. White, K. Kochert, K.C. Simon, C.H. Polman, M.S. Freedman, H.P. Hartung, D.H. Miller, X. Montalban, G. Edan, F. Barkhof, D. Pleimes, E.W. Radu, R. Sandbrink, L. Kappos, and C. Pohl. 2014. Vitamin D as an early predictor of multiple sclerosis activity and progression. *JAMA Neurol* 71:306-314.
8. Ashcroft, G.S., M.A. Horan, and M.W. Ferguson. 1997. The effects of ageing on wound healing: immunolocalisation of growth factors and their receptors in a murine incisional model. *J Anat* 190 (Pt 3):351-365.
9. Asou, H., K. Hamada, K. Uyemura, T. Sakota, and K. Hayashi. 1994. How do oligodendrocytes ensheath and myelinate nerve fibers? *Brain Res Bull* 35:359-365.
10. Back, S.A., T.M. Tuohy, H. Chen, N. Wallingford, A. Craig, J. Struve, N.L. Luo, F. Banine, Y. Liu, A. Chang, B.D. Trapp, B.F. Bebo, Jr., M.S. Rao, and L.S. Sherman. 2005. Hyaluronan accumulates in demyelinated lesions and inhibits oligodendrocyte progenitor maturation. *Nat Med* 11:966-972.
11. Baer, A.S., Y.A. Syed, S.U. Kang, D. Mitteregger, R. Vig, C. Ffrench-Constant, R.J. Franklin, F. Altmann, G. Lubec, and M.R. Kotter. 2009. Myelin-mediated inhibition of oligodendrocyte precursor differentiation can be overcome by pharmacological modulation of Fyn-RhoA and protein kinase C signalling. *Brain* 132:465-481.
12. Baker, M.E. 2011. Origin and diversification of steroids: co-evolution of enzymes and nuclear receptors. *Mol Cell Endocrinol* 334:14-20.
13. Barnett, M.H., and J.W. Prineas. 2004. Relapsing and remitting multiple sclerosis: pathology of the newly forming lesion. *Ann Neurol* 55:458-468.
14. Baron, W., and D. Hoekstra. 2010. On the biogenesis of myelin membranes: sorting, trafficking and cell polarity. *FEBS Lett* 584:1760-1770.
15. Baron, W., E.J. de Vries, H. de Vries, and D. Hoekstra. 1999. Protein kinase C prevents oligodendrocyte differentiation: modulation of actin cytoskeleton and cognate polarized membrane traffic. *J Neurobiol* 41:385-398.
16. Bartzokis, G., M. Beckson, P.H. Lu, K.H. Nuechterlein, N. Edwards, and J. Mintz. 2001. Age-related changes in frontal and temporal lobe volumes in men: a magnetic resonance imaging study. *Arch Gen Psychiatry* 58:461-465.

17. Bartzokis, G., P.H. Lu, K. Tingus, M.F. Mendez, A. Richard, D.G. Peters, B. Oluwadara, K.A. Barrall, J.P. Finn, P. Villablanca, P.M. Thompson, and J. Mintz. 2010. Lifespan trajectory of myelin integrity and maximum motor speed. *Neurobiol Aging* 31:1554-1562.
18. Bauer, J., M. Bradl, W.F. Hickley, S. Forss-Petter, H. Breitschopf, C. Linington, H. Wekerle, and H. Lassmann. 1998. T-cell apoptosis in inflammatory brain lesions: destruction of T cells does not depend on antigen recognition. *Am J Pathol* 153:715-724.
19. Baumann, C.T., P. Maruvada, G.L. Hager, and P.M. Yen. 2001. Nuclear cytoplasmic shuttling by thyroid hormone receptors. multiple protein interactions are required for nuclear retention. *J Biol Chem* 276:11237-11245.
20. Bernardo, A., D. Bianchi, V. Magnaghi, and L. Minghetti. 2009. Peroxisome proliferator-activated receptor-gamma agonists promote differentiation and antioxidant defenses of oligodendrocyte progenitor cells. *J Neuropathol Exp Neurol* 68:797-808.
21. Bethoux, F., D.M. Miller, and R.P. Kinkel. 2001. Recovery following acute exacerbations of multiple sclerosis: from impairment to quality of life. *Mult Scler* 7:137-142.
22. Beyer, M., U. Gimsa, I.Y. Eyupoglu, N.P. Hailer, and R. Nitsch. 2000. Phagocytosis of neuronal or glial debris by microglial cells: upregulation of MHC class II expression and multinuclear giant cell formation in vitro. *Glia* 31:262-266.
23. Blakemore, W.F., and R.J.M. Franklin. 2008. Remyelination in Experimental Models of Toxin-Induced Demyelination. In Advances in multiple Sclerosis and Experimental Demyelinating Diseases. M. Rodriguez, editor Springer Berlin Heidelberg, 193-212.
24. Bogie, J.F., S. Timmermans, V.A. Huynh-Thu, A. Irrthum, H.J. Smeets, J.A. Gustafsson, K.R. Steffensen, M. Mulder, P. Stinissen, N. Hellings, and J.J. Hendriks. 2012. Myelin-derived lipids modulate macrophage activity by liver X receptor activation. *PLoS One* 7:e44998.
25. Bogie, J.F., W. Jorissen, J. Mailleux, P.G. Nijland, N. Zelcer, T. Vanmierlo, J. Van Horssen, P. Stinissen, N. Hellings, and J.J. Hendriks. 2013. Myelin alters the inflammatory phenotype of macrophages by activating PPARs. *Acta Neuropathologica* 1:43.
26. Boven, L.A., M. Van Meurs, M. Van Zwam, A. Wierenga-Wolf, R.Q. Hintzen, R.G. Boot, J.M. Aerts, S. Amor, E.E. Nieuwenhuis, and J.D. Laman. 2006. Myelin-laden macrophages are anti-inflammatory, consistent with foam cells in multiple sclerosis. *Brain* 129:517-526.
27. Bramow, S., J.M. Frischer, H. Lassmann, N. Koch-Henriksen, C.F. Lucchinetti, P.S. Sorensen, and H. Laursen. 2010. Demyelination versus remyelination in progressive multiple sclerosis. *Brain* 133:2983-2998.
28. Brettschneider, J., D. Ecker, A. Bitsch, D. Bahner, T. Bogumil, A. Dressel, E. Elitok, B. Kitze, S. Poser, F. Weber, and H. Tumani. 2002. The macrophage activity marker sCD14 is increased in patients with multiple sclerosis and upregulated by interferon beta-1b. *J Neuroimmun* 133:193-197.
29. Brew, B.J., N.W. Davies, P. Cinque, D.B. Clifford, and A. Nath. 2010. Progressive multifocal leukoencephalopathy and other forms of JC virus disease. *Nat Rev Neurol* 6:667-679.

30. Briscoe, J., A. Pierani, T.M. Jessell, and J. Ericson. 2000. A homeodomain protein code specifies progenitor cell identity and neuronal fate in the ventral neural tube. *Cell* 101:435-445.
31. Brown, N.S., A. Smart, V. Sharma, M.L. Brinkmeier, L. Greenlee, S.A. Camper, D.R. Jensen, R.H. Eckel, W. Krezel, P. Chambon, and B.R. Haugen. 2000. Thyroid hormone resistance and increased metabolic rate in the RXR-gamma-deficient mouse. *J Clin Invest* 106:73-79.
32. Butovsky, O., Y. Ziv, A. Schwartz, G. Landa, A.E. Talpalar, S. Pluchino, G. Martino, and M. Schwartz. 2006. Microglia activated by IL-4 or IFN-gamma differentially induce neurogenesis and oligodendrogenesis from adult stem/progenitor cells. *Mol Cell Neurosci* 31:149-160.
33. Caprariello, A.V., S. Mangla, R.H. Miller, and S.M. Selkirk. 2012. Apoptosis of oligodendrocytes in the central nervous system results in rapid focal demyelination. *Ann Neurol* 72:395-405.
34. Carroll, S.J. 2009. Handbook of the Neuroscience of Aging. Academic Press (Elsevier), London, UK. 690 pp.
35. Chang, A., W.W. Tourtellotte, R. Rudick, and B.D. Trapp. 2002. Premyelinating oligodendrocytes in chronic lesions of multiple sclerosis. *N Engl J Med* 346:165-173.
36. Charles, P., R. Reynolds, D. Seilhean, G. Rougon, M.S. Aigrot, A. Niezgoda, B. Zalc, and C. Lubetzki. 2002. Re-expression of PSA-NCAM by demyelinated axons: an inhibitor of remyelination in multiple sclerosis? *Brain* 125:1972-1979.
37. Chawla, A., J.J. Repa, R.M. Evans, and D.J. Mangelsdorf. 2001. Nuclear receptors and lipid physiology: opening the X-files. *Science* 294:1866-1870.
38. Chen, C.D., J.A. Sloane, H. Li, N. Aytan, E.L. Giannaris, E. Zeldich, J.D. Hinman, A. Dedeoglu, D.L. Rosene, R. Bansal, J.I. Luebke, M. Kuro-o, and C.R. Abraham. 2013. The antiaging protein Klotho enhances oligodendrocyte maturation and myelination of the CNS. *J Neurosci* 33:1927-1939.
39. Chen, H., and M.L. Privalsky. 1995. Cooperative formation of high-order oligomers by retinoid X receptors: an unexpected mode of DNA recognition. *Proc Natl Acad Sci U S A* 92:422-426.
40. Chen, J.D., and R.M. Evans. 1995. A transcriptional co-repressor that interacts with nuclear hormone receptors. *Nature* 377:454-457.
41. Chinetti, G., S. Lestavel, V. Bocher, A.T. Remaley, B. Neve, I.P. Torra, E. Teissier, A. Minnich, M. Jaye, N. Duverger, H.B. Brewer, J.C. Fruchart, V. Clavey, and B. Staels. 2001. PPAR-alpha and PPAR-gamma activators induce cholesterol removal from human macrophage foam cells through stimulation of the ABCA1 pathway. *Nat Med* 7:53-58.
42. Chinetti-Gbaguidi, G., S. Colin, and B. Staels. 2015. Macrophage subsets in atherosclerosis. *Nat Rev Cardiol* 12:10-17.
43. Clifford, D.B., A. De Luca, D.M. Simpson, G. Arendt, G. Giovannoni, and A. Nath. 2010. Natalizumab-associated progressive multifocal leukoencephalopathy in patients with multiple sclerosis: lessons from 28 cases. *Lancet Neurol* 9:438-446.
44. Cohen, J.A., A.J. Coles, D.L. Arnold, C. Confavreux, E.J. Fox, H.P. Hartung, E. Havrdova, K.W. Selmaj, H.L. Weiner, E. Fisher, V.V. Brinar, G. Giovannoni, M. Stojanovic, B.I. Ertik, S.L. Lake, D.H. Margolin, M.A. Panzara, D.A. Compston, and C.-M.I. investigators. 2012. Alemtuzumab versus interferon

beta 1a as first-line treatment for patients with relapsing-remitting multiple sclerosis: a randomised controlled phase 3 trial. *Lancet* 380:1819-1828.
45. Coles, A.J., C.L. Twyman, D.L. Arnold, J.A. Cohen, C. Confavreux, E.J. Fox, H.P. Hartung, E. Havrdova, K.W. Selmaj, H.L. Weiner, T. Miller, E. Fisher, R. Sandbrink, S.L. Lake, D.H. Margolin, P. Oyuela, M.A. Panzara, D.A. Compston, and C.-M.I. investigators. 2012. Alemtuzumab for patients with relapsing multiple sclerosis after disease-modifying therapy: a randomised controlled phase 3 trial. *Lancet* 380:1829-1839.
46. Comi, G., M. Filippi, and J.S. Wolinsky. 2001. European/Canadian multicenter, double-blind, randomized, placebo-controlled study of the effects of glatiramer acetate on magnetic resonance imaging--measured disease activity and burden in patients with relapsing multiple sclerosis. European/Canadian Glatiramer Acetate Study Group. *Ann Neurol* 49:290-297.
47. Committee, N.R.N. 1999. A Unified Nomenclature System for the Nuclear Receptor Superfamily. *Cell* 97:161-163.
48. Compston, A., and A. Coles. 2008. Multiple sclerosis. *Lancet* 372:1502-1517.
49. Confavreux, C., and S. Vukusic. 2006. Age at disability milestones in multiple sclerosis. *Brain* 129:595-605.
50. Cramer, P.E., J.R. Cirrito, D.W. Wesson, C.Y. Lee, J.C. Karlo, A.E. Zinn, B.T. Casali, J.L. Restivo, W.D. Goebel, M.J. James, K.R. Brunden, D.A. Wilson, and G.E. Landreth. 2012. ApoE-directed therapeutics rapidly clear beta-amyloid and reverse deficits in AD mouse models. *Science* 335:1503-1506.
51. Dave, V., Kaul, D, Sharma, M. 2012. Crosstalk between RXR, LXR and VDR within blood mononuclear cellular model. *Indian J Exp Biol* 50:35-40.
52. Davis, B.H., and P.V. Zarev. 2005. Human monocyte CD163 expression inversely correlates with soluble CD163 plasma levels. *Cytometry Part B: Clinical Cytometry* 63B:16-22.
53. Dawson, M.R., A. Polito, J.M. Levine, and R. Reynolds. 2003. NG2-expressing glial progenitor cells: an abundant and widespread population of cycling cells in the adult rat CNS. *Mol Cell Neurosci* 24:476-488.
54. de Monasterio-Schrader, P., O. Jahn, S. Tenzer, S.P. Wichert, J. Patzig, and H.B. Werner. 2012. Systematic approaches to central nervous system myelin. *Cell Mol Life Sci* 69:2879-2894.
55. De Nuccio, C., A. Bernardo, R. De Simone, E. Mancuso, V. Magnaghi, S. Visentin, and L. Minghetti. 2011. Peroxisome proliferator-activated receptor gamma agonists accelerate oligodendrocyte maturation and influence mitochondrial functions and oscillatory Ca(2+) waves. *J Neuropathol Exp Neurol* 70:900-912.
56. DeFronzo, R.A., D. Tripathy, D.C. Schwenke, M. Banerji, G.A. Bray, T.A. Buchanan, S.C. Clement, R.R. Henry, H.N. Hodis, A.E. Kitabchi, W.J. Mack, S. Mudaliar, R.E. Ratner, K. Williams, F.B. Stentz, N. Musi, and P.D. Reaven. 2011. Pioglitazone for Diabetes Prevention in Impaired Glucose Tolerance. *NEJM* 364:1104-1115.
57. Deverman, B.E., and P.H. Patterson. 2012. Exogenous leukemia inhibitory factor stimulates oligodendrocyte progenitor cell proliferation and enhances hippocampal remyelination. *J Neurosci* 32:2100-2109.
58. Diab, A., R.Z. Hussain, A.E. Lovett-Racke, J.A. Chavis, P.D. Drew, and M.K. Racke. 2004. Ligands for the peroxisome proliferator-activated receptor-gamma and the retinoid X receptor exert additive anti-inflammatory effects on experimental autoimmune encephalomyelitis. *J Neuroimmunol* 148:116-126.

59. Diemel, L.T., C.A. Copelman, and M.L. Cuzner. 1998. Macrophages in CNS remyelination: friend or foe? *Neurochem Res* 23:341-347.
60. DiLorenzo, T., J. Halper, and M.A. Picone. 2004. Comparison of Older and Younger Individuals With Multiple Sclerosis: A Preliminary Investigation. *Rehabilitation Psychology* 49:123-125.
61. Drew, P.D., J. Xu, and M.K. Racke. 2008. PPAR-gamma: Therapeutic Potential for Multiple Sclerosis. *PPAR Res* 2008:627463.
62. Duquette, P., T.J. Murray, J. Pleines, G.C. Ebers, D. Sadovnick, P. Weldon, S. Warren, D.W. Paty, A. Upton, W. Hader, R. Nelson, A. Auty, B. Neufeld, and C. Meltzer. 1987. Multiple sclerosis in childhood: Clinical profile in 125 patients. *J Pediatrics* 111:359-363.
63. Durafourt, B.A., C.S. Moore, D.A. Zammit, T.A. Johnson, F. Zaguia, M.C. Guiot, A. Bar-Or, and J.P. Antel. 2012. Comparison of polarization properties of human adult microglia and blood-derived macrophages. *Glia* 60:717-727.
64. Dyall, S.C., G.J. Michael, and A.T. Michael-Titus. 2010. Omega-3 fatty acids reverse age-related decreases in nuclear receptors and increase neurogenesis in old rats. *J Neurosci Res* 88:2091-2102.
65. Ebers, G.C., D.E. Bulman, A.D. Sadovnick, D.W. Paty, S. Warren, W. Hader, T.J. Murray, T.P. Seland, P. Duquette, T. Grey, and et al. 1986. A population-based study of multiple sclerosis in twins. *N Engl J Med* 315:1638-1642.
66. Eckland, D., and M. Danhof. 2000. Clinical pharmacokinetics of pioglitazone. *Exp Clin Endocrin Diab* 108:234-242.
67. Edgar, J.M., M. McLaughlin, H.B. Werner, M.C. McCulloch, J.A. Barrie, A. Brown, A.B. Faichney, N. Snaidero, K.A. Nave, and I.R. Griffiths. 2009. Early ultrastructural defects of axons and axon-glia junctions in mice lacking expression of Cnp1. *Glia* 57:1815-1824.
68. Edin, S., M.L. Wikberg, J. Rutegård, P.-A. Oldenborg, and R. Palmqvist. 2013. Phenotypic Skewing of Macrophages In Vitro by Secreted Factors from Colorectal Cancer Cells. *PLoS ONE* 8:e74982.
69. Emery, B. 2010. Transcriptional and post-transcriptional control of CNS myelination. *Curr Opin Neurobiol* 20:601-607.
70. Eske, K., K. Breitbach, J. Kohler, P. Wongprompitak, and I. Steinmetz. 2009. Generation of murine bone marrow derived macrophages in a standardised serum-free cell culture system. *J Immunol Methods* 342:13-19.
71. Evangelou, N., D. Konz, M.M. Esiri, S. Smith, J. Palace, and P.M. Matthews. 2001. Size-selective neuronal changes in the anterior optic pathways suggest a differential susceptibility to injury in multiple sclerosis. *Brain* 124:1813-1820.
72. Evans, R.M., and D.J. Mangelsdorf. 2014. Nuclear Receptors, RXR, and the Big Bang. *Cell* 157:255-266.
73. Fabriek, B.O., H.J. Møller, R.P.M. Vloet, L.M. van Winsen, R. Hanemaaijer, C.E. Teunissen, B.M.J. Uitdehaag, T.K. van den Berg, and C.D. Dijkstra. 2007. Proteolytic shedding of the macrophage scavenger receptor CD163 in multiple sclerosis. *J Neuroimmunol* 187:179-186.
74. Fancy, S.P., M.R. Kotter, E.P. Harrington, J.K. Huang, C. Zhao, D.H. Rowitch, and R.J. Franklin. 2010. Overcoming remyelination failure in multiple sclerosis and other myelin disorders. *Exp Neurol* 225:18-23.
75. Fancy, S.P., S.E. Baranzini, C. Zhao, D.I. Yuk, K.A. Irvine, S. Kaing, N. Sanai, R.J. Franklin, and D.H. Rowitch. 2009. Dysregulation of the Wnt pathway inhibits timely myelination and remyelination in the mammalian CNS. *Genes Dev* 23:1571-1585.

76. Feinstein, D.L., E. Galea, V. Gavrilyuk, C.F. Brosnan, C.C. Whitacre, L. Dumitrescu-Ozimek, G.E. Landreth, H.A. Pershadsingh, G. Weinberg, and M.T. Heneka. 2002. Peroxisome proliferator-activated receptor-gamma agonists prevent experimental autoimmune encephalomyelitis. *Ann Neurol* 51:694-702.
77. Fields, R.D. 2008. White matter in learning, cognition and psychiatric disorders. *Trends Neurosci* 31:361-370.
78. Fitzner, D., M. Schnaars, D. van Rossum, G. Krishnamoorthy, P. Dibaj, M. Bakhti, T. Regen, U.K. Hanisch, and M. Simons. 2011. Selective transfer of exosomes from oligodendrocytes to microglia by macropinocytosis. *J Cell Sci* 124:447-458.
79. Flesch, I., A. Fruh, and E. Ferber. 1986. Functional comparison of bone marrow-derived macrophages obtained by cultivation in serum-free or serum-supplemented medium. *Immunobiology* 173:72-81.
80. Foote, A.K., and W.F. Blakemore. 2005. Repopulation of oligodendrocyte progenitor cell-depleted tissue in a model of chronic demyelination. *Neuropathol Appl Neurobiol* 31:374-383.
81. Franklin, R.J. 2002. Why does remyelination fail in multiple sclerosis? *Nat Rev Neurosci* 3:705-714.
82. Franklin, R.J., and C. Ffrench-Constant. 2008. Remyelination in the CNS: from biology to therapy. *Nat Rev Neurosci* 9:839-855.
83. Franklin, R.J., and M.R. Kotter. 2008. The biology of CNS remyelination: the key to therapeutic advances. *J Neurol* 255 Suppl 1:19-25.
84. Franklin, R.J., and V. Gallo. 2014. The translational biology of remyelination: past, present, and future. *Glia* 62:1905-1915.
85. Freeman, M.R., and D.H. Rowitch. 2013. Evolving concepts of gliogenesis: a look way back and ahead to the next 25 years. *Neuron* 80:613-623.
86. Fruhbeis, C., D. Frohlich, W.P. Kuo, J. Amphornrat, S. Thilemann, A.S. Saab, F. Kirchhoff, W. Mobius, S. Goebbels, K.A. Nave, A. Schneider, M. Simons, M. Klugmann, J. Trotter, and E.M. Kramer-Albers. 2013. Neurotransmitter-triggered transfer of exosomes mediates oligodendrocyte-neuron communication. *PLoS Biol* 11:e1001604.
87. Gadea, A., A. Aguirre, T.F. Haydar, and V. Gallo. 2009. Endothelin-1 regulates oligodendrocyte development. *J Neurosci* 29:10047-10062.
88. Geurts, J.J., and F. Barkhof. 2008. Grey matter pathology in multiple sclerosis. *Lancet Neurol* 7:841-851.
89. Ginhoux, F., M. Greter, M. Leboeuf, S. Nandi, P. See, S. Gokhan, M.F. Mehler, S.J. Conway, L.G. Ng, E.R. Stanley, I.M. Samokhvalov, and M. Merad. 2010. Fate mapping analysis reveals that adult microglia derive from primitive macrophages. *Science* 330:841-845.
90. Gitik, M., S. Liraz-Zaltsman, P.A. Oldenborg, F. Reichert, and S. Rotshenker. 2011. Myelin down-regulates myelin phagocytosis by microglia and macrophages through interactions between CD47 on myelin and SIRPalpha (signal regulatory protein-alpha) on phagocytes. *J Neuroinflammation* 8:24.
91. Giulian, D., J. Chen, J.E. Ingeman, J.K. George, and M. Noponen. 1989. The role of mononuclear phagocytes in wound healing after traumatic injury to adult mammalian brain. *J Neurosci* 9:4416-4429.
92. Gold, R., H.-P. Hartung, and K.V. Toyka. 2000. Animal models for autoimmune demyelinating disorders of the nervous system. *Molecular Medicine Today* 6:88-91.

93. Goldmann, T., P. Wieghofer, P.F. Muller, Y. Wolf, D. Varol, S. Yona, S.M. Brendecke, K. Kierdorf, O. Staszewski, M. Datta, T. Luedde, M. Heikenwalder, S. Jung, and M. Prinz. 2013. A new type of microglia gene targeting shows TAK1 to be pivotal in CNS autoimmune inflammation. *Nat Neurosci* 16:1618-1626.
94. Goncalves, A.F., N.G. Dias, M. Moransard, R. Correia, J.A. Pereira, W. Witke, U. Suter, and J.B. Relvas. 2010. Gelsolin is required for macrophage recruitment during remyelination of the peripheral nervous system. *Glia* 58:706-715.
95. Griffiths, I., M. Klugmann, T. Anderson, D. Yool, C. Thomson, M.H. Schwab, A. Schneider, F. Zimmermann, M. McCulloch, N. Nadon, and K.A. Nave. 1998. Axonal swellings and degeneration in mice lacking the major proteolipid of myelin. *Science* 280:1610-1613.
96. Groves, A.K., S.C. Barnett, R.J. Franklin, A.J. Crang, M. Mayer, W.F. Blakemore, and M. Noble. 1993. Repair of demyelinated lesions by transplantation of purified O-2A progenitor cells. *Nature* 362:453-455.
97. Guy, J., E.A. Ellis, K. Kelley, and G.M. Hope. 1989. Spectra of G ratio, myelin sheath thickness, and axon and fiber diameter in the guinea pig optic nerve. *The Journal of Comparative Neurology* 287:446-454.
98. Hadas, S., F. Reichert, and S. Rotshenker. 2010. Dissimilar and similar functional properties of complement receptor-3 in microglia and macrophages in combating yeast pathogens by phagocytosis. *Glia* 58:823-830.
99. Hammond, Timothy R., A. Gadea, J. Dupree, C. Kerninon, B. Nait-Oumesmar, A. Aguirre, and V. Gallo. 2014. Astrocyte-Derived Endothelin-1 Inhibits Remyelination through Notch Activation. *Neuron* 81:588-602.
100. Handel, A.E., G. Giovannoni, G.C. Ebers, and S.V. Ramagopalan. 2010. Environmental factors and their timing in adult-onset multiple sclerosis. *Nat Rev Neurol* 6:156-166.
101. Harris, J.J., and D. Attwell. 2012. The energetics of CNS white matter. *J Neurosci* 32:356-371.
102. Haynes, S.E., G. Hollopeter, G. Yang, D. Kurpius, M.E. Dailey, W.B. Gan, and D. Julius. 2006. The P2Y12 receptor regulates microglial activation by extracellular nucleotides. *Nat Neurosci* 9:1512-1519.
103. Hearps, A.C., G.E. Martin, T.A. Angelovich, W.J. Cheng, A. Maisa, A.L. Landay, A. Jaworowski, and S.M. Crowe. 2012. Aging is associated with chronic innate immune activation and dysregulation of monocyte phenotype and function. *Aging Cell* 11:867-875.
104. Henderson, A.P., M.H. Barnett, J.D. Parratt, and J.W. Prineas. 2009. Multiple sclerosis: distribution of inflammatory cells in newly forming lesions. *Ann Neurol* 66:739-753.
105. Hendriks, J.J., H. Slaets, S. Carmans, H.E. de Vries, C.D. Dijkstra, P. Stinissen, and N. Hellings. 2008. Leukemia inhibitory factor modulates production of inflammatory mediators and myelin phagocytosis by macrophages. *J Neuroimmunol* 204:52-57.
106. Henney, J.E. 2000. From the Food and Drug Administration. *JAMA* 283:1131.
107. Heyman, R.A., D.J. Mangelsdorf, J.A. Dyck, R.B. Stein, G. Eichele, R.M. Evans, and C. Thaller. 1992. 9-cis retinoic acid is a high affinity ligand for the retinoid X receptor. *Cell* 68:397-406.

108. Hinks, G.L., and R.J. Franklin. 1999. Distinctive patterns of PDGF-A, FGF-2, IGF-I, and TGF-beta1 gene expression during remyelination of experimentally-induced spinal cord demyelination. *Mol Cell Neurosci* 14:153-168.
109. Hinks, G.L., and R.J. Franklin. 2000. Delayed changes in growth factor gene expression during slow remyelination in the CNS of aged rats. *Mol Cell Neurosci* 16:542-556.
110. Horlein, A.J., A.M. Naar, T. Heinzel, J. Torchia, B. Gloss, R. Kurokawa, A. Ryan, Y. Kamei, M. Soderstrom, C.K. Glass, and et al. 1995. Ligand-independent repression by the thyroid hormone receptor mediated by a nuclear receptor co-repressor. *Nature* 377:397-404.
111. Hu, Y., I. Doudevski, D. Wood, M. Moscarello, C. Husted, C. Genain, J.A. Zasadzinski, and J. Israelachvili. 2004. Synergistic interactions of lipids and myelin basic protein. *Proc Natl Acad Sci U S A* 101:13466-13471.
112. Huang, J.K., A.A. Jarjour, B. Nait Oumesmar, C. Kerninon, A. Williams, W. Krezel, H. Kagechika, J. Bauer, C. Zhao, A. Baron-Van Evercooren, P. Chambon, C. Ffrench-Constant, and R.J. Franklin. 2011. Retinoid X receptor gamma signaling accelerates CNS remyelination. *Nat Neurosci* 14:45-53.
113. Huang, J.T., J.S. Welch, M. Ricote, C.J. Binder, T.M. Willson, C. Kelly, J.L. Witztum, C.D. Funk, D. Conrad, and C.K. Glass. 1999. Interleukin-4-dependent production of PPAR-gamma ligands in macrophages by 12/15-lipoxygenase. *Nature* 400:378-382.
114. Imai, M., M. Watanabe, K. Suyama, T. Osada, D. Sakai, H. Kawada, M. Matsumae, and J. Mochida. 2008. Delayed accumulation of activated macrophages and inhibition of remyelination after spinal cord injury in an adult rodent model. *J Neurosurg Spine* 8:58-66.
115. Ingle, G.T., A.J. Thompson, and D.H. Miller. 2002. Magnetic resonance imaging in primary progressive multiple sclerosis. *J Rehabil Res Dev* 39:261-271.
116. International Multiple Sclerosis Genetics, C., A.H. Beecham, N.A. Patsopoulos, D.K. Xifara, M.F. Davis, A. Kemppinen, C. Cotsapas, T.S. Shahi, C. Spencer, D. Booth, A. Goris, A. Oturai, J. Saarela, B. Fontaine, B. Hemmer, C. Martin, F. Zipp, S. D'alfonso, F. Martinelli-Boneschi, B. Taylor, H.F. Harbo, I. Kockum, J. Hillert, T. Olsson, M. Ban, J.R. Oksenberg, R. Hintzen, L.F. Barcellos, C. Wellcome Trust Case Control, I.B.D.G.C. International, C. Agliardi, L. Alfredsson, M. Alizadeh, C. Anderson, R. Andrews, H.B. Søndergaard, A. Baker, G. Band, S.E. Baranzini, N. Barizzone, J. Barrett, C. Bellenguez, L. Bergamaschi, L. Bernardinelli, A. Berthele, V. Biberacher, T.M.C. Binder, H. Blackburn, I.L. Bomfim, P. Brambilla, S. Broadley, B. Brochet, L. Brundin, D. Buck, H. Butzkueven, S.J. Caillier, W. Camu, W. Carpentier, P. Cavalla, E.G. Celius, I. Coman, G. Comi, L. Corrado, L. Cosemans, I. Cournu-Rebeix, B.A.C. Cree, D. Cusi, V. Damotte, G. Defer, S.R. Delgado, P. Deloukas, A. di Sapio, A.T. Dilthey, P. Donnelly, B. Dubois, M. Duddy, S. Edkins, I. Elovaara, F. Esposito, N. Evangelou, B. Fiddes, J. Field, A. Franke, C. Freeman, I.Y. Frohlich, D. Galimberti, C. Gieger, P.-A. Gourraud, C. Graetz, A. Graham, V. Grummel, C. Guaschino, A. Hadjixenofontos, H. Hakonarson, C. Halfpenny, G. Hall, P. Hall, A. Hamsten, J. Harley, T. Harrower, C. Hawkins, G. Hellenthal, C. Hillier, J. Hobart, M. Hoshi, S.E. Hunt, M. Jagodic, I. Jelčić, A. Jochim, B. Kendall, A. Kermode, T. Kilpatrick, K. Koivisto, I. Konidari, T. Korn, H. Kronsbein, C. Langford, M.

Larsson, M. Lathrop, C. Lebrun-Frenay, J. Lechner-Scott, M.H. Lee, M.A. Leone, V. Leppä, G. Liberatore, B.A. Lie, C.M. Lill, M. Lindén, J. Link, F. Luessi, J. Lycke, F. Macciardi, S. Männistö, C.P. Manrique, R. Martin, V. Martinelli, D. Mason, G. Mazibrada, C. McCabe, I.-L. Mero, J. Mescheriakova, L. Moutsianas, K.-M. Myhr, G. Nagels, R. Nicholas, P. Nilsson, F. Piehl, M. Pirinen, S.E. Price, H. Quach, M. Reunanen, W. Robberecht, N.P. Robertson, M. Rodegher, D. Rog, M. Salvetti, N.C. Schnetz-Boutaud, F. Sellebjerg, R.C. Selter, C. Schaefer, S. Shaunak, L. Shen, S. Shields, V. Siffrin, M. Slee, P.S. Sorensen, M. Sorosina, M. Sospedra, A. Spurkland, A. Strange, E. Sundqvist, V. Thijs, J. Thorpe, A. Ticca, P. Tienari, C. van Duijn, E.M. Visser, S. Vucic, H. Westerlind, J.S. Wiley, A. Wilkins, J.F. Wilson, J. Winkelmann, J. Zajicek, E. Zindler, J.L. Haines, M.A. Pericak-Vance, A.J. Ivinson, G. Stewart, D. Hafler, S.L. Hauser, A. Compston, G. McVean, P. De Jager, S. Sawcer, and J.L. McCauley. 2013. Analysis of immune-related loci identifies 48 new susceptibility variants for multiple sclerosis. *Nature genetics* 45:10.1038/ng.2770.

117. International Multiple Sclerosis Genetics, C., C. Wellcome Trust Case Control, S. Sawcer, G. Hellenthal, M. Pirinen, C.C. Spencer, N.A. Patsopoulos, L. Moutsianas, A. Dilthey, Z. Su, C. Freeman, S.E. Hunt, S. Edkins, E. Gray, D.R. Booth, S.C. Potter, A. Goris, G. Band, A.B. Oturai, A. Strange, J. Saarela, C. Bellenguez, B. Fontaine, M. Gillman, B. Hemmer, R. Gwilliam, F. Zipp, A. Jayakumar, R. Martin, S. Leslie, S. Hawkins, E. Giannoulatou, S. D'Alfonso, H. Blackburn, F. Martinelli Boneschi, J. Liddle, H.F. Harbo, M.L. Perez, A. Spurkland, M.J. Waller, M.P. Mycko, M. Ricketts, M. Comabella, N. Hammond, I. Kockum, O.T. McCann, M. Ban, P. Whittaker, A. Kemppinen, P. Weston, C. Hawkins, S. Widaa, J. Zajicek, S. Dronov, N. Robertson, S.J. Bumpstead, L.F. Barcellos, R. Ravindrarajah, R. Abraham, L. Alfredsson, K. Ardlie, C. Aubin, A. Baker, K. Baker, S.E. Baranzini, L. Bergamaschi, R. Bergamaschi, A. Bernstein, A. Berthele, M. Boggild, J.P. Bradfield, D. Brassat, S.A. Broadley, D. Buck, H. Butzkueven, R. Capra, W.M. Carroll, P. Cavalla, E.G. Celius, S. Cepok, R. Chiavacci, F. Clerget-Darpoux, K. Clysters, G. Comi, M. Cossburn, I. Cournu-Rebeix, M.B. Cox, W. Cozen, B.A. Cree, A.H. Cross, D. Cusi, M.J. Daly, E. Davis, P.I. de Bakker, M. Debouverie, B. D'Hooghe M, K. Dixon, R. Dobosi, B. Dubois, D. Ellinghaus, I. Elovaara, F. Esposito, C. Fontenille, S. Foote, A. Franke, D. Galimberti, A. Ghezzi, J. Glessner, R. Gomez, O. Gout, C. Graham, S.F. Grant, F.R. Guerini, H. Hakonarson, P. Hall, A. Hamsten, H.P. Hartung, R.N. Heard, S. Heath, J. Hobart, M. Hoshi, C. Infante-Duarte, G. Ingram, W. Ingram, T. Islam, M. Jagodic, M. Kabesch, A.G. Kermode, T.J. Kilpatrick, C. Kim, N. Klopp, K. Koivisto, M. Larsson, M. Lathrop, J.S. Lechner-Scott, M.A. Leone, V. Leppa, U. Liljedahl, I.L. Bomfim, R.R. Lincoln, J. Link, J. Liu, A.R. Lorentzen, S. Lupoli, F. Macciardi, T. Mack, M. Marriott, V. Martinelli, D. Mason, J.L. McCauley, F. Mentch, I.L. Mero, T. Mihalova, X. Montalban, J. Mottershead, K.M. Myhr, P. Naldi, W. Ollier, A. Page, A. Palotie, J. Pelletier, L. Piccio, T. Pickersgill, F. Piehl, S. Pobywajlo, H.L. Quach, P.P. Ramsay, M. Reunanen, R. Reynolds, J.D. Rioux, M. Rodegher, S. Roesner, J.P. Rubio, I.M. Ruckert, M. Salvetti, E. Salvi, A. Santaniello, C.A. Schaefer, S. Schreiber, C. Schulze, R.J. Scott, F. Sellebjerg, K.W. Selmaj, D. Sexton, L. Shen, B. Simms-Acuna, S. Skidmore, P.M. Sleiman, C. Smestad, P.S. Sorensen, H.B. Sondergaard, J. Stankovich, R.C. Strange, A.M. Sulonen, E. Sundqvist, A.C. Syvanen, F.

Taddeo, B. Taylor, J.M. Blackwell, P. Tienari, E. Bramon, A. Tourbah, M.A. Brown, E. Tronczynska, J.P. Casas, N. Tubridy, A. Corvin, J. Vickery, J. Jankowski, P. Villoslada, H.S. Markus, K. Wang, C.G. Mathew, J. Wason, C.N. Palmer, H.E. Wichmann, R. Plomin, E. Willoughby, A. Rautanen, J. Winkelmann, M. Wittig, R.C. Trembath, J. Yaouanq, A.C. Viswanathan, H. Zhang, N.W. Wood, R. Zuvich, P. Deloukas, C. Langford, A. Duncanson, J.R. Oksenberg, M.A. Pericak-Vance, J.L. Haines, T. Olsson, J. Hillert, A.J. Ivinson, P.L. De Jager, L. Peltonen, G.J. Stewart, D.A. Hafler, S.L. Hauser, G. McVean, P. Donnelly, and A. Compston. 2011. Genetic risk and a primary role for cell-mediated immune mechanisms in multiple sclerosis. *Nature* 476:214-219.

118. Irvine, K.A., and W.F. Blakemore. 2008. Remyelination protects axons from demyelination-associated axon degeneration. *Brain* 131:1464-1477.

119. Kaiser, C.C., D.K. Shukla, G.T. Stebbins, D.D. Skias, D.R. Jeffery, D. Stefoski, G. Katsamakis, and D.L. Feinstein. 2009. A pilot test of pioglitazone as an add-on in patients with relapsing remitting multiple sclerosis. *J Neuroimmunol* 211:124-130.

120. Karadottir, R., P. Cavelier, L.H. Bergersen, and D. Attwell. 2005. NMDA receptors are expressed in oligodendrocytes and activated in ischaemia. *Nature* 438:1162-1166.

121. Kastner, P., M. Mark, M. Leid, A. Gansmuller, W. Chin, J.M. Grondona, D. Decimo, W. Krezel, A. Dierich, and P. Chambon. 1996. Abnormal spermatogenesis in RXR beta mutant mice. *Genes Dev* 10:80-92.

122. Katagiri, Y., K. Takeda, Z.X. Yu, V.J. Ferrans, K. Ozato, and G. Guroff. 2000. Modulation of retinoid signalling through NGF-induced nuclear export of NGFI-B. *Nat Cell Biol* 2:435-440.

123. Kazawa, T., T. Kawasaki, A. Sakamoto, M. Imamura, R. Ohashi, S. Jiang, T. Tanaka, H. Iwanari, T. Hamakubo, J. Sakai, T. Kodama, and M. Naito. 2009. Expression of liver X receptor alpha and lipid metabolism in granulocyte-macrophage colony-stimulating factor-induced human monocyte-derived macrophage. *Pathol Int* 59:152-160.

124. Keirstead, H.S., and W.F. Blakemore. 1999. The role of oligodendrocytes and oligodendrocyte progenitors in CNS remyelination. *Adv Exp Med Biol* 468:183-197.

125. Kettenmann, H., U.K. Hanisch, M. Noda, and A. Verkhratsky. 2011. Physiology of microglia. *Physiol Rev* 91:461-553.

126. Kirby, B.B., N. Takada, A.J. Latimer, J. Shin, T.J. Carney, R.N. Kelsh, and B. Appel. 2006. In vivo time-lapse imaging shows dynamic oligodendrocyte progenitor behavior during zebrafish development. *Nat Neurosci* 9:1506-1511.

127. Kirk, J., J. Plumb, M. Mirakhur, and S. McQuaid. 2003. Tight junctional abnormality in multiple sclerosis white matter affects all calibres of vessel and is associated with blood-brain barrier leakage and active demyelination. *J Pathol* 201:319-327.

128. Koch-Henriksen, N., and P.S. Sorensen. 2010. The changing demographic pattern of multiple sclerosis epidemiology. *Lancet Neurol* 9:520-532.

129. Komori, M., A. Blake, M. Greenwood, Y.C. Lin, P. Kosa, D. Ghazali, P. Winokur, M. Natrajan, S.C. Wuest, E. Romm, A.A. Panackal, P.R. Williamson,

T. Wu, and B. Bielekova. 2015. CSF markers reveal intrathecal inflammation in progressive multiple sclerosis. *Ann Neurol* n/a-n/a.
130. Kondo, T., and M. Raff. 2000. The Id4 HLH protein and the timing of oligodendrocyte differentiation. *EMBO J* 19:1998-2007.
131. Kornek, B., M.K. Storch, R. Weissert, E. Wallstroem, A. Stefferl, T. Olsson, C. Linington, M. Schmidbauer, and H. Lassmann. 2000. Multiple sclerosis and chronic autoimmune encephalomyelitis: a comparative quantitative study of axonal injury in active, inactive, and remyelinated lesions. *Am J Pathol* 157:267-276.
132. Kotter, M.R., A. Setzu, F.J. Sim, N. Van Rooijen, and R.J. Franklin. 2001. Macrophage depletion impairs oligodendrocyte remyelination following lysolecithin-induced demyelination. *Glia* 35:204-212.
133.
134. Kotter, M.R., C. Zhao, N. van Rooijen, and R.J. Franklin. 2005. Macrophage-depletion induced impairment of experimental CNS remyelination is associated with a reduced oligodendrocyte progenitor cell response and altered growth factor expression. *Neurobiol Dis* 18:166-175.
135. Kotter, M.R., W.W. Li, C. Zhao, and R.J. Franklin. 2006. Myelin impairs CNS remyelination by inhibiting oligodendrocyte precursor cell differentiation. *J Neurosci* 26:328-332.
136. Krauthausen, M., S. Saxe, J. Zimmermann, M. Emrich, M. Heneka, and M. Muller. 2014. CXCR3 modulates glial accumulation and activation in cuprizone-induced demyelination of the central nervous system. *Journal of Neuroinflammation* 11:109.
137. Kremenchutzky, M., G.P.A. Rice, J. Baskerville, D.M. Wingerchuk, and G.C. Ebers. 2006. The natural history of multiple sclerosis: a geographically based study 9: Observations on the progressive phase of the disease. 584-594 pp.
138. Krezel, W., V. Dupe, M. Mark, A. Dierich, P. Kastner, and P. Chambon. 1996. RXR gamma null mice are apparently normal and compound RXR alpha +/-/RXR beta -/-/RXR gamma -/- mutant mice are viable. *Proc Natl Acad Sci U S A* 93:9010-9014.
139. Kuhla, A., T. Blei, R. Jaster, and B. Vollmar. 2011. Aging Is Associated With a Shift of Fatty Metabolism Toward Lipogenesis. *J Gerontol Biol* 66A:1192-1200.
140. Kuhlmann, T., V. Miron, Q. Cui, C. Wegner, J. Antel, and W. Bruck. 2008. Differentiation block of oligodendroglial progenitor cells as a cause for remyelination failure in chronic multiple sclerosis. *Brain* 131:1749-1758.
141. Kurokawa, R., V.C. Yu, A. Naar, S. Kyakumoto, Z. Han, S. Silverman, M.G. Rosenfeld, and C.K. Glass. 1993. Differential orientations of the DNA-binding domain and carboxy-terminal dimerization interface regulate binding site selection by nuclear receptor heterodimers. *Genes Dev* 7:1423-1435.
142. Lampron, A., A. Larochelle, N. Laflamme, P. Prefontaine, M.M. Plante, M.G. Sanchez, V.W. Yong, P.K. Stys, M.E. Tremblay, and S. Rivest. 2015. Inefficient clearance of myelin debris by microglia impairs remyelinating processes. *J Exp Med*
143. Laskin, D.L. 2009. Macrophages and inflammatory mediators in chemical toxicity: a battle of forces. *Chem Res Toxicol* 22:1376-1385.
144. Lassmann, H. 2007. Multiple sclerosis: is there neurodegeneration independent from inflammation? *J Neurol Sci* 259:3-6.

145. Lassmann, H. 2011. Pathophysiology of inflammation and tissue injury in multiple sclerosis: what are the targets for therapy. *J Neurol Sci* 306:167-169.
146. Lassmann, H., J. van Horssen, and D. Mahad. 2012. Progressive multiple sclerosis: pathology and pathogenesis. *Nat Rev Neurol* 8:647-656.
147. Lau, L.W., M.B. Keough, S. Haylock-Jacobs, R. Cua, A. Doring, S. Sloka, D.P. Stirling, S. Rivest, and V.W. Yong. 2012. Chondroitin sulfate proteoglycans in demyelinated lesions impair remyelination. *Ann Neurol* 72:419-432.
148. Laursen, K.B., P.-M. Wong, and L.J. Gudas. 2012. Epigenetic regulation by RARα maintains ligand-independent transcriptional activity. *Nucleic Acids Research* 40:102-115.
149. Lawson, L.J., V.H. Perry, and S. Gordon. 1992. Turnover of resident microglia in the normal adult mouse brain. *Neuroscience* 48:405-415.
150. Lee, Y., B.M. Morrison, Y. Li, S. Lengacher, M.H. Farah, P.N. Hoffman, Y. Liu, A. Tsingalia, L. Jin, P.W. Zhang, L. Pellerin, P.J. Magistretti, and J.D. Rothstein. 2012. Oligodendroglia metabolically support axons and contribute to neurodegeneration. *Nature* 487:443-448.
151. Levine, J.M., R. Reynolds, and J.W. Fawcett. 2001. The oligodendrocyte precursor cell in health and disease. *Trends Neurosci* 24:39-47.
152. Levy, E., G. Xanthou, E. Petrakou, V. Zacharioudaki, C. Tsatsanis, S. Fotopoulos, and M. Xanthou. 2009. Distinct Roles of TLR4 and CD14 in LPS-Induced Inflammatory Responses of Neonates. *Pediatr Res* 66:179-184.
153. Lewis, J., A. Ferrara, T. Peng, M. Hedderson, W. Bilker, C. Quesenberry Jr, D. Vaughn, L. Nessel, J. Selby, and L. Habel. 2014. Cohort Study of Pioglitazone and Bladder Cancer in Patients with Diabetes: Fourth Interim Analysis (8-Year) Report with Data from January 1, 1997 to December 31, 2010. May 30, 2012.
154. Li, M., A.K. Indra, X. Warot, J. Brocard, N. Messaddeq, S. Kato, D. Metzger, and P. Chambon. 2000. Skin abnormalities generated by temporally controlled RXR[alpha] mutations in mouse epidermis. *Nature* 407:633-636.
155. Lloberas, J., and A. Celada. 2002. Effect of aging on macrophage function. *Exp Gerontol* 37:1325-1331.
156. Lonard, D.M., and B.W. O'Malley. 2012. Nuclear receptor coregulators: modulators of pathology and therapeutic targets. *Nat Rev Endocrinol* 8:598-604.
157. Lowe, M., and G. Plosker. 2000. Bexarotene. *Am J Clin Dermatol* 1:245-250.
158. Lu, Q.R., T. Sun, Z. Zhu, N. Ma, M. Garcia, C.D. Stiles, and D.H. Rowitch. 2002. Common developmental requirement for Olig function indicates a motor neuron/oligodendrocyte connection. *Cell* 109:75-86.
159. Lublin, F.D., S.C. Reingold, J.A. Cohen, G.R. Cutter, P.S. Sorensen, A.J. Thompson, J.S. Wolinsky, L.J. Balcer, B. Banwell, F. Barkhof, B. Bebo, Jr., P.A. Calabresi, M. Clanet, G. Comi, R.J. Fox, M.S. Freedman, A.D. Goodman, M. Inglese, L. Kappos, B.C. Kieseier, J.A. Lincoln, C. Lubetzki, A.E. Miller, X. Montalban, P.W. O'Connor, J. Petkau, C. Pozzilli, R.A. Rudick, M.P. Sormani, O. Stuve, E. Waubant, and C.H. Polman. 2014. Defining the clinical course of multiple sclerosis: the 2013 revisions. *Neurology* 83:278-286.

160. Lunemann, J.D., N. Edwards, P.A. Muraro, S. Hayashi, J.I. Cohen, C. Munz, and R. Martin. 2006. Increased frequency and broadened specificity of latent EBV nuclear antigen-1-specific T cells in multiple sclerosis. *Brain* 129:1493-1506.
161. Lutz, M.A., and P.H. Correll. 2003. Activation of CR3-mediated phagocytosis by MSP requires the RON receptor, tyrosine kinase activity, phosphatidylinositol 3-kinase, and protein kinase C zeta. *J Leukoc Biol* 73:802-814.
162. Ma, J., K.F. Tanaka, T. Shimizu, C.C. Bernard, A. Kakita, H. Takahashi, S.E. Pfeiffer, and K. Ikenaka. 2011. Microglial cystatin F expression is a sensitive indicator for ongoing demyelination with concurrent remyelination. *J Neurosci Res* 89:639-649.
163. Mabbott, D.J., M. Noseworthy, E. Bouffet, S. Laughlin, and C. Rockel. 2006. White matter growth as a mechanism of cognitive development in children. *Neuroimage* 33:936-946.
164. Mancuso, P., R.W. McNish, M. Peters-Golden, and T.G. Brock. 2001. Evaluation of phagocytosis and arachidonate metabolism by alveolar macrophages and recruited neutrophils from F344xBN rats of different ages. *Mech Ageing Dev* 122:1899-1913.
165. Mandala, S., R. Hajdu, J. Bergstrom, E. Quackenbush, J. Xie, J. Milligan, R. Thornton, G.J. Shei, D. Card, C. Keohane, M. Rosenbach, J. Hale, C.L. Lynch, K. Rupprecht, W. Parsons, and H. Rosen. 2002. Alteration of lymphocyte trafficking by sphingosine-1-phosphate receptor agonists. *Science* 296:346-349.
166. Martin, R., and H.F. McFarland. 1995. Immunological aspects of experimental allergic encephalomyelitis and multiple sclerosis. *Crit Rev Clin Lab Sci* 32:121-182.
167. Martin, R., H.F. McFarland, and D.E. McFarlin. 1992. Immunological aspects of demyelinating diseases. *Annu Rev Immunol* 10:153-187.
168. Mason, J.L., A. Toews, J.D. Hostettler, P. Morell, K. Suzuki, J.E. Goldman, and G.K. Matsushima. 2004. Oligodendrocytes and progenitors become progressively depleted within chronically demyelinated lesions. *Am J Pathol* 164:1673-1682.
169. Massacesi, L., A.L. Abbamondi, C. Giorgi, F. Sarlo, F. Lolli, and L. Amaducci. 1987. Suppression of experimental allergic encephalomyelitis by retinoic acid. *Journal of the Neurological Sciences* 80:55-64.
170. Matthews, M.A., and D. Duncan. 1971. A quantitative study of morphological changes accompanying the initiation and progress of myelin production in the dorsal funiculus of the rat spinal cord. *J Comp Neurol* 142:1-22.
171. Matusevicius, D., P. Kivisakk, B. He, N. Kostulas, V. Ozenci, S. Fredrikson, and H. Link. 1999. Interleukin-17 mRNA expression in blood and CSF mononuclear cells is augmented in multiple sclerosis. *Mult Scler* 5:101-104.
172. McFarland, H.F., and R. Martin. 2007. Multiple sclerosis: a complicated picture of autoimmunity. *Nat Immunol* 8:913-919.
173. McKenzie, I.A., D. Ohayon, H. Li, J.P. de Faria, B. Emery, K. Tohyama, and W.D. Richardson. 2014. Motor skill learning requires active central myelination. *Science* 346:318-322.

174. McKinnon, R.D., C. Smith, T. Behar, T. Smith, and M. Dubois-Dalcq. 1993b. Distinct effects of bFGF and PDGF on oligodendrocyte progenitor cells. *Glia* 7:245-254.
175. McKinnon, R.D., G. Piras, J.A. Ida, Jr., and M. Dubois-Dalcq. 1993a. A role for TGF-beta in oligodendrocyte differentiation. *J Cell Biol* 121:1397-1407.
176. McMahon, E.J., K. Suzuki, and G.K. Matsushima. 2002. Peripheral macrophage recruitment in cuprizone-induced CNS demyelination despite an intact blood-brain barrier. *J Neuroimmunol* 130:32-45.
177. Mehta, V., W. Pei, G. Yang, S. Li, E. Swamy, A. Boster, P. Schmalbrock, and D. Pitt. 2013. Iron is a sensitive biomarker for inflammation in multiple sclerosis lesions. *PLoS One* 8:e57573.
178. Menéndez-Gutiérrez, M.P., T. Rőszer, L. Fuentes, V. Núñez, A. Escolano, J.M. Redondo, N. De Clerck, D. Metzger, A.F. Valledor, and M. Ricote. 2015. Retinoid X receptors orchestrate osteoclast differentiation and postnatal bone remodeling. *J Clin Invest* 125:809-823.
179. Mia, S., A. Warnecke, X.M. Zhang, V. Malmström, and R.A. Harris. 2014. An optimized Protocol for Human M2 Macrophages using M-CSF and IL-4/IL-10/TGF-β Yields a Dominant Immunosuppressive Phenotype. *Scandinavian J Immunol* 79:305-314.
180. Mikaeloff, Y., G. Caridade, M. Tardieu, S. Suissa, and K.s. group. 2007. Parental smoking at home and the risk of childhood-onset multiple sclerosis in children. *Brain* 130:2589-2595.
181. Mikita, J., N. Dubourdieu-Cassagno, M.S. Deloire, A. Vekris, M. Biran, G. Raffard, B. Brochet, M.H. Canron, J.M. Franconi, C. Boiziau, and K.G. Petry. 2011. Altered M1/M2 activation patterns of monocytes in severe relapsing experimental rat model of multiple sclerosis. Amelioration of clinical status by M2 activated monocyte administration. *Mult Scler* 17:2-15.
182. Miller, D.H., and S.M. Leary. 2007. Primary-progressive multiple sclerosis. *Lancet Neurol* 6:903-912.
183. Miron, V.E., A. Boyd, J.W. Zhao, T.J. Yuen, J.M. Ruckh, J.L. Shadrach, P. van Wijngaarden, A.J. Wagers, A. Williams, R.J. Franklin, and C. Ffrench-Constant. 2013. M2 microglia and macrophages drive oligodendrocyte differentiation during CNS remyelination. *Nat Neurosci*
184. Møller, H.J. 2011. Soluble CD163. *Scandinavian J Clin Lab Invest* 72:1-13.
185. Moore, K.J., E.D. Rosen, M.L. Fitzgerald, F. Randow, L.P. Andersson, D. Altshuler, D.S. Milstone, R.M. Mortensen, B.M. Spiegelman, and M.W. Freeman. 2001. The role of PPAR-gamma in macrophage differentiation and cholesterol uptake. *Nat Med* 7:41-47.
186. Moorman, S.J., and R.I. Hume. 1994. Contact with myelin evokes a release of calcium from internal stores in neonatal rat oligodendrocytes in vitro. *Glia* 10:202-210.
187. Moras, D., and H. Gronemeyer. 1998. The nuclear receptor ligand-binding domain: structure and function. *Curr Opin Cell Biol* 10:384-391.
188. Morell, P., and A.H. Ousley. 1994. Metabolic turnover of myelin glycerophospholipids. *Neurochem Res* 19:967-974.
189. Mozell, R.L., and F.A. McMorris. 1991. Insulin-like growth factor I stimulates oligodendrocyte development and myelination in rat brain aggregate cultures. *J Neurosci Res* 30:382-390.

190. Murtie, J.C., Y.X. Zhou, T.Q. Le, A.C. Vana, and R.C. Armstrong. 2005. PDGF and FGF2 pathways regulate distinct oligodendrocyte lineage responses in experimental demyelination with spontaneous remyelination. *Neurobiol Dis* 19:171-182.
191. Naegele, M., and R. Martin. 2014. The good and the bad of neuroinflammation in multiple sclerosis. *Handbook of Clinical Neurology* 122:59-87.
192. Nagpal, S., S. Friant, H. Nakshatri, and P. Chambon. 1993. RARs and RXRs: evidence for two autonomous transactivation functions (AF-1 and AF-2) and heterodimerization in vivo. *EMBO* 12:2349-2360.
193. Nagy, L., and J.W. Schwabe. 2004. Mechanism of the nuclear receptor molecular switch. *Trends Biochem Sci* 29:317-324.
194. Nataf, S. 2009. Neuroinflammation responses and neurodegeneration in multiple sclerosis. *Rev Neurol (Paris)* 165:1023-1028.
195. Nauta, A.J., N. Raaschou-Jensen, A. Roos, M.R. Daha, H.O. Madsen, M.C. Borrias-Essers, L.P. Ryder, C. Koch, and P. Garred. 2003. Mannose-binding lectin engagement with late apoptotic and necrotic cells. *Eur J Immunol* 33:2853-2863.
196. Nave, K.A. 2010. Myelination and support of axonal integrity by glia. *Nature* 468:244-252.
197. Neumann, H., M.R. Kotter, and R.J. Franklin. 2009. Debris clearance by microglia: an essential link between degeneration and regeneration. *Brain* 132:288-295.
198. Nicholas, R.S., M.G. Wing, and A. Compston. 2001. Nonactivated microglia promote oligodendrocyte precursor survival and maturation through the transcription factor NF-kappa B. *Eur J Neurosci* 13:959-967.
199. Niehaus, A., J. Shi, M. Grzenkowski, M. Diers-Fenger, J. Archelos, H.P. Hartung, K. Toyka, W. Bruck, and J. Trotter. 2000. Patients with active relapsing-remitting multiple sclerosis synthesize antibodies recognizing oligodendrocyte progenitor cell surface protein: implications for remyelination. *Ann Neurol* 48:362-371.
200. Nijeholt, G.J., M.A. van Walderveen, J.A. Castelijns, J.H. van Waesberghe, C. Polman, P. Scheltens, P.F. Rosier, P.J. Jongen, and F. Barkhof. 1998. Brain and spinal cord abnormalities in multiple sclerosis. Correlation between MRI parameters, clinical subtypes and symptoms. *Brain* 121 (Pt 4):687-697.
201. Nimmerjahn, A., F. Kirchhoff, and F. Helmchen. 2005. Resting microglial cells are highly dynamic surveillants of brain parenchyma in vivo. *Science* 308:1314-1318.
202. Norton, W.T., and S.E. Poduslo. 1973. Myelination in rat brain: changes in myelin composition during brain maturation. *J Neurochem* 21:759-773.
203. Nunez, V., D. Alameda, D. Rico, R. Mota, P. Gonzalo, M. Cedenilla, T. Fischer, L. Bosca, C.K. Glass, A.G. Arroyo, and M. Ricote. 2010. Retinoid X receptor alpha controls innate inflammatory responses through the up-regulation of chemokine expression. *Proc Natl Acad Sci U S A* 107:10626-10631.
204. Odegaard, J.I., R.R. Ricardo-Gonzalez, M.H. Goforth, C.R. Morel, V. Subramanian, L. Mukundan, A. Red Eagle, D. Vats, F. Brombacher, A.W.

Ferrante, and A. Chawla. 2007. Macrophage-specific PPARgamma controls alternative activation and improves insulin resistance. *Nature* 447:1116-1120.
205. Ogawa, D., J.F. Stone, Y. Takata, F. Blaschke, V.H. Chu, D.A. Towler, R.E. Law, W.A. Hsueh, and D. Bruemmer. 2005. Liver x receptor agonists inhibit cytokine-induced osteopontin expression in macrophages through interference with activator protein-1 signaling pathways. *Circ Res* 96:e59-67.
206. Olah, M., S. Amor, N. Brouwer, J. Vinet, B. Eggen, K. Biber, and H.W. Boddeke. 2012. Identification of a microglia phenotype supportive of remyelination. *Glia* 60:306-321.
207. Olson, J.K., and S.D. Miller. 2004. Microglia initiate central nervous system innate and adaptive immune responses through multiple TLRs. *J Immunol* 173:3916-3924.
208. O'Meara, R.W., J.P. Michalski, and R. Kothary. 2011. Integrin signaling in oligodendrocytes and its importance in CNS myelination. *J Signal Transduct* 2011:354091.
209. Orthmann-Murphy, J.L., E. Salsano, C.K. Abrams, A. Bizzi, G. Uziel, M.M. Freidin, E. Lamantea, M. Zeviani, S.S. Scherer, and D. Pareyson. 2009. Hereditary spastic paraplegia is a novel phenotype for GJA12/GJC2 mutations. *Brain* 132:426-438.
210. Ousman, S.S., and P. Kubes. 2012. Immune surveillance in the central nervous system. *Nat Neurosci* 15:1096-1101.
211. Pakpoor, J., and S.V. Ramagopalan. 2013. Epstein-Barr virus is a necessary causative agent in the pathogenesis of multiple sclerosis: yes. *Mult Scler* 19:1690-1691.
212. Pasquini, L.A., V. Millet, H.C. Hoyos, J.P. Giannoni, D.O. Croci, M. Marder, F.T. Liu, G.A. Rabinovich, and J.M. Pasquini. 2011. Galectin-3 drives oligodendrocyte differentiation to control myelin integrity and function. *Cell Death Differ* 18:1746-1756.
213. Patrikios, P., C. Stadelmann, A. Kutzelnigg, H. Rauschka, M. Schmidbauer, H. Laursen, P.S. Sorensen, W. Bruck, C. Lucchinetti, and H. Lassmann. 2006. Remyelination is extensive in a subset of multiple sclerosis patients. *Brain* 129:3165-3172.
214. Paz Soldan, M.M., and I. Pirko. 2012. Biogenesis and significance of central nervous system myelin. *Semin Neurol* 32:9-14.
215. Pender, M.P., and S.R. Burrows. 2014. Epstein-Barr virus and multiple sclerosis: potential opportunities for immunotherapy. *Clin Transl Immunology* 3:e27.
216. Penderis, J., S.A. Shields, and R.J. Franklin. 2003. Impaired remyelination and depletion of oligodendrocyte progenitors does not occur following repeated episodes of focal demyelination in the rat central nervous system. *Brain* 126:1382-1391.
217. Perry, V.H., J.A. Nicoll, and C. Holmes. 2010. Microglia in neurodegenerative disease. *Nat Rev Neurol* 6:193-201.
218. Piccio, L., C. Buonsanti, M. Mariani, M. Cella, S. Gilfillan, A.H. Cross, M. Colonna, and P. Panina-Bordignon. 2007. Blockade of TREM-2 exacerbates experimental autoimmune encephalomyelitis. *Eur J Immunol* 37:1290-1301.
219. Plowden, J., M. Renshaw-Hoelscher, C. Engleman, J. Katz, and S. Sambhara. 2004. Innate immunity in aging: impact on macrophage function. *Aging Cell* 3:161-167.

220. Polman, C.H., S.C. Reingold, B. Banwell, M. Clanet, J.A. Cohen, M. Filippi, K. Fujihara, E. Havrdova, M. Hutchinson, L. Kappos, F.D. Lublin, X. Montalban, P. O'Connor, M. Sandberg-Wollheim, A.J. Thompson, E. Waubant, B. Weinshenker, and J.S. Wolinsky. 2011. Diagnostic criteria for multiple sclerosis: 2010 revisions to the McDonald criteria. *Ann Neurol* 69:292-302.
221. Pringle, N.P., H.S. Mudhar, E.J. Collarini, and W.D. Richardson. 1992. PDGF receptors in the rat CNS: during late neurogenesis, PDGF alpha-receptor expression appears to be restricted to glial cells of the oligodendrocyte lineage. *Development* 115:535-551.
222. Prufer, K., A. Racz, G.C. Lin, and J. Barsony. 2000. Dimerization with retinoid X receptors promotes nuclear localization and subnuclear targeting of vitamin D receptors. *J Biol Chem* 275:41114-41123.
223. Ransohoff, R.M., and A.E. Cardona. 2010. The myeloid cells of the central nervous system parenchyma. *Nature* 468:253-262.
224. Ransohoff, R.M., and B. Engelhardt. 2012. The anatomical and cellular basis of immune surveillance in the central nervous system. *Nat Rev Immunol* 12:623-635.
225. Rawji, K.S., and V.W. Yong. 2013. The benefits and detriments of macrophages/microglia in models of multiple sclerosis. *Clin Dev Immunol* 2013:948976.
226. Reichert, F., U. Slobodov, C. Makranz, and S. Rotshenker. 2001. Modulation (inhibition and augmentation) of complement receptor-3-mediated myelin phagocytosis. *Neurobiol Dis* 8:504-512.
227. Richards, J., K. Gabunia, S.E. Kelemen, F. Kako, E.T. Choi, and M.V. Autieri. 2015. Interleukin-19 increases angiogenesis in ischemic hind limbs by direct effects on both endothelial cells and macrophage polarization. *J Mol Cell Cardio* 79:21-31.
228. Richardson, S.K., S.B. Newton, T.L. Bach, J.B. Budgin, B.M. Benoit, J.H. Lin, J.S. Yoon, M. Wysocka, C.S. Abrams, and A.H. Rook. 2007. Bexarotene blunts malignant T-cell chemotaxis in Sezary syndrome: reduction of chemokine receptor 4-positive lymphocytes and decreased chemotaxis to thymus and activation-regulated chemokine. *Am J Hematol* 82:792-797.
229. Richardson, W.D., K.M. Young, R.B. Tripathi, and I. McKenzie. 2011. NG2-glia as multipotent neural stem cells: fact or fantasy? *Neuron* 70:661-673.
230. Ricote M, Snyder CS, Leung H-Y, Chen J, Chien KR, Glass CK Normal hematopoiesis after conditional targeting of RXRα in murine hematopoietic stem/progenitor cells. *J Leuk Biol* 2006; 80 (4):850-861.
231. Ricote, M., A.C. Li, T.M. Willson, C.J. Kelly, and C.K. Glass. 1998. The peroxisome proliferator-activated receptor-gamma is a negative regulator of macrophage activation. *Nature* 391:79-82.
232. Ricote, M., J.T. Huang, J.S. Welch, and C.K. Glass. 1999. The peroxisome proliferator-activated receptor(PPARgamma) as a regulator of monocyte/macrophage function. *J Leukoc Biol* 66:733-739.
233. Rivers, L.E., K.M. Young, M. Rizzi, F. Jamen, K. Psachoulia, A. Wade, N. Kessaris, and W.D. Richardson. 2008. PDGFRA/NG2 glia generate myelinating oligodendrocytes and piriform projection neurons in adult mice. *Nat Neurosci* 11:1392-1401.

234. Robinson, S., and R.H. Miller. 1999. Contact with central nervous system myelin inhibits oligodendrocyte progenitor maturation. *Dev Biol* 216:359-368.
235. Roszer, T., M.P. Menendez-Gutierrez, M. Cedenilla, and M. Ricote. 2013. Retinoid X receptors in macrophage biology. *Trends Endocrinol Metab* 24:460-468.
236. Roszer, T., M.P. Menendez-Gutierrez, M.I. Lefterova, D. Alameda, V. Nunez, M.A. Lazar, T. Fischer, and M. Ricote. 2011. Autoimmune kidney disease and impaired engulfment of apoptotic cells in mice with macrophage peroxisome proliferator-activated receptor gamma or retinoid X receptor alpha deficiency. *J Immunol* 186:621-631.
237. Rotshenker, S., F. Reichert, M. Gitik, R. Haklai, G. Elad-Sfadia, and Y. Kloog. 2008. Galectin-3/MAC-2, Ras and PI3K activate complement receptor-3 and scavenger receptor-AI/II mediated myelin phagocytosis in microglia. *Glia* 56:1607-1613.
238. Ruckh, J.M., J.W. Zhao, J.L. Shadrach, P. van Wijngaarden, T.N. Rao, A.J. Wagers, and R.J. Franklin. 2012. Rejuvenation of regeneration in the aging central nervous system. *Cell Stem Cell* 10:96-103.
239. Safi, R., G.G. Muramoto, A.B. Salter, S. Meadows, H. Himburg, L. Russell, P. Daher, P. Doan, M.D. Leibowitz, N.J. Chao, D.P. McDonnell, and J.P. Chute. 2009. Pharmacological manipulation of the RAR/RXR signaling pathway maintains the repopulating capacity of hematopoietic stem cells in culture. *Mol Endocrinol* 23:188-201.
240. Salzer, J., G. Hallmans, M. Nyström, H. Stenlund, G. Wadell, and P. Sundström. 2013. Vitamin A and systemic inflammation as protective factors in multiple sclerosis. *Multiple Sclerosis Journal* 19:1046-1051.
241. Sarang, Z., G. Joos, E. Garabuczi, R. Ruhl, C.D. Gregory, and Z. Szondy. 2014. Macrophages engulfing apoptotic cells produce nonclassical retinoids to enhance their phagocytic capacity. *J Immunol* 192:5730-5738.
242. Scalfari, A., A. Neuhaus, M. Daumer, G.C. Ebers, and P.A. Muraro. 2011. Age and disability accumulation in multiple sclerosis. *Neurology* 77:1246-1252.
243. Schneider, C., S.P. Nobs, M. Kurrer, H. Rehrauer, C. Thiele, and M. Kopf. 2014. Induction of the nuclear receptor PPAR-gamma by the cytokine GM-CSF is critical for the differentiation of fetal monocytes into alveolar macrophages. *Nat Immunol* 15:1026-1037.
244. Schonberg, D.L., E.Z. Goldstein, F.R. Sahinkaya, P. Wei, P.G. Popovich, and D.M. McTigue. 2012. Ferritin stimulates oligodendrocyte genesis in the adult spinal cord and can be transferred from macrophages to NG2 cells in vivo. *J Neurosci* 32:5374-5384.
245. Schulz, K., A. Kroner, and S. David. 2012. Iron efflux from astrocytes plays a role in remyelination. *J Neurosci* 32:4841-4847.
246. Schumacher, M., R. Hussain, N. Gago, J.P. Oudinet, C. Mattern, and A.M. Ghoumari. 2012. Progesterone synthesis in the nervous system: implications for myelination and myelin repair. *Front Neurosci* 6:10.
247. Serafini, B., L. Muzio, B. Rosicarelli, and F. Aloisi. 2013. Radioactive in situ hybridization for Epstein-Barr virus-encoded small RNA supports presence of Epstein-Barr virus in the multiple sclerosis brain. *Brain* 136:e233.

248. Setzu, A., J.D. Lathia, C. Zhao, K. Wells, M.S. Rao, C. Ffrench-Constant, and R.J. Franklin. 2006. Inflammation stimulates myelination by transplanted oligodendrocyte precursor cells. *Glia* 54:297-303.
249. Shechter, R., and M. Schwartz. 2013. Harnessing monocyte-derived macrophages to control central nervous system pathologies: no longer 'if' but 'how'. *J Pathol* 229:332-346.
250. Shen, S., J. Sandoval, V.A. Swiss, J. Li, J. Dupree, R.J. Franklin, and P. Casaccia-Bonnefil. 2008. Age-dependent epigenetic control of differentiation inhibitors is critical for remyelination efficiency. *Nat Neurosci* 11:1024-1034.
251. Shi, Y., D. Zhang, T.B. Huff, X. Wang, R. Shi, X.M. Xu, and J.X. Cheng. 2011. Longitudinal in vivo coherent anti-Stokes Raman scattering imaging of demyelination and remyelination in injured spinal cord. *J Biomed Opt* 16:106012.
252. Shields, S.A., J.M. Gilson, W.F. Blakemore, and R.J. Franklin. 1999. Remyelination occurs as extensively but more slowly in old rats compared to young rats following gliotoxin-induced CNS demyelination. *Glia* 28:77-83.
253. Shukla, D.K., C.C. Kaiser, G.T. Stebbins, and D.L. Feinstein. 2010. Effects of pioglitazone on diffusion tensor imaging indices in multiple sclerosis patients. *Neurosci Lett* 472:153-156.
254. Shulman, A.I., C. Larson, D.J. Mangelsdorf, and R. Ranganathan. 2004. Structural determinants of allosteric ligand activation in RXR heterodimers. *Cell* 116:417-429.
255. Sica, A., and A. Mantovani. 2012. Macrophage plasticity and polarization: in vivo veritas. *J Clin Invest* 122:787-795.
256. Sica, A., T. Schioppa, A. Mantovani, and P. Allavena. 2006. Tumour-associated macrophages are a distinct M2 polarised population promoting tumour progression: Potential targets of anti-cancer therapy. *Eur J Cancer* 42:717-727.
257. Sim, F.J., C. Zhao, J. Penderis, and R.J. Franklin. 2002. The age-related decrease in CNS remyelination efficiency is attributable to an impairment of both oligodendrocyte progenitor recruitment and differentiation. *J Neurosci* 22:2451-2459.
258. Sim, F.J., G.L. Hinks, and R.J. Franklin. 2000. The re-expression of the homeodomain transcription factor Gtx during remyelination of experimentally induced demyelinating lesions in young and old rat brain. *Neuroscience* 100:131-139.
259. Simons, M., N. Snaidero, and S. Aggarwal. 2012. Cell polarity in myelinating glia: from membrane flow to diffusion barriers. *Biochim Biophys Acta* 1821:1146-1153.
260. Smith, C.M., E. Cooksey, and I.D. Duncan. 2013. Myelin loss does not lead to axonal degeneration in a long-lived model of chronic demyelination. *J Neurosci* 33:2718-2727.
261. Smith, R.S., and K.D. McLeod. 1979. Unusual particle trajectories and structural arrangements in myelinated nerve fibers. *Can J Physiol Pharmacol* 57:1182-1186.
262. Song, W., and X. Wang. 2015. The role of TGFβ1 and LRG1 in cardiac remodelling and heart failure. *Biophys Rev* 7:91-104.
263. Steinman, L. 2001. Multiple sclerosis: a two-stage disease. *Nat Immunol* 2:762-764.

264. Stence, N., M. Waite, and M.E. Dailey. 2001. Dynamics of microglial activation: a confocal time-lapse analysis in hippocampal slices. *Glia* 33:256-266.
265. Stilund, M., A.K. Reuschlein, T. Christensen, H.J. Moller, P.V. Rasmussen, and T. Petersen. 2014. Soluble CD163 as a marker of macrophage activity in newly diagnosed patients with multiple sclerosis. *PLoS One* 9:e98588.
266. Stoffels, J.M., J.C. de Jonge, M. Stancic, A. Nomden, M.E. van Strien, D. Ma, Z. Siskova, O. Maier, C. Ffrench-Constant, R.J. Franklin, D. Hoekstra, C. Zhao, and W. Baron. 2013. Fibronectin aggregation in multiple sclerosis lesions impairs remyelination. *Brain* 136:116-131.
267. Stout, R.D., and J. Suttles. 2005. Immunosenescence and macrophage functional plasticity: dysregulation of macrophage function by age-associated microenvironmental changes. *Immunol Rev* 205:60-71.
268. Streit, W.J., M.B. Graeber, and G.W. Kreutzberg. 1988. Functional plasticity of microglia: a review. *Glia* 1:301-307.
269. Sugama, S., T. Takenouchi, H. Kitani, M. Fujita, and M. Hashimoto. 2007. Activin as an anti-inflammatory cytokine produced by microglia. *J Neuroimmunol* 192:31-39.
270. Sung, B., S. Park, B.P. Yu, and H.Y. Chung. 2006. Amelioration of age-related inflammation and oxidative stress by PPARgamma activator: suppression of NF-kappaB by 2,4-thiazolidinedione. *Exp Gerontol* 41:590-599.
271. Suzuki, K., J.M. Andrews, J.M. Waltz, and R.D. Terry. 1969. Ultrastructural studies of multiple sclerosis. *Lab Invest* 20:444-454.
272. Swift, M.E., A.L. Burns, K.L. Gray, and L.A. DiPietro. 2001. Age-related alterations in the inflammatory response to dermal injury. *J Invest Dermatol* 117:1027-1035.
273. Syed, Y.A., A.S. Baer, G. Lubec, H. Hoeger, G. Widhalm, and M.R. Kotter. 2008. Inhibition of oligodendrocyte precursor cell differentiation by myelin-associated proteins. *Neurosurg Focus* 24:E5.
274. Syed, Y.A., E. Hand, W. Mobius, C. Zhao, M. Hofer, K.A. Nave, and M.R. Kotter. 2011. Inhibition of CNS remyelination by the presence of semaphorin 3A. *J Neurosci* 31:3719-3728.
275. Szalardy, L., D. Zadori, E. Tanczos, M. Simu, K. Bencsik, L. Vecsei, and P. Klivenyi. 2013. Elevated levels of PPAR-gamma in the cerebrospinal fluid of patients with multiple sclerosis. *Neurosci Lett* 554:131-134.
276. Szanto, A., V. Narkar, Q. Shen, I.P. Uray, P.J. Davies, and L. Nagy. 2004. Retinoid X receptors: X-ploring their (patho)physiological functions. *Cell Death Differ* 11 Suppl 2:S126-143.
277. Tabe, Y., M. Konopleva, M. Andreeff, and A. Ohsaka. 2012. Effects of PPARgamma Ligands on Leukemia. *PPAR Res* 2012:483656.
278. Takahashi, K., M. Prinz, M. Stagi, O. Chechneva, and H. Neumann. 2007. TREM2-transduced myeloid precursors mediate nervous tissue debris clearance and facilitate recovery in an animal model of multiple sclerosis. *PLoS Med* 4:e124.
279. Tatsumi, K., H. Takebayashi, T. Manabe, K.F. Tanaka, M. Makinodan, T. Yamauchi, E. Makinodan, H. Matsuyoshi, H. Okuda, K. Ikenaka, and A. Wanaka. 2008. Genetic fate mapping of Olig2 progenitors in the injured adult

cerebral cortex reveals preferential differentiation into astrocytes. *J Neurosci Res* 86:3494-3502.
280. Tippett, E., W.-J. Cheng, C. Westhorpe, P.U. Cameron, B.J. Brew, S.R. Lewin, A. Jaworowski, and S.M. Crowe. 2011. Differential Expression of CD163 on Monocyte Subsets in Healthy and HIV-1 Infected Individuals. *PLoS ONE* 6:e19968.
281. Todorich, B., X. Zhang, B. Slagle-Webb, W.E. Seaman, and J.R. Connor. 2008. Tim-2 is the receptor for H-ferritin on oligodendrocytes. *J Neurochem* 107:1495-1505.
282. Triantafilou, M., and K. Triantafilou. 2002. Lipopolysaccharide recognition: CD14, TLRs and the LPS-activation cluster. *Trends in Immunology* 23:301-304.
283. Trouplin, V., N. Boucherit, L. Gorvel, F. Conti, G. Mottola, and E. Ghigo. 2013. Bone Marrow-derived Macrophage Production. e50966.
284. Tullman, M.J. 2013. A review of current and emerging therapeutic strategies in multiple sclerosis. *Am J Manag Care* 19:S21-27.
285. Tzartos, J.S., G. Khan, A. Vossenkamper, M. Cruz-Sadaba, S. Lonardi, E. Sefia, A. Meager, A. Elia, J.M. Middeldorp, M. Clemens, P.J. Farrell, G. Giovannoni, and U.C. Meier. 2012. Association of innate immune activation with latent Epstein-Barr virus in active MS lesions. *Neurology* 78:15-23.
286. van der Worp, H.B., D.W. Howells, E.S. Sena, M.J. Porritt, S. Rewell, V. O'Collins, and M.R. Macleod. 2010. Can Animal Models of Disease Reliably Inform Human Studies? *PLoS Med* 7:e1000245.
287. van Noort, J.M., and M. Bsibsi. 2009. Toll-like receptors in the CNS: implications for neurodegeneration and repair. *Prog Brain Res* 175:139-148.
288. van Walderveen, M.A., F. Barkhof, M.W. Tas, C. Polman, S.T. Frequin, O.R. Hommes, A.J. Thompson, and J. Valk. 1998. Patterns of brain magnetic resonance abnormalities on T2-weighted spin echo images in clinical subgroups of multiple sclerosis: a large cross-sectional study. *Eur Neurol* 40:91-98.
289. van Wijngaarden, P., and R.J. Franklin. 2013. Ageing stem and progenitor cells: implications for rejuvenation of the central nervous system. *Development* 140:2562-2575.
290. Vereyken, E.J., P.D. Heijnen, W. Baron, E.H. de Vries, C.D. Dijkstra, and C.E. Teunissen. 2011. Classically and alternatively activated bone marrow derived macrophages differ in cytoskeletal functions and migration towards specific CNS cell types. *J Neuroinflammation* 8:58.
291. Vinet, J., H.R. Weering, A. Heinrich, R.E. Kalin, A. Wegner, N. Brouwer, F.L. Heppner, N. Rooijen, H.W. Boddeke, and K. Biber. 2012. Neuroprotective function for ramified microglia in hippocampal excitotoxicity. *J Neuroinflammation* 9:27.
292. Vogel, D.Y., E.J. Vereyken, J.E. Glim, P.D. Heijnen, M. Moeton, P. van der Valk, S. Amor, C.E. Teunissen, J. van Horssen, and C.D. Dijkstra. 2013. Macrophages in inflammatory multiple sclerosis lesions have an intermediate activation status. *J Neuroinflammation* 10:35.
293. Walther, E.U., and R. Hohlfeld. 1999. Multiple sclerosis: side effects of interferon beta therapy and their management. *Neurology* 53:1622-1627.
294. Wang, C., X. Yu, Q. Cao, Y. Wang, G. Zheng, T.K. Tan, H. Zhao, Y. Zhao, Y. Wang, and D. Harris. 2013. Characterization of murine macrophages from bone marrow, spleen and peritoneum. *BMC Immunology* 14:6.

295. Wang, Y., and D. Harris. 2011. Macrophages in renal disease. *J Am Soc Nephrol* 22:21 - 27.
296. Wegner, M. 2008. A matter of identity: transcriptional control in oligodendrocytes. *J Mol Neurosci* 35:3-12.
297. Weinshenker, B.G., B. Bass, G.P. Rice, J. Noseworthy, W. Carriere, J. Baskerville, and G.C. Ebers. 1989. The natural history of multiple sclerosis: a geographically based study. I. Clinical course and disability. *Brain* 112 (Pt 1):133-146.
298. Wiig, H., A. Schroder, W. Neuhofer, J. Jantsch, C. Kopp, T.V. Karlsen, M. Boschmann, J. Goss, M. Bry, N. Rakova, A. Dahlmann, S. Brenner, O. Tenstad, H. Nurmi, E. Mervaala, H. Wagner, F.X. Beck, D.N. Muller, D. Kerjaschki, F.C. Luft, D.G. Harrison, K. Alitalo, and J. Titze. 2013. Immune cells control skin lymphatic electrolyte homeostasis and blood pressure. *J Clin Invest* 123:2803-2815.
299. Wilms, H., T. Schwark, L.O. Brandenburg, J. Sievers, R. Dengler, G. Deuschl, and R. Lucius. 2010. Regulation of activin A synthesis in microglial cells: pathophysiological implications for bacterial meningitis. *J Neurosci Res* 88:16-23.
300. Wolswijk, G. 1998. Chronic stage multiple sclerosis lesions contain a relatively quiescent population of oligodendrocyte precursor cells. *J Neurosci* 18:601-609.
301. Woodruff, R.H., M. Fruttiger, W.D. Richardson, and R.J. Franklin. 2004. Platelet-derived growth factor regulates oligodendrocyte progenitor numbers in adult CNS and their response following CNS demyelination. *Mol Cell Neurosci* 25:252-262.
302. Wuest, S.C., I. Mexhitaj, N.R. Chai, E. Romm, J. Scheffel, B. Xu, K. Lane, T. Wu, and B. Bielekova. 2014. A Complex Role of Herpes Viruses in the Disease Process of Multiple Sclerosis. *PLoS ONE* 9:e105434.
303. Yamasaki, R., H. Lu, O. Butovsky, N. Ohno, A.M. Rietsch, R. Cialic, P.M. Wu, C.E. Doykan, J. Lin, A.C. Cotleur, G. Kidd, M.M. Zorlu, N. Sun, W. Hu, L. Liu, J.C. Lee, S.E. Taylor, L. Uehlein, D. Dixon, J. Gu, C.M. Floruta, M. Zhu, I.F. Charo, H.L. Weiner, and R.M. Ransohoff. 2014. Differential roles of microglia and monocytes in the inflamed central nervous system. *J Exp Med* 211:1533-1549.
304. Yamauchi, T., H. Waki, J. Kamon, K. Murakami, K. Motojima, K. Komeda, H. Miki, N. Kubota, Y. Terauchi, A. Tsuchida, N. Tsuboyama-Kasaoka, N. Yamauchi, T. Ide, W. Hori, S. Kato, M. Fukayama, Y. Akanuma, O. Ezaki, A. Itai, R. Nagai, S. Kimura, K. Tobe, H. Kagechika, K. Shudo, and T. Kadowaki. 2001. Inhibition of RXR and PPARγ ameliorates diet-induced obesity and type 2 diabetes. *J Clin Invest* 108:1001-1013.
305. Yasmin, R., K.T. Yeung, R.H. Chung, M.E. Gaczynska, P.A. Osmulski, and N. Noy. 2004. DNA-looping by RXR tetramers permits transcriptional regulation "at a distance". *J Mol Biol* 343:327-338.
306. Yasmin, R., P. Kannan-Thulasiraman, H. Kagechika, M.I. Dawson, and N. Noy. 2010. Inhibition of mammary carcinoma cell growth by RXR is mediated by the receptor's oligomeric switch. *J Mol Biol* 397:1121-1131.
307. Yednock, T.A., C. Cannon, L.C. Fritz, F. Sanchez-Madrid, L. Steinman, and N. Karin. 1992. Prevention of experimental autoimmune encephalomyelitis by antibodies against alpha 4 beta 1 integrin. *Nature* 356:63-66.

308. You, S.H., H.W. Lim, Z. Sun, M. Broache, K.J. Won, and M.A. Lazar. 2013. Nuclear receptor co-repressors are required for the histone-deacetylase activity of HDAC3 in vivo. *Nat Struct Mol Biol* 20:182-187.
309. Young, K.M., K. Psachoulia, R.B. Tripathi, S.J. Dunn, L. Cossell, D. Attwell, K. Tohyama, and W.D. Richardson. 2013. Oligodendrocyte dynamics in the healthy adult CNS: evidence for myelin remodeling. *Neuron* 77:873-885.
310. Yuen, T.J., J.C. Silbereis, A. Griveau, S.M. Chang, R. Daneman, S.P. Fancy, H. Zahed, E. Maltepe, and D.H. Rowitch. 2014. Oligodendrocyte-encoded HIF function couples postnatal myelination and white matter angiogenesis. *Cell* 158:383-396.
311. Yuen, T.J., K.R. Johnson, V.E. Miron, C. Zhao, J. Quandt, M.C. Harrisingh, M. Swire, A. Williams, H.F. McFarland, R.J. Franklin, and C. Ffrench-Constant. 2013. Identification of endothelin 2 as an inflammatory factor that promotes central nervous system remyelination. *Brain* 136:1035-1047.
312. Zawadzka, M., L.E. Rivers, S.P. Fancy, C. Zhao, R. Tripathi, F. Jamen, K. Young, A. Goncharevich, H. Pohl, M. Rizzi, D.H. Rowitch, N. Kessaris, U. Suter, W.D. Richardson, and R.J. Franklin. 2010. CNS-resident glial progenitor/stem cells produce Schwann cells as well as oligodendrocytes during repair of CNS demyelination. *Cell Stem Cell* 6:578-590.
313. Zhao, C., W.W. Li, and R.J. Franklin. 2006. Differences in the early inflammatory responses to toxin-induced demyelination are associated with the age-related decline in CNS remyelination. *Neurobiol Aging* 27:1298-1307.
314. Zhou, Q., and D.J. Anderson. 2002. The bHLH transcription factors OLIG2 and OLIG1 couple neuronal and glial subtype specification. *Cell* 109:61-73.
315. Zilliacus, J., J. Carlstedt-Duke, J.A. Gustafsson, and A.P. Wright. 1994. Evolution of distinct DNA-binding specificities within the nuclear receptor family of transcription factors. *Proc Natl Acad Sci U S A* 91:4175-4179.